ISSN 2039-6651
anno 2025 numero 102

MISCELLANEA INGV

Fault segmentation and seismotectonics of active thrust systems: the Northern Apennines and Southern Alps laboratories for new Seismic Hazard Assessments in northern Italy (NASA4SHA)

ISTITUTO NAZIONALE DI GEOFISICA E VULCANOLOGIA

102

REGISTRAZIONE AL TRIBUNALE DI ROMA N.178 | 2014, 23 LUGLIO

Rappresentante legale: Presidente INGV
Sede: Via di Vigna Murata, 605 | Roma

www.ingv.it

ISTITUTO NAZIONALE DI GEOFISICA E VULCANOLOGIA

ISSN 2039-6651
anno **2025** numero **102**

MISCELLANEA INGV

Fault segmentation and seismotectonics of active thrust systems: the Northern Apennines and Southern Alps laboratories for new Seismic Hazard Assessments in northern Italy (NASA4SHA)

Selected outcomes and results from the PRIN2020 Project

Editors: Riccardo Caputo[1,2,*], Laura Peruzza[3], Silvio Seno[2,4], Alessandro Tibaldi[2,5], and Emanuela Falcucci[6]

[1]Università di Ferrara, Dipartimento di Fisica e Scienze della Terra, Ferrara, Italy
[2]Centro Interuniversitario per la Sismotettonica 3D con Applicazioni Territoriali (CRUST), Chieti, Italy
[3]Istituto Nazionale di Oceanografia e di Geofisica Sperimentale - OGS, Trieste, Italy
[4]Università degli Studi di Pavia, Dipartimento di Scienze della Terra e dell'Ambiente, Pavia, Italy
[5]Università degli Studi di Milano-Bicocca, Department of Earth and Environmental Sciences, Milan, Italy
[6]Istituto Nazionale di Geofisica e Vulcanologia - INGV, Sezione Roma 1, Italy

**Corresponding author*

Accepted 15 November 2025 | *Accettato* 15 novembre 2025

How to cite | *Come citare* Caputo R., Peruzza L., Seno S., Tibaldi A., and Falcucci E., (2025). Fault segmentation and seismotectonics of active thrust systems: the Northern Apennines and Southern Alps laboratories for new Seismic Hazard Assessments in northern Italy (NASA4SHA). Misc. INGV, 102: 1-152, https://doi.org/10.13127/misc/102

Cover Evidence of Holocene morphogenic earthquakes in the Budoia trench (NE Italy) | *In copertina Evidenze di terremoti morfogenici olocenici nella trincea di Budoia (NE Italia)*

102

NASA4SHA

Research Units

Università degli Studi di Ferrara, Resp. Riccardo Caputo (Project Leader)
Università degli Studi di Pavia, Resp. Silvio Seno
Università degli Studi di Milano-Bicocca, Resp. Alessandro Tibaldi
Istituto Nazionale di Oceanografia e di Geofisica Sperimentale, Resp. Laura Peruzza
Istituto Nazionale di Geofisica e Vulcanologia, Resp. Emanuela Falcucci

The NASA4SHA Project was selected in the frame of the “PRIN: Progetti di ricerca di rilevante interesse nazionale – Bando 2020”, a call of the Italian Ministry of University and Research, following an international peer-review, competing under the main ERC field Physical Sciences and Engineering and coming second in the field Earth System Science - PE10, with an assigned budget of 897,750 euros.

INDEX

Preface

Riccardo Caputo[1,2,*], Laura Peruzza[3], Silvio Seno[2,4], Alessandro Tibaldi[2,5], and Emanuela Falcucci[6]

[1]Università di Ferrara, Dipartimento di Fisica e Scienze della Terra, Ferrara, Italy
[2]Centro Interuniversitario per la Sismotettonica 3D con Applicazioni Territoriali (CRUST), Chieti, Italy
[3]Istituto Nazionale di Oceanografia e di Geofisica Sperimentale - OGS, Trieste, Italy
[4]Università di Pavia, Dipartimento di Scienze della Terra e dell'Ambiente, Pavia, Italy
[5]Università di Milano Bicocca, Dipartimento di Scienze dell'Ambiente e della Terra, Milan, Italy
[6]Istituto Nazionale di Geofisica e Vulcanologia - INGV, Sezione Roma 1, Italy

Corresponding author: rcaputo@unife.it

The PRIN2020 Project aimed at investigating the fault complexities in active thrust systems like those of the Northern Apennines and Southern Alps (NASA; Figure 1), and at quantifying their consequences on standard and pioneer practices of seismic hazard assessments.
We established two distinct, but concatenated, major goals. Firstly, we aimed at better defining the 3D geometry and the kinematics of the thrust systems. This goal can be reached by improving our knowledge on the internal fault hierarchy and earthquake occurrence at specific fault segments, based on a multidisciplinary approach, in which geological, geophysical, remote sensing, seismological, palaeoseismological, geodetic, and morphotectonic datasets are integrated and critically confronted among researchers with different background and expertise. Complementary techniques allow investigating the fault characteristics at different scales and with different resolutions, from the entire seismogenic level of the Earth crust, of as many as possible active segments, for better quantifying the seismotectonic parameters like, maximum credible rupture area, slip-rates and aseismic components, on-/off-fault magnitude-frequency distribution. These results have been obtained by a joint effort of some research units (RUs) and represent one major outcome of the project.
Secondly, another major goal of the project was the release of a prototypal fault displacement hazard assessment (FDHA) in selected locations of Northern Italy. These brand-new analyses are now feasible, thanks to some prototypal tools developed within the *Fault segmentation and seismotectonics of active thrust systems: the Northern Apennines and Southern Alps laboratories for new Seismic Hazard Assessments in northern Italy* (NASA4SHA) Project. They represent an important contribution to seismic risk reduction strategies and for planning prioritization of interventions that should be adopted in such a densely populated and economically important region of Italy.
All project activities can also represent a contribution to the Italian Interuniversity Center for 3D Seismotectonics with territorial applications (CRUST), to which many of the researchers that worked in the NASA4SHA Project belong to. Indeed, the Center promotes research and teaching in Seismotectonics within Italian universities, involving the analysis of long-term and current tectonic activity operating across various temporal and spatial scales to understand the seismic processes controlling seismic hazards.
The collection of short papers included in the present volume is the tip of the iceberg of research performed from May 2022 to May 2025 by ca. 50 research fellows, organized in 5 RUs belonging to the academia, and research institutions. The list of the papers already published as an outcome of the NASA4SHA Project is reported in Appendix at the end of the volume.
A short summary of the contents of this volume is given, and a final section summarizes the lessons learned and potential perspectives.

The background for this research is represented by seismological observations and global tectonics that have driven to basic identification of earthquake-prone areas, however, just in the last decades and for few regions worldwide the location and seismogenic capacity of faults have been fully included in seismic hazard assessment analyses. Earthquake geology with a variety of disciplines contributes to the quantification of earthquake occurrence for known/suspected seismic sources. Accurate 3D geometries of active faults, updated segmentation criteria based on observations of slip partitioning and other fault properties, and state-of-the-art physical models of earthquake behaviour have been proposed in the literature for a more realistic estimate of earthquake recurrences. This kind of multidisciplinary approach is particularly needed in slowly deforming areas, especially in those densely populated and highly industrialized. This is the case of northern Italy where two opposite verging imbricate thrust systems affect the marginal sectors of the Po and Veneto-Friuli plains, which represent our target areas.

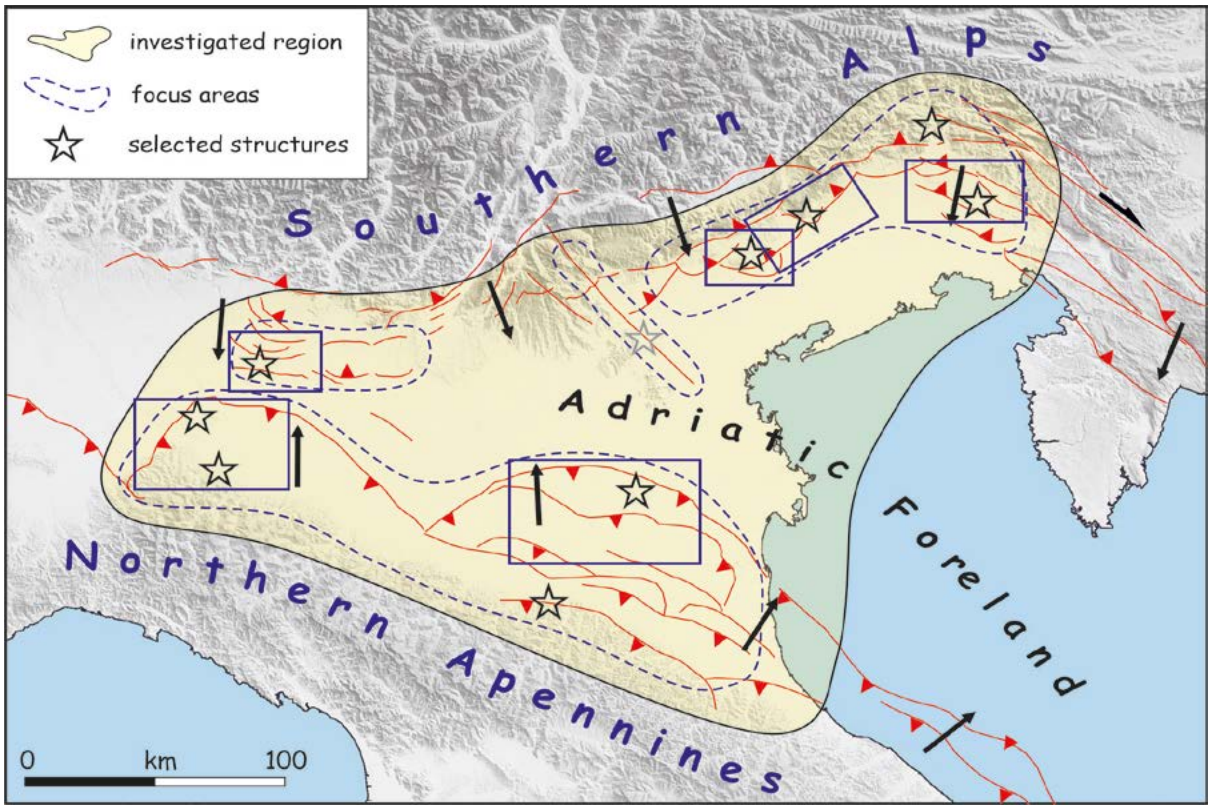

Figure 1 Simplified tectonic map of northern Italy with NASA4SHA targets.

Conceptual framework

Accretionary wedges, especially during their late continental stages, consist of numerous reverse faults, mainly with a low- to intermediate-angle setting and a common vergence. Although single shear zones and slip surfaces could have a relatively simple geometry, the crustal volumes affected by such contractional features are characterized by overstepping and/or overlapping structures, curved geometries (both along strike and downdip), and complex kinematic patterns (either in terms of rake or amount of displacement). During the last million years, the area that now corresponds to northern Italy was affected by a complex geodynamic "engine" [Caputo et al., 2010] that led to stress concentrations/shadows and variable strain rates

both in space and time at different scales [Caputo, 2005]. As a consequence, the identification of the seismogenic sources affecting the external sectors of the NASA region is particularly complex, and it represents a challenge for more realistic SHA, not only for northern Italy, but also for all similar tectonic settings.

From the geological and structural point of view, segment boundaries within major fault zones might influence the initiation and halt of earthquake ruptures, thus controlling the magnitude and rupture propagation patterns during sequences. They correspond to discontinuities such as relay zones and large step-overs, pronounced bends, or branch faults and large cross-faults, and changes in rheology [e.g. Schwartz and Sibson, 1989]. Many of these geologic features are interpreted as higher strength rock-volumes or fault zones, able to stop the propagation of coseismic ruptures (commonly referred to as geometric and structural barriers [Aki, 1979]). On the other hand, being zones of stress concentration barriers can act as nucleation points [King and Nabelek, 1985; Sibson, 1986; Boatwright and Cocco, 1996; Manighetti et al., 2015; Perrin et al., 2016]. Detailed 3D reconstructions at depth and palaeoseismological data contributed to document the behavior of segment boundaries, but literature is primarily focused on strike-slip faults and recently on normal ones [e.g. Faure Walker et al., 2021], whereas low-angle thrusts are indeed the less studied [Biasi and Wesnousky, 2016].

The Po and Veneto-Friuli plains, including their contiguous foothills, are affected by two opposite verging thrust systems (NASA, Figure 1). Arc-shaped geometries of different sizes and curvatures have developed in both orogens, generating a complex system of minor-order structures with different dimensions and seismogenic potential. Although for both thrust belts several seismotectonic investigations have been carried out [e.g. Galadini et al., 2005; Burrato et al., 2008; DISS Working Group, 2018; Martelli et al., 2017; Santulin et al., 2017; Maesano et al., 2015; Maestrelli et al., 2018; Romano et al., 2019; and references therein], the segment boundaries within major seismogenic sources, and especially their possible impact in terms of partial reactivations of the whole structure and maximum credible magnitude that could be released has been not sufficiently treated. Concerning seismicity, the area is affected by minor-to-strong earthquakes, fairly well documented in the last centuries [Rovida et al., 2019], but with some controversial issues, concerning the oldest ones; the instrumental coverage is very different in time and space, and it does not assure a uniform completeness magnitude and homogeneous location uncertainties [Bressan et al., 2019; Sugan and Peruzza, 2011]. Conversely, some 3D geometries are enlightened by microearthquakes [Romano et al., 2019] and have been used for interpreting the geodetic observations too [Anderlini et al., 2020].

This region is affected by small strain-rates, 2-3 mm/a of N-S convergence in the Southern Alps. Therefore, it should be also important to remove any possible hydrological loading effect to enhance the tectonic component of the geodetic observations [Rossi et al., 2018], and calculate the strain-rate field in the region.

Finally, the compilation of national and European fault databases [e.g. DISS Working Group, 2018; Basili et al., 2013] represents a big step forward in Probabilistic Seismic Hazard Assessment (PSHA), but challenges remain in the homogenization of the taxonomy of fault sources, and the transferral of our understanding into quantitative assessments of earthquake potential [e.g. Pace et al., 2018; and references therein].

Recent earthquake sequences in Italy (1976 Friuli, 2012 Emilia-Romagna and 2016-17 Central Apennines) are examples of multiple earthquakes that occurred across a fault system within a period of days to few months; this clustering behaviour is far from unprecedented in the historical past. Although a theoretical framework does exist in PSHA for such behaviour [Yeo and Cornell, 2009; Boyd, 2012], time-dependent SHA as it is practised [e.g. Pace et al., 2006; Peruzza et al., 2011] does not account for such interactions. Similar considerations apply for Fault Displacement Hazard that can have several important applications in the densely urbanized and industrialized area of the Po Plain.

Short description of the project's activities

The main objective of the NASA4SHA Project was to address specific challenges in seismotectonic characterization in contractional systems mainly consisting of blind structures, though local evidence of surface ruptures also occurs; the integration and exchange of research and innovation activities between the involved RUs allowed and can further boost substantial improvements in fundamental components of SHA. Networking and capacity building between RUs were encouraged as well as the adoption of innovative sustainable technologies, giving priority to cutting-edge investigation techniques.
For operational reasons, the several activities have been organized in thematic Work Packages (WPs), strongly linked among each other and basically devoted to:

- Tectonic constraints at depth, with the participation of RUs of UNIPV, UNIFE and OGS, was focused on the characterization of earthquake sources in their complex, 3D geometries (WP1).
- Geodetic strain build-up for slip-rates estimates, with RUs of INGV-OGS-UniFE, was aimed at recognizing the kinematic partitioning occurring in the investigated thrust systems and their segmentation (WP2).
- Remote sensing and morphotectonic analyses (RU UniMIB) attempted at improving the knowledge on the identified segments (WP3).
- Multiscale geophysical surveys (RU UniFE; WP4).
- Palaeoseismological investigations at selected sites (RUs UniFE and INGV; WP5).
- Analogue modelling of thrust barriers (RU UniPV) represented complementary modelling methods capable of investigating different space and time scales (WP6).
- Review of historical and instrumental seismicity (RUs INGV and OGS) attempted at attributing a ranking in terms of the seismogenic potential, for better constraints of the principal seismotectonic parameters, like average slip-rate, maximum credible magnitude, slip per event, recurrence interval, among others (WP7).

Synthesis of the major results

General results and major milestones of the NASA4SHA Project allowed a considerable progress in the knowledge and 3D structural representation of some sectors of Northern Apennines and Southern Alps, with focus on their segmentation and the consequent seismogenic behaviour as well as the development of an interdisciplinary methodological strategy, for building realistic and geologically-constrained seismogenic fault rupture models to be adopted in SHA analyses. Preliminary results have already been presented at national and international congresses and workshops and shared with the scientific community, for further improvements, suggestions and comments.
In the future, all obtained results can be further integrated and critically compared to perform a new conceptual 3D database of major active faults and segments, that gathers all supporting data for the parameterization of as many as possible seismogenic sources, and to assess prototypal assessment of fault displacement seismic hazard of some selected areas.
In the following there is a short summary of the notes included in this volume allowing the reader to have a general idea of the principal activities carried out and the major results. For a more detailed and complete description of research performed and the results obtained in the frame of the NASA4SHA PRIN2020 Project see also the list of publications in the Appendix to this volume.

Structure reconstruction and fault kinematics in the Central Po Plain (Italy): an integrated approach through subsurface data and analogue models

The note by De Matteo and coauthors integrates subsurface seismic data and analogue modeling to reconstruct the buried thrust systems of the Central Po Plain, where the Northern Apennines and Southern Alps fronts converge. Three main thrusts and related anticlines were mapped, revealing heterogeneous slip distribution and along-strike deformation. Sandbox experiments demonstrated that inherited structures significantly influence thrust kinematics, producing non-uniform strain and out-of-sequence reactivation of inner faults. The results enhance the understanding of fault segmentation and slip partitioning relevant for seismic hazard assessment in northern Italy.

Constraining tectonic structures at depth through seismicity revision and tomographic analysis: two case studies in the Eastern Southern Alps (ESA, Italy)

Romano and coauthors performed multidisciplinary analyses of the Montello and Socchieve areas and combined seismicity catalogs, tomographic imaging, and 3D fault modeling to refine crustal structures in the ESA. Local earthquake and attenuation tomography identified high-absorption, fluid-rich zones correlating with methane reservoirs and reduced seismicity, revealing the influence of fluids on fault behavior. The Socchieve 2024 earthquake sequence highlighted active transpressive structures compatible with regional tectonics. The findings demonstrate the efficacy of multi-scale imaging in constraining fault geometry and improving seismic hazard assessment.

A Combined Regional Velocity Field for Northern Italy: new insights into strain accumulation in eastern Southern Alps and Northern Apennines

By merging GNSS datasets from INGV, OGS, and IGM95 networks, Galvani and coauthors produced a unified velocity field for northern Italy. The data reveal two main deformation zones: 2–3 mm/yr NNE-directed shortening across the Ferrara–Romagna Arc and 1.5–2 mm/yr N-directed compression along the Eastern Southern Alps. Strain-rate and dislocation modeling indicate partial fault locking at 8–9 km depth, consistent with interseismic strain accumulation on seismogenic thrusts. These results suggest that both regions are storing elastic strain capable of generating moderate-to-large magnitude earthquakes, refining regional seismic hazard models.

A thirty-year GNSS velocity field - an update for the Northern Apennines and Southern Alps thrust belts: towards a new deformation benchmark

Carnemolla et al. present an updated geodetic analysis of crustal deformation across the Northern Apennines and Southern Alps using GNSS data. The team reanalyzed 29 benchmarks from the historical IGM95 network, combining them with recent 2023 observations to produce a refined velocity field relative to the Eurasian plate. Data were processed using GAMIT/GLOBK software and aligned to the ITRF2014 reference frame. The results reveal a consistent NNE–SSW contractional pattern, in agreement with known Adria microplate kinematics, and show excellent correspondence with nearby continuous GNSS stations. The new dataset allows higher-resolution strain rate calculations, enhancing the understanding of active fault locking and crustal shortening. This reanalysis demonstrates that old cartographic networks can still yield valuable geophysical insights. The study establishes a 2023.0 “zero-point” benchmark for future monitoring, providing a key reference for measuring coseismic, postseismic, and interseismic deformation in northern Italy.

High-precision geometric levelling between Udine and Basagliapenta: a possible key method for detecting recent tectonic deformations at the Eastern Southern Alps front (Friuli, NE Italy)
Marchesini et al. report new high-precision geometric levelling data along a 14 km transect from Udine to Basagliapenta, crossing active thrusts in the Friulian plain. The 2024 survey remeasured and expanded the historical IGM line 110, previously observed in 1977, 1993, and 2004, to detect vertical ground deformation associated with the Pozzuolo and Udine–Buttrio thrust systems. Seven new benchmarks were installed to improve spatial resolution and minimize levelling errors, achieving very high precision ($\sigma^* \approx 0.41$ mm/√km). Analysis of elevation changes between epochs reveals localized uplift between benchmarks 12–09 and 07–04, consistent with known active fronts. The most significant uplift (≈36.7 ± 4.0 mm in 47 years) corresponds to the Udine–Buttrio NW thrust, suggesting a deformation rate of ~0.8 mm/yr, possibly due to aseismic creep. Comparisons with seismic profiles confirm correspondence between surface uplift and buried thrust geometries. Although non-tectonic factors cannot be excluded, the study demonstrates the levelling method's ability to capture subtle crustal deformations over short timescales, establishing a foundation for future geodynamic monitoring of the Eastern Southern Alps.

From surface to crustal depths: the Broni–Sarmato Fault in the context of the Emilia Arc, northern Italy
Tibaldi and coauthors, through morphotectonic mapping, UAV and geoelectrical surveys, and seismic data integration, characterize the Broni–Sarmato thrust as part of the active Stradella fault system within the Emilia Arc. Field evidence, including terrace offsets and triangular facets, indicates Late Pleistocene–Holocene fault activity. Geoelectrical anomalies reveal deformation zones facilitating saline water ascent along structural discontinuities. Seismicity analysis identifies clustered compressional and strike-slip events consistent with SSW–NNE compression. Results collectively support recent tectonic activity and potential seismogenic behavior of the Broni–Sarmato fault.

Application of a C0-class drone for 3D reconstruction and morphotectonic analysis: an example from the Broni-Sarmato Fault, Emilia Arc (Northern Italy)
Using C0-class drones Bonali et al. provide a novel way of conducting morphotectonic analysis in areas with low relief and dense infrastructure. In this study, a DJI Mini 4 Pro was used to create high-resolution 3D models of the Broni–Sarmato Fault (Emilia Arc), revealing previously undocumented decimetre-scale anomalies. The resulting digital surface models (DSMs), orthomosaics and 3D models, which were georeferenced using RTK-mode GCPs, revealed two minor scarps that may have a tectonic origin. These findings support the expansion of near-surface geophysical surveys to improve structural characterisation. The approach adopted demonstrates the effectiveness of UAV photogrammetry, even in semi-urban settings where regulatory and logistical constraints often hinder traditional data collection methods. The collected data provide a valuable foundation for future geological mapping and modelling campaigns.

Terrestrial LiDAR survey to overcome UAV flight restrictions in morphotectonic analyses: an example from the Budoia–Aviano Thrust (NE Italy)
Bonali et al. present a terrestrial LiDAR survey applied to the Budoia-Aviano Thrust (NE Italy) within the framework of the NASA4SHA Project. Due to UAV flight restrictions imposed by the nearby Aviano NATO air base, a handheld GeoSLAM ZEB Horizon scanner coupled with RTK GNSS was employed to acquire high-resolution 3D morphotectonic data. The workflow allowed reconstructing a unified point cloud exceeding 330 million points and a Digital Surface Model (DSM) with centimetre-scale accuracy (~2.7 cm/pixel). The DSM highlights subtle slope

breaks and morphological anomalies potentially linked to shallow deformation structures within the thrust system. Comparison with regional airborne LiDAR datasets confirms the reliability of the SLAM-based approach, which achieved resolutions suitable for (morpho)tectonic analyses. Results demonstrate that portable LiDAR technology represents an effective alternative to UAV photogrammetry, enabling precise documentation of active fault zones in restricted or logistically challenging environments

Deep and Shallow Electrical Resistivity Tomographies on the Budoia-Aviano Thrust (NE Italy)
Rizzo and coauthors investigate the Budoia-Aviano Thrust (NE Italy) by means of a multiscale geophysical approach combining Deep and Shallow Electrical Resistivity Tomography (ERT) with geological and palaeoseismological analyses. The DERT survey, reaching depths of ~1000 m, revealed the subsurface architecture of the Polcenigo-Montereale and Budoia-Aviano thrusts, while high-resolution shallow ERTs (5 to 1 m electrode spacing) allowed to identify near-surface discontinuities affecting Upper Pleistocene-Holocene deposits of the Artugna River alluvial fan. Subsequent trenching at San Martino confirmed the presence of back-verging reverse surficial ruptures and deformation of post-Last Glacial Maximum sediments. These results provide the first evidence of Holocene activation of the Budoia-Aviano thrust, highlighting its seismotectonic significance within the Carnic pre-Alpine front.

Innovative approaches to fault detection: integrating geophones and distributed acoustic sensing (DAS) in the Budoia-Aviano Thrust case study
Suranna and coauthors examine the use of a combination of conventional geophones and Distributed Acoustic Sensing (DAS) to create images of faults along the Budoia–Aviano Thrust (BAT) in the eastern part of the Southern Alps. Four seismic profiles were acquired using explosive sources and dual receiver systems to enable direct comparison. Although geophones provide accurate timing via shot triggers, DAS lacks precise time zero (t_0), which leads to the systematic overestimation of reflector depths by up to two metres for shallow horizons. To address this issue, the authors applied cross-correlation and Bayesian alignment techniques. Despite the limitations of the timing, DAS was able to image the same structures as the geophones, which demonstrates its potential for high-resolution, near-surface seismic analysis. This combined approach improves fault characterisation and contributes to a more accurate seismic hazard assessment.

Bayesian cross-correlation of DAS seismic data using MCMC sampling: a case study from the Budoia–Aviano Thrust (NE Italy)
Suranna and coauthors present a Bayesian approach for aligning Distributed Acoustic Sensing (DAS) seismic data using Markov Chain Monte Carlo (MCMC) sampling, applied to five active-source records from the Budoia-Aviano Thrust in north-eastern Italy. A reference seismic patch was extracted from shot ESP98 and compared to subsequent shots (ESP99-ESP102) by estimating temporal and spatial shifts, stretch, and noise parameters. The MCMC algorithm yielded well-defined posterior distributions, confirming strong feature similarity and stable acquisition conditions. This probabilistic framework enhances traditional cross-correlation by quantifying uncertainty and improving robustness against noise. The results validate the internal consistency of the velocity model and suggest potential for automated DAS monitoring and fault detection.

Recent tectonic activity of the Budoia–Aviano Thrust: the example of the Late Pleistocene–Holocene Artugna alluvial fan (eastern Southern Alps, NE Italy)
In this study Poli and coauthors investigate the recent tectonic activity of the Budoia–Aviano Thrust through geological, geomorphological, stratigraphic, and geophysical analyses of the

Artugna alluvial fan in the eastern Southern Alps. Field mapping, palaeoseismological trenching, electrical resistivity tomography, and radiocarbon dating reveal Late Pleistocene–Holocene deformation affecting alluvial fan sediments and buried paleosols. Fault-related tilting and surface ruptures demonstrate ongoing compressional tectonics along the mountain front. The integration of geological and geophysical data confirms that the Budoia–Aviano structure is an active thrust accommodating present-day crustal shortening, with implications for regional seismic hazard assessment.

Segmentation of the external front of the Eastern Southern Alps: the Arba–Ragogna case study (NE Italy)
Patricelli and coauthors investigate how inherited Dinaric tectonic structures influenced the segmentation of the active frontal thrusts in the Eastern Southern Alps (ESA). Using seismic reflection data, geological mapping, and morphotectonic analysis, they reinterpret the Arba–Ragogna Thrust System as two distinct segments: Arba–Sequals (AS) and Ragogna (RA). This segmentation is controlled by deep Dinaric structures that shaped the propagation of Neogene–Quaternary thrust fronts. The study highlights the polyphase tectonic evolution of the Friuli region, from Mesozoic extension to Cenozoic compression. It allows identifying four active thrust systems-Maniago–Meduno, Toppo–Forgaria, Arba–Sequals, and Ragogna-and shows how their geometry reflects inherited palaeostructures. The authors conclude that structural inheritance plays a fundamental role in fault segmentation and seismic hazard. Segmentation reduces individual seismogenic potential but could lead to linked rupture scenarios.

The influence of pre-existing structures on the foredeep evolution and structural style: the case studio in the Western Emilian Arc, Central Po Plain (Italy)
De Matteo and coauthors investigated how inherited subsurface structures influence the foredeep evolution and structural style of the western Emilian Arc (Italy). Using sandbox analogue models, three scenarios with varying geometric and rheological configurations were tested to evaluate the impact of structural highs and opposing buried thrusts on fault propagation. The experiments reveal that these features promote lateral segmentation, slow deformation rates, and trigger reactivation of internal thrusts. Particle Image Velocimetry (PIV) analysis confirms heterogeneous strain distribution and variable slip rates along the thrust fronts. The most complex model (M3) successfully replicates the arc's non-cylindrical and diachronous geometry, highlighting the tectonic relevance of inherited discontinuities in shaping recent deformation patterns.

Results of historical seismology investigations
Camassi and coauthors present results from historical seismology work aimed at improving Italy's seismic catalogues (CPTI15 v4.0 and DBMI15). The research focuses on moderate or poorly known earthquakes, especially in four key regions: the Emilian plain, Treviso Prealps, Friulian Prealps and Carnia, and the Ferrara area. New documentary evidence revealed previously unknown or neglected earthquakes, such as those in Finale Emilia (1639), Carpi (1761, 1778), and Treviso (1709–1949). Several events were re-evaluated, increasing data points and correcting epicentral parameters. In Ferrara, many supposed medieval earthquakes were proven non-existent, cleaning the catalogue. Overall, the project significantly refines Italy's historical seismic record, improving the accuracy and completeness of seismic hazard models and demonstrating that valuable new information can still emerge from archival research.

Improving seismic catalogs and microseismicity imaging in the Montello area (NE Italy)
Romano and coauthors describe two complementary research streams for the seismically complex Montello–Collalto region: (1) the creation of a unified long-term seismic catalog and (2) the testing of machine-learning-based event detection. The first integrates data from nine local

and national catalogs (1925–2023), reprocessing earthquake locations with improved 1D/3D velocity models to refine the geometry of the Montello thrust system. The second applies the LOC-FLOW machine learning workflow, using PhaseNet for automatic P- and S-wave picking, to detect microseismic sequences such as the 2021 Refrontolo swarm. M_L methods recover most manually identified events but require complementary tools for completeness. Together, these approaches enhance real-time monitoring, distinguish natural from induced seismicity (e.g., near the Collalto gas storage site), and lay the groundwork for advanced hazard assessment and long-term tectonic interpretation.

Advancing multi-scale seismic hazard assessment in Italy: unified moment magnitude catalog and k_0 corrections

Moratto, Saraò, and colleagues report two main advances. First, they compiled a moment magnitude (Mw) catalog for northeastern Italy containing over 11,600 earthquakes (2016–2023) with improved magnitude consistency through an automated near–real-time workflow. A new empirical Mw–M_L relation was derived for the region, confirming stable scaling across small and moderate magnitudes. Second, they introduced k_0 corrections (high-frequency attenuation parameters derived from ambient noise) into source parameter estimations. Applying these corrections allowed reliable corner frequency and stress drop estimates down to Mw ≈ 1.2, improving analysis of microearthquakes. The combined results enhance seismic hazard modeling by providing a robust, continuously updated magnitude database and more accurate physical parameters for small events. These developments strengthen Italian seismic monitoring and inform regional hazard and risk mitigation strategies.

Towards a unified probabilistic fault displacement hazard assessment

Chen and coauthors present a framework integrating physics-based modeling of fault displacements with probabilistic hazard assessment within the OpenQuake Engine. The study models permanent surface deformation due to dip-slip earthquakes (M5.5–7.0) using pseudo-dynamic rupture simulations, capturing variability in fault geometry, slip, and rupture velocity. Results reproduce observed displacement patterns in Central Italy and quantify aleatory and epistemic uncertainties. Building on this, a prototype Probabilistic Fault Displacement Hazard Assessment (PFDHA) module was developed in OpenQuake, enabling transparent, standardized simulations of surface rupture hazard. This integration bridges empirical data and physical modeling, improving estimates for infrastructures crossing active faults. The approach provides a reproducible computational basis for next-generation seismic hazard analysis in compressional tectonic settings such as Northern Italy.

Concluding remarks and possible applications of the results

Northern Italy is affected by low tectonic deformation rates. Most seismogenic sources have been tentatively identified and characterized based on historical observations of earthquake damage and/or by recent instrumental seismicity; only limited investigations provide geological-based constraints [Galadini et al., 2005]. Unfortunately, the time span represented by these data is only a (small) fraction of the typical seismic cycle of these structures. Within the investigated region, corresponding to the frontal sectors of the NASA accretionary wedges, the recognition of the seismogenic sources and especially their seismotectonic characterization is indeed a crucial issue. In this area, tectonic structures consist of complex systems of arcs composed by thrusts, intrinsically interconnected, with strong geometric, kinematic and dynamic lateral variations. It is worth to note that the contractional domains are in general the least known worldwide, and recent reactivations of previously unknown faults [e.g. Brocher et al., 2015]

pose serious questions even for the most advanced fault-based source models [e.g. UCERF3, Field et al., 2017].

All the activities of the 3-years NASA4SHA Project were devoted to improving the knowledge and 3D structural representation of large sectors of NASA, in terms of thrust segmentation and seismogenic behaviour, developing an interdisciplinary strategy principally dedicated to defining ERF models. The relevance of the scientific contribution stems from the innovative methodologies and especially their full integration in a common vision pivoted on SHA. The multidisciplinary approach represents the real added value of the NASA4SHA Project. Indeed, in slowly deforming areas like northern Italy, it aims to define two main tools: a consistent one able to improve the methodologies for active fault system analysis and a merging multidata storage tool able to improve the estimates of earthquake recurrence.

Recent developments in data availability, computational resources, and scientific knowledge, partly achieved also in the frame of the NASA4SHA Project are creating new opportunities for incorporating 3D geometries and multiple strands of seismotectonic information into more sophisticated seismic-hazard models, for a better quantification of different expressions of earthquake potential. Seismic events have an impact on society at a variety of social and economic scales. As a consequence, collecting and analysing data of different spatial coverage and resolution, collected from a blend of large- and local-scale, and information at depth, represent a technological breakthrough that bring challenges, particularly by disrupting established patterns of work and providing new skills. The multidisciplinary approach of NASA4SHA Project was also planned for representing a fertile source of novel scientific questions contributing to justify the proposed framework needed to address these questions in an efficient and timely manner.

The impact of the obtained results may be remarkable both from economic and social point of view. As a matter of fact, the most urbanized and industrialized regions of Italy are within and/or close to the areas investigated by the NASA4SHA Project; despite the degree of seismicity is not the highest of Italy, the region is characterized by a very high risk as the 2012 Emilia seismic sequence has shown [Mucciarelli and Liberatore, 2014; Regione Emilia-Romagna, 2017; Meroni et al., 2017].

Human and financial losses can be mitigated through making informed decisions based on where future earthquakes may occur, how often they might occur and how strong the ground will shake. Such information is the purpose of SHA and should be applied in building codes, insurance models and public policies: on these means is based a stronger socio-economic resilience, enhanced preparedness as well as public risk awareness. Therefore, the technological and social innovation of the Project are in perfect agreement with, and certainly contributed to, some of the main topics of the Italian “Programma Nazionale della Ricerca 2021-2027”. In particular, the results of this project revealed to be useful i) from a pre-disaster perspective, to consider the root causes of earthquakes in northern Italy and ii) during an ongoing sequence, to provide the reconstruction of the 3D fault pattern and segmentation of potential seismogenic sources to identify earthquake-fault connection.

References

Aki, K., (1979). *Characterization of barriers on an earthquake fault*. J. Geophy. Res., 84, B11, 6140-6148. https://doi.org/10.1029/JB08iB11p06140

Anderlini, S., Vannoli, P., Basili, R., Fracassi, U., & Valensise, G. (2020). *A revised seismogenic framework for Italy*. Solid Earth, 11, 1681-1702. https://doi.org/10.5194/se-11-1681-2020

Basili, R., Vannoli, P., Burrato, P., Fracassi, U., and Valensise, G., (2013). *The SHARE fault database*. https://doi.org/10.6092/INGV.IT-SHARE-EDSF

Biasi, G.P., and Wesnousky, S.G., (2016). *Steps and gaps in ground ruptures: empirical bounds on rupture propagation* Bull. Seism. Soc. Am., 106(3), 1110-1124. https://doi.org/10.1785/0120150175

Boatwright, J., and Cocco, M., (1996), *Frictional constraints on crustal faulting*. J. Geophy. Res., 101, B6, 13895-13909. https://doi.org/101(B6), 13895-13909

Boyd, O.S., (2012). *Fault geometry and ground motion prediction*. Bull. Seism. Soc. Am., 102(1), 1-14. https://doi.org/10.1785/0120110008

Bressan, G., Gentili, S., and Rossi, G., (2019). *Seismicity and stress field in northeastern Italy*. Boll. Geofis. Teor. Appl., 60(3), 301-316. https://doi.org/10.4430/bgta0300

Brocher, T.M., Aagaard, B.T., Simpson, R.W., and Jachens, R.C., (2015). *USGS 3D velocity model for northern California*. Seismol. Res. Lett., 86(1), 1–10. https://doi.org/10.1785/0220150004

Burrato, P., Poli, M.E., Vannoli, P., Zanferrari, A., Basili, R., and Galadini, F., (2008). *Sources of Mw 5+ earthquakes in northeastern Italy and western Slovenia: an updated view based on geological and seismological evidence.* Tectonophys., 453(1-4), 157-176.

Caputo, R. (2005). *Stress variability and brittle tectonic structures*. Earth-Science Reviews, 70(1-2), 103-127. https://doi.org/10.1016/j.earscirev.2004.11.005

Caputo, R., Poli E., and Zanferrari A., (2010). *Neogene-Quaternary tectonic stratigraphy of the eastern Southern Alps, NE Italy*. J. Struct. Geol., 32(7), 1009-1027. https://doi.org/10.1016/j.jsg.2010.06.004

DISS Working Group, (2018). *Database of Individual Seismogenic Sources (DISS), Version 3.2.1*. https://doi.org/10.6092/INGV.IT-DISS3.2.1

Faure Walker, J., Wedmore, L.N.J., and Roberts, G.P., (2021). *Fault segmentation dataset*. https://www.pangaea.de/tok/09c7ec39625747f42e0676292d3ee3d04b72bde8.

Field, E.H., Milner, K.R., and Shaw, J.H., (2017). *UCERF3 update*. Seismol. Res. Lett., 88(5), 1251-1260. https://doi.org/10.1785/0220170045

Galadini, F., Poli, M.E., and Zanferrari, A., (2005). *Seismogenic sources in the eastern Southern Alps*. Geophys. J. Int., 161, 739-762. https://doi.org/10.1111/j.1365-246X.2005.02571.x

King, G., and Nabelek, J., (1985). *Role of fault bends in the initiation and termination of earthquake rupture.* Science, 228,4702, 984-987. https://doi.org/10.1126/science.228.4702.984

Maesano, F.E., D'Ambrogi, C., and Civetta, L., (2015). *Seismic source modeling in Italy*. Tectonophysics, 646, 1-15. https://doi.org/10.1016/j.tecto.2014.12.007

Maestrelli, D., Bonini, M., Corti, G., and Sani, F., (2018), *Fault segmentation and stress field*. Tectonophysics, 745, 1-20. https://doi.org/10.1016/j.tecto.2017.12.006

Manighetti, I., Caulet, C., De Barros, L., Perrin, C., Cappa, F., and Gaudemer,Y., (2015). *Generic along-strike segmentation of Afar normal faults, East Africa: Implications on fault growth and stress heterogeneity on seismogenic fault planes*. Geochem. Geophys. Geosyst., 16(2), 443-467. https://doi.org/10.1002/2014GC005691

Martelli, L., Santulin,M., Sani, F., Tamaro, A., Bonini, M., Rebez, A., Corti, G., and Slejko, D., (2017). *Seismic hazard of the Northern Apennines based on 3D seismic sources.* J. Seismol., 21, 1251-1275. https://doi.org/10.1007/s10950-017-9665-1

Meroni, F., Zonno, G., and Azzaro, R., (2017). *Risk perception and preparedness*. Int. J. Disaster Risk Sci., 8(4), 353-365. https://doi.org/10.1007/s13753-017-0142-9

Mucciarelli, M., and Liberatore, D., (2014). *Seismic vulnerability in Italy*. Bull. Earthq. Eng., 12(5), 2111-2116. https://doi.org/10.1007/s10518-014-9602-3

Pace, B., Peruzza, L., and Zucconi, D., (2006). *Fault segmentation and recurrence*. Bull. Seism. Soc. Am., 96(4A), 1282-1300. https://doi.org/10.1785/0120040231

Pace, B., Visini, F., and Peruzza, L., (2018). *Seismic hazard modeling*. Nat. Hazards Earth Syst. Sci., 18(5), 1349-1373. https://doi.org/10.5194/nhess-18-1349-2018

Perrin, C., Manighetti, I., Ampuero, J.-P., Cappa, F., and Gaudemer, Y., (2016). *Location of largest earthquake slip and fast rupture controlled by along-strike change in fault structural maturity due to*

fault growth. J. Geophys. Res., 121(5), 3666-3685. https://doi.org/10.1002/2015JB012671
Peruzza, L., Pace, B., and Visini, F., (2011). *Seismic hazard sensitivity*. Bull. Seism. Soc. Am., 101(6), 3068-3081. https://doi.org/10.1785/0120090276
Regione Emilia-Romagna, (2017). *Informazioni sul terremoto*. https://www.regione.emilia-romagna.it/terremoto
Romano, F., Cinti, F.R., and Meletti, C., (2019*). Fault segmentation and rupture scenarios*. Seismol. Res. Lett., 90(2A), 1-10. https://doi.org/ 10.1785/0220180387
Rossi, G., Maesano, F.E., and D'Ambrogi, C., (2018). *Seismic source characterization*. Pure Appl. Geophys., 175(5), 1712-1730. https://doi.org/10.1007/s00024-017-1712-x
Rovida, A., Locati, M., Camassi, R., Lolli, B., and Gasperini, P., (2019). *Catalogo Parametrico dei Terremoti Italiani (CPTI15), versione 2.0*. Istituto Nazionale di Geofisica e Vulcanologia (INGV). https://doi.org/10.13127/CPTI/CPTI15.2
Santulin, M., Tamaro, A., Rebez, A., Slejko, D., Sani, F., Martelli, L., Bonini, M., Corti, G., Poli, M.E., Zanferrari, A., et al., (2017). *Seismogenic zonation as a branch of the logic tree for the new Italian seismic hazard map – MPS16: a preliminary outline*. Boll. Geof. Teor. Appl., 58(4), 313-342. https://doi.org/10.4430/bgta0216
Schwartz, D.P., and Sibson, R.H. (Eds), (1989). *Fault Segmentation and Controls of Rupture Initiation and Termination*. Open-File Report 89-315.
Sibson, R.H., (1986). *Earthquakes and rock deformation in crustal fault zones*. Ann. Rev. Earth Planet. Sci., 14(1), 149-175.
Sugan, M., and Peruzza, L., (2011). *Distretti sismici del Veneto*. Boll. Geof. Teor. Appl., 52(Supplement), s3-s90. https://doi.org/10.4430/bgta0057
Yeo, G.L., and Cornell, C.A., (2009). *Stochastic characterization and decision bases under time-dependent aftershock risk in performance-based earthquake engineering*. Earthq. Eng. Struct. Dyn., 38(8), 1013-1037. https://doi.org/10.1002/ege.840

Structure reconstruction and fault kinematics in the Central Po Plain (Italy): an integrated approach through subsurface data and analogue models

Ada De Matteo[1,2,*], Daniel Barrera Acosta[1,2], Giovanni Toscani[1,2], and Silvio Seno[1,2]

[1]Università di Pavia, Dipartimento di Scienze della Terra e dell'Ambiente, Pavia, Italy
[2]Centro Interuniversitario per la Sismotettonica 3D con Applicazioni Territoriali (CRUST), Chieti, Italy

Corresponding author: ada.dematteo@unipv.it

Introduction

The research project aims to investigate the fault complexities in active thrust systems of Northern Italy and their consequences on Seismic Hazard Assessment (SHA). Main goals are (i) to better defining the 3D geometry and the kinematics of the thrust systems, suggesting scenarios of slip partitioning and constraints on earthquake occurrences in selected sectors of the Northern Apennines and Southern Alps and (ii) to release a prototypal Fault Displacement Hazard Assessment (FDHA) in selected sectors of Northern Italy.
Our Research Unit (RU) was responsible for the analysis of the western portion of the Emilian Arc (Figure 1) throughout the development of two main activities: (i) tectonic constraint at depth; (ii) analogue modelling of thrust barriers. An integrated approach combining the analysis of subsurface data and analogue modeling was employed to study the Pliocene-Pleistocene fault kinematics of the central Po Plain (Italy), a tectonically complex area where the Northern Apennines and the Southern Alps outermost fronts are buried under the deposits filling the foredeep basin of the two opposite verging thrust-fold belts.

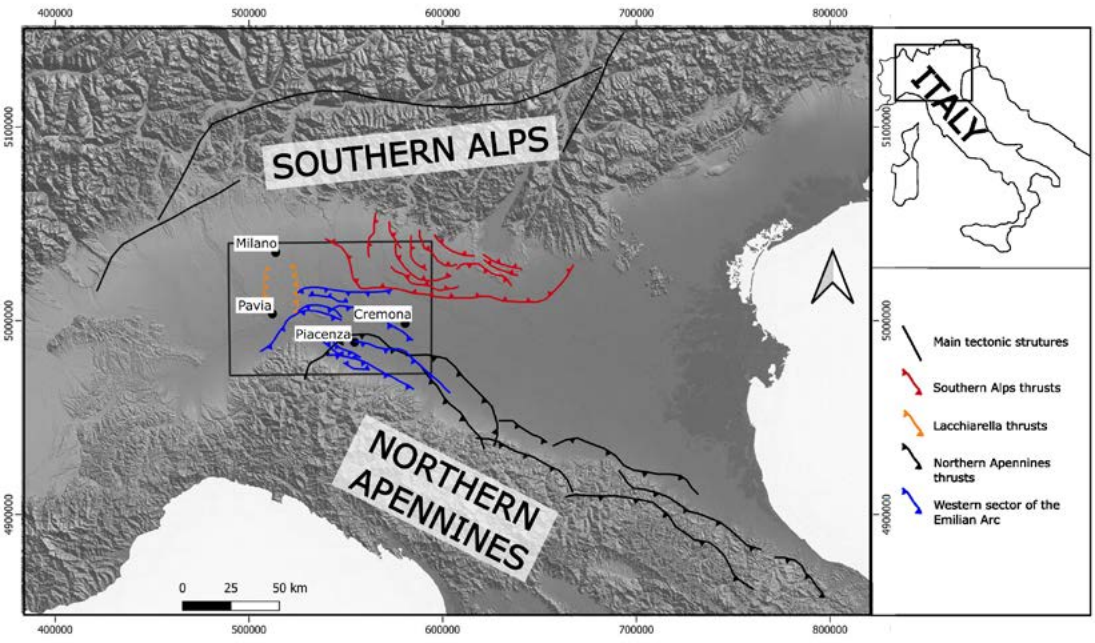

Figure 1 Geological setting of the Emilian Arc.

For the tectonic constraint at depth of our study area, 2D seismic reflection profiles surveying the outermost fronts of the thrust systems have been analysed using several software packages available at the RU. Taking advantage of the fact that, at the same time as the PRIN Project, a PhD program was underway aimed at mapping the structures of the Emilian Arc, a dataset consisting of 2305 TWT seismic lines and almost 220 wells has been analysed across the Northern Apennines arcs.
In order to better understand the kinematics of the arc-shaped thrusts characterising the westernmost sector of the Emilian Arc, interacting with the presence of opposite-verging thrusts (i.e. the South-Alpine thrusts), analogue modelling have been carried out. In particular, these models can reveal if deformation takes place homogeneously along strike or if it is segmented since the initial stages of thrust growth. Moreover, they are a useful instrument to analyse the strain distribution along the outermost front of the arcs. Two sets of models have been achieved aimed at reproducing i) a single arcuate thrust fault and ii) a set of structural arcs and associated recesses.

Tectono-stratigraphic reconstruction and fault kinematics

A dense grid of seismic reflection profiles and well data allowed the reconstruction of the main underground structures and their lateral continuity/discontinuity. In particular, we mapped the main Pliocene-Pleistocene surfaces and a system of three main thrusts and related anticlines belonging to the Northern Apennines buried front, and the deep structures associated to the Southern Alps buried fronts (Figure 2).

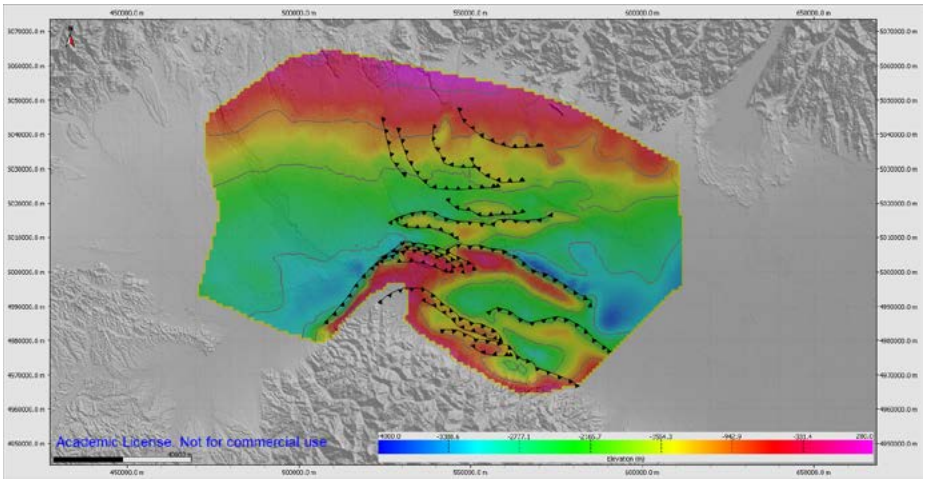

Figure 2 Subsurface reconstructed map (major faults and depth of the Pliocene base).

The tectono-stratigraphic reconstruction was achieved revising the literature in order to choose the unconformities to build a basin-scale model and identifying the wells characterised by a good correlation to cover the full extent of the study area. Progressively, the geophysical interpretation also included the depth conversion of the horizons employing a three-dimensional velocity model that accounts for the geometry of the interpreted horizons and the velocity taken from the available checkshots and VSP measurements. Finally, we fulfilled the interpretation of the reflectors selected to represent the defined surface picks within the basin, following seismic stratigraphy and sequence stratigraphy principles.

Restoring the cross sections, the cumulative deformation distribution and long-term slip-rates have been estimated with a probabilistic approach considering the age and slip uncertainties. This allowed to detect i) where and how the deformation is partitioned along strike, ii) on which segment(s) strain is mainly concentrated and iii) when most of the deformation occurred. The main goal of this activity is to define different sectors of contiguous structures composing the arcs, to describe and tentatively quantify the slip differences between the different sectors of the arcs.

Analogue models

In order to investigate the factors controlling this kinematic complexity, a set of analogue models was carried out to simulate the influence of the mapped structural highs and related rheological variations of the central Po Plain subsurface.
We built a sandbox with three fixed sides and one movable side, driven by a PC-controlled hydraulic piston. Then we laid some layers of coloured sand (with different rheology in different places to simulate the inhomogeneities in the field) and placed two blocks at the base to simulate the presence of two structural highs which, according to our data, interfere with the advance of the Apennine front (Figure 3).

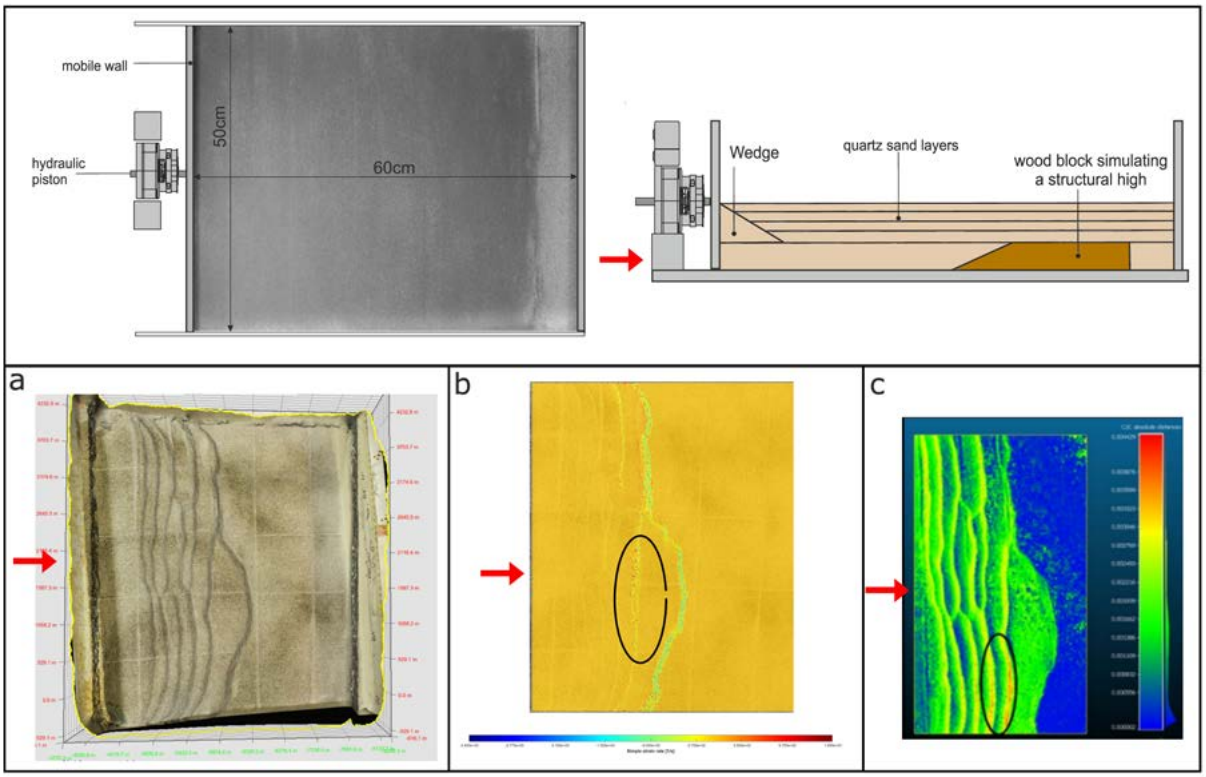

Figure 3 Analogue models. On the top: the set-up of our models consisting of quartz sand layers, wood blocks used to simulate the presence of structural highs as Lacchiarella and South-Alpine. Red arrow indicates the direction of compression. On the bottom: a) 3D of the model at the end of the experiment; b) simple strain rate map of one of the last moments of the experiment; c) deformation map of one of the last moments of the experiment. Black circles highlight the faults that show higher values of strain rate and displacement than the youngest one.

To estimate the vertical and horizontal deformations, we monitored the experiments using four digital cameras. Image sets were processed into sequences of 3-D surface models using structure-from-motion photogrammetry, allowing vertical deformation analyses (AgiSoft MetaShape Professional). Horizontal deformation was assessed by tracking feature displacements within the vertical camera image sequence using PIVlab (a free and open-source Particle Image Velocimetry - PIV - software) [Thielicke and Stamhuis, 2014], which also allowed to determine the strain rates along the outermost front of the modelled arc.
Moreover, at the end of the deformation, the model was cut, and different sections were observed and quantitatively analysed for creating 3D reconstructions of the displacement pattern.
Sand box models analysis demonstrates that the presence of inherited structures and/or buried fronts related to opposite-verging thrust-belts significantly affect both kinematics and spatial distribution (along-strike variations) of tectonic deformation (Figure 2). The slip distribution and the along-strike deformation become therefore rather inhomogeneous. Also, the thrust kinematics does not follow the usual sequence of deformation from the inner to the outer sectors of the chain, but show evidence of out-of-sequence reactivation of inner thrusts because the PIV analysis shows that these thrusts register higher strain values than the outer ones. In the same passages, external thrusts show little or no activity during the final deformation phases.

Concluding remarks

As part of the NASA4SHA Project, the tectono-stratigraphic structure of a portion of the Emilian Arc facing the buried southern Alpine fronts was reconstructed in detail based on both subsurface data and observations derived from analogue models. Based on the analysis of the buried structures, their offsets and slip rates, we suggest that the evolutionary history of the Emilian Arc has been influenced by the presence of inherited structures, the effects of which are visible both in the geometry of the main structures (asymmetrical and arcuate) and in the slip distribution along the strike of the main fault planes.

References

Thielicke, W., and Stamhuis, E., (2014). *Pivlab towards user-friendly, affordable and accurate digital particle image velocimetry in matlab*. Journal of Open Research Software, 2 (1), e30. https://doi.org/10.5334/jors.bl

Constraining tectonic structures at depth through seismicity revision and tomographic analysis: two case studies in the ESA (Eastern Southern Alps, Italy)

Maria Adelaide Romano[1,*], Fatemeh Abdi[1], Gualtiero Böhm[1], Piero Brondi[1], Rita de Nardis[2,3], Luca De Siena[4], Marco Garbin[1], Mariangela Guidarelli[1], Giusy Lavecchia[2,3], Andrea Magrin[1], Luca Moratto[1], Vincenzo Picotti[5], Matteo Picozzi[1], Enrico Priolo[1], Marco Santulin[1], Angela Saraò[1], Daniele Spallarossa[1,6], Monica Sugan[1], Donato Talone[2,3], Luigi Zampa[1], and Laura Peruzza[1]

[1]Istituto Nazionale di Oceanografia e di Geofisica Sperimentale - OGS, Trieste, Italy
[2]Università "G. d'Annunzio", Chieti-Pescara, Italy
[3]Centro Interuniversitario per la Sismotettonica 3D con Applicazioni Territoriali (CRUST), Chieti, Italy
[4]Alma Mater Studiorum - Università di Bologna, Bologna, Italy
[5]ETH | Eidgenössische Technische Hochschule, Zürich, Switzerland
[6]Università degli Studi di Genova, Genoa, Italy

Corresponding author: aromano@ogs.it

1. Introduction and objectives

The Eastern Southern Alps (ESA), in particular the Montello region and the neighboring Friuli sector, represent a tectonically complex and seismically active area that lies on the boundary between the Adria microplate and the Eurasian plate. Both sub-regions are characterized by active faults and historical seismicity, which make them susceptible to future earthquakes.
As part of the Work Package 1 of the PRIN Project NASA4SHA, we conducted multidisciplinary studies that reviewed and integrated geological, seismological and geophysical data with two main objectives: 1) improving earthquake location to obtain reliable seismicity patterns, and performing tomographic analyses to constrain the structural-geological interpretation; 2) gaining a deeper understanding of the 3D setting of seismogenic faults and of the processes involved in earthquake generation (e.g. by understanding the role of underground fluids).
Our ultimate goal was to provide new data and observations to improve seismic hazard assessment in these areas and enable stakeholders to take action for seismic risk mitigation.

2. Montello area

The Montello area in the Veneto region of northeastern Italy is a tectonically active zone at the front of the eastern Southern Alps, but most of the active faults are hidden beneath the sediments of the Venetian plain.
Since 2012, the Collalto seismic network (RSC) has been recording microseismicity in the region, primarily to monitor an underground gas storage facility [Priolo et al., 2015]. While no man-made seismicity has been detected until now, the network has revealed very valuable to get new insights into the seismotectonics of the area, thanks to the detailed and high-quality seismic catalog it has provided over the years. Indeed, the spatial distribution of natural microearthquakes recorded clearly depicted the geometry of the Montello thrust, as a plane gently dipping to the northwest, locally interrupted by high-angle faults [Romano et al., 2019]. Moreover, in August 2021, an extremely productive sequence of 407 microearthquakes occurred near Refrontolo (TV) at a depth of 9 km, involving a southeast-dipping zone, well

distinct from the main Montello thrust. The swarm was not felt by the population (M_{Lmax} 2.5) and was almost invisible for the national and regional seismic networks, but thanks to the high-resolution data recorded by RSC, it indicated clear ruptures on steep, pre-stressed, antithetic faults and significant aseismic creep in the Montello thrust system, providing important insights into the regional seismic behavior [Peruzza et al., 2022; 2023].

In the frame of the NASA4SHA PRIN project, the seismic catalog of RSC, and specifically the best constrained locations of earthquake occurred from January 2012 to October 2022 (Figure 1), has been used for carrying out both the local earthquake and the seismic attenuation tomography of the study area, and visualizing the local crustal structure in terms of seismic velocities or scattering and absorption contrasts.

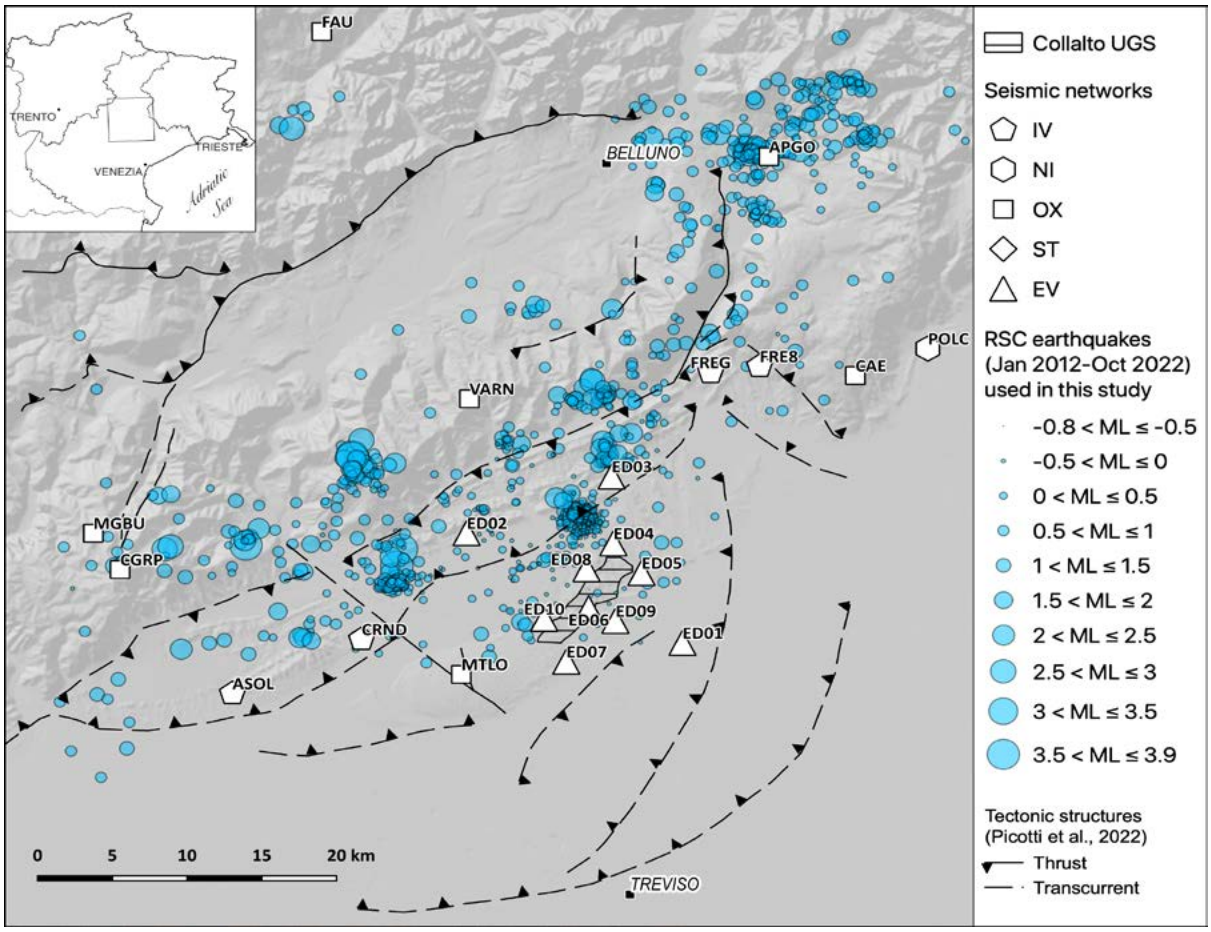

Figure 1 Map of the Montello area monitored by the RSC (network code EV) with the earthquake dataset (light blue circles) used for carrying out two types of tomography of the crustal structure. The seismic events are sized according to their magnitude; the small white polygons are the seismic stations represented according to their network; the dashed polygon in the middle is the Collalto underground gas storage; the dashed or solid black lines are the buried or exposed faults according to Picotti et al. [2022].

Local earthquake tomography (LET) was performed with an improved version of Cat3D software, which essentially uses an iterative approach to determine earthquake hypocenters and to estimate P- and S-wave velocities by inverting travel-time data in multi-parametric 3D models. The upgrade of the software consists of a time residual analysis after each tomographic step within the iterative process, which provides more accurate estimates of hypocentral depth, the most critical parameter in the location estimations [Moratto et al., 2025]. A local velocity

model for P wave, and imaging of the VP/VS can be obtained. Several tests on the first results have been done, but some sensitivity analyses are still ongoing.
Seismic attenuation tomography (SAT) was performed with the MuRAT3.0 code [De Siena et al., 2014], which creates models of scattering and absorption considering different segments of the seismogram; in particular, the scattering uses the so called peak delay, i.e. the time last between the earthquake origin time and the maximum peak of the seismogram envelope, while the absorption uses the inverse coda quality factor evaluated through the envelope decay of the coda waveform. We recall that seismic wave scattering provides a diagnostic measure of the degree of rock fracturing, as it is strongly influenced by heterogeneities associated with crack density and orientation. In contrast, seismic wave absorption is predominantly controlled by the presence and distribution of fluids within the pore space, reflecting fluid–rock interactions at the microscopic scale.
Therefore, SAT is an effective geophysical method for imaging geological structures, particularly useful in detecting rock melts, fractures, and strain conditions. While widely applied in volcanic environments due to its sensitivity to fluids, experimental validation of this sensitivity remains limited. Talone et al. [2024; 2025a] apply SAT in the Montello area with the goals of validating the method using a known fluid-rich environment (natural gas reservoir), and of producing the first multi-scale attenuation model of the area. The results were interpreted alongside geological and seismic data [Romano et al., 2024; Talone et al., 2025b], in the light of the recent work done by Picotti et al. [2022], and key findings are:

1. regionally, the models confirm known tectonic structures (e.g., Montello thrust) and reveal additional minor faults;
2. locally, high-absorption zones correspond to methane-rich areas, confirming the method's fluid sensitivity;
3. high-attenuation zones at depth correlate inversely with seismicity, suggesting deep fluids may influence tectonic behavior.

These results support the potential for more comprehensive, multi-disciplinary studies of seismotectonic in the region. On this basis, the authors are currently working on a preliminary 3D structural-geologic model of the region, developed with Geomodeller software, and incorporating all available geological and geophysical data.

3. Socchieve area

On March 27, 2024, a magnitude 4.6 earthquake occurred near the village of Socchieve in the Friuli region of northeastern Italy. It was the strongest earthquake in the last 22 years in this region [1], which was hit by a magnitude M6.4 quake in 1976 (Figure 2). In the following two months, the Socchieve event was followed by around 100 aftershocks ($0.1 \leq M \leq 3.4$), which were recorded by the OGS seismic monitoring system [2].
Due to the importance of the event and thanks to the very good coverage of the seismic networks currently in operation, a detailed analysis of the sequence was carried out to determine the geometry and kinematics of the responsible fault, and to better understand the seismotectonic context [Romano et al., 2025].
The most important steps were: 1) integration of data from seismic and accelerometric stations, including those not normally used for seismic monitoring of the area; 2) manual picking of P- and S-wave arrival times and first-motion polarities; 3) application of absolute location algorithm (NonLinLoc) with a local 3D velocity model, and relative location method (HypoDD) for a highly accurate estimation of the hypocentral depth; 4) calculation of the focal mechanisms (using the FPFIT and SKHASH codes) and solution of the moment tensor for the largest events.

Subsequently, the geometric and kinematic relationship between the earthquake sequence and the known tectonic structures reported both in the ITHACA catalogue [ITHACA Working Group, 2019] and in the Database of the Active Faults of FVG Region [Marchesini et al., 2023] in the study area was investigated by combining the 3D mapping of the relocated seismicity with fault plane solutions.
The Socchieve sequence delineates a very clear, high angle, transpressive structure, and although no direct relationship to the known faults has yet been found, the causative fault is compatible with the seismotectonic setting of the area.

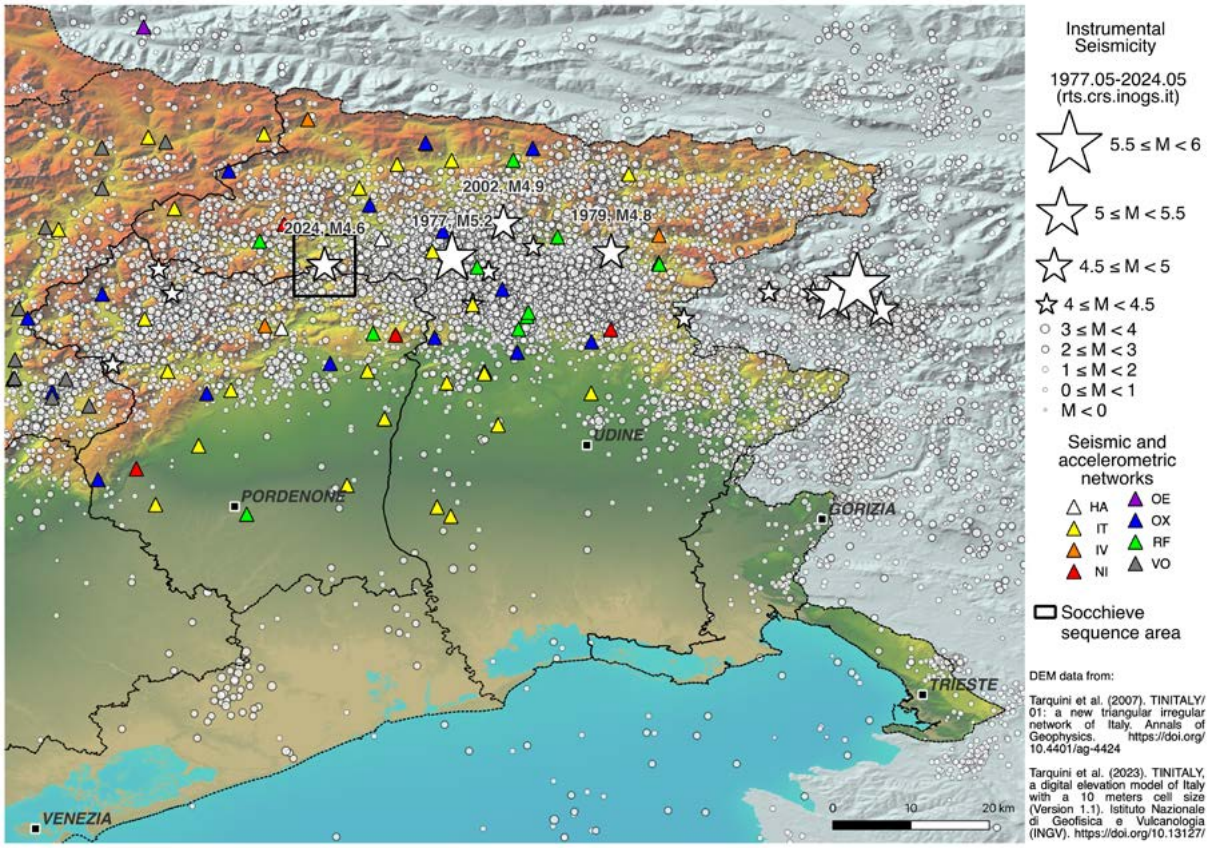

Figure 2 Map of the Friuli-Venezia Giulia region representing the instrumental seismicity occurred from 1977 to November 2024, the Socchieve sequence area (black rectangle), and the seismic and accelerometric networks used in this study.

4. Conclusion and outlook

These studies collectively emphasize the importance of multi-disciplinary, multi-scale imaging in active tectonic regions, and in particular:

- fault geometry and segmentation in the ESA can now be constrained with greater confidence, aiding seismic hazard models;
- seismic attenuation tomography proves effective in delineating potential fault damage zones, especially useful for monitoring gas storage infrastructure;
- the Socchieve sequence underlines the importance of monitoring seismically quiet regions that may host blind or unknown faults.

Future research may pave the way for improved hazard resilience and resource management.

Acknowledgments

The research activities here described have been carried out in the frame of the Italian PRIN Project (Research Projects of National Interest) “Fault segmentation and seismotectonics of active thrust systems: the Northern Apennines and Southern Alps laboratories for new Seismic Hazard Assessments in northern Italy (NASA4SHA)”, PI R. Caputo, UR Responsible L. Peruzza, and they are related to the Work Package 1 “Tectonic constraints at depth”.

References

De Siena, L., Thomas, C., and Aster, R., (2014). *Multi-scale reasonable attenuation tomography analysis (MuRAT): An imaging algorithm designed for volcanic regions.* Journal of Volcanology and Geothermal Research, 277, 22–35. https://doi.org/10.1016/j.jvolgeores.2014.03.009

ITHACA Working Group (2019). *ITHACA (ITaly HAzard from CApable faulting), A database of active capable faults of the Italian territory*. Version December 2019. ISPRA Geological Survey of Italy. Web Portal http://sgi2.isprambiente.it/ithacaweb/Mappatura.aspx

Marchesini, A., Poli, M.E., Bonini, L., Busetti, M., Piano, C., Dal Cin, M., et al., (2023). *Linee guida per l’utilizzo della banca dati georiferita delle faglie attive della Regione Friuli Venezia Giulia.* Servizio Geologico - Regione Autonoma Friuli Venezia Giulia, 64 pp.

Moratto, L., Böhm, G., and Romano, M.A., (2025). *Use of time residuals to improve Local Earthquake Tomography in the Montello area (Southeastern Alps, Italy)*. IAGA/IASPEI Joint Scientific Meeting 2025, Lisbona, 31 August-5 September 2025. https://hdl.handle.net/20.500.14083/44226

Peruzza, L., Romano, M.A., Guidarelli, M., Moratto, L., Garbin, M., and Priolo, E., (2022). *An unusually productive microearthquake sequence brings new insights to the buried active thrust system of Montello (Southeastern Alps, Northern Italy).* Front. Earth Sci. 10:1044296. https://doi.org/10.3389/feart.2022.1044296

Peruzza, L., Romano, M.A., Guidarelli, M., Moratto, L., Garbin, M., and Priolo, E., (2023). *A sneak peek under the Prosecco vineyards*. Atti del 41° GNGTS, Bologna, 7-9 febbraio 2023. https://hdl.handle.net/20.500.14083/30064

Picotti, V., Romano, M.A., Ponza, A., Guido, F.L., and Peruzza, L., (2022). *The Montello Thrust and the Active Mountain Front of the Eastern Southern Alps (Northeast Italy).* Tectonics, 41, e2022TC007522. https://doi.org/10.1029/2022TC007522

Priolo, E., Romanelli, M., Plasencia Linares, M.P., Garbin, M., Peruzza, L., Romano, M.A., Marotta, P., Bernardi, P., Moratto, L., Zuliani, D., and Fabris, P., (2015). *Seismic Monitoring of an Underground Natural Gas Storage Facility: The Collalto Seismic Network.* Seismological Research Letters, 86 (1), 109–123. https://doi.org/10.1785/0220140087

Romano, M.A., Peruzza, L., Garbin, M., Priolo, E., and Picotti, V., (2019). *Microseismic Portrait of the Montello Thrust (Southeastern Alps, Italy) from a Dense High-Quality Seismic Network*. Seismological Research Letters, 90 (4), 1502-1517. https://doi.org/10.1785/0220180387

Romano, M., Picotti, V., and Peruzza, L., (2024). *3D model of the Montello–Collalto area from geological, geophysical and seismological data*. Workshop CRUST 2024, Chieti, 23-25 giugno 2024. https://hdl.handle.net/20.500.14083/40403

Romano, M.A., Brondi P., Magrin A., et al. (2025). *Recent Seismic Activity in Friuli (NE Italy): The M4.6 Socchieve Earthquake Sequence and Its Preliminary Seismotectonic Interpretation*. Atti del 43° GNGTS 2025, Bologna, 11-14 febbraio 2025. https://ricerca.ogs.it/handle/20.500.14083/42925

Talone, D., Romano, M.A., De Siena, L., Guidarelli, M., Peruzza, L., Lavecchia, G., and de Nardis, R., (2024). *Unveiling the characteristics of the eastern Southern Alps boundary thrust and the*

"Collalto Stoccaggio" gas storage with multi-scale attenuation tomography. Workshop CRUST 2024, Chieti, 23-25 giugno 2024. https://hdl.handle.net/20.500.14083/40404

Talone, D., Romano, M.A., De Siena, L., Guidarelli, M., Santulin, M., Peruzza, L., Lavecchia, G., and de Nardis, R., (2025a). *Multi-scale attenuative imaging of the Collalto UGS area and the Montello thrust system (eastern Southern Alps, Italy)*. Atti del 43° GNGTS 2025, Bologna, 11-14 febbraio 2025. https://hdl.handle.net/20.500.14083/42924

Talone, D., Romano, M.A., De Siena, L., Guidarelli, M., Santulin, M., Peruzza, L., Lavecchia, G., and de Nardis, R., (2025b). *Underground gas storage as benchmark for seismic attenuation tomography in a tectonically complex region (north-eastern Italy)*. Geophysical Research Letters, 52, e2025GL117956. https://doi.org/10.1029/2025GL117956

Sitography

[1] http://www.crs.inogs.it/bollettino/RSFVG
[2] https://terremoti.ogs.it/

A combined regional velocity field for Northern Italy: new insights into strain accumulation in eastern Southern Alps and Northern Apennines

Alessandro Galvani[1], Daniele Cheloni[*,1], Grazia Pietrantonio[1], Matteo Albano[1], Carla Braitenberg[2], Fabio Brighenti[3,4], Francesco Carnemolla[4,5], Giorgio De Guidi[4,5], Roberto Devoti[1], Salvatore Giuffrida[4,5], Andrea Magrin[6], Davide Russo[3,4], Alberto Pellegrinelli[3], Giuliana Rossi[6], Salvatore Stramondo[1], Lavinia Tunini[6], and David Zuliani[6]

[1]Istituto Nazionale di Geofisica e Vulcanologia - INGV, Rome, Italy
[2]Università di Trieste, Dipartimento di Matematica e Geoscienze, Trieste, Italy
[3]Università di Ferrara, Dipartimento di Fisica e Scienze della Terra, Ferrara, Italy
[4]Centro Interuniversitario per la Sismotettonica 3D con Applicazioni Territoriali (CRUST), Chieti, Italy
[5]Università di Catania, Dipartimento di Scienze Biologiche Geologiche e Ambientali, Catania, Italy
[6]Istituto Nazionale di Oceanografia e di Geofisica Sperimentale - OGS, Trieste, Italy

Corresponding author: daniele.cheloni@ingv.it

Introduction

Understanding the seismogenic potential of major active thrust faults in the eastern Southern Alps (SA) and Northern Apennines (NA) is essential for assessing seismic hazard in northern Italy, a region characterized by high population density, critical infrastructures, and significant economic assets. Even moderate earthquakes in this area can cause substantial damage, emphasizing the need for detailed knowledge of the active tectonic structures and their potential to generate large seismic events. The active tectonics of the eastern SA is governed by the convergence between the Adriatic and Eurasian plates, with present-day rates increasing from west to east, reaching up to ~2 mm/yr in the Friuli region [*e.g.*, D'Agostino et al., 2005; Devoti et al., 2017; Tunini et al., 2024]. This convergence is accommodated by continental collision in the eastern SA, which marks the northeasternmost boundary of the active Alpine orogen. The region is characterized by active thrust faulting, actively growing anticlines, and drainage anomalies along the mountain front [*e.g.*, Galadini et al., 2005].

Although historical seismicity along the eastern SA front is relatively sparse, several damaging events have been documented [Rovida et al., 2020] (Figure 1). These include the 1695 M6.5 Asolo earthquake associated with the Bassano-Cornuda thrust [*e.g.*, Burrato et al., 2008]; the 1873 M6.3 Bellunese and the 1936 M6.1 Bosco del Cansiglio events associated with the Polcenigo-Maniago thrust system [*e.g.*, Burrato et al., 2008]; and the 1976 M6.4 Friuli earthquake linked to the Susans-Tricesimo thrust system [*e.g.*, Patricelli et al., 2022]. Two of the strongest events, those of 1348 (M7.0) and 1511 (M6.9), have more uncertain locations. The 1348 event has been attributed to the Periadriatic Thrust [*e.g.*, Galadini et al., 2005], while the 1511 sequence likely involved the intersection of the Alpine and Dinaric systems [*e.g.*, Falcucci et al., 2018]. The seismogenic potential of the area west of the 1976 sequence remains uncertain, due to the absence of documented M>6 earthquakes in the historical catalog [Rovida et al., 2020]. These observations have led some authors to propose the existence of seismic gaps along some segments of the eastern SA external thrust front [*e.g.*, Galadini et al., 2005; Cheloni et al., 2014]. A revision of the historical data is, however, ongoing, opening to new interpretations of the seismic potential of this area [*e.g.* Camassi et al., 2024; Barbano et al., 2025].

In the Northern Apennines, active shortening is accommodated by an external fold-and-thrust system buried beneath thick Pliocene-Quaternary sediments, the Ferrara Arc, which

absorbs approximately 2 mm/yr of active shortening according to recent GNSS data [*e.g.*, Devoti et al., 2017]. The region exhibits relatively low seismicity, with only a few moderate historical events [Rovida et al., 2020], such as the 1570 M5.8 Ferrara earthquake, the 1996 M5.4 event, and the 2012 M6.1 and M6.0 Emilia sequence.

Previous geodetic studies in the eastern SA have estimated locking depths around 10 km and slip-rates between 1 and 2.4 mm/yr, with significant along-strike variability in fault coupling, ranging from highly locked segments (*e.g.*, Polcenigo-Maniago) to weakly coupled or creeping zones (*e.g.*, Cansiglio) [D'Agostino et al., 2005; Cheloni et al., 2014; Serpelloni et al., 2016; Anderlini et al., 2020]. In contrast, the NA remains less well characterized. While GNSS data indicate shortening rates of ~2 mm/yr across the thrust front [Serpelloni et al., 2016; Devoti et al., 2017], detailed knowledge of individual segment behavior is still limited.

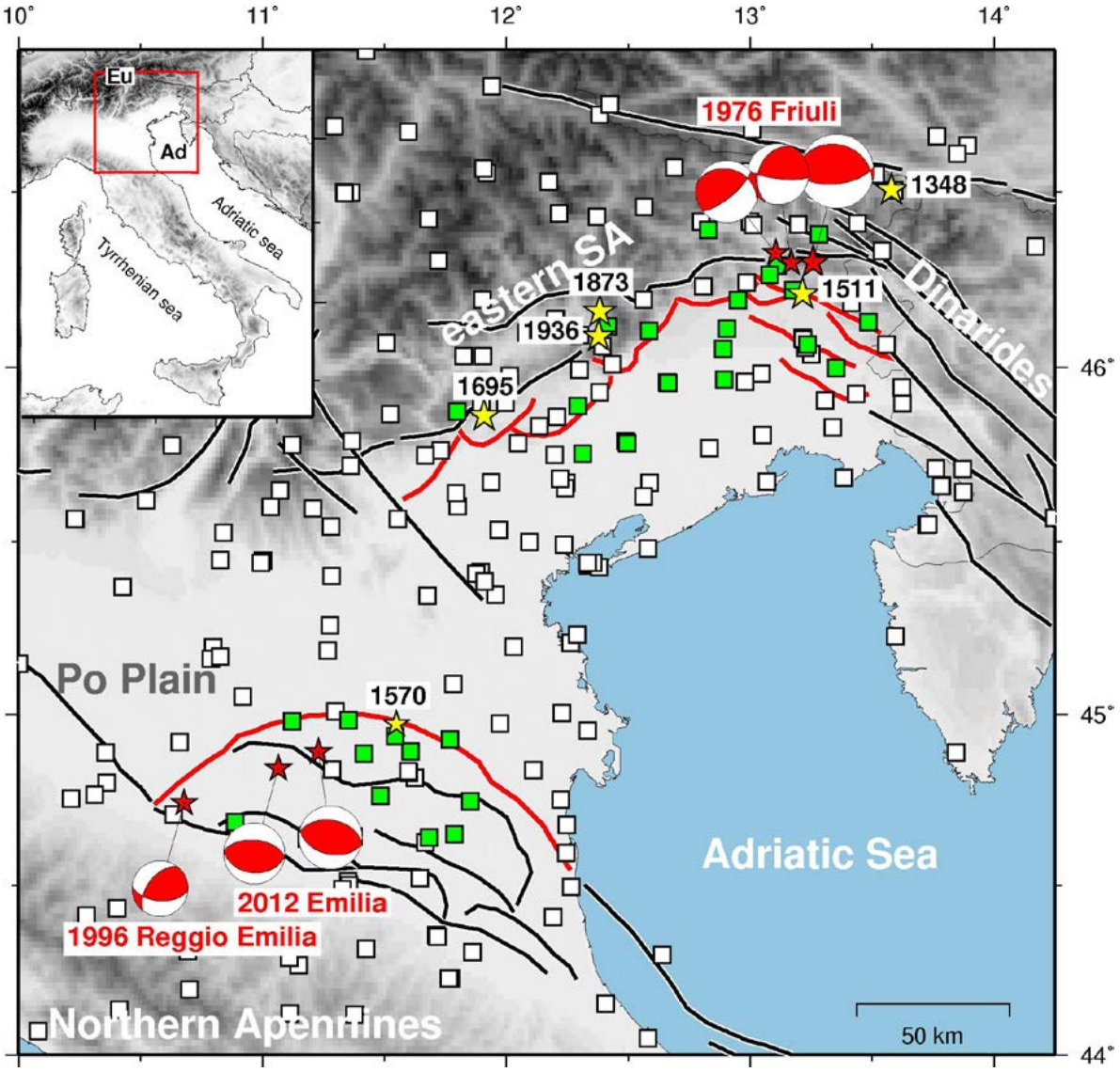

Figure 1 Simplified seismotectonic setting of the study region. The solid lines represent the main fault segments of the eastern Southern Alps, Dinarides and Northern Apennines. Solid red lines mark the main active thrust faults selected for investigation within the NASA4SHA project. Yellow stars indicate the epicenters of major historical earthquakes, with labeled event dates [Rovida et al., 2020]; red stars represent the location of the major instrumental seismic events [Aoudia et al., 2000; Selvaggi et al., 2001; Scognamiglio et al., 2012] and their moment tensor solutions. The white squares are the locations of permanent GNSS sites, while the green ones are the locations of the re-surveyed IGM95 vertices.

This study is part of the PRIN 2020 NASA4SHA Project (*Fault segmentation and seismotectonics of active thrust systems: the Northern Apennines and Southern Alps laboratories for New Seismic Hazard Assessment in northern Italy*). The project aims to define the geometry and kinematics of the main compressive fault systems in the eastern Southern Alps and Northern Apennines, through a multidisciplinary approach that integrates geological, geophysical, seismological, palaeoseismological, and geodetic methods at both regional and local scales. In the present note, we focus on quantifying strain accumulation along key compressive structures using both continuous and newly acquired discontinuous Global Navigation Satellite Systems (GNSS) observations. In particular, we employ a GNSS velocity solution for northern Italy that combines two independent datasets from INGV (Istituto Nazionale di Geofisica e Vulcanologia) and OGS (Istituto Nazionale di Oceanografia e di Geofisica Sperimentale). In addition, we measured selected stations of the IGM95 (Istituto Geografico Militare) geodetic network along local transects orthogonal to the main thrust systems. By analyzing interseismic GNSS velocities, we aim to resolve localized patterns of strain accumulation, providing insights into ongoing seismotectonic processes and identifying segments that may be more prone to future significant earthquakes.

GNSS Data and velocity field

We analyzed data from continuous GNSS stations across the entire study area, sourced from the RING (Rete Integrata Nazionale GPS) and FReDNet (Friuli Regional Deformation Network) networks, which are managed by INGV and OGS, respectively, as well as from other permanent GNSS networks managed by various institutions. Additionally, we re-surveyed selected vertices (29 benchmarks) of the IGM95 geodetic network (Figures 1 and 2), focusing on local transects that are orthogonal to the main compressive structures. These benchmarks were established in the early 1990s and re-measured during densification campaigns between 2001 and 2004, providing long time spans of observations.

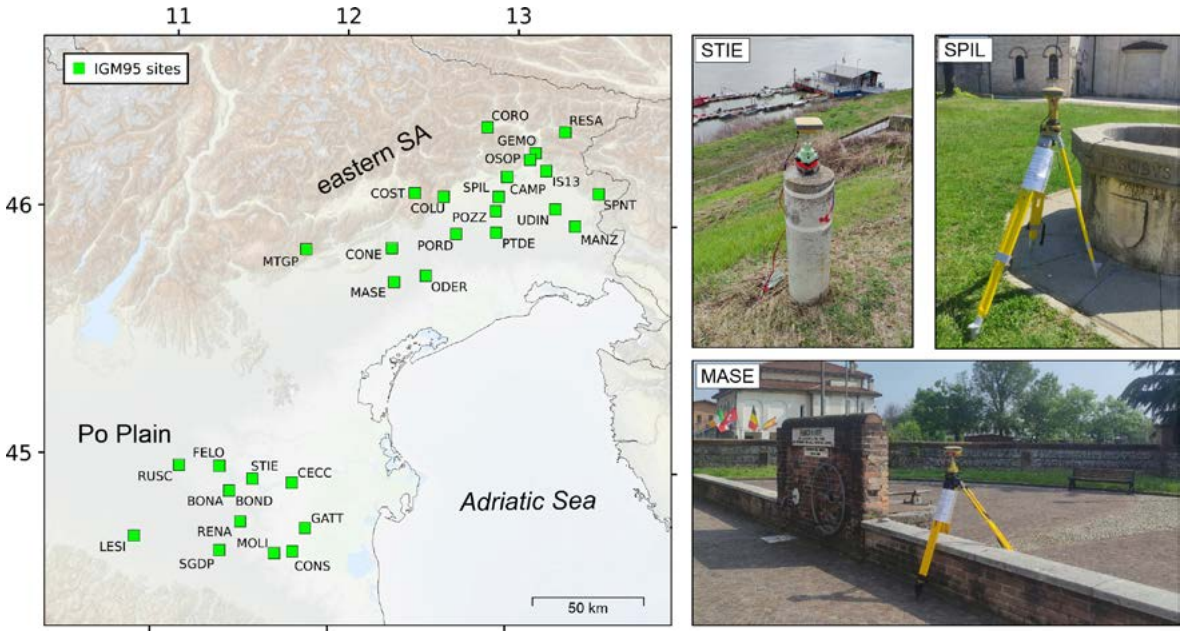

Figure 2 Re-surveyed IGM95 vertices. On the left, a map of the GNSS stations from the IGM95 network (green squares). On the right, photographic examples of IGM95 benchmarks that were re-occupied during the survey.

We then compared the new discontinuous GNSS observations with previous measurements made by IGM (Istituto Geografico Militare) at the same vertices. The reoccupation of IGM95 benchmarks enables a kinematic assessment of structures belonging to the Emilian Apennine and South-Alpine tectonic systems. The IGM95 network was created for cartographic and topographic applications, for this reason most of the IGM95 beckmarks do not follow restrictive geodetic requirements for geophysical applications (duration, stability, use of tripod [Anzidei et al., 2008]. In our opinion, these aspects are probably compensated for by the robust long-term velocity estimates (30 years as of 2023), which are derived from a benchmark network selected according to strict criteria [De Guidi et al., 2017]. The selection prioritized: a) location relative to active structures, b) installation prior to the year 2000 to ensure long time series, c) local geotechnical and anthropogenic stability, and d) a high number of previous reoccupations. Field surveys were conducted using dual-frequency geodetic GNSS receivers, with observation sessions of at least 24 hours per site to ensure high-precision positioning. The data were processed by Gamit-Globk software using double-difference phase observation with ambiguity resolutions, precise orbits and adopting the absolute phase center model for receiver and satellite antenna. The preliminary velocity field is expressed in the IRTF14 reference frame with respect to the Eurasian plate [Altamimi et al., 2017], producing a consistent time series that extends from 1994 to present.

In this study, we present the regional GNSS velocity field publicly available on Zenodo [https://doi.org/10.5281/zenodo.17120299], which was derived by combining three distinct velocity fields: i) the OGS velocity solution [Tunini et al., 2024]; ii) the INGV velocity solution, produced following the methodology of Devoti et al. [2017] and publicly available on Zenodo [https://doi.org/10.5281/zenodo.17107303], both of which encompass the northern sector of Italy; and iii) a velocity field derived from the re-measurement of selected vertices of the IGM95 geodetic network [Carnemolla et al., 2024]. The resulting velocity field is expressed in the ITRF2014 reference frame, with respect to the Eurasian plate [Altamimi et al., 2017]. The combination procedure follows the method outlined in Devoti et al. [2017], employing a linear least-squares approach. This method treats each velocity field as a sample of the true velocity field, with the combined velocity field providing the best estimate of the true velocities.

The horizontal velocity field shown in Figure 3a highlights two main deformation zones in Northern Italy: a NNE-oriented shortening of approximately 2-3 mm/yr across the Ferrara Arc, which borders the Po Plain in the outer sector of the Northern Apennines (NA), and a N-directed shortening of about 1.5-2 mm/yr along the southern front of the eastern Southern Alps (SA). The vertical velocities (Figure 3b) show a slight uplift in the northern part of the eastern SA in agreement with previous, independent observations [Areggi et al., 2023], and confirm the well-known subsidence in the eastern Po Plain. Despite the limited redundancy of the discontinuous IGM95 data, the horizontal velocities derived from these benchmarks are consistent with the solutions from the permanent networks (yellow arrows in Figure 3a).

Strain-rate and dislocation modelling

In order to estimate the strain-rate field, the slip rate and locking depth of the main compressive structures along the central-eastern SA and NA, we analyze the combined GNSS data, which provides an improved spatial coverage of both near- and far-field areas compared to previous studies [e.g., D'Agostino et al. 2005; Cheloni et al. 2014; Serpelloni et al. 2016; Devoti et al. 2017], also due to the integration of discontinuous IGM95 benchmarks that densify the permanent network. Strain accumulation is assessed through a two-step approach. First, we estimate the strain-rate field using geodetic data; subsequently, we apply dislocation modeling to infer interseismic locking depths and slip-rates along selected fault segments. The strain-rate

was obtained by applying the optimal interpolation of the spatially discretized geodetic data algorithm [Shen et al., 2015]. This method allowed to generate a continuous strain-rate field of the study area. The GNSS-derived strain-rate field clearly delineates the major fault zones in northern Italy, such as the active front of the eastern SA, and the Ferrara Arc in the external part of the NA. In addition, in the easternmost sector of the study area, strain-rate also appears to be high around the Dinaric strike-slip fault systems in western Slovenia (Figure 4). Notably, the direction of the compressive axis is perpendicular to the major thrust faults in the eastern SA and NA (Figure 4).

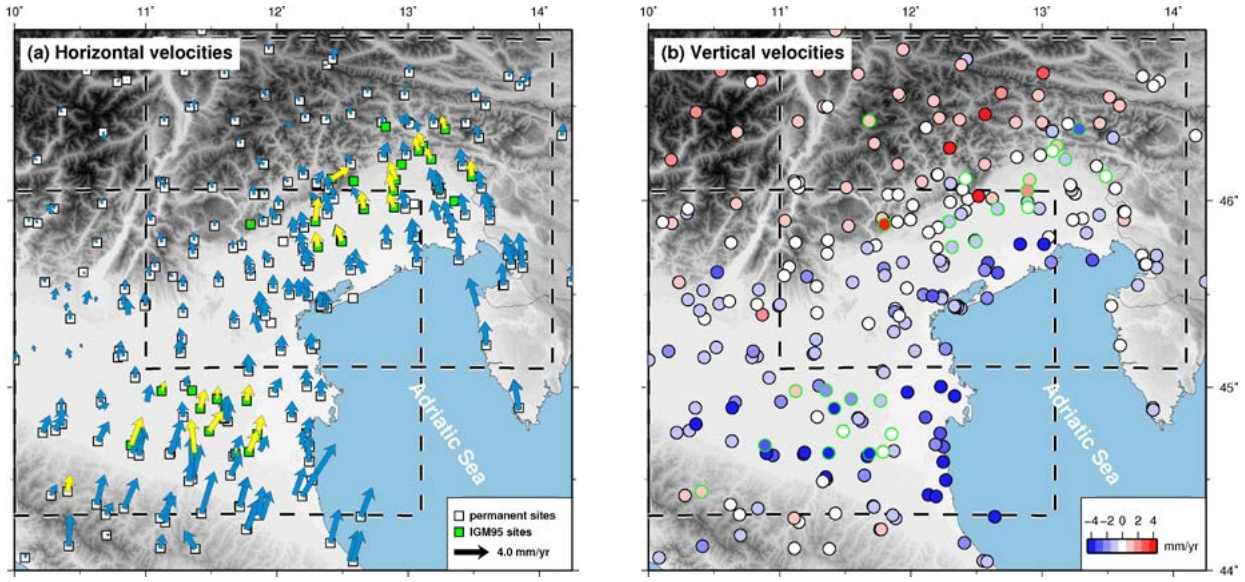

Figure 3 Map of the combined GNSS velocity field. (a) Horizontal GNSS velocities in the Eurasian-fixed reference frame. The white squares represent the location of permanent sites, while the green ones are the locations of the re-surveyed IGM95 vertices, with estimated velocities (blue and yellow arrows, respectively). The dashed boxes represent the areas of Figures 4 and 5. (b) Vertical velocities of the combined solution: the circles with the green borders represent the re-surveyed IGM95 vertices. Error ellipses are not shown here for clarity of the figure.

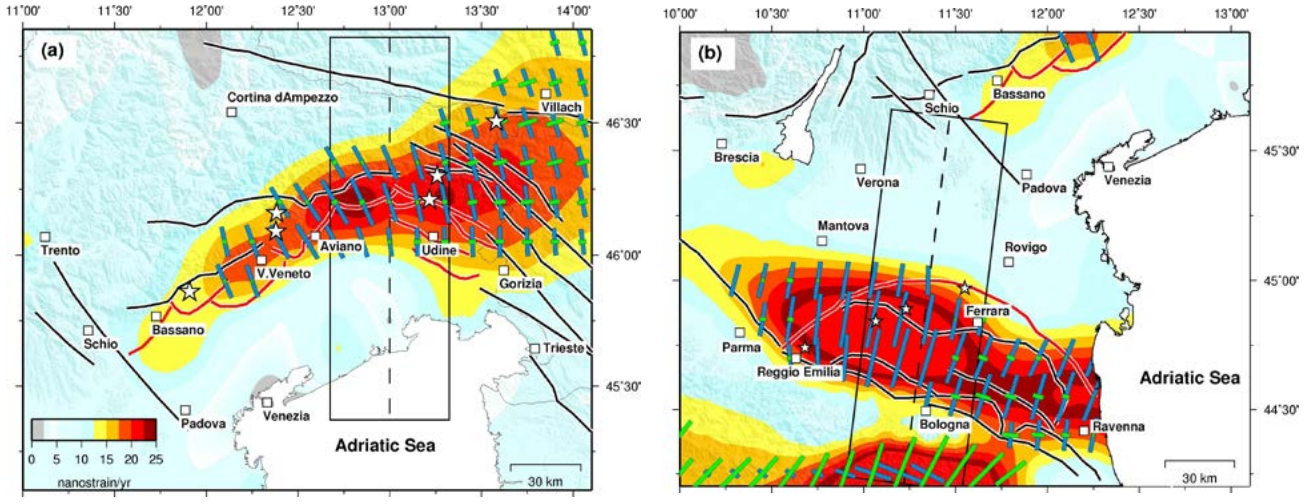

Figure 4 Map of the second invariant of the strain-rate tensor. (a) Strain-rate field along the eastern SA and part of the Dinarides. (b) Strain-rate field along the NA. Blue (compressional) and green (extensional) bars represent the principal strain directions. White stars indicate the locations of major earthquakes (see Figure 1 for details).

High strain-rates (25-40 nanostrain/yr) are observed across the southern front of the eastern SA (Figure 4a) and across the Ferrara Arc in the external part of the NA (Figure 4b), in agreement with previous studies [*e.g.*, Bennett et al., 2012; Serpelloni et al., 2016]. This is consistent with the fact that the convergence between the Adriatic and Eurasian plates is not purely compressional but has a significant oblique component. Along the southern front of the eastern EA, the strain-rates vary, decreasing towards W-SW, and transitioning to a transpressional regime towards E-NE in correspondence with the intersection of the Alpine and Dinarides systems. Along the NA, the maximum strain-rates are linked to the Ferrara Arc.
In the second step, we applied dislocation modelling (i.e., creeping dislocations in an elastic half-space [Okada, 1992]) to estimate interseismic slip-rate and locking depth along two selected segments of the eastern SA and NA (Figure 5). In order to interpret the crustal motion across the active fronts of the central-eastern SA and NA, we rotate the GNSS velocity field in a reference frame defined by the minimization of the residual horizontal velocities of stations located on the Venetian-Friulian plane lying therefore far from the active SA and NA front. Accordingly, the motion of stations across the external thrust front of the eastern SA is consistent with an average north-directed shortening of 1-2 mm/yr along the mountain front. Similarly, stations across the Ferrara-Romagna Arc in the NA exhibit a shortening rate of 2-3 mm/yr.
We then constructed two profiles across the study area, perpendicular to the major thrusts, by projecting the velocity vectors within a 50 km-wide swath. These two profiles, extending over a length of 160 km, were selected because they both cross areas affected by the most recent seismic sequences within the study region: the 1976 Friuli sequence (M6.4) and the 2012 Emilia sequence (M6.1 and 6.0). The observed horizontal velocities were compared with the surface deformation resulting from the slip on a two-dimensional planar dislocation, locked at a specific depth. Our analysis indicates that, in the eastern SA the thrust systems in the Friuli area are subjected to aseismic slip at the base of the brittle section of the faults at approximately 8 km-depth (Figure 5, top panels). Similarly, in the NA, the investigated segment of the Ferrara Arc presents a locking depth of approximately 9 km (Figure 5, bottom panels), aligning closely with the coseismic slip distribution of the 2012 Emilia earthquake [*e.g.* Cheloni et al., 2016].

Discussion and concluding remarks

Our integrated geodetic analysis provides new constraints on the present-day deformation patterns and seismogenic behavior of major thrust faults in the eastern Southern Alps and Northern Apennines. The GNSS velocity and strain-rate fields clearly delineate zones of active shortening across both regions, revealing peak strain accumulation along the southern front of the eastern SA and the Ferrara Arc. Dislocation modeling along representative transects confirms that these fault systems are partially locked, with estimated locking depths around 8-9 km and slip-rates consistent with geodetic shortening. These findings suggest that the investigated thrust segments are accumulating elastic strain and may be capable of generating moderate to large earthquakes, as exemplified by the 1976 Friuli and 2012 Emilia sequences. Our results support the existence of active and potentially hazardous fault zones in areas with sparse historical seismicity, highlighting the importance of geodetic data for identifying seismic gaps and refining seismic hazard assessments in northern Italy.
Future work will expand this analysis to include additional transects across other key segments of the thrust fronts, in order to better characterize along-strike variations in fault coupling and improve the resolution of seismic hazard models at the regional scale.

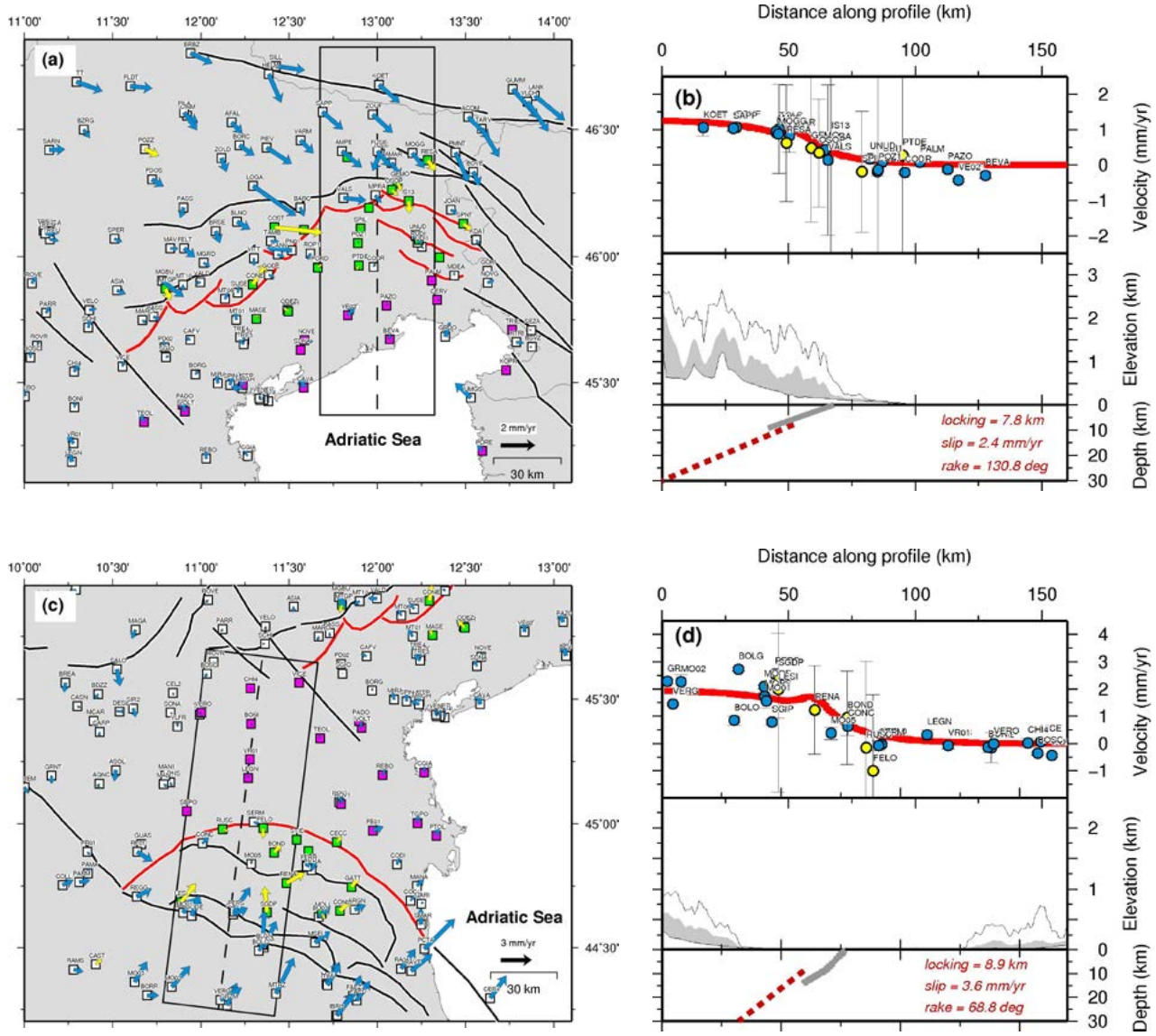

Figure 5 GNSS velocity field expressed in the Adria reference frame. (a, c) Estimated velocities at continuous (blue arrows) and discontinuous (yellow arrows) GNSS sites in the eastern Southern Alps (a) and Northern Apennines (c). Violet squares mark the sites used to define the local reference frame. Boxes highlight velocities projected perpendicular to the strike of the eastern SA front (Friuli region) and the Ferrara Arc, respectively. (b, d) Fault-perpendicular velocity profiles for the SA and NA regions: observed velocities (blue and yellow circles for continuous and discontinuous GNSS sites, respectively), synthetic velocities (solid red line), dislocation model results (dashed red line), topography, and coseismic fault planes from the 1976 Friuli [Cheloni et al., 2012] and 2012 Emilia [Cheloni et al., 2016] earthquakes (solid gray lines).

References

Altamimi, Z., Metivier, L., Rebischung, P., Rouby, H., and Collilieux, X., (2017). *ITRF2014 plate motion model.* Geophysical Journal International, 209 (3), 1906-1912. https://doi.org/10.1093/gji/ggc136

Anderlini, L., Serpelloni, E., Tolomei, C., De Martini, P.M., Pezzo, G., Gualandi, A., and Spada, G., (2020). *New insights into active tectonics and seismogenic potential of the Italian Southern Alps from vertical geodetic velocities.* Solid Earth, 11 (5), 1726–1737. https://doi.org/10.5194/se-11-1681-2020

Anzidei, M., Baldi, P., and Serpelloni, E., (2008). *The coseismic ground deformations of the 1997 Umbria-Marche earthquakes: a lesson for the development of new GPS networks*. Annals of Geophysics, 51 (2-3). https://doi.org/10.4401/ag-3029

Aoudia, A., Saraó, A., Bukchin, B., and Suhadolc, P., (2000). *The 1976 Friuli (NE Italy) thrust faulting earthquake: a reappraisal 23 years later*. Geophysical Research Letters, 27 (4), 573-576. https://doi.org/10.1029/1999GL011071

Areggi, G., Pezzo, G., Merryman Boncori, J.P., Anderlin, L., Rossi, G., Serpelloni, E., Zuliani, D. and Bonini, L., (2023). *Present-day surface deformation in North-East Italy using In-SAR and GNSS data*. Remote Sensing, 15 (1704). https://doi.org/10.3390/rs15061704

Barbano, M.S., Baranello, S., Rossetti, A., Castelli, V., Camassi, R., (2025). *Updating knowledge on 18th century Carnia earthquakes*. XLIII Convegno Nazionale del G.N.G.T.S., February 2025, Bologna.

Bennett, R.A., Serpelloni, E., Hreinsdottir, S., Brandon, M.T., Buble, G., Basic, T., Casale, G., Cavaliere, A., Anzidei, M., Marjonovic, M., Minelli, G., Molli, G. and Montanari, A., (2012). *Syn-convergent extension observed using the RETREAT GPS network, northern Apennines, Italy*. Journal of Geophysical Research, 117 (B4). https://doi.org/10.1029/2011JB008744

Burrato, P., Poli, M.E., Vannoli, P., Zanferrari, A., Basili, R., and Galadini F., (2008). *Sources of Mw 5+ earthquakes in northeastern Italy and western Slovenia: An updated view based on geological and seismological evidence*. Tectonophysics, 453, 157-176. https://doi.org/10.1016/j.tecto.2007.07.009

Camassi, R., Castelli, V., Serpelloni, E., and Pondrelli, S., (2024). *Reappraising the 25 February 1695 Asolano Earthquake*. Seismological Research Letters, 95 (1), 526–538. https://doi.org/10.1785/0220230238

Carnemolla, F., Brighenti, F., De Guidi, G., Di Pietro, A., Fabbri, P., Giuffrida, S., Magrin, A., Rossi, G., Russo, R., Tunini, L., and Zuliani, D., (2024). *Update of the Northern Apennines and Southern Alps velocity field from historical GNSS measurements to the '0 point'*. XLII Convegno Nazionale del G.N.G.T.S., Febbraio 2024, Ferrara.

Cheloni,D., D'Agostino, N., D'Anastasio, E., and Selvaggi, G., (2012). *Reassessment of the source of the 1976 Friuli, NE Italy, earthquake sequence from the joint inversion of high-precision levelling and triangulation data*. Geophysical Journal International, 190 (2), 1279-1294. https://doi.org/10.1111/j.1365-246X.2012.05561.x

Cheloni, D., D'Agostino, N., and Selvaggi, G., (2014). *Interseismic coupling, seismic potential, and earthquake recurrence on the southern front of the Eastern Alps (NE Italy)*. Journal of Geophysical Research, 119 (5), 4448-4468. https://doi.org/10.1002/2014JB010954

Cheloni, D., Giuliani, R., D'Agostino, N., Mattone, M., Bonano, M., Fornaro, G., Lanari, R., Reali, D., and Atzori, S., (2016). *New insights into fault activation and stress transfer between en echelon thrusts: The 2012 Emilia, Northern Italy, earthquake sequence*. Journal of Geophysical Research, 121 (6), 4742-4766. https://doi.org/10.1002/2016JB012823

D'Agostino, N., Cheloni, D., Mantenuto, S., Selvaggi, G., and Michelini, A., (2005). *Strain accumulation in the southern Alps (NE Italy) and deformation at the northeastern boundary of Adria observed by CGPS*. Geophysical Research Letters, 32 (19), 1-4. https://doi.org/10.1029/2005GL024266

De Guidi, G., *et al.*, (2017). *Brief communication: Co-seismic displacement on 26 and 30 October 2016 (Mw 5.9 and 6.5) - earthquakes in central Italy from the analysis of a local GNSS network*. NHESS 17, 1885-1892. https://doi.org/10.5194/nhess-17-1885-2017

Devoti, R. *et al.* (2017). *A Combined Velocity Field of the Mediterranean Region*. Annals of Geophysics, 60 (2), 1-16. https://doi.org/10.4401/ag-7059

Falcucci, E., Poli, M.E., Galadini, F., Scardia, G., Paniero, G., and Zanferrari, A., (2018). *First evidence of active transpressive surface faulting at the front of the eastern Southern Alps, northeastern Italy: insight on the 1511 earthquake seismotectonics*. Solid Earth, 9, 911-922.

https://doi.org/10.5194.se-9-911-2018

Galadini. F., Poli, M.E., and Zanferrari, A., (2005). *Seismogenic sources potentially responsible for earthquakes with M > 6 in eastern Southern Alps (Thiene-Udine sector, NE Italy).* Geophysical Journal International, 161, 739-762. https://doi.org/10.1111/j.1365-246X.2005.02571.x

Okada, Y., (1992). *Internal deformation due to shear and tensile faults in a half space.* Bulletin of the Seismological Society of America, 82, 1018-1040. https://doi.org/10.1785/BSSA0820021018

Patricelli, G., Poli, M.E., and Cheloni, D., (2022). *Structural Complexity and Seismogenesis: The Role of the Transpressive Structures in the 1976 Friuli Earthquakes (Eastern Southern Alps, NE Italy).* Geosciences, 12 (227): 1-31. https://doi.org/10.3390/geosciences12060227

Rovida, A., Locati, M., Camassi, R., Lolli, B., and Gasperini, P., (2020). *The Italian earthquake catalogue CPTI15.* Bulletin of Earthquake Engineering, 18 (7), 2953-2984. https://doi.org/10.1007/s10518-020-00818-y

Scognamiglio, L., *et al.*, (2012). *Pianura Padana Emiliana seismic sequence: Locations, moment tensors and magnitudes.* Annals of Geophysics, 55, 549-559. https://doi.org/10.4401/ag-6146

Selvaggi G., *et al.*, (2001). *The Mw = 5.4 Reggio Emilia 1996 earthquake: Active compressional tectonics in the Po Plain, Italy.* Geophysical Journal International, 144, 1-13. https://doi.org/10.1046/j.0956-540X.2000.01255.x

Serpelloni, E., Vannucci, G., Anderlini, L. and Bennett, R.A., (2016). *Kinematics, seismotectonics and seismic potential of the eastern sector of the European Alps from GPS and seismic deformation data.* Tectonophysics 688: 157-181. https://doi.org/10.1016/j.tecto.2016.09.026

Shen, Z.-K., Wang, M., Zeng. Y., and Wang, F., (2015). *Optimal Interpolation of Spatially Discretized Geodetic Data.* Bulletin of Seismological Society of America, 105 (4), 2117-2127. https://doi.org/10.1785/0120140247

Tunini, L., Magrin, A., Rossi, G., and Zuliani, D., (2024). *Global Navigation Satellite System (GNSS) time series and velocities about a slowly convergent margin processed on high-performance computing (HPC) clusters: products and robustness evaluation.* Earth System Science Data, 16, 1083-1106. https://doi.org/10.5194/essd-16-1083-2024

A thirty-year GNSS velocity field - an update for the Northern Apennines and Southern Alps thrust belts: towards a new deformation benchmark

Francesco Carnemolla[1,2], Fabio Brighenti[2,3], Giorgio De Guidi[1,2,*], Adriano Di Pietro[3], Paolo Fabris[4], Salvatore Giuffrida[1,2], Andrea Magrin[4], Giuliana Rossi[5], Davide Russo[2,3], Lavinia Tunini[4], and David Zuliani[4]

[1]Università di Catania, Dipartimento di Scienze Biologiche Geologiche e Ambientali, Catania, Italy
[2]Centro Interuniversitario per la Sismotettonica 3D con Applicazioni Territoriali (CRUST), Chieti, Italy
[3]Università di Ferrara, Dipartimento di Fisica e Scienze della Terra, Ferrara, Italy
[4]Istituto Nazionale di Oceanografia e di Geofisica Sperimentale - OGS, Trieste, Italy

Corresponding author: giorgio.deguidi@unict.it

Introduction

The relative convergence between the African and Eurasian plates drives active crustal shortening and seismicity across the Italian Peninsula, primarily accommodated by the thrust systems of the Northern Apennines and the Southern Alps [Galdini et al., 2005; Vannoli et al., 2015]. These regions have hosted moderate historical earthquakes, and a detailed understanding of their present-day deformation is a cornerstone of modern seismic hazard assessment [Carafa et al., 2015; DISS Working Group, 2021].
Global Navigation Satellite System (GNSS) data have been a key instrument to understand and quantify the ongoing kinematics in the Mediterranean region [Serpelloni et al., 2013; Devoti et al., 2017]. Continuous GNSS (cGNSS) networks, such as the RING (Managed by INGV) and FReDNet (managed by OGS) in Italy, provide valuable data and products to support geophysical studies in a regional or national scale. However, the spatial density of permanent stations can be insufficient to resolve strain localization across specific faults in terms of local scale [Cheloni et al., 2014]. Discrete GNSS measurements offer a cost-effective method to densify measurements at critical locations, thereby enhancing the spatial resolution of the strain rate field in a specific area [Bennet et al., 2003].
The IGM95 network, established between 1993 and 1995, was created for cartographic and topographic applications, for this reason most of the IGM95 beckmarks do not follow restrictive geodetic requirements for geophysical applications (duration, stability, use of tripod [Anzidei et al., 2008]) but in our opinion, this network represents a valuable, yet underexploited, geodetic heritage. While its monuments and observation sessions do not always meet the strictest geodetic standards for geophysical applications [Anzidei et al., 2008], the three-decade temporal baseline offers the possibility to obtain a valuable regional or local velocity field in the kinematic analysis.
This study, conducted within the PRIN 2020 NASA4SHA Project, aims to a) reanalyze the entire dataset from 29 IGM95 sites, including a new occupation; b) compute a refined, long-term velocity field for the Northern Apennines and Southern Alps; c) compare and validate this field to the existing cGNSS velocity field; d) derive an updated strain-rate pattern and establish a definitive geodetic “0-point” (epoch 2023.0) to serve as a benchmark for quantifying future ground deformation.

Data and Methods

We reoccupied 29 benchmarks of the IGM95 network (Figure 1), focusing on transects orthogonal to the main thrust fronts. Site selection prioritized monument stability, original establishment date (1993-1995), and a history of multiple occupations. In particular, these criteria were defined in De Guidi et al., 2017 and later refined in Pirrotta et al., 2021, useful to locate new geodetic benchmarks and to monitor the active deformation.

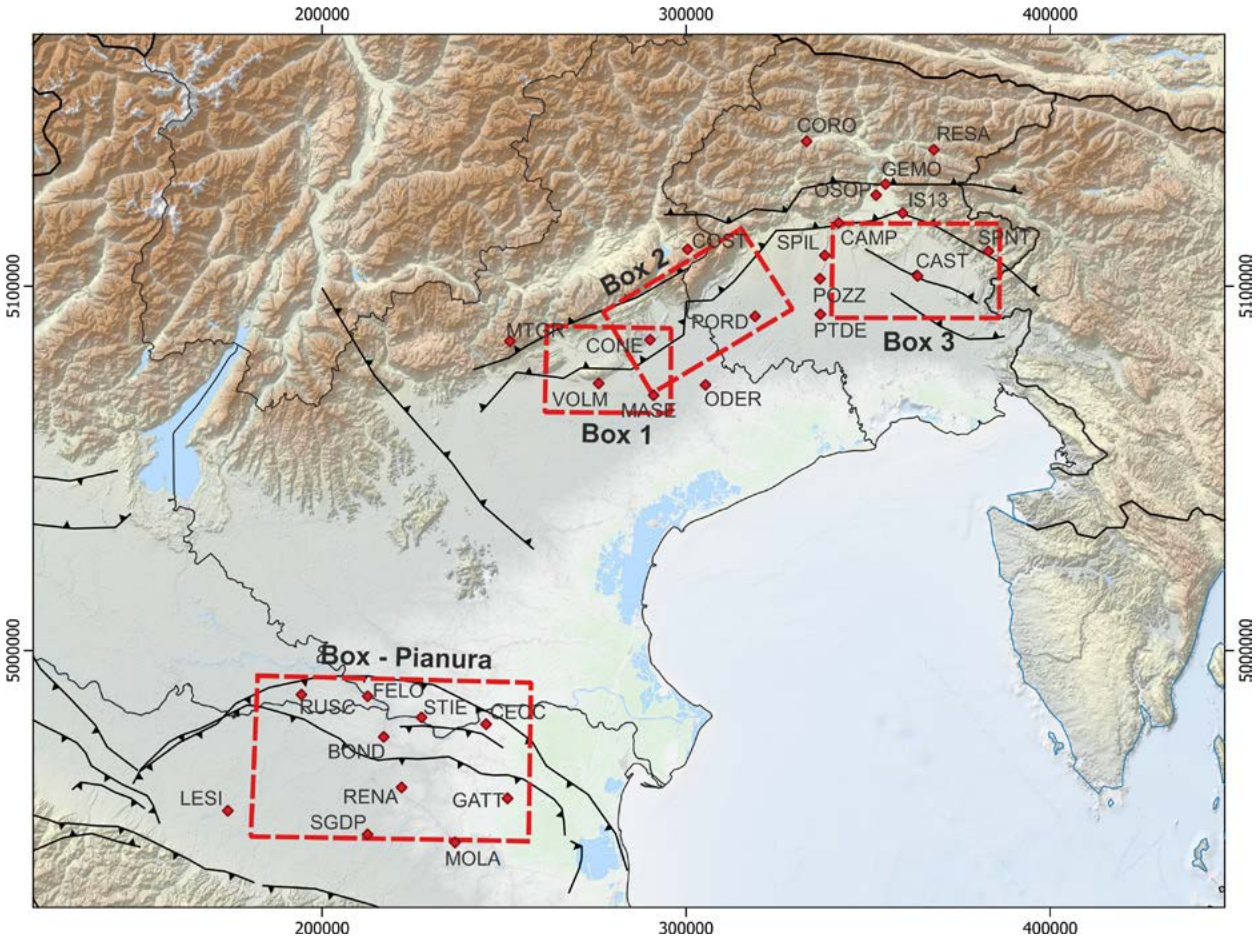

Figure 1 Map of the study area showing the 29 IGM95 points reoccupied during the 2023 campaigns.

However, these criteria could not always be met. Eight points (SPNT, PTDE, POZZ, MOLI, IS13, GEMO, CONS, CAMP) were built during a network densification phase (2000-2001), and four points (VOLM, PTDE, POZZ and MOLI) had only one prior occupation. The duration of previous occupation decreased over time, from an average of ~4.5 hours in 1993 to ~2 hours in campaigns from 2000 onward (Figure 2a). Furthermore, we used the tripods in most of the benchmarks, so the stability of the tripods is an important aspect to consider, in fact some benchmarks presented problems documented during our field campaigns (Figure 2b).

We processed all GNSS data from the historical campaigns and the 2023 survey using the GAMIT/GLOBK software (version 10.71) [Herring et al., 2018]. The processing strategy adhered to well established methodologies for high-precision geodetic analyses [Dong et al., 1998; Serpelloni et al., 2013].

We used double-difference phase observations with ambiguity resolution. Applied precise satellite orbits and clock products from the International GNSS Service (IGS). Used the absolute phase center model for both receiver and satellite antennas. Modeled tropospheric delay using

the VMF1 mapping function and estimated zenith path delays as stochastic parameters. Applied models for solid Earth tides, ocean tidal loading, and pole tide. Daily loosely constrained solutions from GAMIT were combined into a single network solution using GLOBK. The combined solution was aligned to the ITRF2014 reference frame [Altamini et al., 2017] by applying a seven-parameter Helmert transformation, using a subset of well-distributed IGS reference stations. Finally, velocities were expressed in the IRTF14 reference frame with respect to the Eurasian plate [Altamini et al., 2017].

Site positions from all campaign epochs were used to estimate linear velocities. We performed a critical analysis of the coordinate time series (Figure 3). Outliers were identified and removed based on a 2-sigma threshold. For sites showing non-linear behavior (*e.g.*, SGDP and PORD), we report velocities with caution, noting their potential unreliability for tectonic interpretation. The velocity uncertainties were derived from the full covariance matrix of the linear regression, providing a realistic estimate of the long-term velocity error.

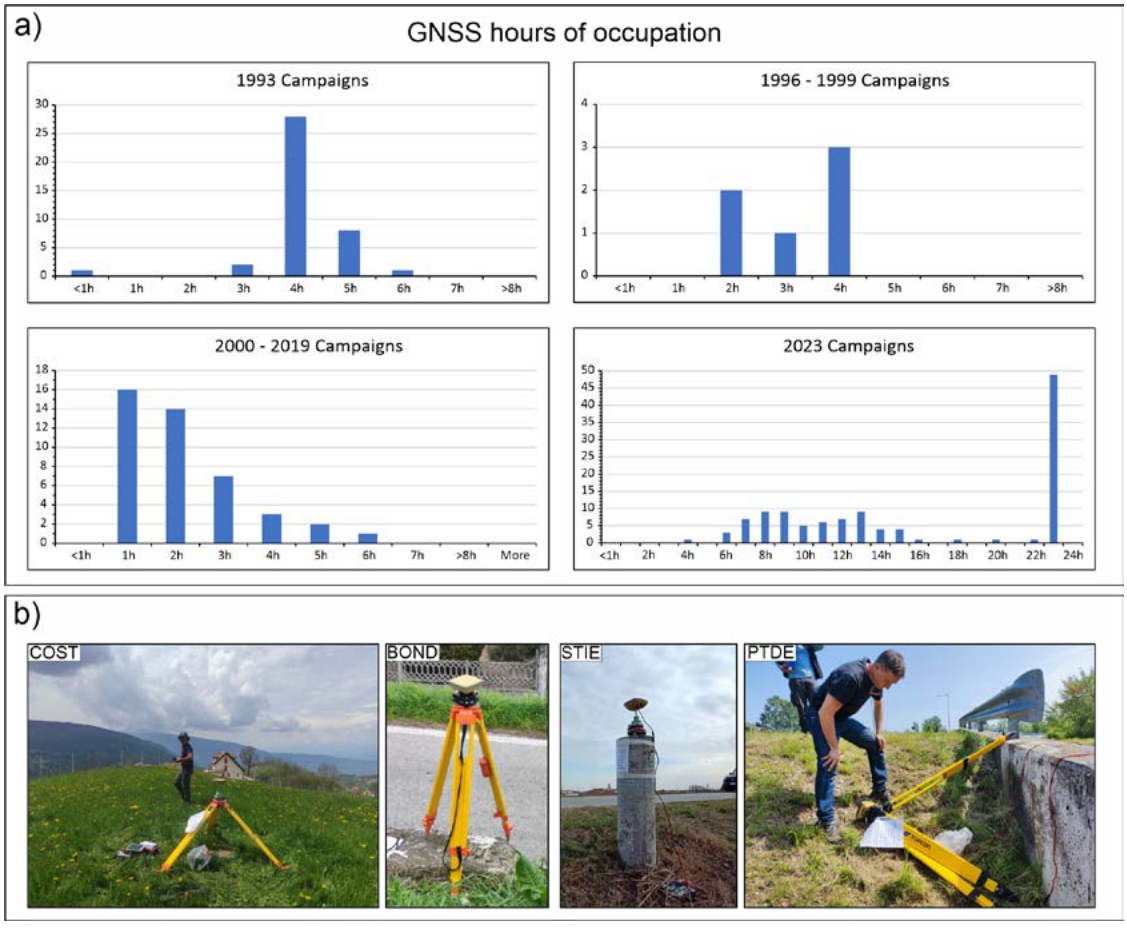

Figure 2 a) Graphs illustrating the occupation time (in hours) of each group of campaigns starting from the first campaign in 1993 to the last campaign carried out by the GeoDynamic and GeoMatic Lab of the University of Catania. b) Photographs from the field campaign showing examples of occupation setups and potential monument stability issues encountered at some benchmarks.

Results

The preliminary velocity field with respect to the Eurasian plate is shown in Figure 4. The velocities depict a pattern consistent with the regional NNE–SSW oriented compression.

Sites in the Po Plain and the frontal thrusts show minimal residual motion relative to Eurasia, while sites within the orogenic belts exhibit slightly higher velocities, reflecting the internal deformation of the thrust wedges. The overall pattern is coherent and aligns with the large-scale kinematics of the Adria microplate [Serpelloni et al., 2013; Devoti et al., 2017].
To validate our campaign-derived velocities, we compared them with time series from nearby permanent stations of the RING [INGV RING Working Group, 2016] and FredNet [OGS, 2016] networks (Friuli Regional Deformation Network). The velocities of reoccupied IGM95 sites show remarkable agreement with the long-term trends of the permanent GNSS stations (*e.g.*, the velocity of point LESI is consistent with the nearby permanent station MODE00ITA). This cross-validation confirms the reliability of our processing strategy and the quality of the long-term velocity estimates derived from the IGM95 campaign data, despite the shorter observation sessions.

Discussion

The updated velocity field allows for a higher-resolution calculation of the strain rate tensor across the study area, by applying the methodology called The “Gaussian Filter” or “Gaussian Smoother” Approach [Kreemer et al., 2014], we can delineate areas of elevated strain accumulation, which likely correspond to segments of the thrust system that are locked and are at present loading elastic strain. Integrating this geodetic strain with active fault databases [Carafa et al., 2015; DISS Working Group, 2021] provides a direct input for physically based probabilistic seismic hazard models. The improved spatial resolution from our campaign data helps to bridge the gap between regional-scale models and fault-specific behavior.
Our study demonstrates that historical geodetic networks, even those designed for cartography, can be repurposed for high-value geophysical research. The primary limitation -shorter observation sessions- is counterbalanced by the long temporal baseline, which effectively averages out short-term noise and allows the tectonic signal to emerge. This approach provides a cost-effective model for enhancing geodetic monitoring in other seismically active regions with existing, but outdated, campaign networks.
The central outcome of this work is the establishment of a “0-point” benchmark. We formally define this as the comprehensive kinematic model -comprising coordinates and velocities for all 29 sites at a reference epoch of 2023.0 - presented in this study. This dataset serves as a foundational datum against which future geodetic measurements can be compared. It will be critically important for:

- quantifying coseismic displacements: providing the pre-seismic interseismic velocity field to accurately measure the static offset of future earthquakes;
- monitoring postseismic transients: serving as the starting point for analyzing the relaxation processes following a major seismic event;
- constraining intersesimic models: providing a high-quality dataset for refining mechanical models of fault locking depth and slip deficit.

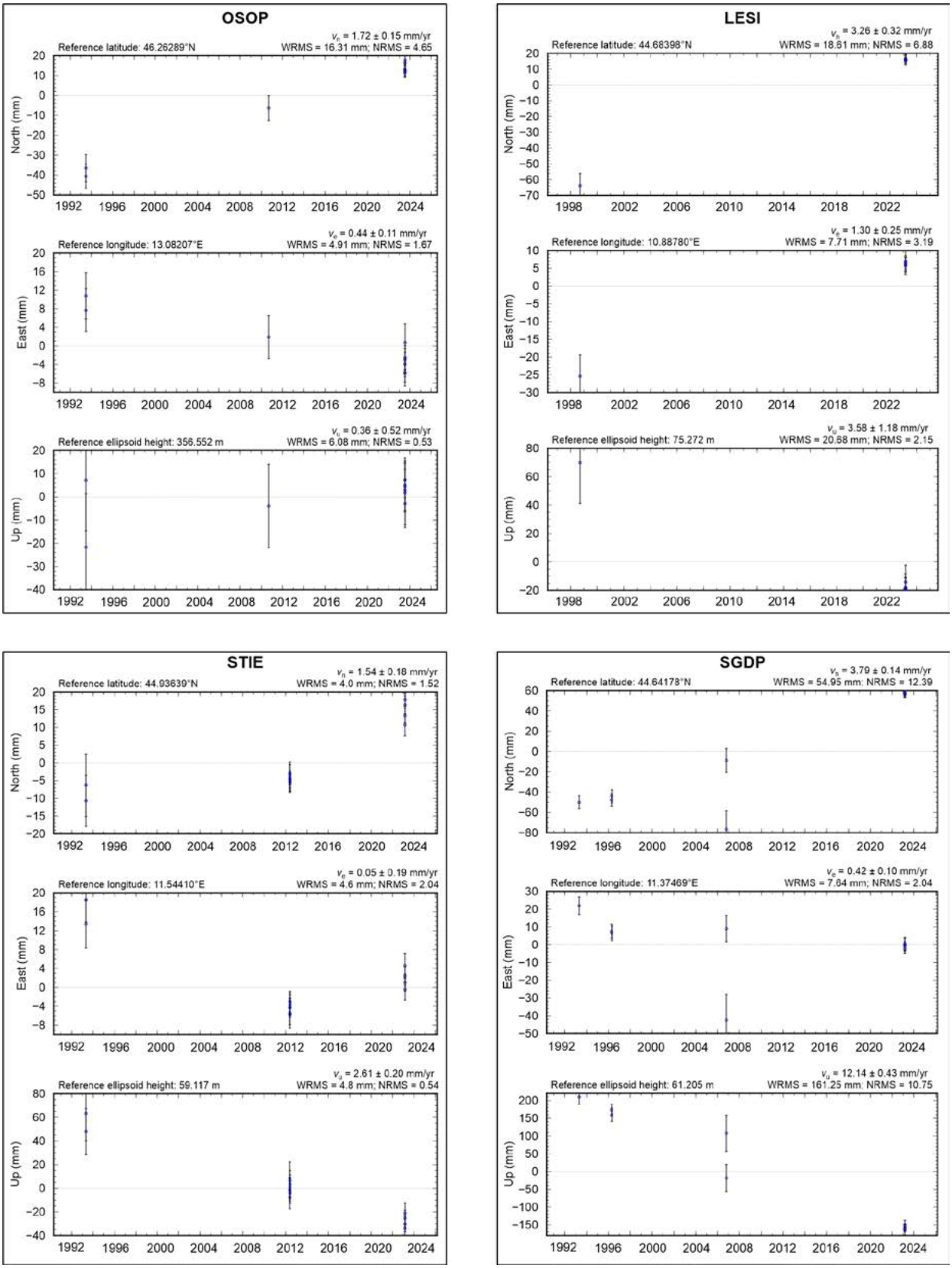

Figure 3 Representative examples of coordinate time series from the IGM95 benchmarks. The panels show the North, East, and Up components for selected stations. Top row (*e.g.*, OSOP and LESI): Examples of sites with a clear linear trend, supporting a reliable velocity estimate. Bottom row (*e.g.*, STIE and SGDP): Examples of sites exhibiting outliers, large formal errors, or non-linear behavior, which complicates the interpretation of a steady tectonic velocity.

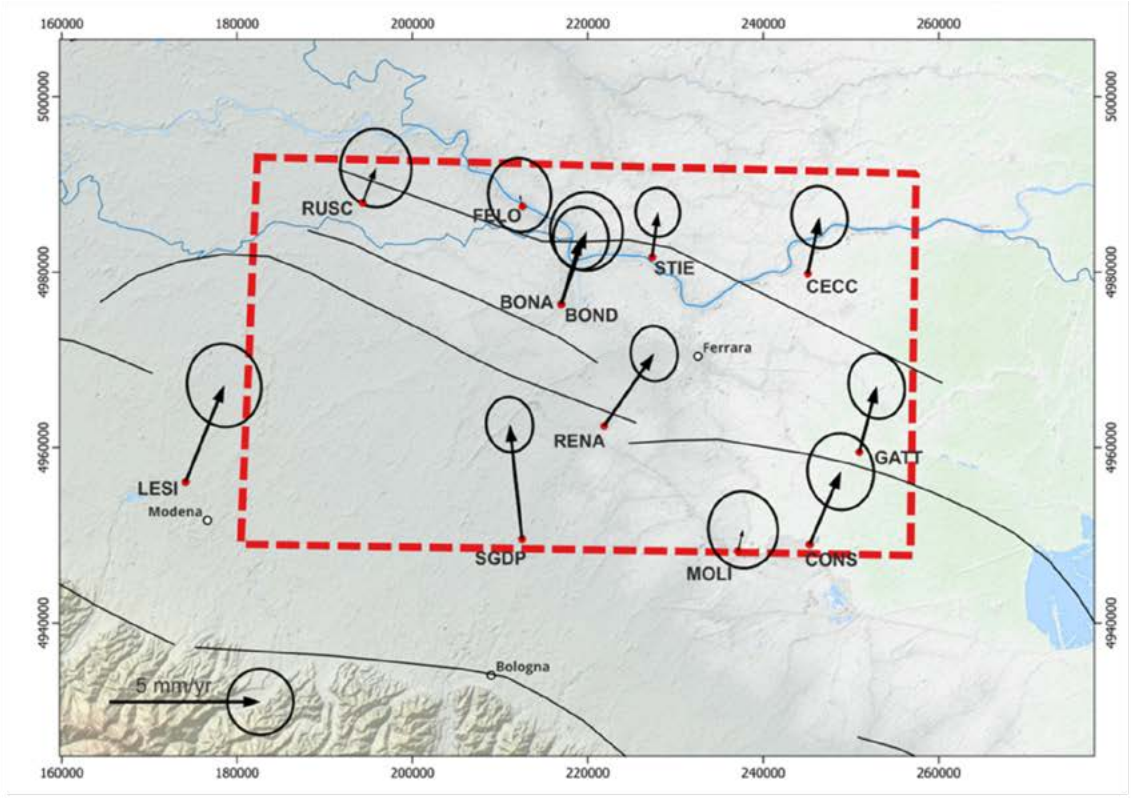

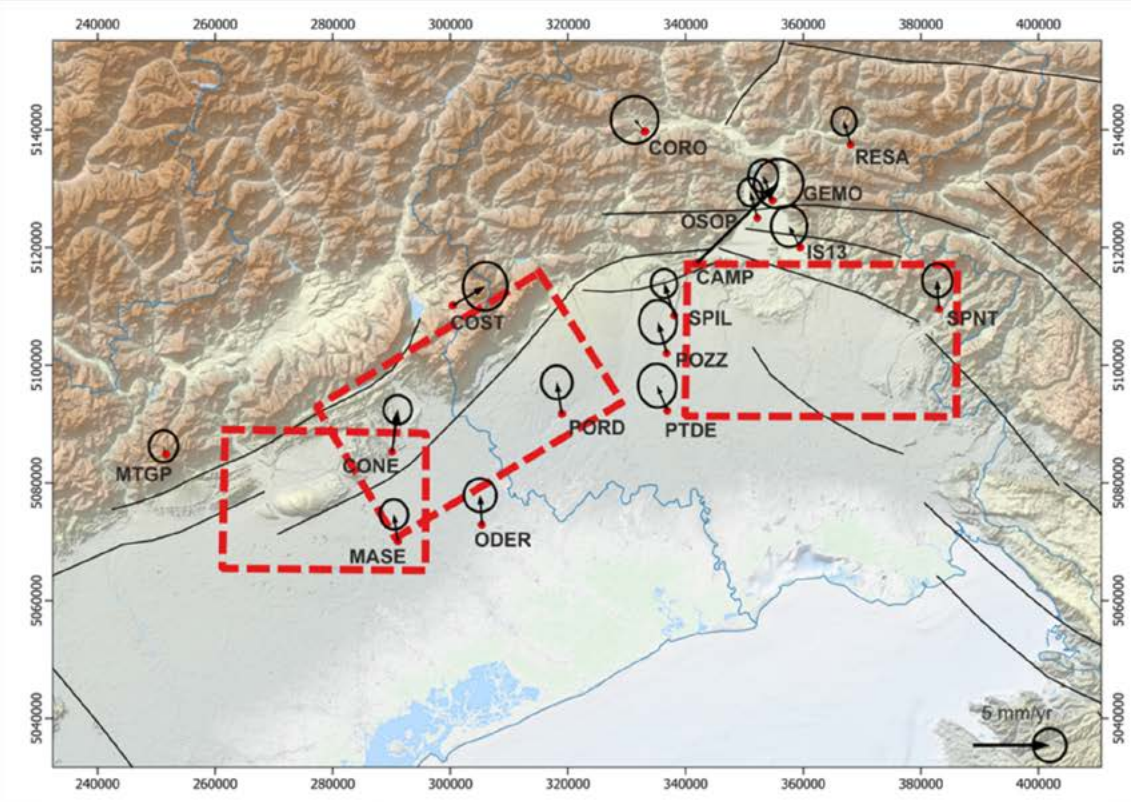

Figure 4 Velocity field obtained from the IGM95 points, referred to the Eurasian plate. Error ellipses represent 2-sigma uncertainties. The background shows the topography of the region.

Conclusions

We have produced an updated and validated velocity field for the Northern Apennines and Southern Alps thrust belts by reanalyzing three decades of GNSS data from the IGM95

network, including a new 2023 campaign. Although the topographic aim of the IGM95 network, which is not compatible with the current high precision geodetic occupation; its long time series can minimize the errors of the obtained velocities of the benchmarks effectively selected by the previous criteria. The results confirm the ongoing compressive deformation and provide enhanced spatial detail on strain accumulation. In the future, our velocity field combined with that obtained from the GNSS permanent station (RING, FredNet, public and private agencies networks) [Galvani et al., 2025] can be useful to obtain a new detailed strain field to better characterize the north Apennines and Southern Alps thrust belts. We have transformed a historical cartographic network into a valuable geophysical tool and established a definitive "0-point" geodetic benchmark for 2023.0. This benchmark is an essential resource for the scientific community, enabling precise quantification of future crustal deformation and contributing to a more accurate assessment of seismic hazard in northern Italy.

References

Altamimi, Z., Métivier, L., and Collilieux, X., (2017). *ITRF2014 plate motion model*. Geophysical Journal International, 209(3), 1906-1912. https://doi.org/10.1093/gji/ggx136

Anzidei, M., Baldi, P., and Serpelloni, E., (2008). *The coseismic ground deformations of the 1997 Umbria-Marche earthquakes: A lesson for the development of new GPS networks*. Annals of Geophysics, 51(2/3), 27-43. https://doi.org/10.4401/ag-3029

Bennett, R.A., Wernicke, B.P., Niemi, N.A., Friedrich, A.M., and Davis, J.L., (2003). *Contemporary strain rates in the northern Basin and Range province from GPS data*. Tectonics, 22(2). https://doi.org/10.1029/2001TC001355

Carafa, M.M.C., Bird, P,. and Valensise, G., (2015). *A geodetic strain rate model for the Italian region*. Geophysical Journal International, 200(2), 1117-1134. https://doi.org/10.1093/gji/ggu446

Cheloni, D., et al., (2014). *New insights into the crustal structure of the Po Plain (Northern Italy) from seismic exploration data*. Tectonophysics, 636, 345-359. https://doi.org/10.1016/j.tecto.2014.08.006

De Guidi, G., Vecchio, A., Brighenti, F., Caputo, R., Carnemolla, F., Di Pietro, A., Lupo, M., Maggini, M., Marchese, S., Messina, D., Monaco, C., and Naso, S., (2017). *Brief communication: Co-seismic displacement on 26 and 30 October 2016 (Mw = 5.9 and 6.5) – earthquakes in central Italy from the analysis of a local GNSS network.* Natural Hazards Earth System Sciences, 17, 1885–1892, https://doi.org/10.5194/nhess-17-1885-2017

Devoti, R., Esposito, A., Pietrantonio, G., Pisani, A.R., and Riguzzi, F., (2017). *A combined velocity field of the Mediterranean region*. Annals of Geophysics, 60(2). https://doi.org/10.4401/ag-7059

DISS Working Group, (2021). *Database of Individual Seismogenic Sources (DISS), Version 4.0*. https://doi.org/10.13127/diss3.3.0

Dong, D., Herring, T.A., and King, R.W., (1998). *Estimating regional deformation from a combination of space and terrestrial geodetic data*. Journal of Geodesy, 72(4), 200-214. https://doi.org/10.1007/s001900050161

Galadini, F., Poli, M.E., and Zanferrari, A., (2005). *Seismogenic sources potentially responsible for earthquakes with M ≥ 6 in the eastern Southern Alps (Thiene-Udine sector, NE Italy)*. Geophysical Journal International, 161(3), 739.762. https://doi.org/10.1111/j.1365-246X.2005.02571.x

Galvani, A., Pietrantonio, G., Devoti, R., (2025). *Combined GNSS velocity field for Northern Italy (NASA4SHA project)*. [Data set]. Zenodo. https://doi.org/10.5281/zenodo.17120300

Herring, T.A., King, R.W., Floyd, M.A., and McClusky, S.C. (2018). *GAMIT Reference Manual, GPS Analysis at MIT, Release 10.7*. Department of Earth, Atmospheric and Planetary Sciences,

MIT. https://doi.org/10.13140/RG.2.2.22894.36161

Kreemer, C., Blewitt, G., and Klein, E.C., (2014). *A geodetic plate motion and Global Strain Rate Model*. Geochemistry, Geophysics, Geosystems, 15(10), 3849-3889. https://doi.org/10.1002/2014GC005407

OGS (Istituto Nazionale Di Oceanografia E Di Geofisica Sperimentale), (2016). *Friuli Regional Deformation Network Data Center (1.0)*. OGS (Istituto Nazionale Di Oceanografia E Di Geofisica Sperimentale) [data set], https://doi.org/10.6092/frednet

Pirrotta, C., Barberi, G., Barreca, G., Brighenti, F., Carnemolla, F., De Guidi, G., Monaco, C., Pepe, F., Scarfì, L., (2021). *Recent Activity and Kinematics of the Bounding Faults of the Catanzaro Trough (Central Calabria, Italy)*. New Morphotectonic, Geodetic and Seismological Data. Geosciences, 11, 405. https://doi.org/10.3390/geosciences11100405

Serpelloni, E., Faccenna, C., Spada, G., Dong, D., and Williams, S.D.P., (2013). *Vertical GPS ground motion rates in the Euro-Mediterranean region: New evidence of velocity gradients at different spatial scales along the Nubia–Eurasia plate boundary*. Journal of Geophysical Research: Solid Earth, 118(11), 6003-6024. https://doi.org/10.1002/2013JB010102

Vannoli, P., Burrato, P., and Valensise, G., (2015). *The seismotectonics of the Po Plain (Northern Italy): Tectonic diversity in a blind faulting domain*. Pure and Applied Geophysics, 172(5), 1105-1142. https://doi.org/10.1007/s00024-014-0873-0

High-precision geometric levelling between Udine and Basagliapenta: a possible key method for detecting recent tectonic deformations at the Eastern Southern Alps front (Friuli, NE Italy)

Andrea Marchesini[1], Alberto Pellegrinelli[2], Giulia Patricelli[1,3,4,*], Francesco Carnemolla[4,5], Laura Monti[2], Davide Russo[3,4], Giorgio De Guidi[4,5], and Maria Eliana Poli[1,4]

[1]Università di Udine, Dipartimento di Scienze AgroAlimentari, Ambientali e Animali, Udine, Italy
[2]Università di Ferrara, Dipartimento di Ingegneria, Ferrara, Italy
[3]Università di Ferrara, Dipartimento di Fisica e Scienze della Terra, Ferrara, Italy
[4]Centro Interuniversitario per la Sismotettonica 3D con Applicazioni Territoriali (CRUST), Chieti, Italy
[5]Università di Catania, Dipartimento di Scienze Biologiche, Geologiche e Ambientali, Catania, Italy

Corresponding author: giulia.patricelli@uniud.it

Introduction

In the framework of the PRIN2020 "Fault segmentation and seismotectonics of active thrust systems: the Northern Apennines and Southern Alps laboratories for new Seismic Hazard Assessments in northern Italy (NASA4SHA)", new geodynamic hints have been collected through topographic method in the Friuli Plain, which support the recent activity of the easternmost portion of the Southalpine external front.
The Italian Military Geographic Institute (IGM) high-precision levelling line number 110 intersects at high angle the possible surface traces of active buried tectonic structures named Pozzuolo Thrust-system (which includes the Pozzuolo-Medea and Pozzuolo2 transpressive planes) and Udine-Buttrio thrust [Marchesini et al., 2023]. In this contest, the high-precision levelling measurement method could allow us to assess the vertical component of present surface deformations during a short period.

Seismotectonic setting

The study area belongs to the Quaternary front of the Eastern Southern Alps, characterized by south-to southeast-verging fold-and-thrust belt that have been active from the Middle Miocene to the Present and extend from Veneto region to eastern Friuli. During the Quaternary, the Southern Alpine front propagated into the Venetian-Friulian piedmont plain, which currently represents its foreland (Figure 1). In the eastern sector, the geometry of the tectonic structures is strongly influenced by structural features inherited from the Palaeogene (Dinaric) deformation phase. During this stage, west-southwest-verging folds and thrusts affected most of the Friuli region. The outermost front of the Dinaric chain is represented by the Palmanova thrust Auct., which extends NW-SE beneath the Quaternary deposits of the Friulian plain. In the frame of the Neogene-Quaternary stress field, these structures were reactivated with a transpressive kinematics, producing widespread evidence of surface deformation in the Friulian piedmont plain. Examples include the so-called "isolated relieves" of Pozzuolo, Variano, Orgnano, and Carpeneto, involving the conglomerates of the Friuli Supersynthem (Upper Pliocene-Pleistocene) [Venturini et al., 1987; Zanferrari et al., 2008; Fontana et al., 2019; Patricelli and Poli, 2020; Marchesini et al., 2023]. The innermost sector of the piedmont plain is affected by the low-angle Udine-Buttrio NW thrust, which is responsible for the uplift

of the Pasian di Prato high near Udine, where pre-Last Glacial Maximum conglomerates of the Friuli Supersynthem crop out [Zanferrari et al., 2008].

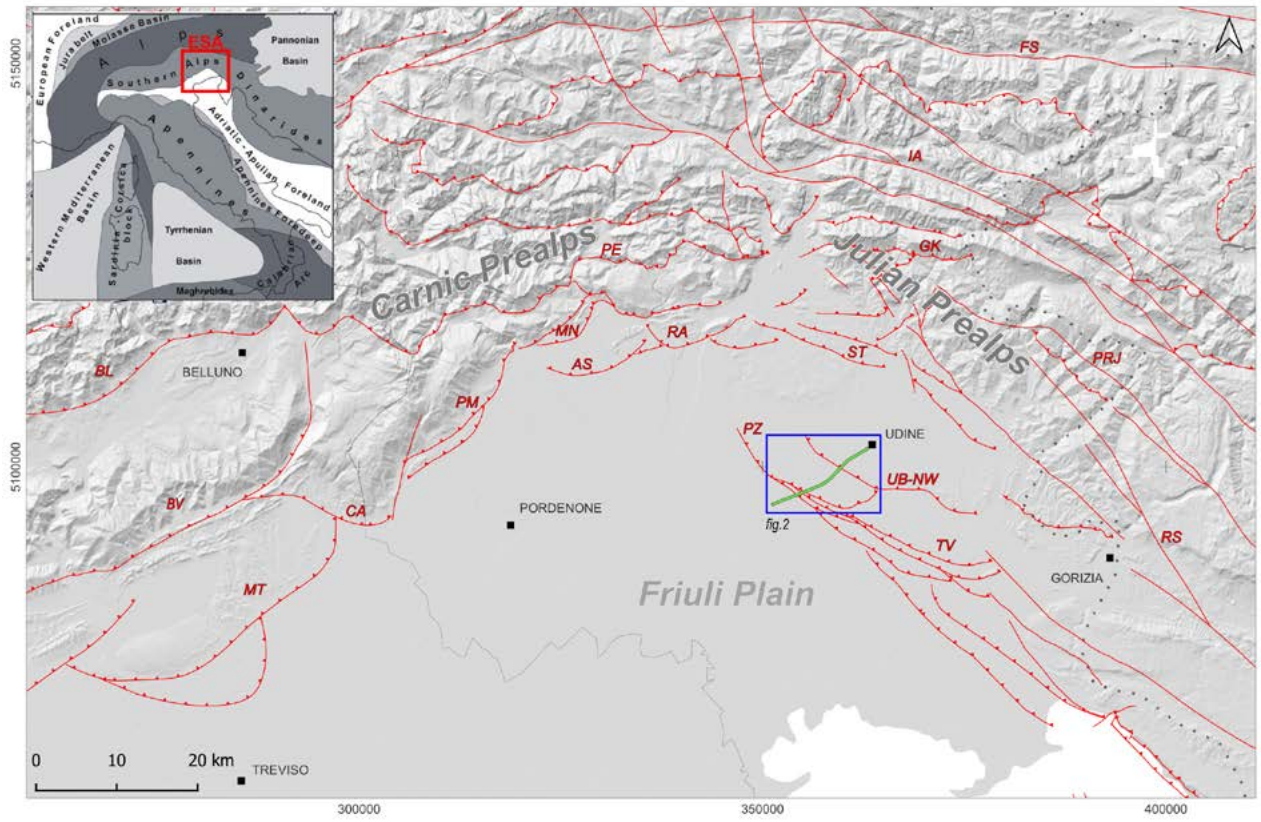

Figure 1 Structural sketch map of Eastern Southern Alps. The green line represents the measured high-precision IGM levelling line number 110; blue box represents the area mapped in Figure 2. Faults acronyms: AS: Arba-Sequals th., BL: Belluno th., BV: Bassano-Valdobbiadene th., CA: Cansiglio th., FS: Fella-Sava fs., GK: Gemona-Kobarid th., IA: Idrija-Ampezzo fs., MN: Maniago th., MT: Montello th., PE: Periadriatic th., PM: Polcenigo-Montereale th., PRJ: Predjama f., PZ: Pozzuolo ts., RA: Ragogna th., RS: Rasa f., ST: Susans-Tricesimo th., TV: Trivignano th., UB-NW: Udine-Buttrio NW th. RS: EPSG 6708.

New materialisations and data acquisition

During February 2024, we planned and carried out the repetition of the high-precision levelling measurement on the existing benchmarks (hereinafter: BMs) along the IGM line 110 and on other newly constructed ones. The measurement line started in Udine and extended southwestwards for approximately 14 km crossing a difference in altitude of about -50 m. The changes in height over time were calculated by comparing the variation in elevation difference between a pair of common marks in two epochs, using measurement data from previous epochs: 1977, 1993 and 2004.

Planning the acquisition campaign and processing the data for each available epoch involved collecting, carefully reading and digitising monographs and plano-altimetric data, analytically verifying the field logbooks and cross-comparing the state of markers (and artefacts) over time with field inspections and updating the monographs to estimate tampering or unreported substitutions.

Before the survey, a site inspection was carried out in order to assess the condition and the existence of those BMs. More in details, 11 BMs already measured in 2004 were occupied in 2024; 3 useful BMs, created by other materialisations, were also found. Finally, where logistically possible, 7 BMs were materialised to replace the lost markers and reduce the distance between the existing BMs to no more than approximately 800 m. This helped us to limit the error and to densify the measurements at the intersection with the traces of structures defined as active [Zanferrari et al., 2008; Patricelli and Poli, 2020; Marchesini et al., 2023] (Figure 2).
In this contest, the high-penetration industrial reflection seismic lines A and B (gently supplied by ENI), located perpendicular to the active tectonic structures and therefore parallel to the IGM line trace, as well as line C intersecting the measured levelling line towards north-west (Figure 2), allowed us to compare the interpretation of the topographic results with the observed subsurface tectonic deformations on the seismic lines.

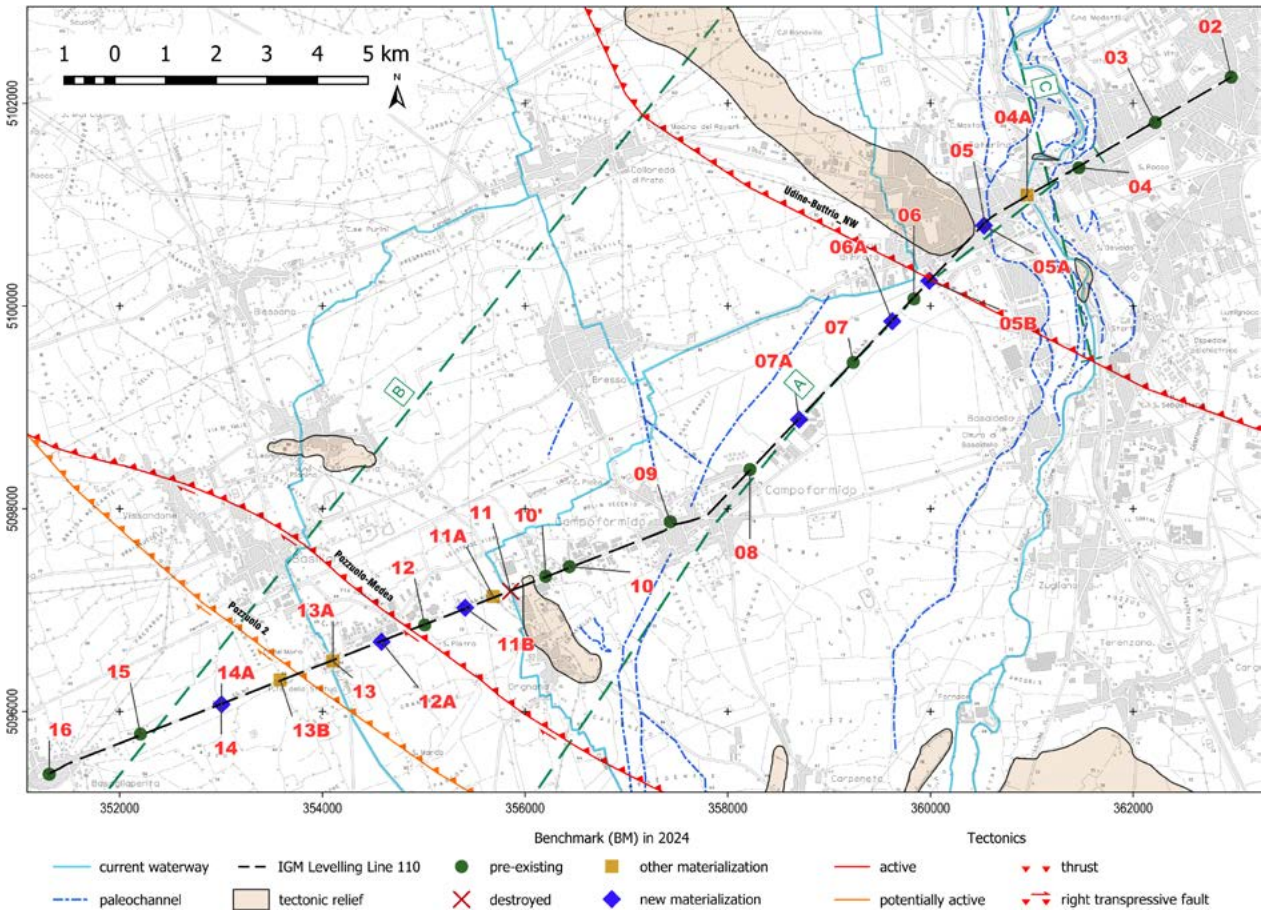

Figure 2 Planimetry of the benchmarks of the IGM levelling line 110 (measured in 2024), thrusts (from Patricelli and Poli [2020]), geological and geodynamic hints (from Marchesini et al. [2023]). RS: EPSG 6708.

Figure 3 shows the precision of the levelling measurement for the 2024 campaign. In general, the discrepancy between consecutive BMs meets the very high-precision specifications, except for the section crossing the bridge over the motorway (between BM 04 and 04A) due to vibrations induced by traffic above and below, even though the measurements were carried out on a winter Sunday morning.

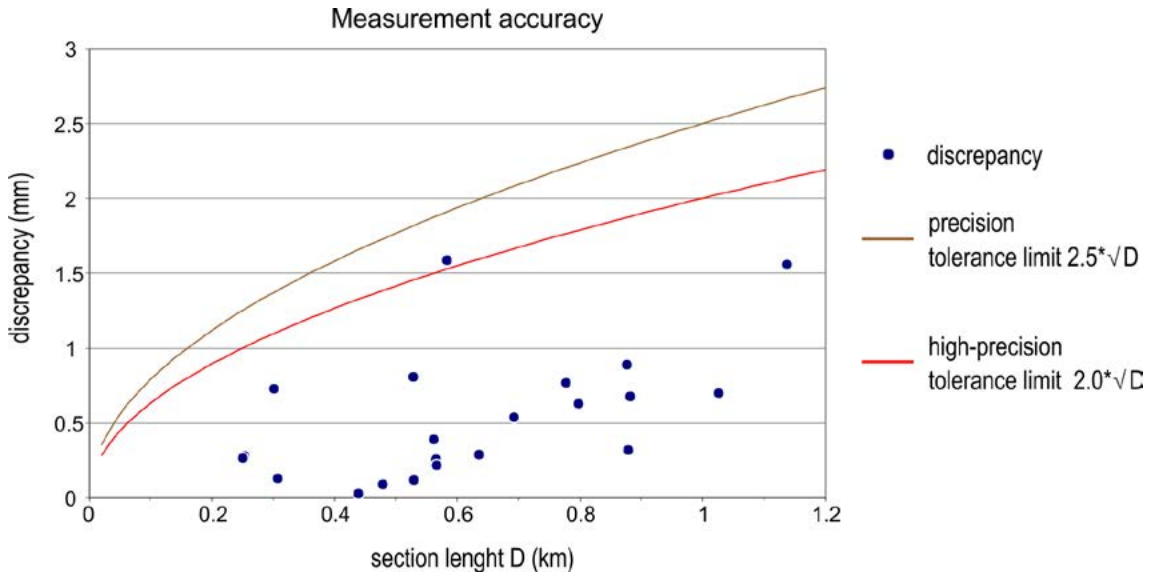

Figure 3 Precision of the levelling measurement for the 2024 campaign.

Table 1 reports the kilometric errors (σ*) for each epoch. The improved kilometric error in 2024 is also due to the shorter runs resulting from the new BMs.

epoch	σ* (mm/km)
1977	0.483
1993	0.491
2004	0.546
2024	0.411

Table 1 Kilometric errors σ* for each epoch.

Method and elaborations

The height variations between the BMs are invariant with respect to the altimetric reference, therefore it is not essential to have a point of known absolute height that remains unchanged over time. Since the regional-scale geodynamics indicates uplift from south to north, the BM with zero height variation between epochs was set to the south-west, in the first BM measured in 2024 (BM 16, Basagliapenta), which also has the advantage of being common to all epochs. For each elevation change between BM markers common to two epochs, the standard deviation is calculated. The graphs in Figures 4 and 5 show the elevation changes between epochs on the y-axis and the distance from BM 16 to BM 02 (Udine) on the x-axis. This allows the graph to be read from left to right along the line from approximately south-west to north-east.
Figure 4a summarizes the overall graph of cumulative elevation changes from BM 16 along the measured levelling trace, in the intervals 1993-1977, 2004-1993, and 2024-2004 [Marchesini et al., 2025]. These are intervals of 16, 11, and 20 years, respectively. In figures 4a and 4b, the curve of the height variations over time is continuous between adjacent BMs, while dashed between non-adjacent BMs where there was no pair of identical markers between two epochs. The BMs numbers are in red, while the positions of the new 2024 BMs are represented by brown circles outside the chart. The linear interpolation (dotted line, same colour), indicative of the general trend for each epoch, considers all the sections between BMs without filtering.

The calculation of the residuals (from the general trend of each interval) is shown in figure 4b. This is a representation to emphasize local deformations. This graph highlights that between BMs 16 and 14 (possibly extending to BM 12, as suggested by the 1977-1993 dataset), the trend remains nearly flat. In contrast, a more complex pattern emerges from BM 12 onwards, with two peaks indicating relative uplift. The first of these occurs between BMs 12 and 09, while the second, more pronounced and consistent, between BMs 07 and 04.
Although in figures 4a and 4b the error bars are shown at 1, deformation analyses are conducted considering 2 error bars, which are always referred to in the interpretation.

Geodynamic considerations

The general deformation trends are not univocal. However, the graph in Figure 4b highlights local deformations common to the three intervals probably due to the above mentioned active tectonic structures. In order to verify whether the observed anomalies in the trend can be attributed to tectonic activity, we compared the deformations obtained through levelling data (Figures 4a and 4b) with the geological and geomorphological evidence (including deformed surfaces interpreted from seismic lines, fault scarps, isolated reliefs, etc.), that testify recent-to-present surface deformation associated to the active thrust fronts affecting the area [Zanferrari et al., 2008].
In this contest, Figure 4c shows the altimetric profile with some geological hints, while Figure 4d presents a geological cross section along the trace of the levelling line, extracted from the 3D structural model derived from seismic lines interpretation [Patricelli and Poli, 2020].
Both figures highlight that the area showing the two positive residuals (between BMs 12 and 04) corresponds to the uplifted zone identified through geological and geophysical techniques and associated with the outer front of the thrust belt. In contrast, no significant vertical deformation is detected in the footwall of the active front - corresponding to the Pozzuolo transpressive fault system - across all the three intervals.
In the north-eastern portion of the levelling line, the maximum relative height variation over the three intervals is observed near BM 06, in correspondence with the active Udine-Buttrio NW thrust. This structure shows surface evidence of both geological and geomorphological recent activity, such as the Pasian di Prato structural high made up of the Friuli Supersynthem conglomerates.
However, while the residuals observed between BMs 07 and 04 could possibly reflect the deformational effects of the Udine thrust, those between BMs 12 and 09 do not allow for a clear interpretation, due to the discontinuity of the graph, even though consistent with the general uplift trend. In this contest, in the Orgnano area, surface deformation referable to the Pozzuolo fault system is well documented in a post-LGM time interval, as evidenced by a series of structural highs producing several metres-high scarps in LGM deposits. Therefore, it remains uncertain whether the levelling method is capable of capturing this tectonic activity over the past few decades. Notably, the plot shows a lack of continuity across all the three intervals from BM 14 to BM 10 (Figure 4b).
In the northernmost portion (BM 04 to BM 02), both available graphs (2004-1993 and 2024-2004) show a declining pattern. This localised subsidence may be linked to a paleo-Cormor stream channel, where thicker alluvial deposits could lead to differential compaction. Identifying and mapping these paleo-channels may help to clarify the origin and timing of the deformation.
Figure 5 shows the fragmentary graph of the cumulative difference in height from BM 16 between the same marks of the few common BMs residues in the interval 2024-1977.

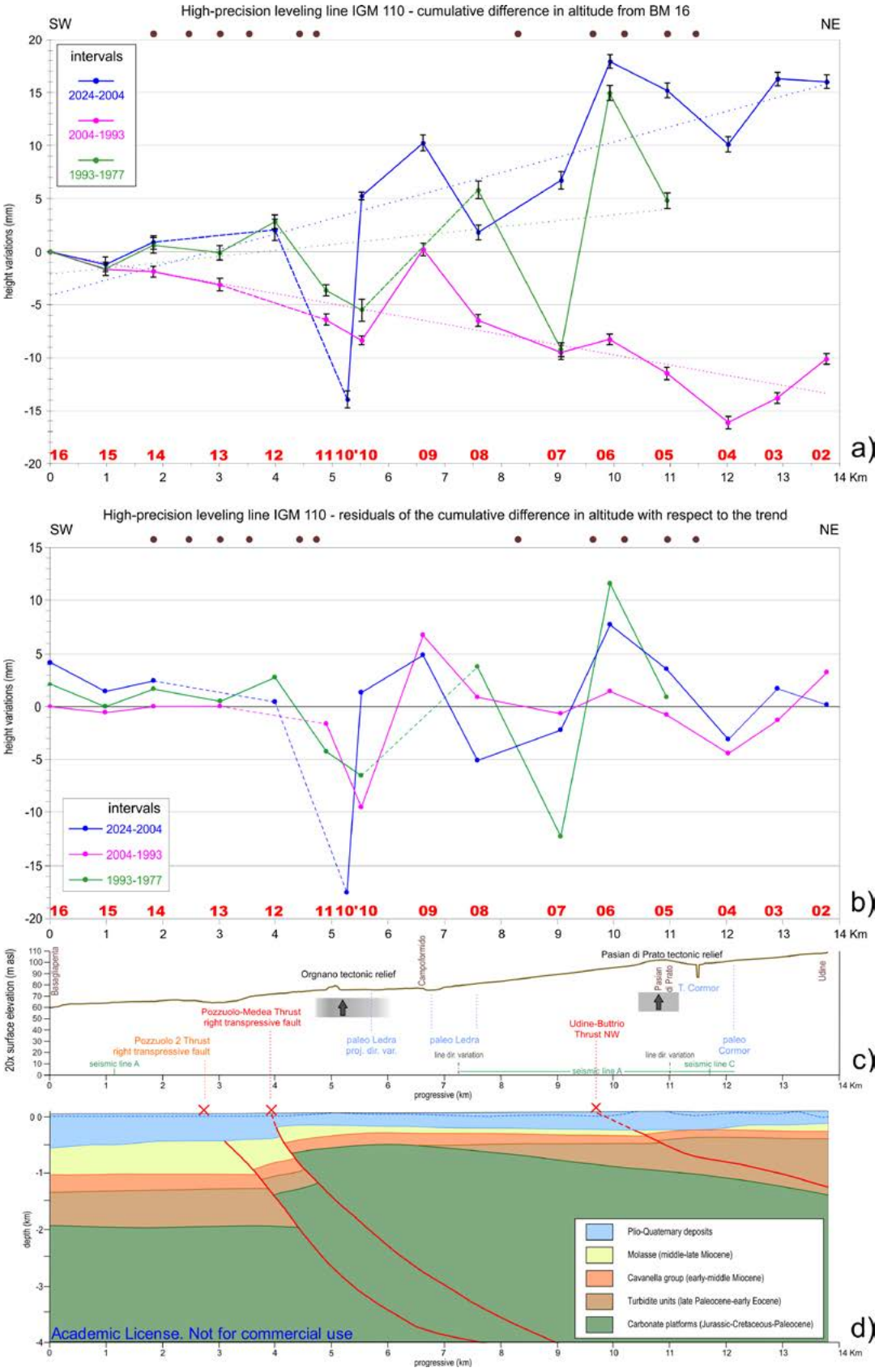

Figure 4 (front page) (a) elevation change between epochs from BM 16 (Basagliapenta) to BM 02 (Udine) with 1σ error bars to avoid graphic overlaps. The BMs numbers are in red, the positions of the new 2024 BMs are in brown circles outside the chart, in the upper part; b) calculation of the residuals from the general trend of each interval, without error bars to avoid graphic overlaps; (c) altimetric profile with vertical exaggeration of 20x and geodynamic hints; (d) geological cross section extracted from the 3D model derived from seismic lines; dashed blue line: top of the conglomerates.

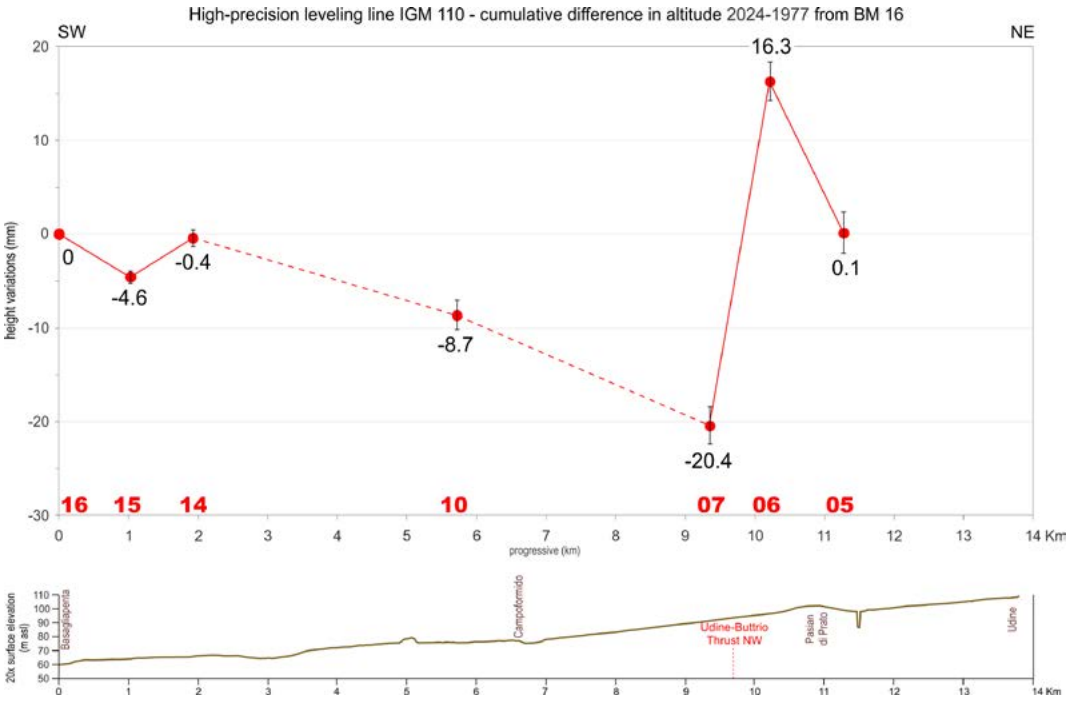

Figure 5 Graph and values of the cumulative difference in height from BM 16 between the same residual BM markers in common in the interval 2024-1977. Error bars 2σ.

Since the graph is not continuous across the Pozzuolo system, the available data do not allow for a reliable quantification of the cumulative elevation change over time referable to the frontal transpressive system (Pozzuolo system). Therefore, it is currently impossible to estimate the system's short-term deformation rate.

Across the Udine-Buttrio NW thrust, between BM 06 and BM 07, a relative uplift of 36.7 ± 4.0 mm (2σ) in the last 47 years has been observed. This corresponds to a short-term deformation rate of approximately 0.8 mm/yr. Long-term throw rates (late LGM corresponding to 23.0-21.0 kyr cal BP) derived from geological data are 0.17–0.18 mm/yr [Patricelli and Poli, 2020]; the local uplift rates estimated through the topographic method appear to be higher. In this regard, it is worth remarking that the analysed deformations represent only 0.2% of the time elapsed since the LGM and are confined to an 800 m section, compared with geological evidence suggesting broader-scale deformation.

The results presented are in good agreement with the structural model of the area. They highlight that the Southalpine external front in eastern Friuli is uplifting relative to the undeformed foreland, which is represented by the Friulian Plain. The key aspect of this study, which deserves further investigation, is that despite the moderate-to-low uplift rates of the analysed structures, topographic levelling measurements -covering a time span of approximately 50 years- are able to detect cumulative deformation even over short time periods.

It is important to note that it is currently impossible to clearly distinguish how much of the variation in altitude measured through the topographic method is due to purely tectonic processes.

Indeed, the effects of seasonal and historical water table fluctuations (at depths between 35 and 44 m) on the topographic surface can be considered negligible. However, other factors such as local compaction, palaeogeographic evolution, and sedimentary dynamics, are likely to have contributed to the recorded elevation changes.

Further implications arise when comparing the estimated deformation rates with the distribution of historical and instrumental seismicity. Given the low to absent seismic activity

in recent times, it is reasonable to hypothesise that the Udine-Buttrio thrust accommodates deformation through aseismic creep rather than through stick-slip behaviour.
Thanks to the new BMs materialised for the present work, future re-measurements will enable more accurate sampling of the recorded surface deformation effects, both on a regional scale and for the accommodation across single tectonic structures.
We thank Alberto Beinat (University of Udine) for the logistical support.

References

Fontana, A., Monegato, G., Rossato, S., Poli, M. E., Furlani, S., and Stefani, C.. (2019). *Carta delle unità geologiche della pianura del Friuli Venezia Giulia alla scala 1:150.000 e note illustrative*. Regione Autonoma Friuli Venezia Giulia - Servizio Geologico. ISBN: 978-88-89637-14-2.

Marchesini, A., Poli, M.E., Bonini, L., Busetti, M., Piano, C., Dal Cin, M., Paiero, G., Areggi, G., Civile, D., Ponton, M., Patricelli, G., Tamaro, A., and Gruppo di lavoro Faglie attive FVG, (2023). *Linee guida per l'utilizzo della banca dati georiferita delle faglie attive della Regione Friuli Venezia Giulia*. Servizio Geologico - Regione Autonoma Friuli Venezia Giulia, 76 pp, ISBN 9788894039474.

Marchesini, A., Pellegrinelli, A., Patricelli, G., Carnemolla, F., Monti, L., and Russo, D., (2025). *High-precision geometric levelling between Udine and Basagliapenta: a key method for detecting recent tectonic deformations at the Eastern Southern Alps front (NE Italy)*. 43rd National Conference of the GNGTS, Bologna, Italy.

Patricelli, G., and Poli, M.E., (2019). *3D geometry of NE-Friuli Quaternary faults (NE Italy)*. EGU General Assembly 2019, Vienna, Austria.

Patricelli, G., and Poli, M.E., (2020). *Quaternary tectonic activity in the north-eastern Friuli Plain (NE Italy)*. Boll. Geof. Teor. Appl., 61, 309-332. https://doi.org/10.4430/bgta0319

Venturini, S., (1987) *Nuovi dati sul Tortoniano del sottosuolo della Pianura Friulana*. Gortania - Atti Museo Friulano Storia Naturale, 9, 5-16.

Zanferrari, A., Avigliano, R., Monegato, G., Paiero, G., Poli, M.E., and Stefani, C., (2008). *Carta Geologica e Note Illustrative della Carta Geologica d'Italia alla scala 1:50.000*. ISPRA. ISBN: 978-88-9311-025-9.

From surface to crustal depths: the Broni-Sarmato Fault in the context of the Emilia Arc, northern Italy

Alessandro Tibaldi[1,2,*], Rita de Nardis[2,3], Patrizio Torrese[2,4], Sofia Bressan[1], Martina Pedicini[1], Donato Talone[2,3], Fabio Luca Bonali[1,2], Noemi Corti[1], Elena Russo[1,2], and Giusy Lavecchia[2,3]

[1]Università di Milano Bicocca, Dipartimento di Scienze dell'Ambiente e della Terra, Milan, Italy
[2]Centro Interuniversitario per la Sismotettonica 3D con Applicazioni Territoriali (CRUST), Chieti, Italy
[3]Università "G. d'Annunzio", Dipartimento di Scienze Psicologiche, della Salute e del Territorio, Chieti, Italy
[4]Università di Pavia, Dipartimento di Scienze dell'Ambiente e della Terra, Pavia, Italy

Corresponding author: alessandro.tibaldi@unimib.it

Introduction and geological background

The outermost sector of the Northern Apennines is buried under a thick pile of Pliocene-Pleistocene deposits, locally up to 7-8 km [Bigi et al., 1990]. The convergence here is accommodated by thrusting and folding [Burrato et al., 2003; Zuffetti and Bersezio, 2020; Lavecchia et al., 2021], but orientations of structures are scattered and their relationships with seismicity are not always well constrained, also for the low amount of instrumental seismicity, especially in the central-western part of the buried front. This corresponds to the Monferrato Arc and Emilia Arc, the latter being the object of the present study. Two major northward-verging and rejuvenating thrust systems may be recognized in the Emilia Arc. From south to north, they are: 1) the pede-Apennine Thrust Front (PTF, sensu Boccaletti et al. [1985]), where our detailed Broni-Sarmato study area is located, which borders the Miocene Northern Apennines outcropping fold-and-thrust belt, and 2) the thrusts of the “Emilia Southern and Central Po Plain Structures”, buried beneath the Po Plain alluvial deposits [Toscani et al., 2014], active at least up to early Pleistocene according to surface and subsurface data [Maesano et al., 2015; Zuffetti et al., 2018] (Figure 1).
Mainly based on morphotectonic data, the activity in Quaternary times of a 35 km-long thrust belonging to the Emilia PTF and recognized between the localities of Montebello and Sarmato (Figure 2a) has been proposed by Benedetti et al. [2003]. They suggested that the fault, named Stradella thrust, has variable cumulative surface throws in the range of 2-25 m and scarp degradation, suggesting a recent offset of the terrace surfaces (10-100 ka BP). The Stradella fault is composed of two segments located east-ward and west-ward of the Broni locality (Figure 2). We concentrated our field efforts on the 18 km-long eastern segment, named Broni-Sarmato fault. We applied different methodologies that comprise field morphostructural mapping, analyses of aerial photos, surveys carried out with an Unmanned Aerial Vehicle (UAV), GPS, and geoelectrical surveys across the thrust scarp. The length of this structure and its closeness to several large towns indicate relevance for the seismic hazard and risk. Consequently, further analyses are required to better assess the possible existence of the thrust and define its characteristics. Due to the lack of relevant seismic activity associated with the Stradella fault, we enlarged the seismotectonic and earthquake data analysis to the whole Emilia Arc. We integrated geological and seismological data from literature with new focal mechanisms to build a 3D geometric-kinematic fault model of the overall fault pattern and its association with instrumental earthquakes.

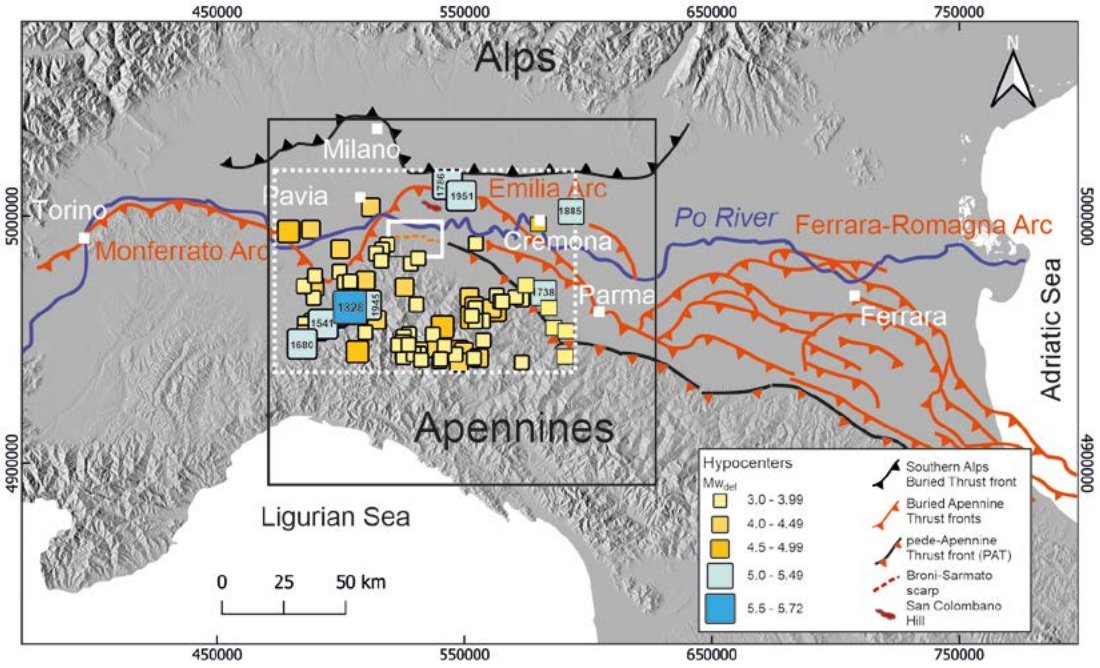

Figure 1 Location map of the local and regional study areas (boxes) in the framework of the regional main structures, simplified from Tibaldi et al. [2023]. The northernmost part of the Apennine fold-and-thrust belt is characterized by three major arcs (from west to east: the Monferrato Arc, the Emilia Arc, and the Ferrara-Romagna Arc), buried under Po Plain sediments. Hypocenters, from 1000 A.D. to 2020, within the dotted white rectangle are extrapolated from CPTI15 [Rovida et al., 2021] and ISIDe [ISIDe Working Group, 2007]. The smallest white box shows the location of Figure 2; the box with dotted white line is the area where earthquakes are shown; the box with black line shows the location of Figures 4a and 5.

The Stradella fault and the Broni-Sarmato scarp

The Broni-Sarmato scarp (Figure 2a) limits three main fluvial terraces –composed of Apennine clays and sands– distinguishable by their elevation and weathering degree. Apennine tributaries of the Po River have generated these terraces (T1, T2, and T3 in Figure 2a) due to the continuous lifting of the area, which has been dated to the middle Pleistocene (T2-T3), and to the latest Pleistocene (T1) [Benedetti et al., 2003]. The northern limit of these terraces is characterised by triangular facets and perched valleys, features that support the hypothesis of a tectonic origin of the scarp.

The trace of this scarp is not continuous along the area; indeed, it is characterized by several left- and right-stepping segments, with a separation in the order of 60 to 260 m. It is also affected by one large right-stepping with a separation of 1.8 km between the villages of Casa Olmo and Castel San Giovanni. 30 high-precision GPS profiles across the scarp indicate heights in the range 6-23 m. Measurements along a minor scarp located at the foot of the main scarp are indicated in Figure 2b.

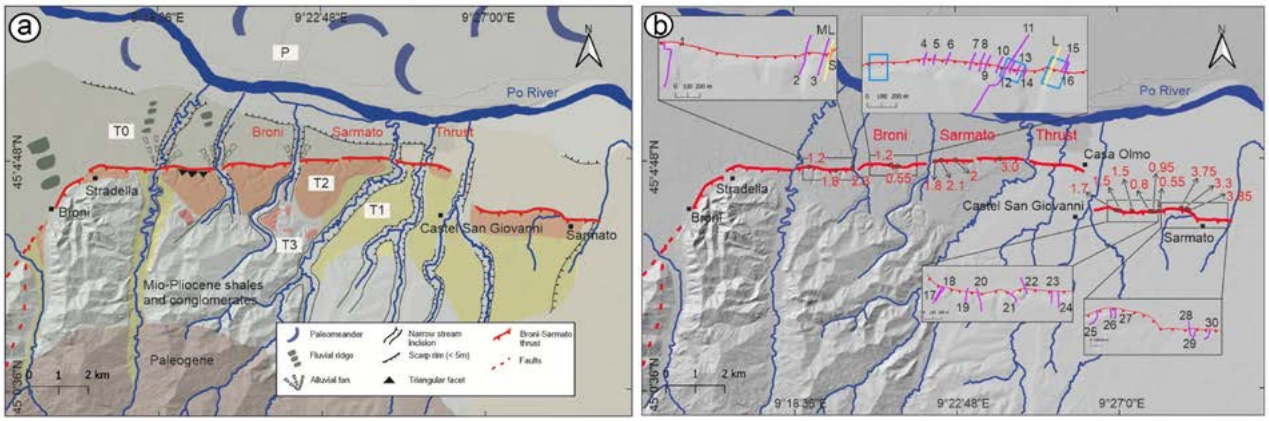

Figure 2 a) Geological and geomorphological map of the study area (small white rectangle in Figure 1) after Tibaldi et al. [2023]. T1, T2, T3 mark Quaternary fluvial terraces. T0 Holocene. Triangular facets identified from the analysis of LIDAR data are reported. b) Location of GPS profiles (purple lines), ERT surveys (yellow and orange lines), and drone-flight areas (blue squares). Height (m) of the minor escarpment of the Broni-Sarmato structure is reported.

Geoelectrical surveys

In the inverse resistivity models (Figure 3), warm colours (from green to red) are associated with freshwater-saturated clayey-to-sandy deposits, cool colours (from purple to blue) are associated with brackish water-saturated sandy deposits or freshwater-saturated clays. Our models pointed out the presence of zones of the subsoil affected by brackish water contaminations which are likely localised along structural discontinuities (A, D, E discontinuities in Figure 3). The origin of these Na-Cl rich waters is connected to the brines (very high-density fluids) that are remnants of evaporated marine waters in the late Messinian (Late Miocene), trapped at the bottom of the Po plain aquifer. The uprising of saline waters is facilitated by these structural discontinuities, which represent preferential flow paths and facilitate the flow towards the surface and the mixing of deep saline waters with shallow fresh waters [Pilla et al., 2010]. Horizontal interruption and vertical dislocation of a shallow, high resistivity layer (dislocated into Z and Y, X and W bodies) allowed the recognition of structural discontinuities B, C, and F. These discontinuities appear to be associated with the uprising of brackish water to a lesser extent than the other discontinuities, as revealed by detailed profile S alone. Among the discontinuities revealed by the inverse resistivity models, we identified the main discontinuity (A), which is recognisable on all profiles. Discontinuity A is associated with minor structures B and C, which are found on all the profiles; the other two small, shallow structures are revealed by the detailed profile S alone. Integrating the topographic analysis and the geoelectrical profiles, we identify the Broni-Sarmato fault as a wide zone of deformation at the shallowest level extending from point B to point D in Profile L of Figure 3.

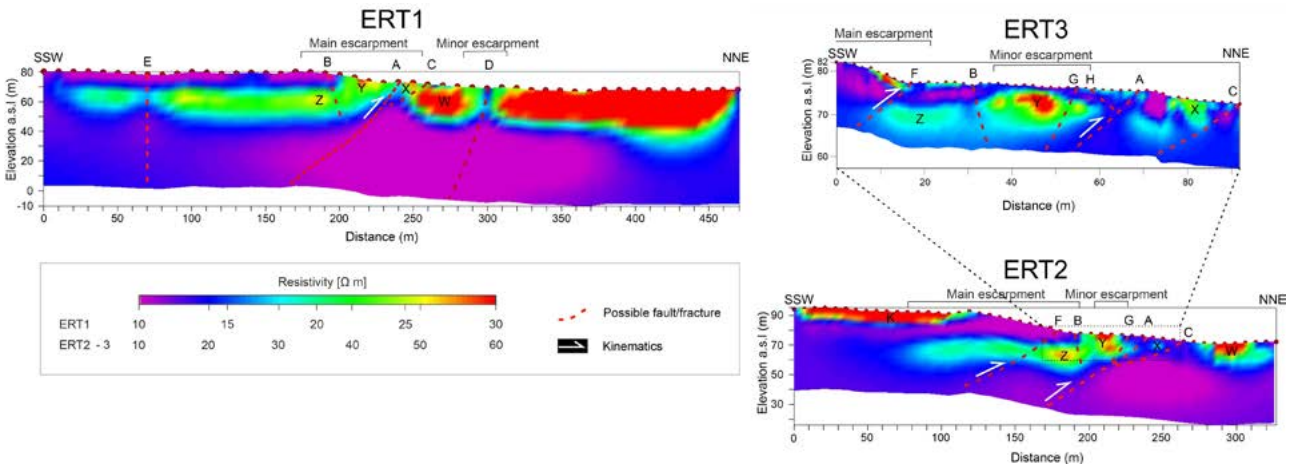

Figure 3 Electrical Resistivity Tomography (ERT) profiles with different length, depth of investigation and resolution acquired across the studied Broni-Sarmato deformation zone in a NNE-SSW orientation. For location see Figure 2b. The profiles are roughly orthogonal to the thrust scarps. ERT1 is the longest (length 470 m), ERT2 is shorter (329 m), providing depth of investigation down to about 70 m and 50 m, respectively. ERT3 is the shortest (94 m), providing high accuracy at shallow depths of ca. 15 m. Modified after Tibaldi et al. [2023].

Earthquake distribution and kinematics

The instrumental seismicity occurred in north-western Italy in the 1985-2020 time interval (Figure 4a), mainly localized south and south-west of the PTF. It is characterized by small-to-moderate-sized earthquakes with magnitude 0.1 ≤ M_L ≤ 4.9 and a low seismicity rate. In instrumental times, unlike the Ferrara-Romagna Arc, which experienced the Emilia 2012 seismic sequence (Mw 6.1), the study area was not affected by significant seismic activity, but only by minor events that never exceeded magnitude M_L 4.9. The major seismic sequence occurred in December 2008 at lower crustal depths (depth 19-20 km, M_L 4.9). The other event of M_L 4.9 that affected the area occurred in 2012 at sub-crustal depth (depth 60 km). The shallow seismicity (<10-12 km) along the Emilia Arc is not well constrained, while the deeper earthquakes, prevailing occurring at lower crustal depths (20-30 km), as well as the events occurring in the southern part of the study area, are better located also due to the local seismic networks.

The compilation of FMs from literature and the 7 new ones (Figure 4), computed in this study, well depicts the kinematic distribution of the study area. The new focal solutions provide additional information in areas where few FMs were previously available.

It is possible to observe that the study area undergoes a compressional-extensional pair (Figure 5a), and it is possible to identify three spatially distinct groups with rather homogeneous kinematics. The seismic events with reverse solutions are predominant in the central-eastern sector at the lower crust and subcrustal depths (see red-bordered group of FMs in Figure 5a). The southern-western events present a normal kinematics compatible with the northward prosecution of Lunigiana and Garfagnana extensional fault systems (Figures 5a and 5c); the strike-slip solutions characterize the western flank of the outer buried front of the Emilia Arc, giving it an asymmetric shape. The P and T average kinematics axes show a sub-horizontal SSW–NNE and SW-NE- trend, respectively (Figure 5b). The seismicity is not uniformly distributed, but rather clustered in specific zones, mainly close to known active faults (Figure 5e). The cluster analysis (Figures 5c and 5a) highlights 16 groups characterized by different energy released and mainly located to the south-eastern portion of the study area.

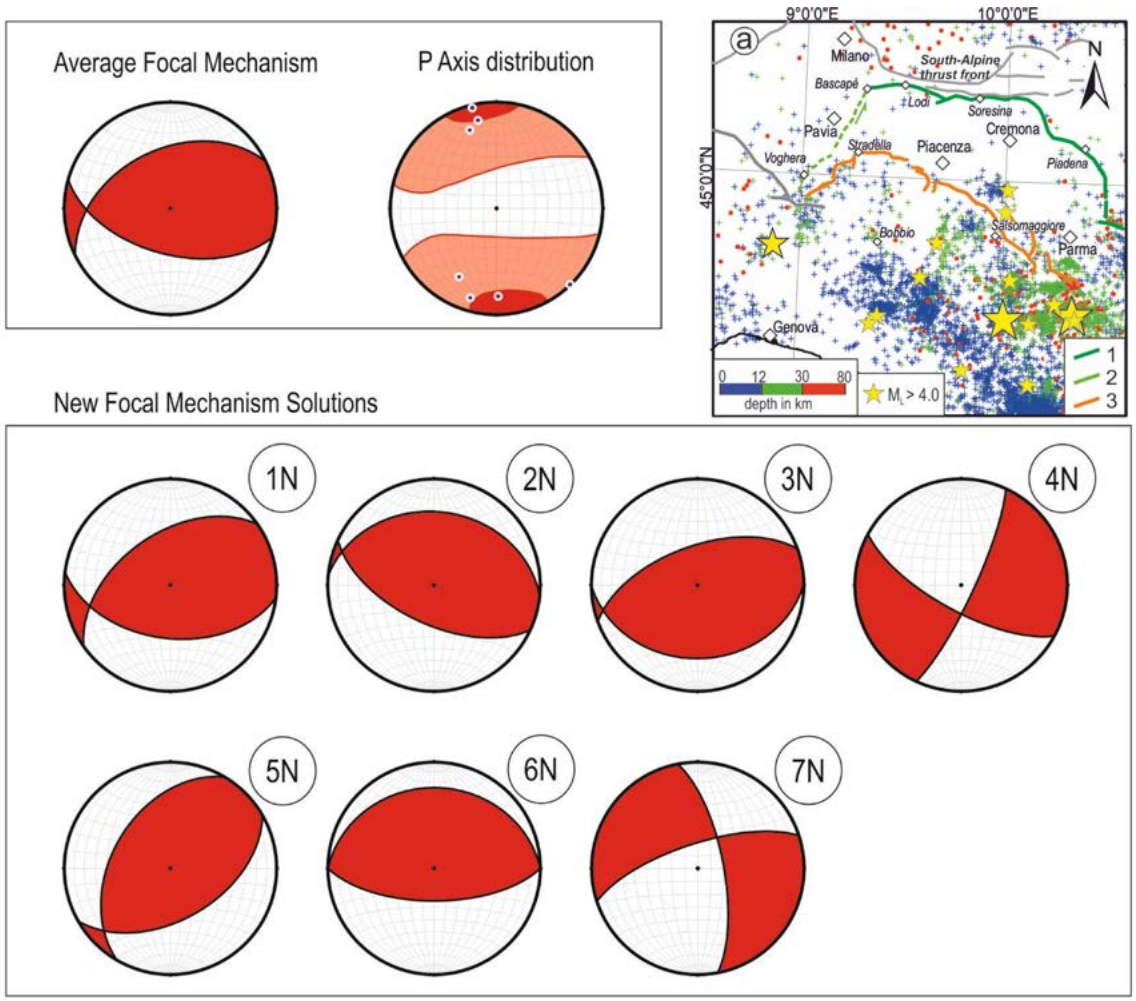

Figure 4 New focal mechanism solutions. The box "a" shows the seismicity south of the Stradella-Salsomaggiore thrust and in the Emilia Arc as computed considering the Italian Seismic Bulletin from 1985 to 2020 (0.4≤ML≤4.9).

Taking into account the prevailing depth range and kinematics, five clusters typology can be identified:

1. shallow extensional clusters (8, 9, 10, 11), localized along with the termination and northward prosecution of the Lunigiana-Garfagnana extensional fault system (LU-GA in Figure 5c);
2. shallow compressional clusters (1, 4), localized on the hanging-wall side of the Stradella-Salsomaggiore Arc;
3. shallow compressional clusters (6, 16) on the footwall side of the Stradella-Salsomaggiore Arc, possibly linked with the Cremona or Pavia Arcs basal detachments;
4. lower crust compressional clusters with almost pure dip-slip kinematics and an average NE-SW P-axis (2, 3, 12, 13, 14, 15), localized on the hanging-wall side of the Stradella-Salsomaggiore Arc, possibly linked with the Stradella thrust (cluster 2), the outermost SW-dipping frontal thrust of the Emilia Arc (clusters 3, 12, 15), and one of its deep backthrust (e.g., cluster 14);
5. shallow to lower crust strike-slip clusters (5 and 7) located along the Voghera-Pavia (Figure 5) north-western side of the Emilia Arc, with a NNE-SSW-trending P-axis.

Cluster 6, located between Parma and Piacenza towns, and cluster 15, both with reverse kinematics, are the most significant clusters in terms of energy released among shallow and deeper earthquakes respectively (M_L max 4.0, 1991, and M_L max 4.9, 2008 in Figure 5d).

Discussion and conclusions

The surface evidence of activity of the Stradella thrust is smooth, and the instrumental seismic activity at the fault hanging-wall is very minor, although with a little evidence of well-compatible reverse kinematics, which does not allow a simple direct answer on its potential seismogenic nature. In any case, due to a multi-scale and multi-disciplinary approach, we have collected several clues that support the presence of a compressional recent tectonic activity.

1. Along the Broni-Sarmato segment of the Stradella fault, a morpho-structural survey showed the presence of a major scarp (6-23 m-high) that has a rectilinear trace in plan view, with some left-stepping and right-stepping geometries. This evidence, together with other lithostratigraphic and geomorphological clues, indicates that the main scarp has not been created by the activity of the Po River. Instead, the general geometry of the scarp, the presence of hanging valleys and triangular facets, the offsets of Middle-latest Pleistocene terraces, and the over-incision of rivers in the uplifted block indicate that the origin of the scarp should be tectonic. The height and geometry of the scarp indicate that it resulted from successive incremental motions along a south-dipping reverse fault.
2. The geoelectrical surveys suggest the presence of a wide zone of shallow deformation at the Broni-Sarmato scarp, which represents a preferential flow path for deep saline waters and facilitates the flow towards the surface. Horizontal interruption and vertical dislocation of a shallow, high-resistivity layer also revealed by geoelectrical surveys suggest that the Broni-Sarmato fault possibly produced shallow deformation along vertical and inclined zones.
3. The age of the various offset terraces and the age of the deformed deposits visible in the geoelectrical sections reveal that the fault scarps developed until the Latest Pleistocene and, probably, the Holocene.
4. The 3D earthquake-fault association along the pede-Apennine thrust front, in the rear of the Emilia Arc, shows smooth evidence of NNE-directed compressional activity associated with the Stradella thrust, but more consistent data in support of seismogenic activity of the southernmost prosecution of the structure, along the Salsomaggiore thrust.
5. We identified three spatially distinct groups of earthquakes with rather homogeneous kinematics. The seismic events with reverse solutions are predominant in the central-eastern sector at the lower crust and subcrustal depths. The southern-western events present a normal kinematics compatible with the northward prosecution of Lunigiana and Garfagnana extensional fault systems. The strike-slip solutions characterize the western flank of the outer buried front of the Emilia Arc.
6. The P axes of already published and newly calculated FMs indicate an active SSW–NNE compression. This state of stress is compatible with the orientation and kinematics of the reverse Broni-Sarmato fault.

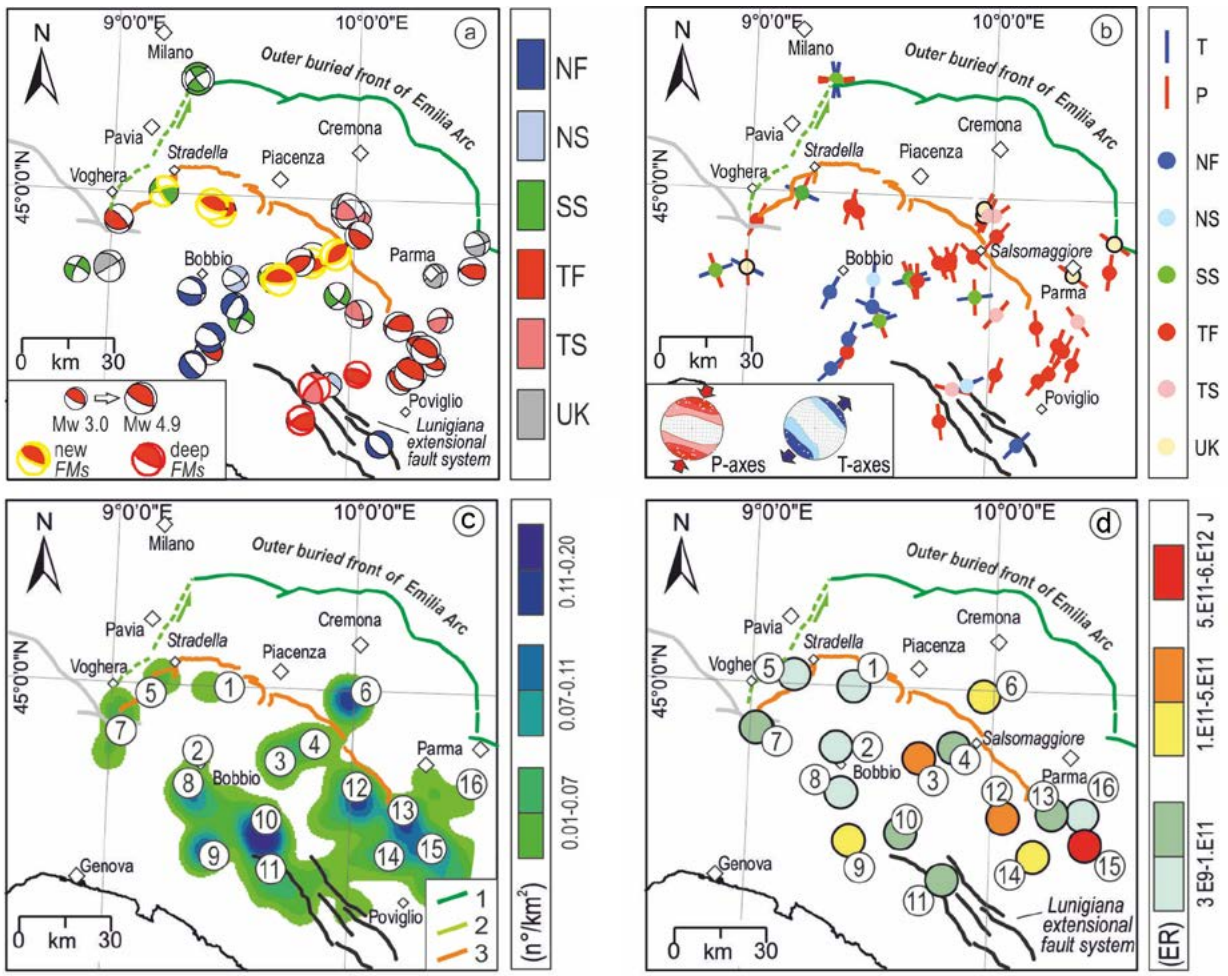

Figure 5 Seismicity analysis in the tectonic framework of the study area. (a) Map of the new (yellow colored border) and compiled focal mechanisms categorized following the Zoback kinematic classification. (b) Map of the P and T axis distribution of FM solutions. The left lower inset represents the P and T axis distribution and the average axes of the reverse/reverse oblique and normal/normal oblique FMs, respectively. (c) Map of the seismicity clusters detected by the Kernel Density Estimation (KDE) in geospatial analysis. LU-GA = Lunigiana-Garfagnana extensional fault system. (d) Map of the energy released by each selected cluster.

Acknowledgments

The work has been carried out under the framework of the CRUST - Interuniversity Center for 3D Seismotectonics with Territorial Applications, and under the aegis of the International Lithosphere Program, Task Force II. We acknowledge PetEx that provided the Move 2019.1 suite software license, and we thank Daniele Spallarossa and his colleagues for providing us the waveforms of the Regional Seismic Network of Northwestern Italy RSNI.

References

Benedetti, L.C., Tapponnier, P., Gaudemer, Y., Manighetti, I., and Van der Woerd, J., (2003). *Geomorphic evidence for an emergent active thrust along the edge of the Po Plain: The Broni-Stradella fault: evidence for an emergent thrust along the Po plain*. J. Geophys. Res., 108. https://doi.org/10.1029/2001JB001546

Bigi, G., Cosentino, D., Parotto, M., Sartori, R. and Scandone, P., [Eds.] (1990). *Structural Model of Italy (1:500.000)*, CNR-Progetto finalizzato geodinamica, Sheets 1 e 2, SELCA, Firenze.

Boccaletti, M., Coli, M., Eva, C., Ferrari, G., Giglia, G., Lazzarotto, A., Merlanti, F., Nicolich, R., Papani, G., and Postpischl, D., (1985). *Considerations on the seismotectonics of the Northern Apennines*. Tectonophysics, 7-38.

Burrato, P., Ciuffi, F., and Valensise, G., (2003). *An inventory of river anomalies in the Po Plain, Northern Italy: evidence for active blind thrust faulting.* Annals of Geophysics, 46. https://doi.org/10.4401/ag-3459

ISIDe Working Group, (2007). *Italian Seismological Instrumental and Parametric Database (ISIDe).* Istituto Nazionale di Geofisica e Vulcanologia (INGV). https://doi.org/10.13127/ISIDE (accessed 13 March 2022)

Lavecchia, G., de Nardis, R.D., Ferrarini, F., Cirillo, D., Bello, S., and Brozzetti, F., (2021). *Regional seismotectonic zonation of hydrocarbon fields in active thrust belts: a case study from Italy. In Building knowledge for geohazard assessment and management in the Caucasus and other orogenic regions* (pp. 89-128). Springer, Dordrecht.

Maesano, F.E., D'Ambrogi, C., Burrato, P., and Toscani, G., (2015). *Slip-rates of blind thrusts in slow deforming areas: Examples from the Po Plain (Italy).* Tectonophysics, 643, 8-25. https://doi.org/10.1016/j.tecto.2014.12.007

Pellegrini, G.B., and Vercesi, P.L., (1995). *Considerazioni morfoneotettoniche sulla zona a sud del Po tra Voghera (PV) e Sarmato (PC).* Atti Tic. Sci. Terra, 38, 95–118.

Pilla, G., Torrese, P., and Bersan, M., (2010). *Application of hydrochemical and preliminary geophysical surveys within the study of the saltwater uprising occurring in the Oltrepò Pavese plain aquifer.* Bollettino di Geofisica Teorica ed Applicata, 51 (4).

Rovida, A., Locati, M., Camassi, R., Lolli, B., Gasperini, P., and Antonucci, A., (eds) (2021). *Italian Parametric Earthquake Catalogue (CPTI15), version 3.0.* Istituto Nazionale di Geofisica e Vulcanologia (INGV). https://doi.org/10.13127/CPTI/CPTI15.3

Tibaldi, A., de Nardis, R., Torrese, P., Bressan, S., Pedicini, M., Talone, D., Bonali, F.L., and Lavecchia, G., (2023). *A multi-scale approach to the recent activity of the Stradella thrust in the seismotectonic context of the Emilia Arc (northwestern Italy).* Tectonophysics, 857, 229853. https://doi.org/10.1016/j.tecto.2023.229853

Toscani G., Bonini, L., Ahmad, M.I., Di Bucci, D., Di Giulio, A., Seno, S., and Galuppo, C., (2014). *Opposite verging chains sharing the same foreland: Kinematics and interactions through analogue models (Central Po Plain, Italy).* Tectonophysics, 633, 268-282. https://doi.org/10.1016/j.tecto.2014.07.019.

Zuffetti, C., Bersezio, R., Contini, D., and Petrizzo, M.R., (2018). *Geology of the San Colombano hill, a Quaternary isolated tectonic relief in the Po Plain of Lombardy (Northern Italy).* Journal of Maps, 14, 199–211. https://doi.org/10.1080/17445647.2018.1443166

Zuffetti, C., and Bersezio, R., (2020). *Morphostructural evidence of Late Quaternary tectonics at the Po Plain-Northern Apennines border (Lombardy, Italy).* Geomorphology, 364, 107245. https://doi.org/10.1016/j.geomorph.2020.107245

Application of a C0-Class Drone for 3D Reconstruction and Morphotectonic Analysis: An Example from the Broni–Sarmato Fault, Emilia Arc (Northern Italy)

Fabio Luca Bonali[1,2,*], Lorenzo Suranna[1], Alessandro Luppino[1], Giovanni Piccio[1], Sofia Brando[1], Giovanni Toscani[2,3], Patrizio Torrese[3], and Alessandro Tibaldi[1,2]

[1]Università di Milano Bicocca, Dipartimento di Scienze dell'Ambiente e della Terra, Milan, Italy
[2]Centro Interuniversitario per la Sismotettonica 3D con Applicazioni Territoriali (CRUST), Chieti, Italy
[3]Università di Pavia, Dipartimento di Scienze dell'Ambiente e della Terra, Pavia, Italy

Corresponding author: fabio.bonali@unimib.it

Introduction and geological background

The outermost sector of the Northern Apennines is buried beneath a thick succession of Plio-Pleistocene deposits, locally reaching 7-8 km in thickness [Bigi et al., 1990]. Convergence in this region is accommodated by a complex system of thrusts and folds [Burrato et al., 2003; Zuffetti and Bersezio, 2020; Lavecchia et al., 2021]. However, structural orientations are often scattered, and the relationships between fault geometry and seismicity remain poorly constrained due to the limited instrumental seismic record, particularly in the central-western portion of the buried front. This area corresponds to the Monferrato and Emilia arcs, the latter representing the focus of this study. Within the Emilia Arc, two major north-verging thrust systems can be distinguished. From south to north, these include: (1) the Pede-Apennine Thrust Front (PTF; [Boccaletti et al., 1985]), which bounds the outcropping Miocene fold-and-thrust belt of the Northern Apennines and hosts the Broni-Sarmato sector investigated in this work; and (2) the buried thrusts of the Emilia Southern and Central Po Plain Structures [Toscani et al., 2014], active at least until the Early Pleistocene according to surface and subsurface evidence [Maesano et al., 2015; Zuffetti et al., 2018] (Figure 1).

The Broni-Sarmato scarp and study objectives

Based on morphotectonic evidence, Benedetti et al. [2003] identified Quaternary activity along a 35-km-long segment of the Emilia Pede-Apennine Thrust Front (PTF) between Montebello and Sarmato, known as the Stradella Thrust. Cumulative surface offsets of 2-25 m and degraded scarps suggest late Quaternary reactivations (10-100 ka BP). The fault comprises two main segments east and west of Broni (Figure 2), with the eastern one -here termed the Broni-Sarmato Fault- representing the focus of this study. The Broni-Sarmato scarp (Figure 2a) bounds three main fluvial terraces composed of Apennine clays and sands, which differ in elevation and degree of weathering. These terraces (T1, T2, T3 in Figure 2a), formed by Po River tributaries during progressive uplift of the area, are dated to the middle (T2-T3) and late Pleistocene (T1) [Benedetti et al., 2003]. The northern margin of the terraces shows triangular facets and perched valleys, further supporting a tectonic origin of the scarp. The fault trace is discontinuous and segmented, with left- and right-stepping sections separated by 60-260 m, and a major right step of about 1.8 km between Casa Olmo and Castel San Giovanni. Thirty high-precision GPS profiles across the scarp indicate vertical offsets of 6-23 m [Tibaldi et al., 2023]. Measurements along a minor scarp at the base of the main fault are reported in Figure 2b.

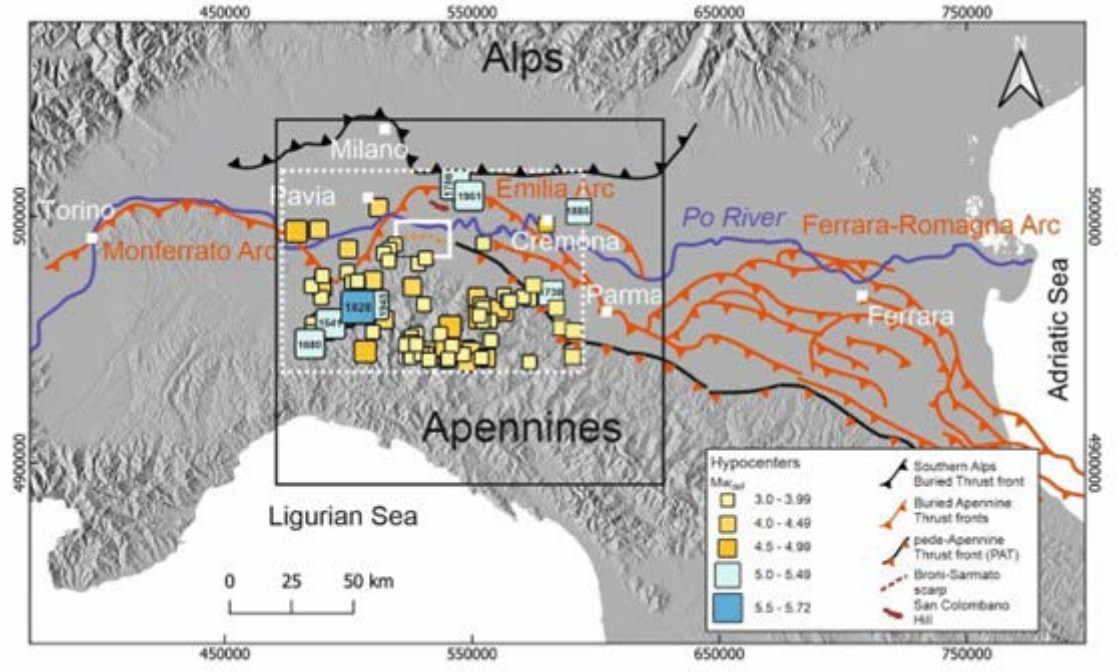

Figure 1 Location of the study areas (highlighted boxes) within the broader structural framework of the Northern Apennines, modified after Tibaldi et al. [2023]. The northern sector of the Apennine fold-and-thrust belt comprises three main arcuate systems, arranged from west to east as the Monferrato, Emilia, and Ferrara-Romagna arcs, all buried beneath the Quaternary infill of the Po Plain. Earthquake hypocenters occurring between 1000 A.D. and 2020 inside the white dashed rectangle are derived from the CPTI15 catalogue [Rovida et al., 2022] and the ISIDe database [ISIDe Working Group, 2007].

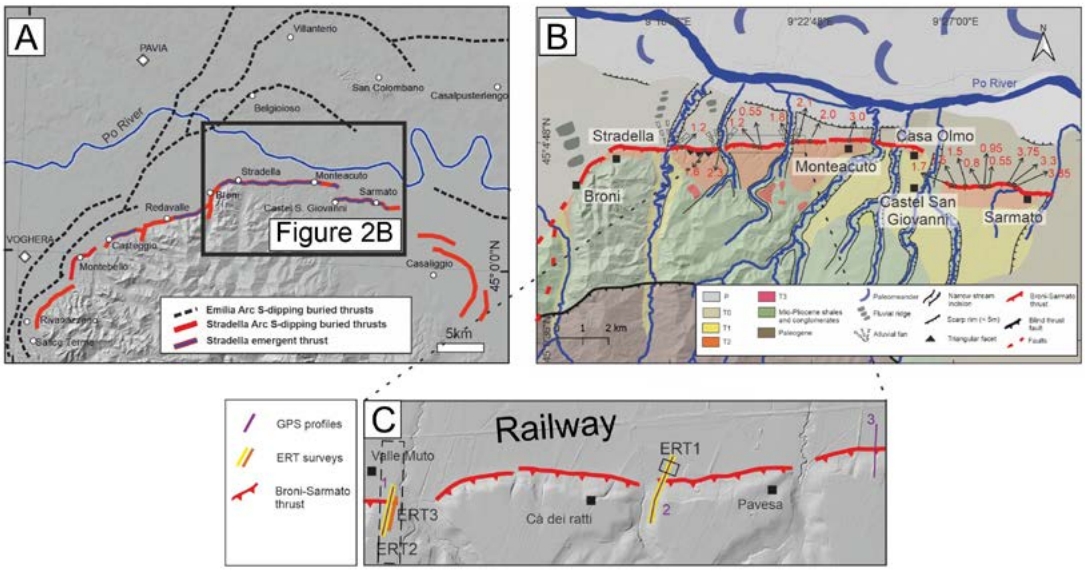

Figure 2 Tectonic and morphotectonic framework of the Stradella-Salsomaggiore Arc. (a) Regional setting and trace of the Stradella Thrust (modified after [Bigi et al., 1990; Martelli et al., 2017; CARG, 2016]). The black box marks the Broni-Sarmato segment studied by Tibaldi et al. [2023]. (b) Geological and geomorphological map of the area (modified after Tibaldi et al. [2023]). Colours show Palaeogene, Miocene-Pliocene, and Quaternary units. Fluvial terraces (T1-T3) differ in elevation and weathering, while T0 marks the coalescent surface of the Apennine River deposits. (c) Locations of GPS profiles (purple), ERT surveys (yellow/orange), and the UAV-surveyed area of this study (black squares) along the Broni-Sarmato Thrust, parallel to the local railway.

In this study, we present a high-resolution dataset obtained through UAV-based photogrammetry, acquired with a C0-class drone (DJI Mini 4 Pro), demonstrating its effectiveness in detecting and quantifying minor fault scarps that were not highlighted by Benedetti et al. [2003], but may represent potential sites for further investigation. The compact and lightweight UAV platform enabled ultra-low-altitude image acquisition with centimetric spatial resolution, ideally suited to identify subtle geomorphic features associated with active deformation. A major operational advantage of using a C0-class UAV lies in its compliance with the European "Open" category (subcategory A1) regulation, which allows safe and legal flights over roads, buildings, and people, provided that no gatherings are present. This regulatory framework makes it possible to perform detailed morphotectonic investigations even in inhabited or infrastructure-dense areas representing conditions where heavier UAVs (≥250 g) require specific authorization or operational limitations. Given the proximity of the Broni-Sarmato structure to several urban areas and the absence of clear seismic signatures, detailed UAV-based analyses were performed to better characterize its surface expression and morphotectonic features. The identified minor scarps are the target of forthcoming near-surface geophysical surveys, including Electrical Resistivity Tomography (ERT) and shallow seismic profiling, aimed at further constraining their subsurface geometry and assessing their possible tectonic origin. The specific area selected for the UAV survey and subsequent 3D reconstruction is shown in Figure 2c.

Methodology

Prior to field operations, flight restrictions and airspace conditions for the study area were verified through the Italian d-Flight platform [1], ensuring full compliance with national and European UAV regulations. The total survey area was subsequently subdivided into smaller flight sectors to optimize battery use, maintain visual line-of-sight control, and minimize potential interference with local bird activity. All flights were carried out using a DJI Mini 4 Pro (C0-class drone equipped with a 12 Mpx camera) at a constant altitude of 60 m above the take-off point. Image acquisition was performed manually, as this UAV model does not support automated or pre-programmed flight paths. The camera captured images at two-second intervals during continuous flight, with speeds ranging between 3 and 6 m/s to ensure sufficient image overlaps and minimize motion blur. This configuration allowed the collection of high-resolution, nadir-oriented imageries suitable for subsequent Structure-from-Motion (SfM) photogrammetric processing, following workflows similar to those described by Bonali et al. [2019] and Fallati et al. [2019]. The chosen parameters ensured a dense image network and accurate ground coverage.

We collected a total of 989 photographs, as shown in Figure 3. Each image contains EXIF metadata, including the GPS position referenced to the WGS84 datum, which was used for initial geolocation during the photogrammetric processing. Agisoft Metashape was selected as the processing platform because of its user-friendly interface, intuitive workflow, and the high quality of the point clouds it produces, which have made it one of the most widely adopted Structure-from-Motion (SfM) software packages within the geological and geomorphological research community [Benassi et al., 2017; Burns and Delparte, 2017; Cook, 2017; Bonali et al., 2019]. Prior to model reconstruction, the image overlap was verified and found to be greater than 90% within the survey area, consistent with the adopted acquisition strategy. The first alignment step was performed in low-quality mode to ensure rapid assessment of image geometry and camera position. Subsequently, a photo quality check was carried out, and only images with quality value greater than 0.7 were retained for further processing.

The entire image set was then aligned in high-quality mode using Agisoft Metashape Professional (Agisoft LLC, 2023), allowing the software to use the full resolution of each photograph during

image matching. Both Generic and Reference (GPS) preselection settings were enabled to enhance matching accuracy and computational efficiency by exploiting the approximate camera positions recorded in the EXIF metadata. This process generated the sparse point cloud (tie points) and optimized the estimated camera parameters, providing the basis for the subsequent dense point cloud reconstruction. According to the Agisoft Metashape Professional v.2.0 User Manual (Agisoft LLC, 2023), the sparse point cloud consists of automatically detected tie points identified across overlapping images during the alignment phase. These tie points are used to refine both the internal camera calibration parameters and the external orientation of each image, forming the geometric foundation for the later stages of dense reconstruction and 3D model generation. Following image alignment, the dense point cloud was generated in high-quality mode using Mild depth filtering. This configuration allowed the reconstruction of the model at the maximum possible resolution, minimizing the loss of detail and avoiding excessive smoothing of small-scale topographic features. The adopted parameters ensured an optimal balance between accuracy and processing efficiency, resulting in a high-fidelity representation of the surveyed surface.

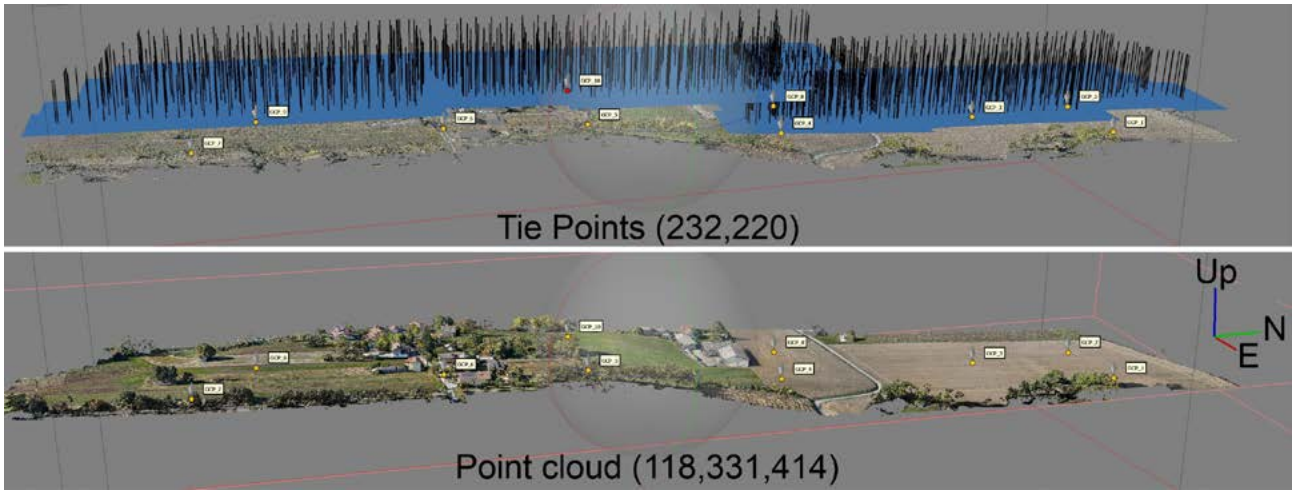

Figure 3 Three-dimensional view of the photogrammetric processing in Agisoft Metashape. Top: sparse point cloud showing the distribution of tie points (232,220) used for camera alignment and the positions of the photographs acquired with the DJI Mini 4 Pro UAV during the survey. Bottom: high-quality dense point cloud (118,331,414 points) representing the detailed surface morphology of the Broni-Sarmato survey area. The yellow markers indicate the Ground Control Points (GCPs) used for georeferencing.

The use of the high-quality setting was particularly effective for capturing the subtle morphology of minor scarps and slope breaks along the Broni-Sarmato Fault, which are often poorly expressed in lower-resolution models. The resulting dense point cloud formed the basis for the subsequent generation of the Digital Surface Model (DSM) and orthomosaic, used for morphotectonic interpretation and quantitative analyses. Before the production of the DSM, the dense point cloud was georeferenced using ten Ground Control Points (GCPs) acquired in the field with an Emlid Reach RS+ GNSS receiver operating in Real-Time Kinematic (RTK) mode. The receiver was connected to the SPIN GNSS network managed by the Regione Lombardia [2], which provided real-time differential corrections.

Because the study area is a natural environment with few permanent and clearly recognizable features, the GCPs were collected on artificial targets placed on the ground prior to the UAV flight. These targets were evenly distributed across the survey area to ensure homogeneous spatial control and minimize geometric distortion during model scaling (Figure 3). The RTK coordinates were further corrected using the EGM2008 global geoid model, ensuring accurate

conversion from ellipsoidal to orthometric heights. The integration of RTK and geoid corrections provided centimetric accuracy in both planimetric and vertical components. This georeferencing step ensured that the resulting DSM and orthomosaic were properly scaled and geographically consistent. Additionally, the dense point cloud can be used to generate fully navigable 3D models and tiled reconstructions that can be shared on the web [3] or explored through immersive Virtual Reality systems [Tibaldi et al., 2020], providing an effective tool for scientific visualization, education, and public dissemination of morphotectonic data.

Results and applications

The photogrammetric workflow produced a sparse point cloud (tie points) and a high-quality dense point cloud (Figure 3), which served as the basis for generating the Digital Surface Model (DSM), the orthomosaic, and the 3D Tiled Model of the Broni–Sarmato survey area (Figure 4). The DSM has a spatial resolution of 4.23 cm/pixel, while the orthomosaic reaches a ground resolution of 2.11 cm/pixel (Figure 4).

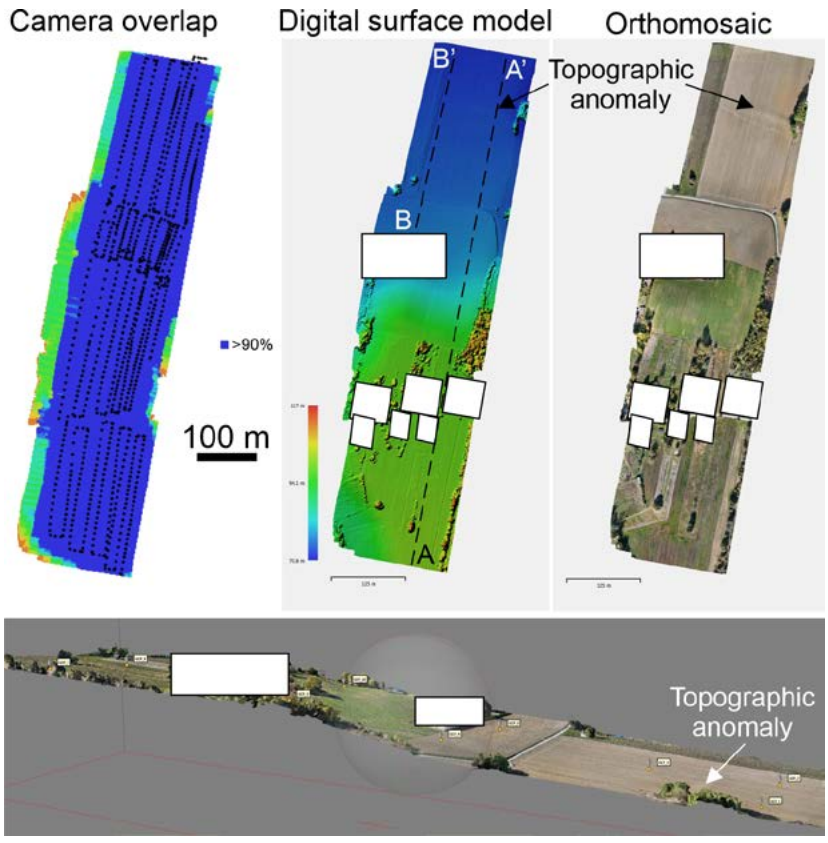

Figure 4 Results of the UAV photogrammetric processing for the Broni-Sarmato survey area. Top: camera overlap map showing that the area of interest is characterized by an image overlap greater than 90% (left); Digital Surface Model (DSM) coloured by elevation (centre); and orthomosaic derived from the same dataset (right). The newly detected scarp is highlighted in both the DSM and the orthomosaic. Bottom: perspective view of the 3D Tiled Model, showing the same area, where the new scarp is clearly visible. Private buildings were excluded from the visual outputs and masked with white rectangles for privacy reasons.

The UAV survey covered an elongated area of approximately 865 m (N-S) × 210 m (E-W), corresponding to about 0.18 km², along the Broni-Sarmato fault zone (Figures 2-4). These

high-resolution products provide a detailed and accurate representation of the surveyed sector, allowing the recognition of subtle morphotectonic features that were not detectable in previous lower-resolution topographic datasets.

The DSM highlights fine-scale elevation variations along the main fault scarp and adjacent terraces, while the orthomosaic provides a realistic visual context for mapping and field validation. Thanks to these high-resolution models, two previously unmapped minor scarps were identified in the northernmost meadow area, which were not visible in earlier DEMs or cartographic products. The integration of the DSM and orthomosaic enabled the precise location and quantitative measurement of minor scarps height and morphological anomalies, which represent key parameters for identifying and characterizing recent/active deformation.

Topographic profiles A-A′ and B-B′ (Figure 5), extracted from the DSM, clearly show subtle slope breaks of 21, 43, and 71 cm in height, identified at three different points along the two topographic profiles. These features correspond to minor scarps that have now been validated in the field (Figure 5), but were not detected on previous lower-resolution DSM models.

The two scarps showing height differences of 43 and 71 cm correspond to the location of a secondary road and, although an anthropogenic origin cannot be excluded, the southern portion of the topographic profile remains higher than the northern segment.

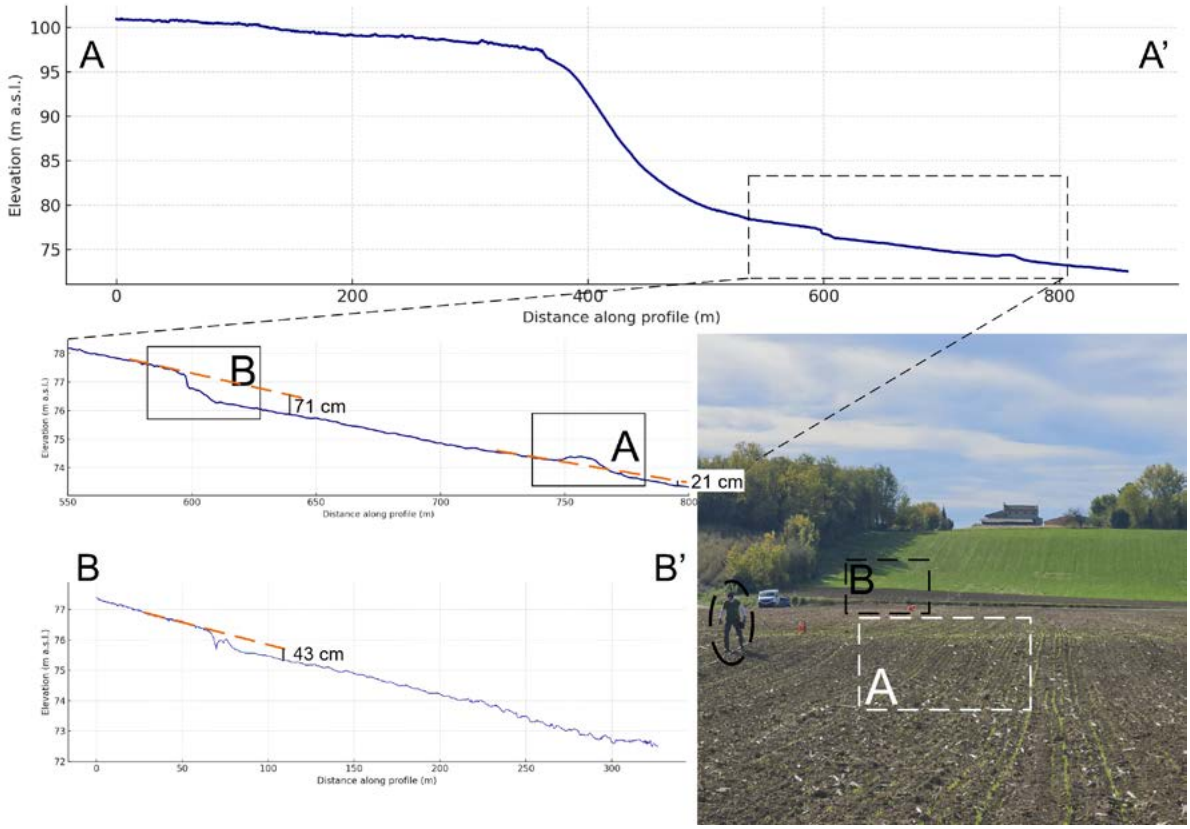

Figure 5 DSM-derived topographic profiles and corresponding field view. Top: complete profile A-A′ showing the overall topographic gradient and the location of the analysed sector (dashed box). Middle: enlarged view of the 550-800 m portion of the profile, highlighting subtle slope breaks associated with features A and B, showing height differences of 21 and 71 cm, respectively. Bottom: detail of profile B-B′ showing a height difference of 43 cm. The red dashed segments represent the projected continuation of the slope, emphasizing the height differences along the topographic profiles. Right: field photograph indicating the location of the analysed sectors A and B, where gentle morphological steps are visible on the cultivated surface. The locations of profiles A-A′ and B-B′ are shown in Figure 4. All topographic profiles are vertically exaggerated to better highlight the morphological anomalies.

This configuration suggests a possible uplift of the southern sector, which should be verified through further investigations, including near-surface geophysical methods such as ERT, seismic, and GPR profiling. In addition, the area showing a bulging-like morphology and a vertical difference in elevation of about 21 cm may also deserve further investigation.
Overall, these results demonstrate the effectiveness of lightweight UAV-based photogrammetry for the high-precision detection of topographic anomalies with a potential morphotectonic origin, and for detailed mapping in low-relief and semi-urban environments.
The significance of these results lies primarily in the identification of previously unrecognized topographic anomalies, expressed as decimetre-scale scarps. These observations clearly call for further investigations to determine whether such features are of tectonic or anthropogenic origin.

Concluding remarks

The UAV-derived models revealed subtle morphological anomalies along the Broni-Sarmato fault zone, including minor scarps and a local bulging area, which deserve geophysical investigations to assess if they reflect shallow deformation or anthropogenic modifications. In light of these results, the investigations proposed by Tibaldi et al. [2023] should be expanded by extending the ERT2 profile northwards, across the anomalies detected by drone photogrammetry. This integrated approach will better constrain the shallow geometry and recent activity of the Broni-Sarmato Fault.

References

Benassi, F., Dall'Asta, E., Diotri, F., Forlani, G., Morra di Cella, U., Roncella, R., and,Santise, M., (2017). *Testing accuracy and repeatability of UAV blocks oriented with GNSS-supported aerial triangulation*. Remote Sensing, 9, 172. https://doi.org/10.3390/rs9020172

Benedetti, L.C., Tapponnier, P., Gaudemer,Y., Manighetti, I,. and Van der Woerd, J,. (2003). *Geomorphic evidence for an emergent active thrust along the edge of the Po Plain: the Broni-Stradella fault*. Journal of Geophysical Research, 108, 2238. https://doi.org/10.1029/2001JB001546

Bigi, G., Cosentino, D., Parotto, M., Sartori, R., and Scandone, P., (Eds.) (1990). *Structural Model of Italy (1:500,000)*. CNR–Progetto Finalizzato Geodinamica, SELCA, Firenze

Boccaletti, M., Coli, M., Eva, C., Ferrari, G., Giglia, G., Lazzarotto, A., Merlanti, F., Nicolich, R., Papani, G., and Postpischl, D., (1985). *Considerations on the seismotectonics of the Northern Apennines*. Tectonophysics, 117, 7-38. https://doi.org/10.1016/0040-1951(85)90234-3

Bonali, F.L., Tibaldi, A., Marchese, F., Fallati, L., Russo, E., Corsini, A., and Savio, G., (2019). *UAV-based photogrammetry and geostructural analysis of rock slopes: a new approach for the study of inaccessible outcrops*. Geomorphology, 350, 106913. https://doi.org/10.1016/j.geomorph.2019.106913

Burns, J.H.R., and Delparte, D., (2017). *Comparison of commercial structure-from-motion photogrammety software used for underwater three-dimensional modeling of coral reef environments*. The International Archives of the Photogrammetry, Remote Sensing and Spatial Information Sciences, 42, 127-131

Burrato, P., Ciuffi, F., and Valensise, G., (2003). *An inventory of river anomalies in the Po Plain, Northern Italy: evidence for active blind thrust faulting*. Annals of Geophysics, 46, 865-882. https://doi.org/10.4401/ag-3459

CARG, (2016). *Carta geologica d'Italia, scale 1:50,000, Voghera sheet n.178*. ISPRA

Cook, K.L., (2017). *An evaluation of the effectiveness of low-cost UAVs and structure-from-motion for geomorphic change detection*. Geomorphology, 278, 195-208. https://doi.org/10.1016/j.

geomorph.2016.11.009
Fallati, L., Bonali, F.L., and Giannecchini, R., (2019). *UAV-based analysis of slope instability processes: comparison with traditional field methods*. Geomatics, Natural Hazards and Risk, 10, 1870-1888. https://doi.org/10.1080/19475705.2019.1650125
ISIDe Working Group, (2007). *Italian Seismological Instrumental and Parametric Database (ISIDe)*. Istituto Nazionale di Geofisica e Vulcanologia (INGV). https://doi.org/10.13127/ISIDE (accessed 13 March 2022)
Lavecchia, G., De Nardis, R., Ferrarini,F., Cirillo, D., Bello, S. and Brozzetti, F., (2021). *Regional seismotectonic zonation of hydrocarbon fields in active thrust belts: a case study from Italy*. In: Building Knowledge for Geohazard Assessment and Management in the Caucasus and Other Orogenic Regions. Springer, Dordrecht, pp. 89-128.
Maesano, F.E., D'Ambrogi, C., Burrato, P., and Toscani, G., (2015). *Slip rates of blind thrusts in slow deforming areas: examples from the Po Plain (Italy)*. Tectonophysics, 643, 8-25. https://doi.org/10.1016/j.tecto.2014.12.007
Martelli, L., Santulin, M., Sani, F., Tamaro, A., Bonini, M., Rebez, A., Corti, G., and Slejko, D., (2017). *Seismic hazard of the Northern Apeninnes based on 3D seismic sources*. Journal Seismology, 21, 1251-1275. https://doi.org/10.1007/s10950-017-9665-1
Rovida, A., Locati, M., Camassi, R., Lolli, B., Gasperini, P., and Antonucci, A., (2022). *Italian Parametric Earthquake Catalogue (CPTI15), version 4.0*. Istituto Nazionale di Geofisica e Vulcanologia (INGV). https://doi.org/10.13127/CPTI/CPTI15.4
Tibaldi, A., Bonali, F.L., Vitello, F., Delage, E., Nomikou, P., Antoniou, V., and Whitworth, M., (2020). *Real world–based immersive Virtual Reality for research, teaching and communication in volcanology*. Bulletin of Volcanology, 82(5), 38. https://doi.org/10.1007/s00445-020-01377-6
Tibaldi, A., de Nardis, R., Torrese, P., Bressan, S., Pedicini, M., Talone, D., Bonali, F.L., and Lavecchia., G., (2023). *A multi-scale approach to the recent activity of the Stradella thrust in the seismotectonic context of the Emilia Arc (northwestern Italy)*. Tectonophysics, 857, 229853. https://doi.org/10.1016/j.tecto.2023.229853
Toscani, G., Bonini, L., Ahmad, M.I., Di Bucci, D., Di Giulio, A., Seno, S., and Galuppo, C., (2014). *Opposite verging chains sharing the same foreland: kinematics and interactions through analogue models (Central Po Plain, Italy)*. Tectonophysics, 633, 268-282. https://doi.org/10.1016/j.tecto.2014.07.019
Zuffetti, C., and Bersezio, R., (2020). *Morphostructural evidence of Late Quaternary tectonics at the Po Plain–Northern Apennines border (Lombardy, Italy)*. Geomorphology, 364, 107245. https://doi.org/10.1016/j.geomorph.2020.107245
Zuffetti, C., Bersezio, R., Contini, D., and Petrizzo, M.R., (2018). *Geology of the San Colombano hill, a Quaternary isolated tectonic relief in the Po Plain of Lombardy (Northern Italy)*. Journal of Maps, 14, 199-211. https://doi.org/10.1080/17445647.2018.1443166

Sitography

[1] https://www.d-flight.it/new_portal/
[2] https://www.regione.lombardia.it/wps/portal/istituzionale/HP/DettaglioServizio/servizi-e-informazioni/enti-e-operatori/territorio/sistema-informativo-territoriale-sit/spin-gnss-posizionamento-satellitare/spin-gnss-posizionamento-satellitare
[3] https://geovires.unimib.it/

Terrestrial LiDAR survey to overcome UAV flight restrictions in morphotectonic analyses: an example from the Budoia–Aviano Thrust (NE Italy)

Fabio Luca Bonali[1,2,*], Lorenzo Suranna[1], Alessandro Luppino[1], Noemi Corti[1], Alberto Villa[1], Giovanni Piccio[1], Sofia Brando[1], Giulia Patricelli[3,4], Enzo Rizzo[4], Maria Eliana Poli[3], and Alessandro Tibaldi[1,2]

[1]Università di Milano Bicocca, Dipartimento di Scienze dell'Ambiente e della Terra, Milan, Italy
[2]Centro Interuniversitario per la Sismotettonica 3D con Applicazioni Territoriali (CRUST), Chieti, Italy
[3]Università di Udine, Dipartimento di Scienze AgroAlimentari, Ambientali e Animali, Udine, Italy
[4]Università di Ferrara, Dipartimento di Fisica e Scienze della Terra, Ferrara, Italy

Corresponding author: fabio.bonali@unimib.it

Introduction

The study area is situated along the outer Pliocene–Quaternary deformation front of the Eastern Southern Alps (ESA) accommodating about 2-3 mm/yr of crustal shortening, as inferred from GNSS-based geodetic observations [Devoti et al., 2011; Serpelloni et al., 2016; Areggi et al., 2023]. This sector is characterised by a belt of curved, WSW–ENE-oriented, SSE-verging thrusts that disrupt Late Pleistocene to Holocene sediments of the Friulian piedmont plain [Galadini et al., 2005; Poli et al., 2021; 2024]. Among these structures, the Polcenigo-Montereale Thrust System comprises multiple SSE verging branches, including the Budoia-Aviano (BA) and Vigonovo (VI) thrusts, both displaying geological and geomorphological indications of ongoing deformation, including pre-LGM conglomerate outcrops, upwarping of the late Pleistocene–Holocene Artugna alluvial fan, drainage anomalies, and morphological scarps (Figure 1) [Poli et al., 2015].

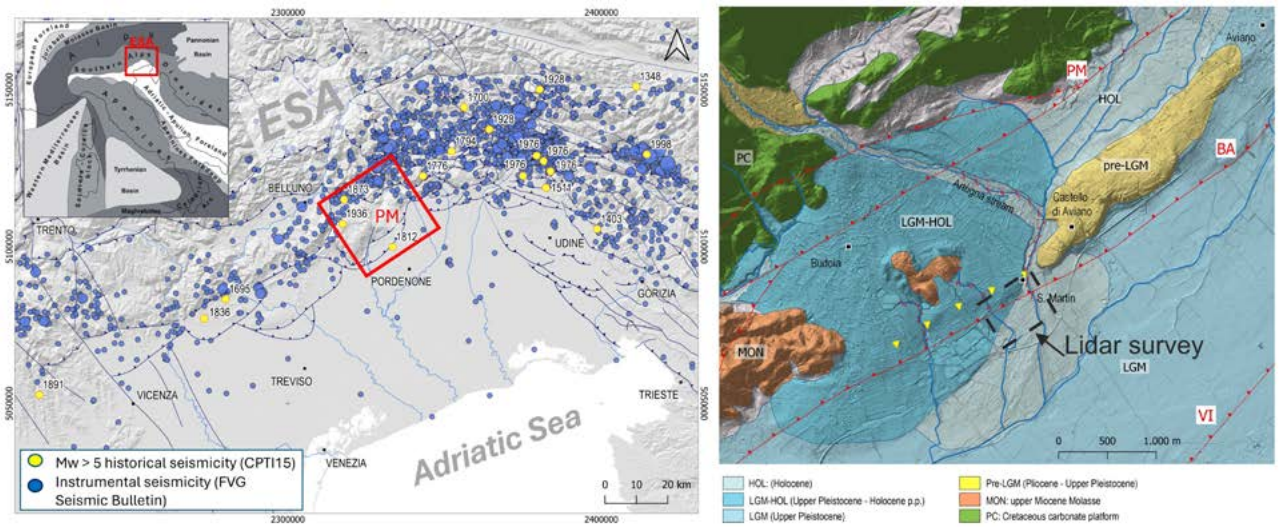

Figure 1 Tectonic and seismic framework of the study area, located at the front of the Carnic Prealpine sector of the Eastern Southern Alps. In the left panel, active faults and instrumental/historical earthquakes [Patricelli et al., 2024; Rovida et al., 2022] are shown. In the right panel, morphotectonic map of the investigated area (modified after Poli et al. [2015]).

Geophysical investigation also highlighted anomalies at depth, possibly related to the recent tectonic activity of the Budoia-Aviano and Vigonovo Thrusts [Rizzo et al., 2024]. In this note, we provide a detailed 3D documentation and analysis of the BA fault zone using a high-resolution, ground-based LiDAR approach. The dataset was acquired with a handheld GeoSLAM ZEB Horizon scanner, enabling the collection of precise morphotectonic information in an area where unmanned aerial vehicle (UAV) operations are prohibited due to the proximity of the Aviano NATO air base (ENAC D-Flight restricted area; Figure 2).

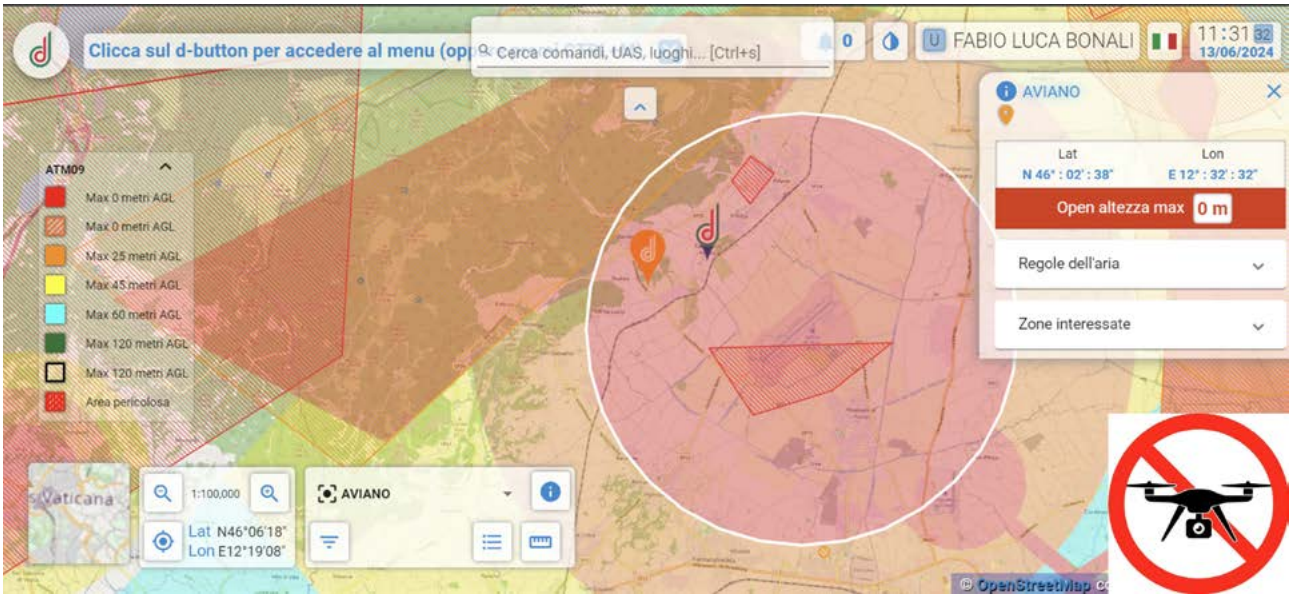

Figure 2 Screenshot from the D-Flight web application [1] showing the airspace restrictions around the Aviano area. The study site (orange marker) lies entirely within the no-fly zone (maximum altitude 0 m AGL) imposed due to the presence of the Aviano NATO air base, which prevents the use of UAVs for photogrammetric surveys. The "drone prohibited" logo was manually added to the image for illustrative purposes.

The results demonstrate that SLAM-based terrestrial LiDAR can achieve spatial resolutions and accuracies comparable to UAV photogrammetry while fully complying with airspace regulations. This approach highlights the potential of portable LiDAR mapping as an effective alternative for studying active fault zones in restricted or logistically challenging environments.

Methodology

Fieldwork was carried out along the BA using a GeoSLAM ZEB Horizon handheld LiDAR coupled with an Emlid Reach RS+ GNSS receiver operating in Real-Time Kinematic (RTK) mode for ground control. To improve efficiency and ensure stable data acquisition, a custom metallic backpack mount was adapted to host the GeoSLAM sensor, its data logging unit, and the RTK antenna (Figure 3). This configuration allowed the operator to perform the survey autonomously even over extended areas, maintaining optimal line-of-sight and positioning stability.

During acquisition, the operator periodically stopped for approximately 10 seconds at selected locations to allow the GeoSLAM system to register fixed reference points, while the same points were simultaneously logged in the GNSS mobile application. The paired measurements

were subsequently employed to achieve absolute georeferencing of the point cloud using the WGS84 reference datum and UTM Zone 33N coordinate system.

Figure 3 Custom backpack-mounted configuration used for the GeoSLAM ZEB Horizon handheld LiDAR survey. The metallic frame was adapted to host the scanner, the data logging unit, and the Emlid Reach RS+ GNSS antenna (operating in RTK mode), allowing autonomous data collection and accurate georeferencing of the point cloud. The system enabled the operator to perform extended surveys efficiently, even across large areas, as shown in the central panel. The right panels show details of the GeoSLAM ZEB Horizon unit and the Emlid Reach RS+ GNSS antenna.

Scanning paths were executed along the main morphotectonic features over an area of roughly 0.4 km². The acquired data were processed using GeoSLAM Connect and GeoSLAM Draw, resulting in a high-resolution Digital Surface Model (DSM) with a spatial resolution of ~2.7 cm/pixel. The integrated LiDAR–RTK workflow achieved a mean RMSE of 0.02–0.03 m, consistent with previously reported performance values [Urban et al., 2024; Petrov et al., 2024]. At the beginning of the acquisition phase, the survey area was subdivided a priori into four smaller sectors, each surveyed individually to optimize data collection and instrument performance. All scanning sessions shared a common network of Ground Control Points (GCPs) acquired in RTK mode, ensuring precise alignment among the different datasets. This strategy allowed effective management of acquisition time and data size while maintaining consistent georeferencing accuracy.
The four point clouds (Figure 4) were referenced and merged in GeoSLAM Connect, producing a single unified point cloud for the area of interest. This dataset was then imported into Agisoft Metashape, where it was processed to generate the final high-resolution Digital Surface Model (DSM) used for subsequent morphotectonic analysis, with a final resolution of 2.7 cm/pixel.

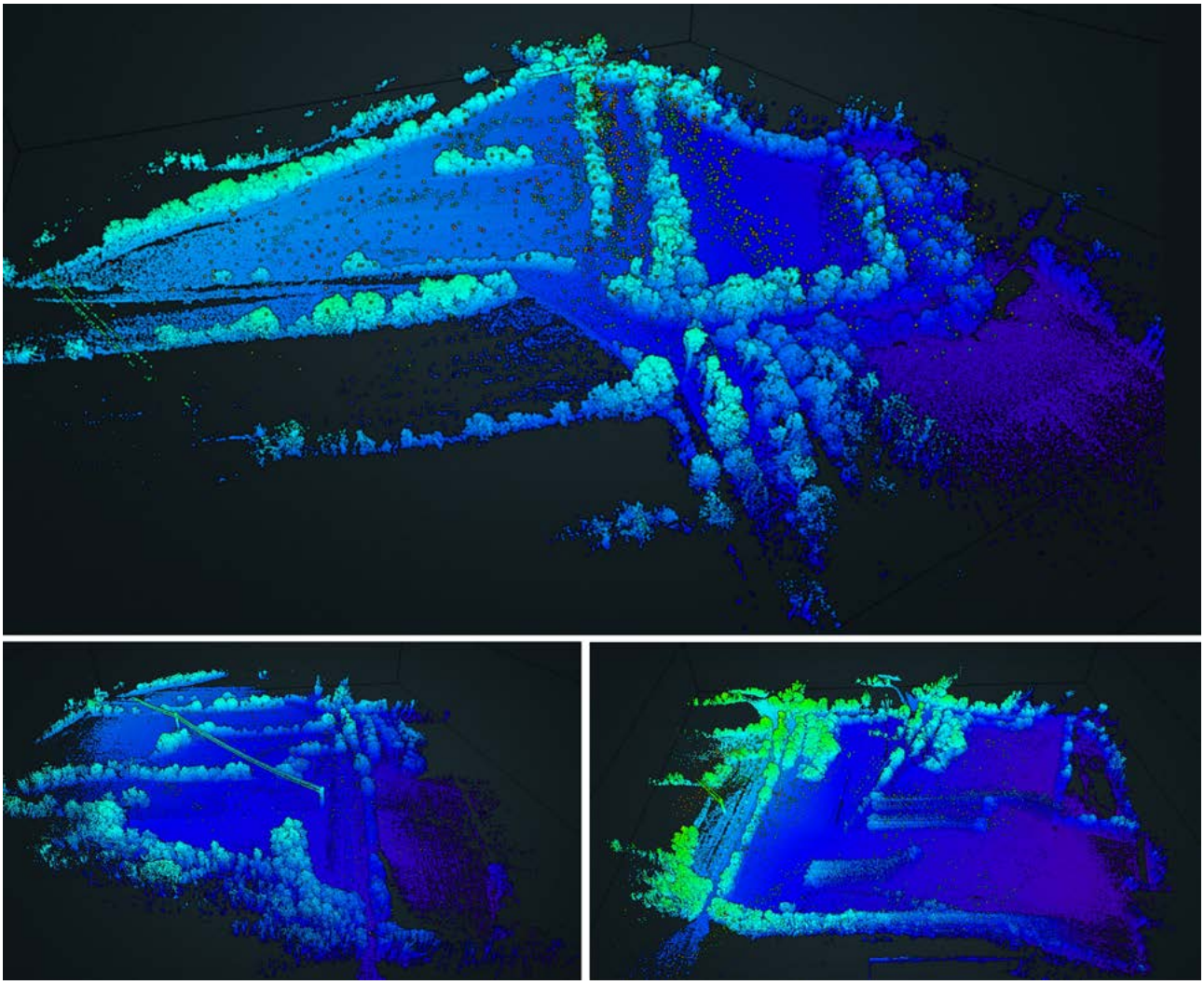

Figure 4 Preliminary results of the GeoSLAM survey showing three of the four independently acquired point clouds corresponding to the subdivided survey areas along the Budoia-Aviano Thrust. Each coloured cloud (blue-green-purple scale) represents one of the scanned sectors, illustrating differences in elevation. These datasets were later merged and processed to generate the high-resolution DSM.

Results and applications

The first outcome of the survey was the generation of a single, unified point cloud (Figure 5), produced in GeoSLAM Connect by merging the four individual scans acquired in the field. This was made possible by the use of a common network of RTK Ground Control Points (GCPs), which ensured precise spatial consistency among the datasets. The automatic alignment provided by GeoSLAM Connect significantly reduced the need for manual post-processing, resulting in a seamless 3D representation of the surveyed area.

This unified point cloud forms the basis for all subsequent analyses, including the production of the high-resolution Digital Surface Model (DSM) in Agisoft Metashape (Figure 6) and the identification of morphological features that deserve further studies to understand if they are associated with the Budoia–Aviano Thrust.

Moreover, the newly generated DSM can also be used as a reference dataset to extract accurate X, Y, Z information for the integration of Ground Penetrating Radar, seismic, and Electrical Resistivity Tomography (ERT) surveys, allowing more precise topographic correction and interpretation of geophysical data along the investigated profiles.

Previous morphotectonic and paleoseismological analyses and geophysical investigations [Patricelli et al., 2024; Rizzo et al., 2024] already suggested the presence of shallow structural features within the SE-verging Budoia-Aviano fault system, including a north-directed back-thrust component and secondary fault strands detected by ERT and GPR profiles.

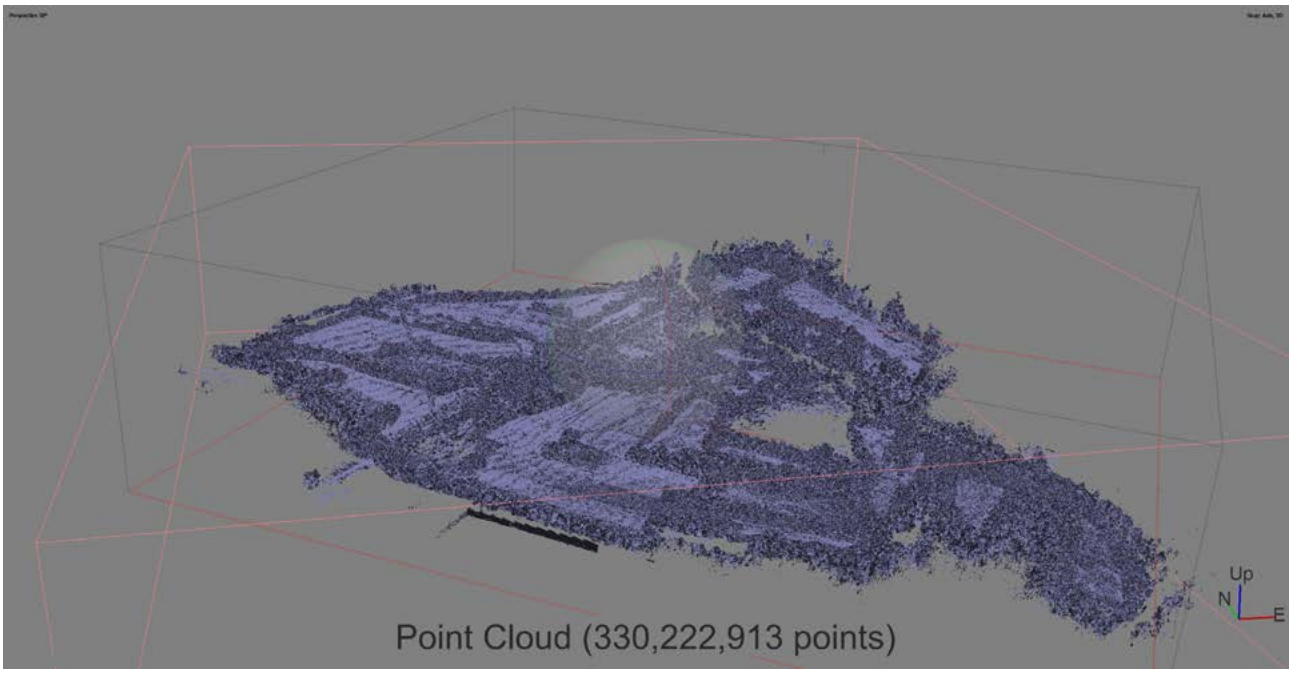

Figure 5 Unified point cloud generated automatically in GeoSLAM Connect by merging the four individual scans acquired along the Budoia–Aviano Thrust (BA). The common RTK Ground Control Points ensured accurate spatial alignment among the sectors, resulting in a seamless dataset containing more than 330 million points. This integrated point cloud represents the basis for subsequent DSM generation and morphotectonic analysis.

Building on this framework, several topographic profiles were extracted from high-resolution DSMs (Figures 6 and 7), including those generated through SLAM-based method (Figure 6), across the cultivated areas to detect subtle slope breaks and elevation variations potentially associated with active deformation. The SLAM-derived DSM proved particularly effective in highlighting minor morphological anomalies that may be related either to shallow tectonic deformation or to depositional processes, such as those shaping the alluvial fan surfaces. These newly identified features highlight additional sectors that warrant detailed investigation.

In the example shown in Figure 8, the high-resolution A-A′ DSM profile reveals a distinct slope break, transitioning from a gently southeast-dipping surface to a nearly flat area. This feature is also recognisable in the DSM derived from the regional LiDAR point cloud (LAZ format) of Friuli Venezia Giulia, whereas the DSM generated with Agisoft Metashape achieved a spatial resolution of 20.6 cm/pixel (Figure 7).

Although the main slope break at approximately 125 m along the transect could coincide with the distal portion of the late Pleistocene–Holocene Artugna alluvial fan, which has been eroded by Holocene and present-day alluvial deposits, further irregularities in the topographic profile are also observed in the southeastern portion of the transect (Figure 8). There, the upward-convex topography and minor slope breaks may indicate the presence of very shallow deformation structures, likely related to minor faulting or folding within the Budoia–Aviano Thrust system (Figure 8). The latter represents an example of surface morphology that can be further investigated through high-resolution ERT and GPR surveys.

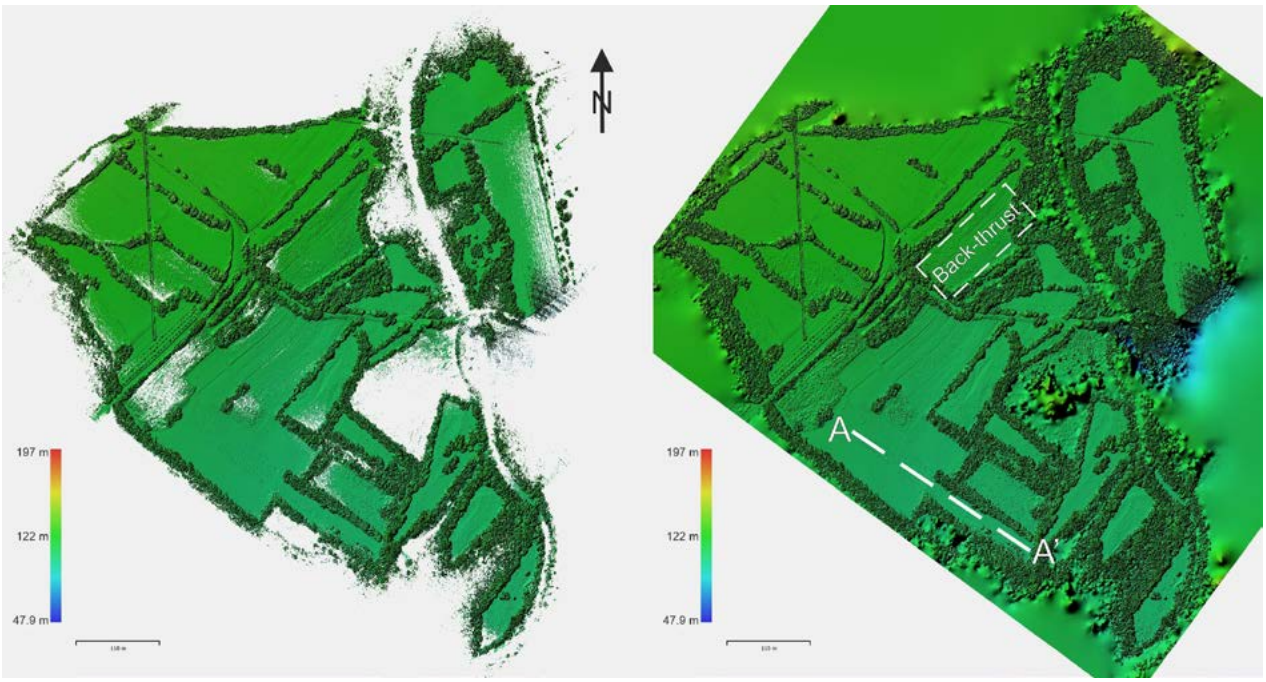

Figure 6 High-resolution Digital Surface Model (DSM) generated from the unified GeoSLAM point cloud and processed in Agisoft Metashape. The DSM, visualised at 2.7 cm/pixel resolution with an elevation colour scale ranging from 47.0 m to 197 m a.s.l., shows a slightly wider elevation range than Figure 7 due to interpolation effects. It highlights subtle topographic variations along the Budoia–Aviano Thrust area. The green–blue colour gradient enhances the morphological expression of the fault scarp and adjacent terraces. The left panel shows the DSM without interpolation, preserving the original no-data gaps, whereas the right panel displays the same model after interpolation to fill these areas.

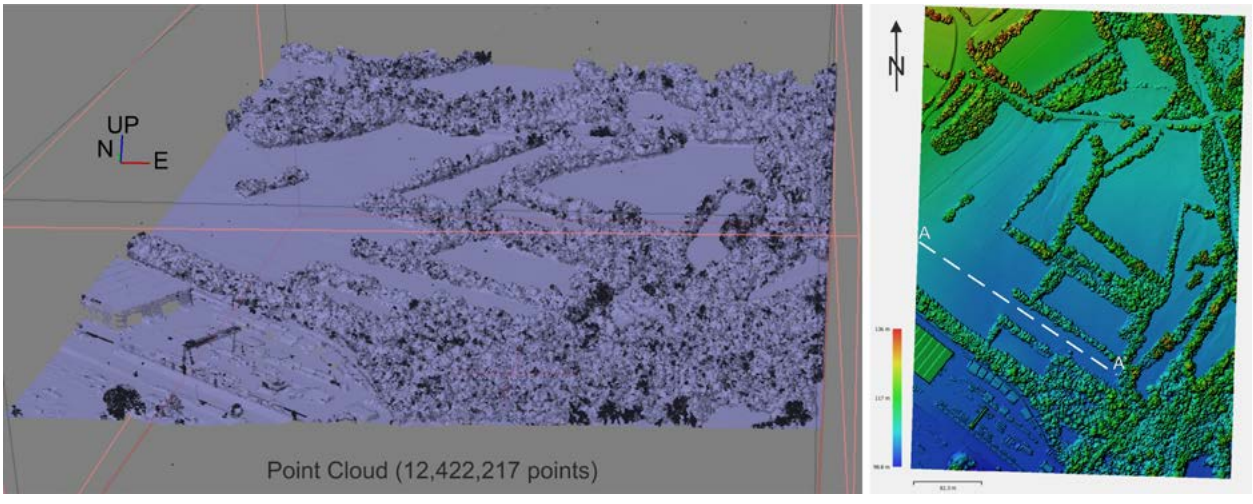

Figure 7 Left panel: Point cloud from the LiDAR dataset of Friuli Venezia Giulia. Right panel: Derived high-resolution Digital Surface Model (DSM; 20.6 cm/pixel). The elevation colour scale, ranging from 98.8 m to 136 m a.s.l., highlights subtle topographic variations along the Budoia-Aviano Thrust area.

Discussion and conclusions

The GeoSLAM-based handheld LiDAR approach proved to be a reliable and efficient method for large-area 3D surveys in restricted or operationally complex environments where UAV flights are not permitted. The technique produced high-resolution point clouds and detailed Digital Surface Models capable of capturing subtle morphological features with centimetric accuracy, which in this area can be further studied to highlight possible morphotectonic structures. Although it provides slightly lower absolute precision compared to static terrestrial or airborne laser scanning, the method ensures rapid, autonomous, and safe data acquisition across wide sectors, even in vegetated or uneven terrain.
In our case, it reproduces the same overall morphology as the FVG LiDAR survey, with slightly higher detail, as shown in Figure 8. Overall, this workflow demonstrates that mobile LiDAR technology represents a valuable and versatile tool for active tectonic studies, particularly valuable in areas affected by flight restrictions or where UAV-based photogrammetry cannot be employed, such as in correspondence of the Budoia–Aviano Thrust in the Eastern Southern Alps.

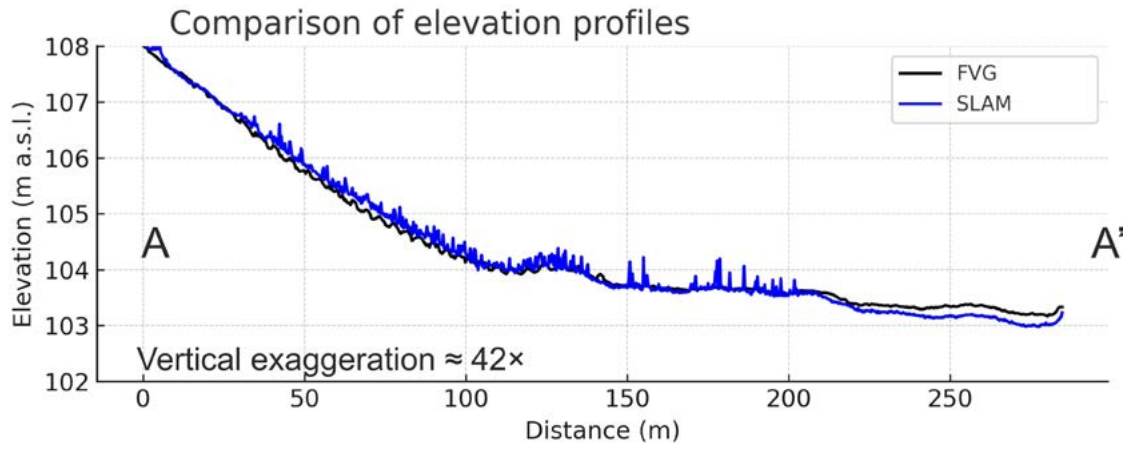

Figure 8 Comparison between two DSM-derived topographic profiles from the Budoia-Aviano Thrust area (LiDAR FVG in black; SLAM-based DSM in blue), showing a gentle slope break near 150 m along the transect. Vertical exaggeration ≈ ×42. The location of topographic transect A-A′ is shown in Figures 6 and 7.

References

Areggi, G., Pezzo, G., Merryman Boncori, J.P., Anderlin, L., Rossi, G., Serpelloni, E., Zuliani, D., and Bonini, L., (2023). *Present-day surface deformation in North-East Italy using InSAR and GNSS data*. Remote Sensing, 15(1704). https://doi.org/10.3390/rs15061704

Devoti, R., Esposito, A., Pietrantonio, G., Pisani, A., and Riguzzi,F. (2011). *Evidence of large-scale deformation patterns from GPS data in the Italian subduction boundary*. Earth and Planetary Science Letters, 311, 230-241. https://doi.org/10.1016/j.epsl.2011.09.034

Galadini, F., Poli, M.E., and Zanferrari, A., (2005). *Seismogenic sources potentially responsible for earthquakes with M > 6 in eastern Southern Alps (Thiene–Udine sector, NE Italy)*. Geophysical Journal International, 161, 739-762. https://doi.org/10.1111/j.1365-246X.2005.02571.x

Patricelli, G., Poli, M.E., Falcucci, E., Gori, S., Paiero, G., Rizzo, E., and Caputo, R., (2024). *First evidence of Holocene activity and surface displacement of the Budoia–Aviano Thrust System in north-eastern Italy, unravelled through the integration of geological, geophysical and*

paleoseismological analyses. EGU General Assembly Conference Abstracts, 16527.
Petrov, S., Dimitrov, S., and Ihtimanski, I., (2024). *Integrated application of geospatial technologies for digital twining of urbanized territories for microscale urban planning*. In Tenth International Conference on Remote Sensing and Geoinformation of the Environment (RSCy2024) (Vol. 13212, pp. 34-48). SPIE.
Poli, M.E., Monegato, G., Zanferrari, A., Falcucci, E., Marchesini, A., Grimaz, S., Malisan, P. and Del Pin, E., (2015). *Seismotectonic characterization of the western Carnic pre-alpine area between Caneva and Meduno (NE Italy, Friuli)*. DPC-INGV–S1 Project: Base-knowledge improvement for assessing the seismogenic potential of Italy (D6/a2.1).
Poli, M.E., Falcucci, E., Gori, S., Monegato, G., Zanferrari, A., Affatato, A., Baradello, L., Böem, G., Dal Bo, I., Del Pin, E., Forte, E., Grimaz, S., and Marchesini, A., (2021). *Paleoseismological evidence for historical ruptures along the Meduno Thrust (eastern Southern Alps, NE Italy)*. Tectonophysics, 818. https://doi.org/10.1016/j.tecto.2021.229071
Poli, M.E., Patricelli, G., Monegato, G., and Zanferrari, A., (2024). *Structural inheritances, fault segmentation and seismogenic potential at the front of the eastern Southern Alps (central Carnic Prealps, NE Italy)*. Tectonophysics, 883. https://doi.org/10.1016/j.tecto.2024.230390
Rizzo, E., Giampaolo, V., Mucchi, F., Boldrin, P., De Martino, G., Poli, M.E., Patricelli, G., Marchesini, A., and Caputo, R., (2024). *Multiscale geophysical investigation on the Budoia–Aviano Thrust System (NE Italy): first results*. GNGTS 2024 Proceedings.
Rovida, A., Locati, M., Camassi, R., Lolli, B., Gasperini, P., and Antonucci, A., (2022). *Catalogo Parametrico dei Terremoti Italiani (CPTI15), versione 4.0*. Istituto Nazionale di Geofisica e Vulcanologia (INGV). https://doi.org/10.13127/CPTI/CPTI15.4
Serpelloni, E., Vannucci, G., Anderlini, L., and Bennett, R.A., (2016). *Kinematics, seismotectonics and seismic potential of the eastern sector of the European Alps from GPS and seismic deformation data*. Tectonophysics, 688, 157–181. https://doi.org/10.1016/j.tecto.2016.09.026
Urban, R., Štroner, M., Braun, J., Suk, T., Kovanič, Ľ., and Blistan, P. (2024). *Determination of accuracy and usability of a SLAM scanner GeoSLAM ZEB Horizon: A bridge structure case study*. Applied Sciences, 14(12), 5258. https://doi.org/10.3390/app14125258

Sitography

[1] https://www.d-flight.it/new_portal/
[2] https://www.ingv.it/monitoraggio-e-infrastrutture/sorveglianza/servizio-di-sorveglianza-sismica

Deep and Shallow Electrical Resistivity Tomographies on the Budoia-Aviano Thrust (NE Italy)

Enzo Rizzo[1,2,3,*], Maria Eliana Poli[3,4], Giulia Patricelli[1,3,4], Vincenzo Giampaolo[2], G. De Martino[2], F. Mucchi[1], Alessandro Marchesini[4], Paola Boldrin[1], Fabio Luca Bonali[5], and Riccardo Caputo[1,3]

[1]Università di Ferrara, Dipartimento di Fisica e Scienze della Terra, Ferrara, Italy
[2]Consiglio Nazionale delle Ricerche, Istituto di Metodologie per l'Analisi Ambientale, Tito, Italy
[3]Centro Interuniversitario per la Sismotettonica 3D con Applicazioni Territoriali (CRUST), Chieti, Italy
[4]Università di Udine, Dipartimento di Scienze AgroAlimentari, Ambientali e Animali, Udine, Italy
[5]Università di Milano Bicocca, Dipartimento di Scienze dell'Ambiente e della Terra, Milan, Italy

Corresponding author: enzo.rizzo@unife.it

Introduction

The research group was involved in the NASA4SHA PRIN2020 Project (*Fault segmentation and seismotectonics of active thrust systems: the Northern Apennines and Southern Alps laboratories for new Seismic Hazard Assessments in northern Italy*), which aims to explore the complexity of faults in active thrust systems in the Northern Apennines and Southern Alps of Italy. The study area, located within the external Pliocene-Quaternary front of the Eastern Southalpine Chain (Friuli, NE Italy), is characterized by distinct WSW-ENE trending and S-verging reverse fault planes, arranged in thrust systems that affect the Quaternary succession. The Deep and Shallow Electrical Resistivity Tomography were integrated to define a multiscale geophysical approach on the Budoia-Aviano thrust system, which is part of the Polcenigo–Montereale fault system. Adopting a multilayer approach, the integration of geological and morphotectonic field surveys with geophysical investigations and paleoseismological analyses enabled the detection of the Budoia-Aviano backthrust, revealing the first evidence of its activation during the Late Pleistocene to Holocene.

Geological setting

The study area is located in the pre-Alpine Carnic belt, where the first hilly terrains overlook the Friulian plain. The geophysical investigations were carried out in the territory of the Budoia village, where Galadini et al. [2005] and Poli et al. [2015], based on previous morphotectonic surveys, identify the presence of the Budoia-Aviano blind thrust (BA), which belongs to the Polcenigo-Montereale (PM) reverse fault system (Figure 1). The identified Polcenigo-Montereale reverse fault system is considered the source of the 1873 earthquake (Mw 6.3) in the Belluno area [Galadini et al., 2005; Burrato et al., 2008] and extends across the pre-Alpine Carnic belt from Polcenigo to Montereale Valcellina. It consists of a main fault (Polcenigo-Montereale) and several smaller S-verging splays, including the Budoia-Aviano fault, which are buried in the Late Pleistocene foreland plain. The Polcenigo-Montereale thrust (PM) overlaps the Calcare del Cellina Cretaceous carbonates on the upper Miocene-Pliocene Molasse and the Budoia-Aviano (BA) thrust causes the outcrop of upper Miocene-Pliocene Molasse and pre-Last Glacial Maximum (LGM) units on the Pliocene-Quaternary deposits of the alluvial piedmont plain [Patricelli et al., 2024].
The study area is located within a large Λate Pleistocene alluvial fan built by the Artugna Ριωερ. The alluvial fan exhibits significant morphological anomalies linked to the presence of active

faults belonging to the Polcenigo-Montereale system [Galadini et al., 2005; Burrato et al., 2008; Poli et al., 2015]. Specifically, the Budoia-Aviano thrust is believed to be responsible for the deformation of the Late Pleistocene alluvial fan of the Artugna stream and the drainage anomalies observed within the fan itself.

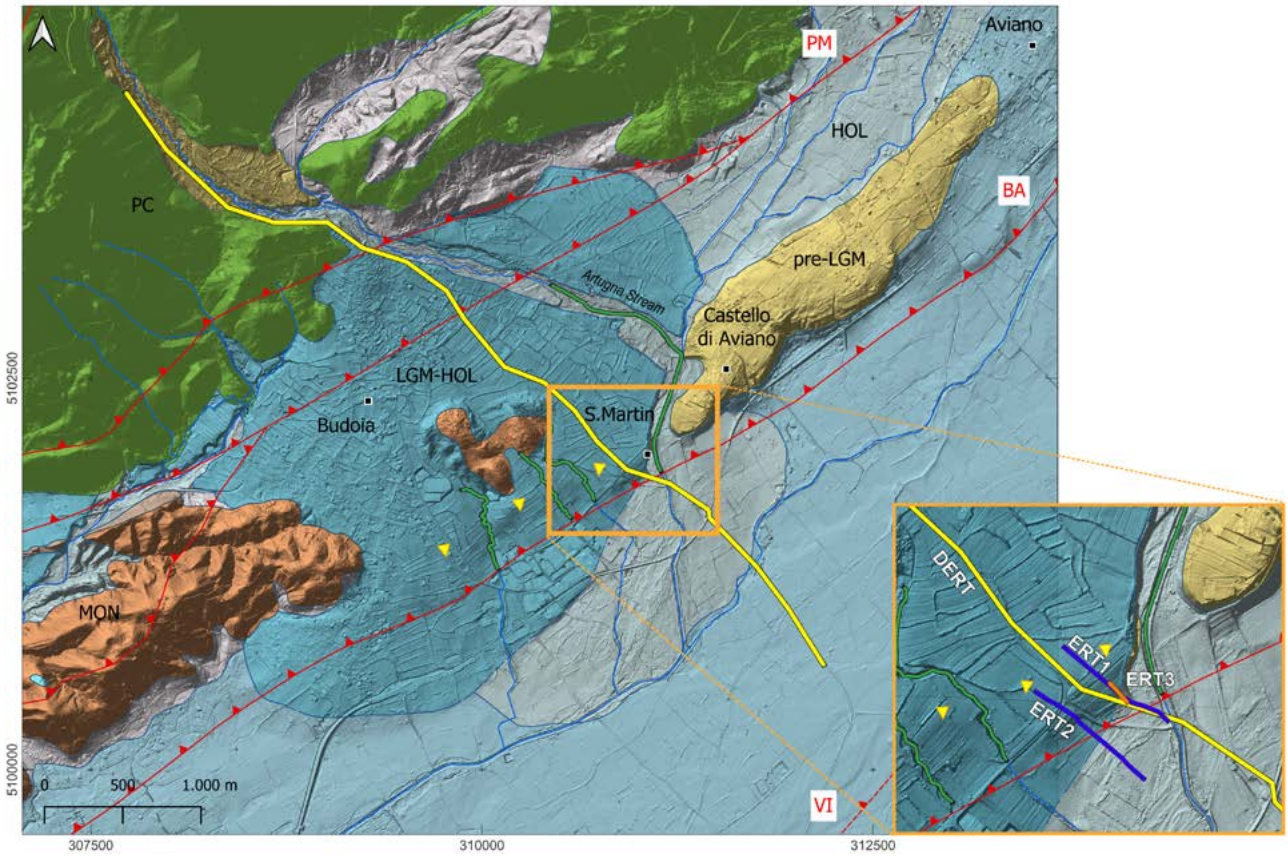

Figure 1 Geological map of the investigated area. PC: Jurassic-Cretaceous Carbonate Platform; LGM-HOL: Upper Pleistocene-Holocene *p.p.* alluvial fan of the Artugna river; pre-LGM: Pliocene-Upper Pleistocene conglomerates; MON: upper Miocene-Pliocene Molasse; PM: Polcenigo-Montereale thrust; BA: Budoia-Aviano thrust; VI: Vigonovo thrust. The long yellow line represents the DERT profile, while the shortest blue lines the ERT1 and ERT2 and the orange one is the ERT3 (modified from Poli et al. [2015]).

Geophysical methods

The ERT method is a cost-effective, user-friendly, and reliable geophysical tool widely used across various geological fields. It is arguably the most popular geophysical technique for near-surface exploration, but there is great attention to improving the efficiency and the capability of the ERT method in deep geological investigations. Therefore, a Deep ERT method was introduced increasing the spacing between the electrodes used for injecting currents into the ground (A and B) and for receiving the voltage signals (M and N). In order, to use large distance between the two couples of electrodes in the DERT method the emitting and receiving systems are generally decoupled and the dipole-dipole array configuration is generally adopted. The current injecting system is physically separated from the receiving one and the distance between the two dipoles (r) is gradually increased along a selected profile on the surface to obtain the 2D resistivity patterns of deep geological sections [Balasco et al., 2023].

The DERT instrumentation is a multichannel system designed and implemented by CNR-IMAA [Rizzo et al., 2004]. It is characterized by a high power transmitter (10 kVA up to 1000V, 20 Amp) to inject the current and several receivers (Campbell datalogger at 1Hz) for the drop of potential acquisitions. Each data logger station consists of four electrodes placed to have av MN distance approximately between 300 and 900 m. This configuration allowed to extend the DERT investigation over approximately 6000 m and it provided a subsurface investigation depth of around 1000 m. The dataloggers were also connected to a GPS receiver so that the clock were used for data processing.
After acquisition, the acquired data were processed using few principal steps [Rizzo and Giampaolo, 2019]: i) alignment of the injected current and drop of potential acquisition data, ii) data filtering, iii) FFT analysis, and iv) apparent resistivity calculation. Finally, the electrical resistivity 2D model along the defined profile of the investigated area is thus obtained by applying an inversion algorithm approach of the elaborated apparent electrical resistivity data. This DERT approach was carried out across the Polcenigo-Montereale thrust system (Figure 1) to define the origin of the morphological features observed in the investigated area and to reconstruct the tectonic architecture at depth.
While the DERT survey primarily targeted the relatively deep subsurface geological features, a series of high-resolution shallow geophysical surveys were also conducted near the major morphotectonic scarps along the Budoia-Aviano thrust fault. Two shallow Electrical Resistivity Tomographies (ERT) with an electrode spacing of approximately 5 m and one very shallow ERT with an electrode spacing of approximately 1 m were carried out to constrain the best location(s) for digging the palaeoseismological trench.

Results

Figure 2 shows the 2D tomography model obtained from processing the data acquired along the DERT profile. The 2D electrical resistivity image was processing using ERTlab software [Morelli and LaBrecque, 1996], which employs a regularized least-squares inversion algorithm with smoothness constraints minimizing the objective function that combines data misfit and model roughness, applying regularization to stabilize the solution in the presence of noise.

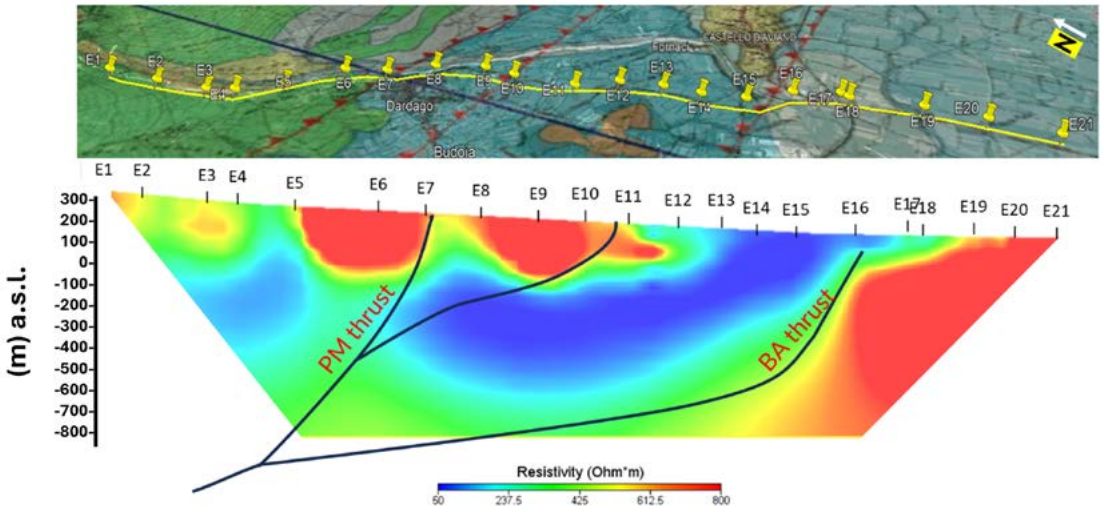

Figure 2 DERT model with the interpretation of the two main thrust systems: Polcenigo-Montereale (PM) and the Budoia-Aviano (BA) thrusts.

The model highlights a resistivity range from 50 to 1000 Ω·m, and it can be divided in three electro-layers: EL1: electrical resistivity values <100 Ω·m; EL2: electrical resistivity values between 100 and 500 Ω·m; EL3: electrical resistivity values >500 Ω·m.
The DERT image can be interpreted taking into account the geological setting of the investigated area. The two main thrust systems, Policenigo-Montereale (PM) and the Budoia-Aviano (BA), are well identified in the depth with the lateral contrast of the electro-layers. The first fault branch of the PM thrust is located between the electrodes E7 and E8, where a relative good lateral resistivity contrast is well identified. The second branch of the PM thrust is well identified between the electrode E10 and E11, where the lateral resistivity contrast between the two electro-layers EL3 and EL1 could be associated with the overlaps of the Jurassic-Cretaceous Carbonate Platform (PC) on the upper Miocene-Pliocene Molasse (MPM). Therefore, the MPM formation should be associated with the electrolayer EL1, where relative low resistivity values are highlighted in the DERT model and these values also extend deep underground. Continuing eastwards, there is a new well lateral contrast in electrical resistivity below the electrodes E16, which can be associated with the BA thrust. This resistivity contrast between the EL 1 and EL3 could be associated with the geological contact between the upper MPM units with the LGM gravelly and pre-LGM (Last Glacial Maximum) conglomeratic units. Moreover, this resistivity contrast is clearly visible deep down and does not appear to reach the surface, because the pre-LGM conglomeratic units are covered by LGM gravels of the Cellina river alluvial fan (Vivaro syntem, Late Pleistocene in age).
Shallow tomographies were performed at electrode 16 of DERT, to better analyze the most superficial portion of the BA thrust. The Figure 3 shows the shallow ERTs acquired at the San Martino locality, where two parallel palaeoseismological trenches were excavated after the geophysical acquisitions [Patricelli et al., 2024; Poli et al., 2024].

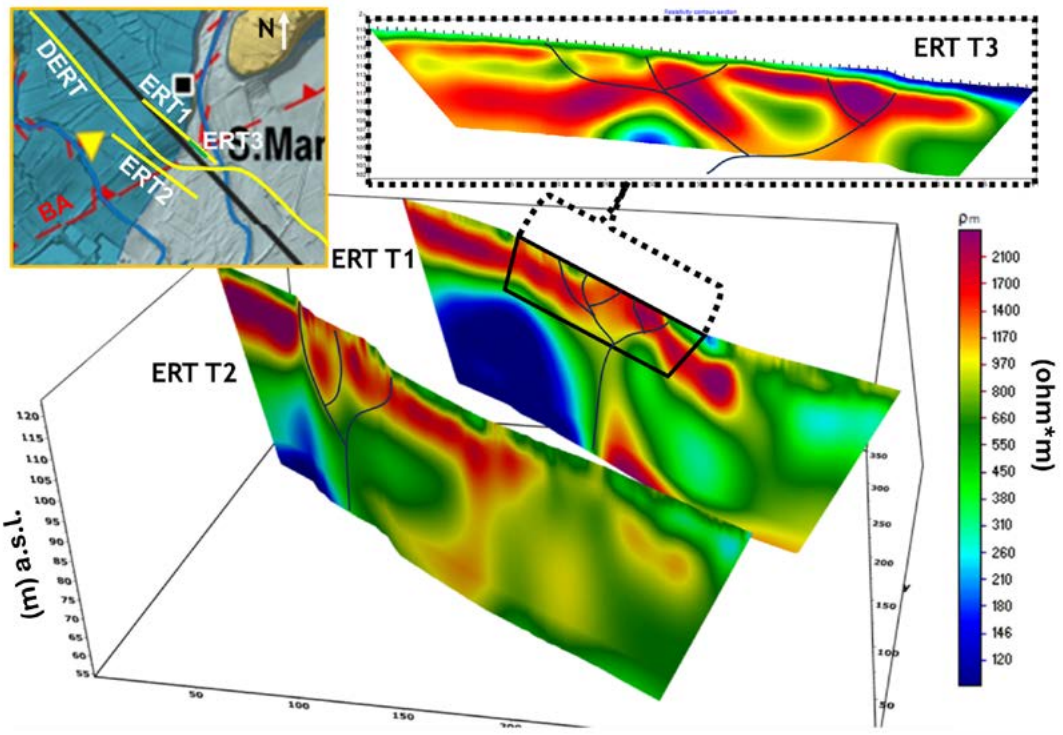

Figure 3 Shallow ERTs across the Budoia-Aviano (BA) thrust. ERT 1 and ERT3 were carried out where two parallel palaeoseismological trenches were excavated at the San Martino locality. The ERT2 was acquired across the same morphological scarp associated to the BA thrust. In black the interpreted faults.

The ERT 1 and ERT2 highlight the resistivity models up to 50 m with a resistivity range between 100 to 2500 Ω·m. In general, three electro-layers could be clearly recognized: EL1 with resistivity values <250 Ω·m; EL2 with resistivity values between 250 and 800 Ω·m; EL3 with resistivity values > 800 Ω·m. The 5 m electrode spacing ERT highlighting the high-angle discontinuity separating at depth the low resistivity body (EL 1) to the North, interpreted as the fractured upper Miocene-Pliocene Molasse, from EL2 to the South associated to the Last Glacial Maximum (LGM) gravels of the Cellina River alluvial fan (Vivaro syntem, Late Pleistocene in age). The deep discontinuity propagates upwards affecting the high-resistivity electro-layer (EL3) interpreted as the late Pleistocene-Holocene Artugna alluvial fan.
The ERT3 depicts the resistivity model up to 10 m characterizing the EL3 resistivity layer described before. The high resolution resistivity ERT highlights the shallow alluvial fan of the Artugna River, where most of the resistivity values are > 800 Ω·m. Only two electro-layer EL1 (< 250 Ω·m) are well depicted, the deeper one could be associated with the upper Miocene-Pliocene Molasse and the shallow one with the humid soil of the alluvial fan. Moreover, the ERT3 resistivity model shows many discontinuities within the high resistivity electro-layer, highlighting a set of dipping surfaces displacing the geological layers of the late Pleistocene-Holocene alluvial deposits of the Artugna River.

Concluding remarks

This research activity highlighted a geophysical survey where several electrical resistivity tomographies were carried out for the purpose of a multiscale application to characterize the Budoia-Aviano thrust system. In order to carry out multiscale geophysical investigations, the ERT survey was first conducted using a Deep approach (Deep Electrical Resistivity Tomography-DERT) for obtaining a general overview of the study area and identify large-scale tectonic structures (up to 1000 m). Indeed, the DERT was able to identify the deep characteristics of the BA thrust system. Subsequently, detailed ERTs were carried out to better characterize the shallower subsurface deformation associated to the BA thrust system. Therefore, two ERTs with an electrode distance of 5 m allowed to characterize the shallow deformed areas up to 50 m-depth. An additional shallow ERT was carried out with an electrode spacing of 1 m which provided even higher resolution up to 10 m-depth. The latter was performed at the same site where ERT1 was carried out. This showed a clear discontinuity, particularly in the most resistive electro-layer, and this discontinuity is likely associated to reactivation(s) along the Budoia-Aviano thrust system. Finally, two parallel palaeoseismological trenches were excavated at the San Martino locality, exposing late LGM-to-Holocene alluvian fan deposits of the Artugna River. The trenches highlight several geological information depicting a back-verging reverse planes of the Budoia-Aviano thrust system, testifying the occurrence of intense deformation since the post-Last Glacial Maximum and represent the first evidence of latest Pleistocene-Holocene activation within the Carnic prealpine area between Polcenigo and Montereale [Patricelli et al., 2024].

References

Balasco, M., Lapenna, V., Rizzo, E., and Telesca, L., (2022). *Deep Electrical Resistivity Tomography for geophysical investigations: the state of the art and future directions*. Geosciences, 12, 438. https://doi.org/10.3390/geosciences12120438

Burrato, P., Poli, M.E., Vannoli, P., Zanferrari, A., Basili, R., and Galadini, F., (2008). *Sources of Mw 5+ earthquakes in northeastern Italy and western Slovenia: an updated view based on*

geological and seismological evidence. Tectonophysics, 453(1-4), 157-176.

Galadini, F., Poli, M.E., and Zanferrari, A., (2005*). Seismogenic sources potentially responsible for earthquakes with M≥ 6 in the eastern Southern Alps (Thiene-Udine sector, NE Italy)*. Geophysical Journal International, 161(3), 739-762.

Morelli, G., and LaBrecque, D.J., (1996). *Advances in ERT modeling*. European Journal of Environmental and Engineering Geophysics, 1, 171–186.

Patricelli, G., Poli, M.E., Falcucci,E., Gori, S., Paiero, G., Rizzo, E., Marchesini, A., and Caputo, R., (2024). *First evidence of Holocene activity and surface diplacement of the Budoia-Aviano Thrust System in north-eastern Italy, unravelled through the integration of geological, geophysic and paleoseismological analyses*. EGU General Assembly 2024, Vienna, Austria, 14-19 Apr 2024, EGU24-16527 https://doi.org/10.5194/egusphere-egu24-16527, 2024.

Poli, M.E., Monegato, G., Zanferrari, A., Falcucci, E., Marchesini, A., Grimaz, S., Malisan, P. and Del Pin, E. (2015). *Seismotectonic characterization of the western Carnic pre-alpine area between Caneva and Meduno (Ne Italy, Friuli)*. DPC-INGV-S1 Project "Base-knowledge improvement for assessing the seismogenic potential of Italy" (D6/a2.1).

Poli M.E., Patricelli G., Falcucci E., Gori S., Rizzo E., Marchesini A. and Caputo R. (2024). *New palaeoseismological evidence of coseismic surface rupture across the Carnic Prealpine front (NE-Italy): the Budoia-Aviano Thrust System*. GNGTS 2024.

Rizzo, E., Colella, A., Lapenna, V., and Piscitelli, S., (2004). *High-resolution images of the fault controlled High Agri Valley basin (Southern Italy) with deep and shallow Electrical Resistivity Tomographies*. Physics and Chemistry of the Earth, 29, 321-327.

Rizzo, E., and Giampaolo, V., (2019). *New deep electrical resistivity tomography in the High Agri Valley basin (Basilicata, Southern Italy)*. Geomatics, Natural Hazards and Risk, 10:1, 197-218. https://doi.org/10.1080/19475705.2018.1520150

Innovative approaches to fault detection: integrating geophones and distributed acoustic sensing (DAS) in the Budoia-Aviano Thrust case study

Lorenzo Suranna[1], Nicola Piana Agostinetti[1], Grazia Maria Caielli[1,2], Fabio Luca Bonali[1,3,*], Roberto De Franco[1,2], Noemi Corti[1,3], Alberto Villa[1], Marta Arcangeli[1], Alessandro Tibaldi[1,3]

[1]Università di Milano Bicocca, Dipartimento di Scienze dell'Ambiente e della Terra, Milan, Italy
[2]Consiglio Nazionale delle Ricerche, Istituto di Geologia Ambientale e Geoingegneria, Roma, Italy
[3]Centro Interuniversitario per la Sismotettonica 3D con Applicazioni Territoriali (CRUST), Chieti, Italy

Corresponding author: fabio.bonali@unimib.it

Introduction and geological framework

The eastern Southern Alps represent a key area for understanding the interaction between Alpine and Dinaric deformation. This region is characterized by ENE-WSW-striking, south-verging thrusts that accommodate the indentation of the Adria microplate beneath the Eastern Alps (Figure 1). The Budoia-Aviano Thrust (BAT) is one of the main structures in this sector, forming part of the Polcenigo-Montereale Thrust System, which uplifts Miocene molasses and pre-LGM deposits over Pliocene-Quaternary alluvial units.
Geomorphic indicators such as uplifted fans, diverted streams, and linear scarps testify to the Quaternary activity of the BAT. Given the significant historical seismicity in the Friuli region [Rovida et al., 2022], constraining the geometry of the BAT is crucial for improving seismic hazard assessment. Within this context, this study investigates the potential of combining conventional seismic acquisition with Distributed Acoustic Sensing (DAS) to improve fault imaging at multiple scales. The project as part of the NASA4SHA PRIN Project, integrates geological, geomorphological, and geophysical analyses to refine models of active deformation and fault segmentation in northern Italy.

Data acquisition and methodology

Four seismic lines were acquired across the Budoia-Aviano area, using a controlled shotgun source and two receiver systems: conventional 4.5 Hz geophones (5 m spacing) and a Distributed Acoustic Sensing (DAS) fiber-optic cable (1 m channel spacing). Both systems recorded the same shots, thus enabling also a direct comparison.
The DAS array transforms every meter of fiber into a virtual sensor by detecting strain via laser backscatter. This setup provides high-density data, but introduces specific challenges, such as oversampling noise, poor coupling, and lack of precise time-zero synchronization. Standard software (Visual SUNT, Rayfract) was used for geophone data, while DAS data required custom pre-processing and alignment through cross-correlation techniques.

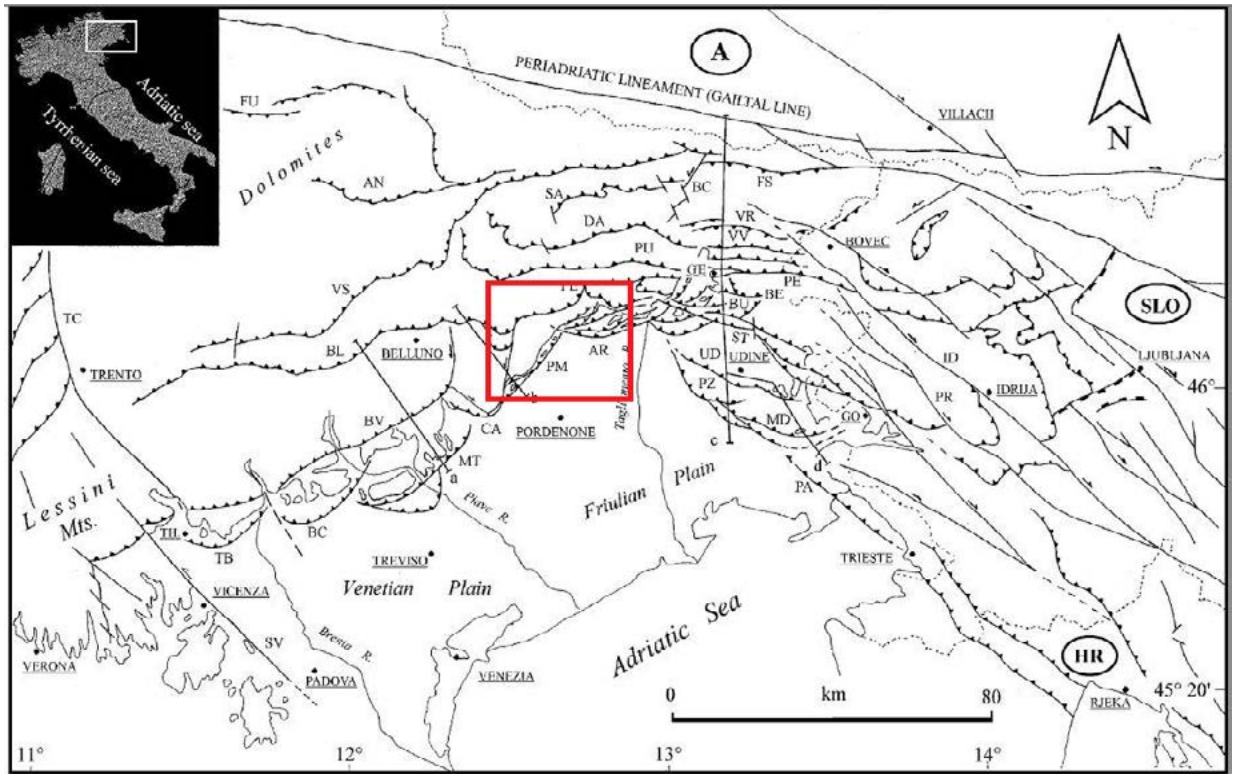

Figure 1 Regional tectonic and seismic setting showing the location of the Budoia-Aviano Thrust (red box). Legend (towns): TH, Thiene; GE, Gemona; GO, Gorizia. Legend (structures): TC, Trento-Cles fault; FU, Funes fault; AN, Antelao fault; MT, Montello fault; CA, Cansiglio fault; PM, Polcenigo-Maniago fault; AR, Arba-Ragogna fault; PE, Periadriatic thrust; PU, Pinedo-Uccea fault; DA, Dof-Auda fault; SA, Sauris fault; BC, But-Chiarsò fault; FS, Fella-Sava fault; VR, Val Resia fault; VV, Val Venzonassa fault; BE, Bernarda fault; BU, Buia fault; ST, Susans-Tricesimo fault; UD, Udine-Buttrio fault; PZ, Pazzuolo fault; MD, Medea fault; PA, Palmanova fault; ID, Idrija fault; PR, Predjama fault. Modified from Poli et al. [2021].

Results and discussion

DAS has the potential to revolutionize near-surface seismic imaging thanks to its dense spatial sampling and the ability to repurpose existing fiber-optic cables as seismic arrays. However, one of the main obstacles to using DAS for active-source experiments is the absence of a precise shot initiation time (t_0). Unlike conventional geophone systems, which are physically connected to the shot trigger and record the absolute start of each seismic event, DAS interrogators operate independently of the source.

As a result, the first sample in a DAS record does not correspond to the true explosion time, but instead reflects the internal clock of the interrogator.

This missing reference point has direct consequences for seismic analyses. In geophone data, travel times can be measured with respect to the exact moment of energy release, ensuring that velocity models and reflector depths are correctly tied to the survey geometry. In DAS data, arrivals are only aligned relative to one another, while their absolute position along the time axis remains uncertain. Even a small constant delay of just a few milliseconds propagates into significant errors in derived parameters:

- velocity estimation becomes biased because first-break picks are systematically shifted;
- reflector depths are overestimated, especially for shallow interfaces where

millisecond-scale differences correspond to meters of error;
- comparison with geophone results becomes problematic, as apparent discrepancies may stem not from the subsurface, but from acquisition timing. Faced with this limitation, discarding the DAS dataset would have meant losing the opportunity to test a promising technology under real conditions.

To overcome this problem and still extract meaningful information, two complementary strategies were adopted. First, a direct comparison between DAS and geophone acquisitions was carried out, analyzing how the absence of t_0 manifests in practice by comparing velocity and depth estimates for the same explosive shots.
Second, a Bayesian cross-correlation approach using MCMC sampling was developed to evaluate relative similarity between DAS shot gathers without requiring absolute timing. This probabilistic framework not only identifies the best alignment between seismic patches but also quantifies uncertainty, providing a robust alternative to deterministic correlation. Together, these experiments address both the methodological and practical sides of the t_0 problem.

Comparison between geophone and DAS acquisition

A detailed comparison was made between seismic data recorded simultaneously with a conventional geophone array and with a DAS system. Both datasets correspond to the same explosive shot, ensuring that the subsurface response is directly comparable. The approach focuses on the velocity analysis, reflector depth estimation, and the methodological implications of the observed differences. Particular attention is given to the absence of a precise time-zero (t_0) in DAS acquisition, which introduces a systematic bias in travel-time measurements and propagates through subsequent stages of seismic interpretation.
The comparison highlights how this lack of absolute timing affects both the estimation of seismic velocities and the calculation of reflector depths. In conventional geophone acquisitions, the shot trigger provides an exact temporal reference, allowing travel times to be measured from the true initiation of the seismic event. In DAS systems, by contrast, the interrogator operates asynchronously, meaning that each recorded trace is internally timed, but lacks a link to the physical instant of the energy release.
As a result, first arrivals in the DAS dataset are aligned only relative to one another, and the entire record may be shifted along the time axis by a constant offset. This delay, although small, in the order of a few milliseconds, translates into measurable depth discrepancies when velocity models are computed.
By directly comparing the two datasets (Figures 2 and 3), the study quantifies the effect of this offset: shallow reflectors imaged at 3.6 and 11.8 m-depth in the geophone data appear at 5.6 and 12.7 m, respectively, in the DAS results. These differences confirm that the absence of time-zero in DAS introduces a systematic overestimation of depth, particularly for shallow interfaces where even millisecond delays correspond to several meters of error.
Nevertheless, the DAS and geophone datasets consistently image the same reflectors, demonstrating that, despite timing uncertainty, the DAS system captures coherent structural information suitable for comparative analysis once appropriate alignment and correction procedures are applied.

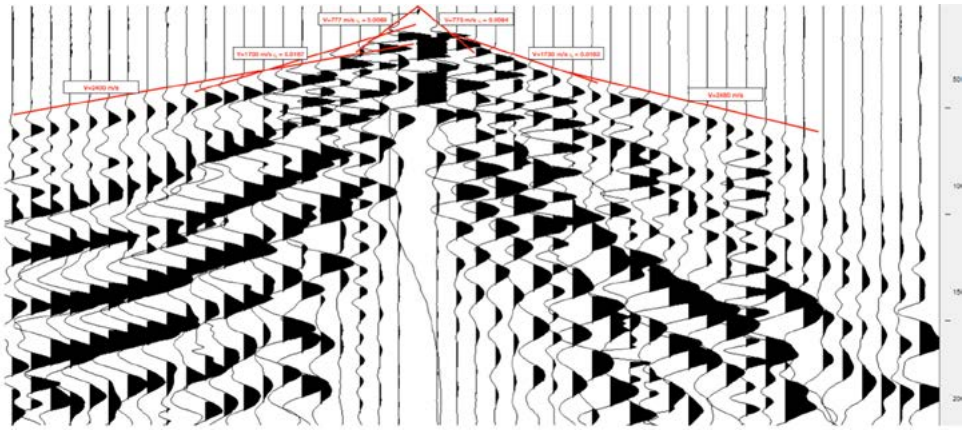

Figure 2 Shot gather recorded with 4.5 Hz geophones spaced every 5 m. Red curves represent the best-fitting hyperbolic travel-times obtained during velocity analysis, yielding reflector depths at approximately 3.6 and 11.8 m.

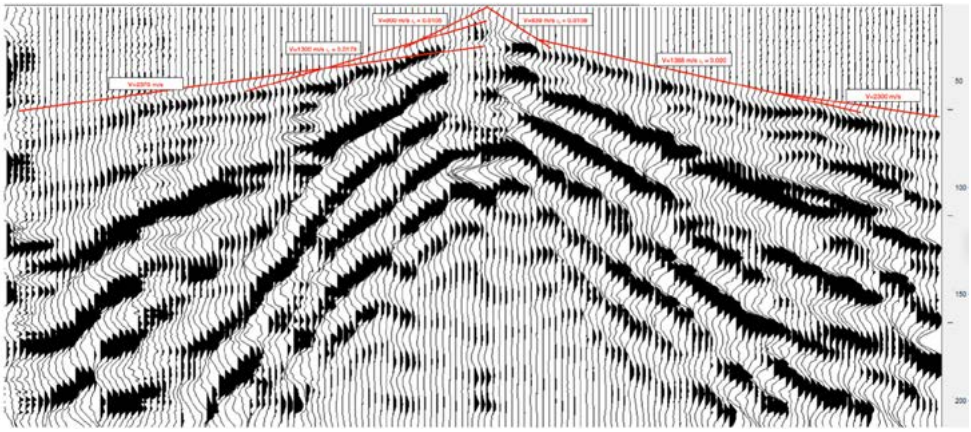

Figure 3 Shot gather recorded with DAS at 1 m channel spacing. Red curves indicate the velocity functions used in the analysis, with reflector depths estimated at ~5.6 and 12.7 m. The systematic shift relative to the geophone results reflects the uncertainty in the shot-time (time zero) of the DAS data.

The seismic survey was designed for direct comparison between the two systems:

- geophone array: vertical 4.5 Hz sensors spaced every 5 m, connected to a system with shot-triggering mechanism, ensuring accurate t_0;
- DAS array: fiber-optic cable interrogated with 4 m gauge length, 1 m spacing. Operated independently of the trigger, so t_0 was not directly recorded;
- source: the same explosive charge for both, guaranteeing identical subsurface response.

This geometry provides an ideal framework for assessing consistency between geophones and DAS in velocity determination and reflector(s) imaging. In seismic refraction analysis, the intercept-time (plus-minus) method relates intercept time (t_0) to layer thickness, assuming horizontal layering [Sheriff and Geldart, 1995]:

$$h = \frac{t_0 \cdot V_1}{2cos\left(arcsin\left(\frac{V_1}{V_2}\right)\right)}$$

where, h = thickness of the first layer, t_0 = intercept time, $V1$ = velocity of first layer, $V2$ = velocity of underlying layer.

At the investigated site, velocity analysis revealed two main reflectors. In geophone data, reflectors were identified at ~3.6 and 11.8 m depth. In DAS data, the same reflectors appeared at ~5.6 and 12.7 m depth. This consistent overestimation in DAS reflects the effect of missing t_0. The differences between geophone and DAS results cannot be attributed to geometry or processing, since both datasets followed identical workflows. They stem from the absence of precise time-zero in DAS recordings; indeed, in geophone data, the trigger provides absolute arrival reference, while in DAS data, arrivals are relatively aligned, without absolute reference.

This produces systematic time shifts, propagating as overestimated reflector depths. The effect is strongest for shallow reflectors (2 m difference for the first interface) and smaller for deeper ones (~1 m for the second interface).

The systematic differences are thus not due to velocity estimation errors but to the t_0 issue. Reconstruction of time zero, via alignment of first arrivals or cross-correlation, introduces uncertainty that manifests as delay. When propagated through the intercept-time method, it inflates depth estimates, especially for shallow horizons. Despite this, both methods consistently detect the same interfaces, confirming DAS's potential for structural imaging once timing corrections are implemented.

Conclusions and outlooks

This study highlights the complementary roles of geophones and DAS in subsurface imaging. Geophones produce high-quality data for both reflection and refraction surveys, while DAS - although affected by timing and coupling limitations - offers high-resolution near-surface imaging. The t_0 issue remains a central limitation, introducing depth overestimation in DAS data, yet it can be mitigated through cross-correlation and probabilistic analysis. Integrating both systems enables a multi-scale characterization of the Budoia-Aviano Thrust, improving our understanding of active deformation in the Eastern Southern Alps and informing future seismic hazard assessments.

References

Poli, M.E., Falcucci, E., Gori, S., Monegato, G., Zanferrari, A., Affatato, A., Baradello, L., Böhm, G., Dal Bo, I., Del Pin, E., Forte, E., Grimaz, S., and Marchesini, A., (2021). *Paleoseismological evidence for historical ruptures along the Meduno Thrust (eastern Southern Alps, NE Italy)*. Tectonophysics, 818, 229071. https://doi.org/10.1016/j.tecto.2021.229071

Rovida, A., Locati, M., Camassi, R., Lolli, B., Gasperini, P., and Antonucci, A., (2022). *Italian Parametric Earthquake Catalogue (CPTI15), version 4.0*. INGV. https://doi.org/10.13127/CPTI/CPTI15.4

Sheriff, R.E., and Geldart, L.P., (1995). *Exploration seismology*. Cambridge University Press, 2nd edition. https://doi.org/10.1017/CBO9781139168359

Bayesian cross-correlation of DAS seismic data using MCMC sampling: a case study from the Budoia-Aviano Thrust (NE Italy)

Lorenzo Suranna[1,*], Nicola Piana Agostinetti[1], Grazia Maria Caielli[1,2], Fabio Luca Bonali[1,3], Roberto De Franco[1,2], Noemi Corti[1,3], Alessandro Tibaldi[1,3]

[1]Università di Milano Bicocca, Dipartimento di Scienze dell'Ambiente e della Terra, Milan, Italy
[2]Consiglio Nazionale delle Ricerche, Istituto di Geologia Ambientale e Geoingegneria, Roma, Italy
[3]Centro Interuniversitario per la Sismotettonica 3D con Applicazioni Territoriali (CRUST), Chieti, Italy

Corresponding author: l.suranna@campus.unimib.it

Introduction and geological framework

The eastern Southern Alps represent a key area for understanding the interaction between Alpine and Dinaric deformation. This region is characterized by ENE-WSW-striking, south-verging thrusts that accommodate the indentation of the Adriatic microplate beneath the Eastern Alps (see Figure 1 of Suranna et al. [this volume]). The Budoia-Aviano Thrust (BAT) is one of the main structures in this sector, forming part of the Polcenigo-Montereale Thrust System, which uplifts Miocene molasses and pre-LGM deposits over Pliocene-Quaternary alluvial units.
Geomorphic indicators such as uplifted fans, diverted streams, and linear scarps testify to the Quaternary activity of the BAT. Given the significant historical seismicity in the Friuli region [Rovida et al., 2022], constraining the geometry of the BAT is crucial for seismic-hazard assessment. Within this context, this study investigates the potential of combining conventional seismic acquisition with Distributed Acoustic Sensing (DAS) to improve fault imaging at multiple scales. The present research has been developed in the frame of the NASA4SHA PRIN Project, which integrates geological, geomorphological, and geophysical analyses to refine models of active deformation and fault segmentation in northern Italy. This note represents a companion paper of Suranna et al. [this volume].

Data and Methodology

The dataset consists of five DAS shot records (ESP98.h5 to ESP102.h5) acquired near Aviano, northeastern Italy. Each file represents a distinct active-source experiment recorded along the same buried fiber-optic cable interrogated with a Febus A1-R system. The sampling rate is 250 Hz, with 221 samples per trace and 1 m spatial channel spacing.
Shot ESP98 was chosen as the reference gather due to its high signal-to-noise ratio. A rectangular feature patch was manually selected within this shot, corresponding to channels 100-150 and samples 6600-6700 (Figure 1). This region contains a coherent seismic arrival that serves as the target feature for subsequent cross-correlation with the remaining shots.

Bayesian Feature Matching via MCMC

To assess feature similarity, a Bayesian Markov Chain Monte Carlo (MCMC) sampler was implemented using custom Python functions. The sampler explores five parameters:

- t_0: vertical (temporal) shift,
- c_0: horizontal (spatial) shift,
- h_1: horizontal stretch factor,
- h: hyper-parameter related to the noise standard deviation.

Priors for these parameters were defined empirically, centered around the geometry of the reference patch. Each MCMC chain ran for 10,000-30,000 iterations for each candidate shot (ESP99-ESP102), producing posterior distributions that describe the likelihood of feature similarity.

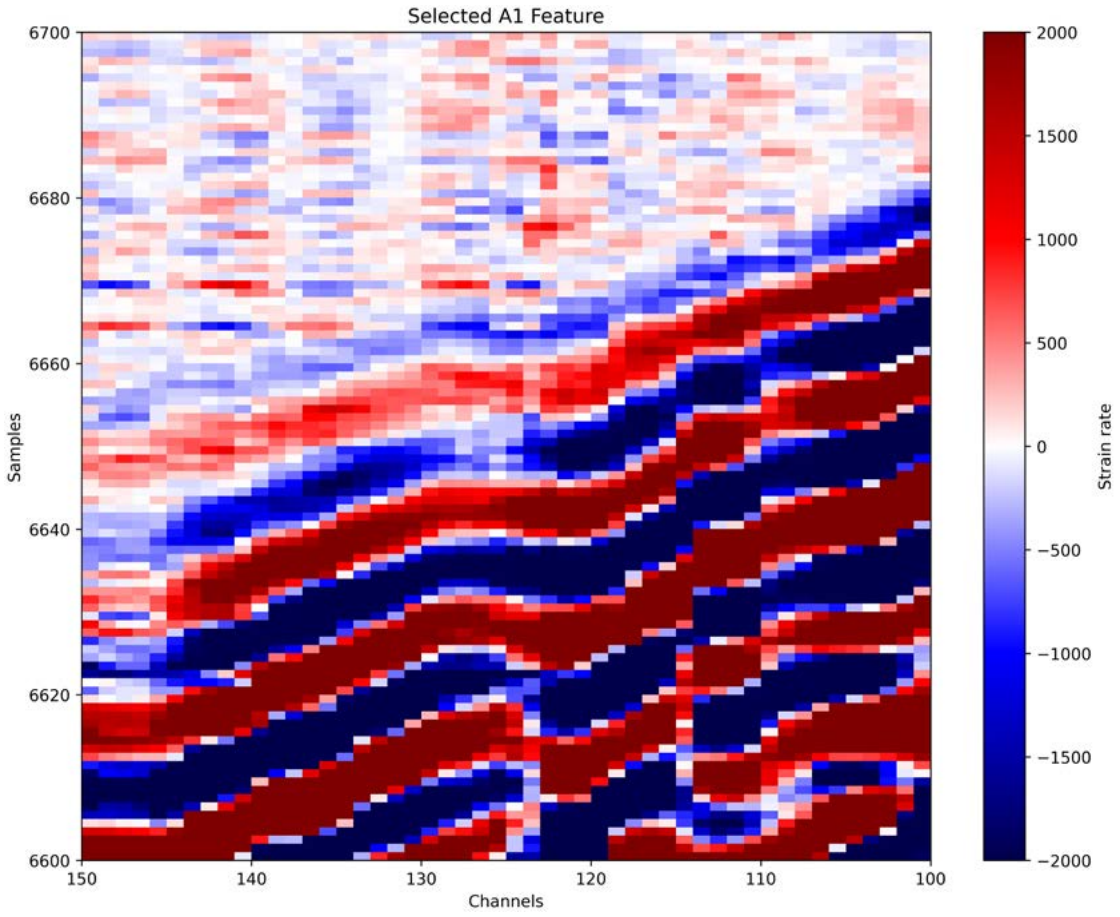

Figure 1 Reference DAS patch (channels 100-150, samples 6600-6700) extracted from shot ESP98 and used as target feature A_1 for MCMC cross-correlation.

Likelihood and Sampling Scheme

The likelihood function evaluates the misfit between the reference patch A_1 and a candidate patch A_2 as:

$$L(A_1, A_2) = \sum \frac{(A_1 - B_2)^2}{\sigma^2 \cdot 10^{2h}}$$

where represents the *a priori* estimated noise level and h is the hierarchical hyperparameter controlling misfit weighting. At each iteration, a candidate patch is proposed and accepted according to the Metropolis-Hastings criterion [Metropolis et al., 1953].

Results

The MCMC approach successfully identified coherent seismic features between the reference shot ESP98 and subsequent shots ESP99–ESP102. For each comparison, the algorithm converged to a well-defined *a posteriori* distribution, indicating a strong similarity between the extracted patches. In particular, the match between ESP98 and ESP100 displayed the highest *a posteriori* probability, reflecting minimal temporal and spatial offsets between reference and candidate features (Figure 2). The *a posteriori* distributions for t_0 and c_0 were narrow and unimodal, implying a high-confidence match. Conversely, broader posteriors for stretch h_1 or amplitude scaling suggest minor variations in local coupling or wavelet amplitude between shots.

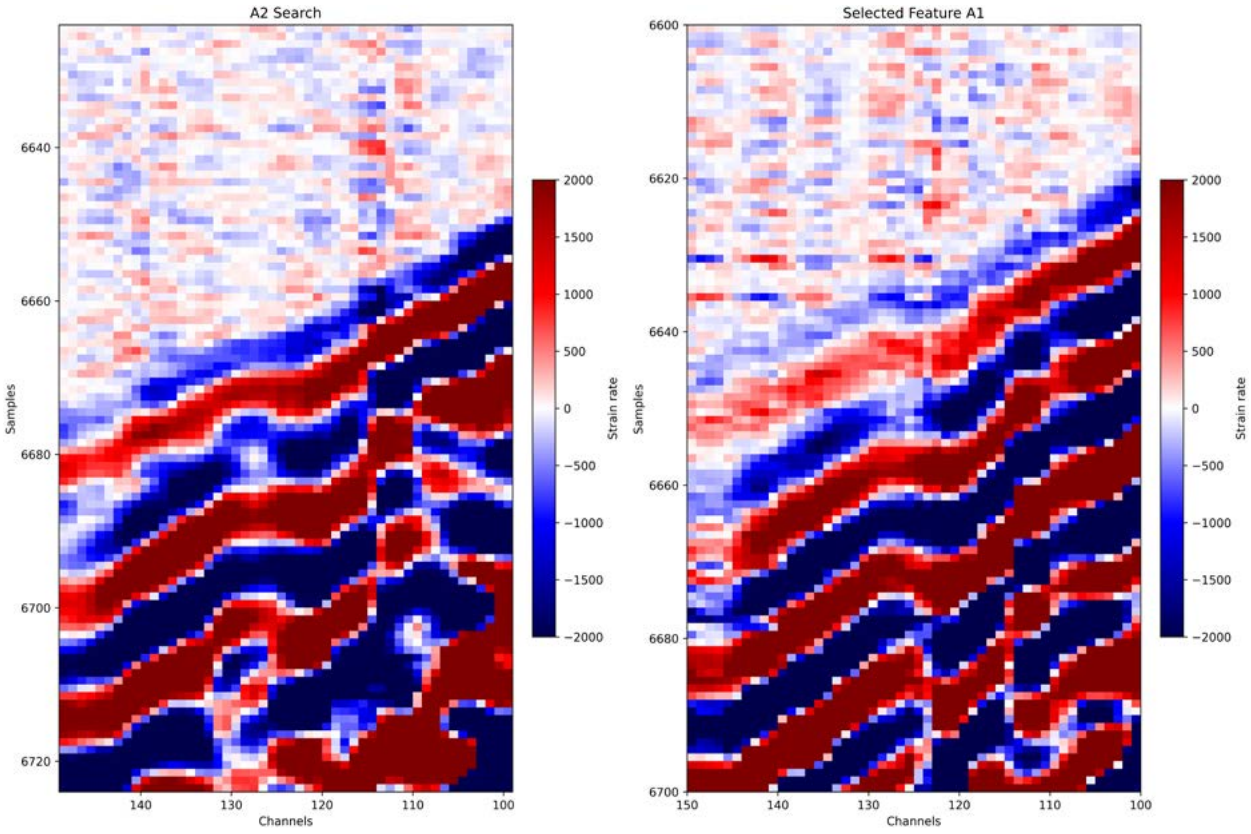

Figure 2 Comparison between the reference patch from ESP98 and the matched patch from ESP100 after MCMC alignment. The strong visual similarity supports the high posterior probability of the match.

Discussion and geophysical implications

The MCMC-based Bayesian framework offers several methodological and geophysical advantages. Methodologically, it provides a probabilistic alternative to traditional cross-correlation, enabling uncertainty quantification in feature matching. The hierarchical error model and noise parameter make the approach robust to amplitude fluctuations and acquisition noise, both of which are common in DAS recordings.

From a geophysical perspective, the consistent matching of seismic features across multiple shots suggests stable source conditions and homogeneous fiber coupling along the tested segment. The stretch factor $h_1 \approx 1$ indicates negligible geometric distortion, reinforcing the accuracy of the acquisition setup.

Furthermore, identifying coherent arrivals between shots confirms the internal consistency of the velocity model used for the Budoia-Aviano area. This method can also help detecting subtle fault-related reflections or scattering zones if applied to longer DAS profiles with multiple active sources.

Conclusions

The application of MCMC-based Bayesian sampling to Distributed Acoustic Sensing (DAS) data demonstrates its capability to detect and quantify recurring seismic features across multiple shot gathers. By jointly estimating translation, stretch, amplitude, and noise parameters, the method provides both the best-fit alignment and associated uncertainty.
The analysis of shots ESP98-ESP102 from the Budoia-Aviano Thrust area reveals strong coherence between acquisitions, confirming stable source conditions and effective coupling. The Bayesian approach thus represents a powerful addition to DAS data analysis, complementing conventional geophysical interpretation and enhancing confidence in seismic feature tracking. Future developments may include integrating MCMC feature detection into automated pipelines for real-time DAS monitoring and combining Bayesian inference with machine learning to accelerate convergence on large datasets.

References

Suranna, L., Piana, Agostinetti N., Caielli, G.M., Bonali, F.L., De Franco, R., Corti, N., Villa, A., Arcangeli, M., and Tibaldi, A., (2025). *Innovative approaches to fault detection: integrating geophones and distributed acoustic sensing (DAS) in the Budoia-Aviano Thrust case study*. Miscellanea INGV 102, in this volume.

Metropolis, N., Rosenbluth, A.W., Rosenbluth, M.N., Teller, A.H., and Teller, E., (1953). *Equations of state calculations by fast computing machines*. J. Chem. Phys., 21, 1087-1091. https://doi.org/10.1063/1.1699114

Rovida, A., Locati, M., Camassi, R., Lolli, B., Gasperini, P., and Antonucci, A., (2022). *Catalogo Parametrico dei Terremoti Italiani (CPTI15), versione 4.0*. Istituto Nazionale di Geofisica e Vulcanologia. https://doi.org/10.13127/CPTI/CPTI15.4

Recent tectonic activity of the Budoia-Aviano Thrust: the example of the Late Pleistocene-Holocene Artugna alluvial fan (eastern Southern Alps, NE Italy)

Maria Eliana Poli[1,2,*], Giulia Patricelli[1,2,4], Emanuela Falcucci[3], Stefano Gori[3], Enzo Rizzo[2,4], Giovanni Paiero[1], Andrea Marchesini[1], Angela Franceschet[1,5], Davide Russo[2,4], Paola Boldrin[4], Aaron Sobbe[4], and Riccardo Caputo[2,4]

[1]Università di Udine, Dipartimento di Scienze AgroAlimentari, Ambientali e Animali, Udine, Italy
[2]Centro Interuniversitario per la Sismotettonica 3D con Applicazioni Territoriali (CRUST), Chieti, Italy
[3]Istituto Nazionale di Geofisica e Vulcanologia, Osservatorio Nazionale Terremoti, Rome, Italy
[4]Università di Ferrara, Dipartimento di Fisica e Scienze della Terra, Ferrara, Italy
[5]Università di Trieste, Dipartimento di Scienze della Vita, Trieste, Italy

Corresponding author: eliana.poli@uniud.It

Introduction and seismotectonic setting

In the framework of the PRIN2020 "*Fault segmentation and seismotectonics of active thrust systems: the Northern Apennines and Southern Alps laboratories for new Seismic Hazard Assessments in northern Italy (NASA4SHA)*", we made a multidisciplinary and multiscale seismotectonic study on the Budoia-Aviano Thrust which is an external splay of the larger Polcenigo-Montereale fault system located in the western Carnic Prealps (Friuli, NE Italy).
The investigated area is part of the external Pliocene-Quaternary front of the eastern Southern Alps (ESA) where geodetic (GNSS) time series [Devoti et al., 2011; Serpelloni et al., 2016; Areggi et al., 2023] show a crustal shortening rate of about 2-3 mm/yrs. In the Carnic Prealps, the external front of ESA consists in a series of arch-shape WSW-ENE trending, SSE verging presently mostly believed as blind thin-skinned thrusts, affecting the Late Pleistocene-Holocene piedmont Friuli Plain [Galadini et al., 2005; Poli et al., 2021; 2024]. In particular, the Polcenigo-Montereale Thrust System (Figure 1), where the Mesozoic Friuli Carbonate Platform overthrust the Neogene Southalpine Molasse, extends from the Caneva to Montereale Valcellina towns and consists of a series of S-verging splays that show evidence of recent tectonic activity: the Aviano-Budoia and the Vigonovo thrusts, respectively [Poli et al., 2015].
According to the currently available catalogue of historical seismicity (the DBMI Catalogue [Locati et al., 2022]) the area was hit by some historical destructive earthquakes, like the 1776 Tramonti (Mw = 5.78, Io = 8-9); the 1794 Alpi Carniche (Mw = 6.04, Imax = 9); the 1812 Sequals (Mw = 5.7; Imax = 7-8); the 1873 Alpago (Mw = 6.3; Imax = 9-10) and the 1936 Cansiglio (Mw = 6.1; Imax = 9) earthquakes. Concerning the instrumental seismicity (from 1977 to Present), we distinguish the area of Claut that was hit by frequent medium-to-low seismic events (max magnitude 4.3, 1996-04-13 earthquake; [Bernardis et al., 1996]). In this contest, Galadini et al. [2005] indicate the Polcenigo-Montereale Thrust System as the seismogenic source of the aforementioned 1873 Alpago earthquake.

Methodology

The area was analysed by means of a multidisciplinary and multiscale approach that includes:

1. Morphotectonic investigations with analysis of high-resolution Digital Elevation Model provided by the Friuli Venezia Giulia Region in order to define possible morphotectonic

features across the investigated area. In case of morphological surface anomalies, we performed detailed field surveys to verify whether they indicate active, progressively growing, fault-related anticlines (drainage anomalies, uplifted and/or tilted palaeosurfaces, scarps) (Figure 2).

2. Multiscale geophysical surveys, encompassing a range of techniques, each providing different insights into the studied fault system. By applying a range of geophysical techniques at different scales of investigation, the proposed methodology in the study involved the use of deep and shallow Electrical Resistivity Tomographies (hereafter ERT) [Rizzo et al., 2004], and Ground-Penetrating Radar (hereafter GPR) techniques to upscale the understanding of buried geological structures and identify optimal sites for the excavation of palaeoseismological trenches (Figures 3 and 4).
3. Palaeoseismological trenches, excavated where morphotectonic analyses and geophysical survey indicate possible shallow-to-surficial effects of tectonic activity. Two trenches (BU1 and BU2 in Figure 3) were dug to achieve detailed geometric (trend, size, depth), kinematic (slip vector, cumulative displacement, slip per event), dynamic (maximum expected magnitude) and chronological (slip-rate and mean recurrence interval) parameters for seismotectonic assessments. Radiocarbon dating on the Late Pleistocene-Holocene continental deposits were carried out by Beta Analytic.

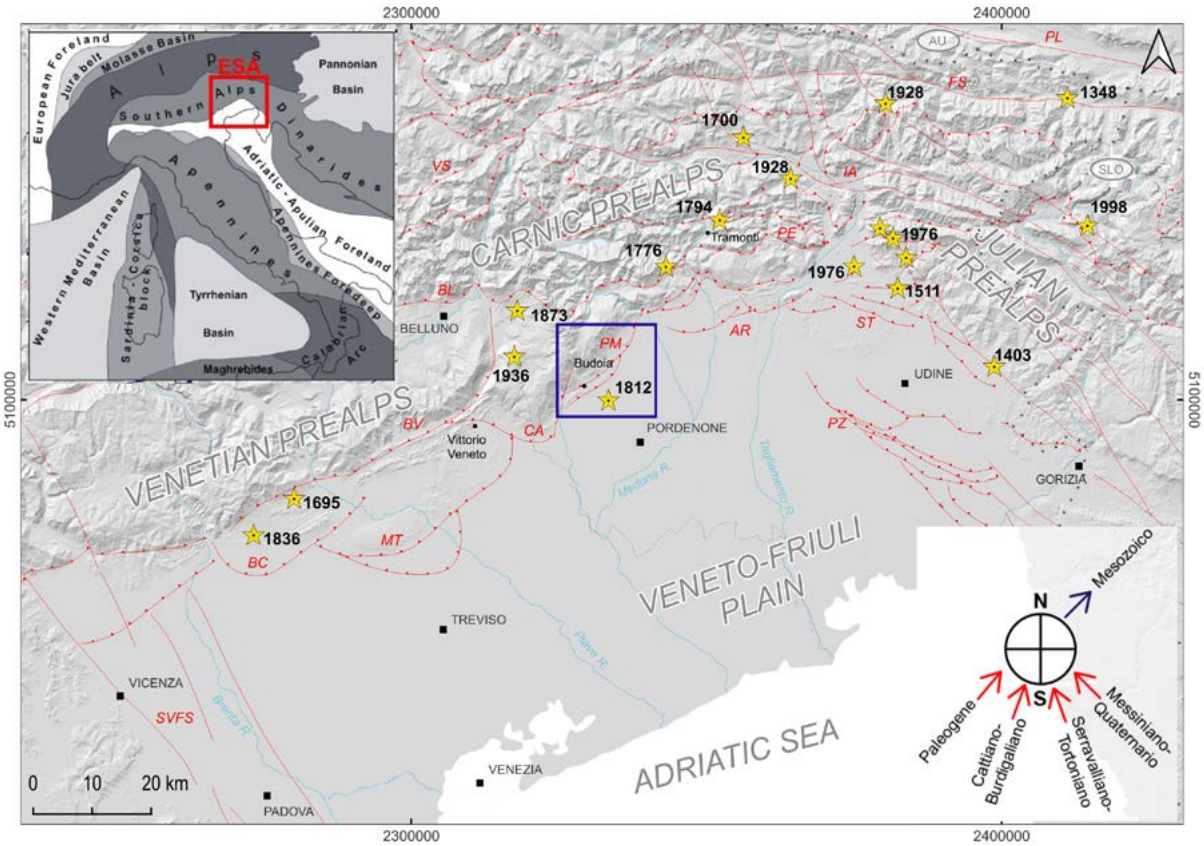

Figure 1 Structural sketch map of the Eastern Southern Alps. Blue rectangle is the study area. Yellow stars are the M>5.5 historical and instrumental seismic events during the last millennium. AR: Arba-Ragogna Th., BC: Bassano-Cornuda Th., BL: Belluno Th., BV: Bassano-Vittorio Veneto Th., CA: Cansiglio Th., FS: Fella-Sava f., IA: Idrija-Ampezzo fs., MT: Montello Th., PE: Periadriatic Th., PL: Periadriatic Lineament, PM: Polcenigo-Montereale Th., PZ: Pozzuolo Th., ST: Susans-Tricesimo Th., SVFS: Schio-Vicenza fault-system., VS: Valsugana Th.

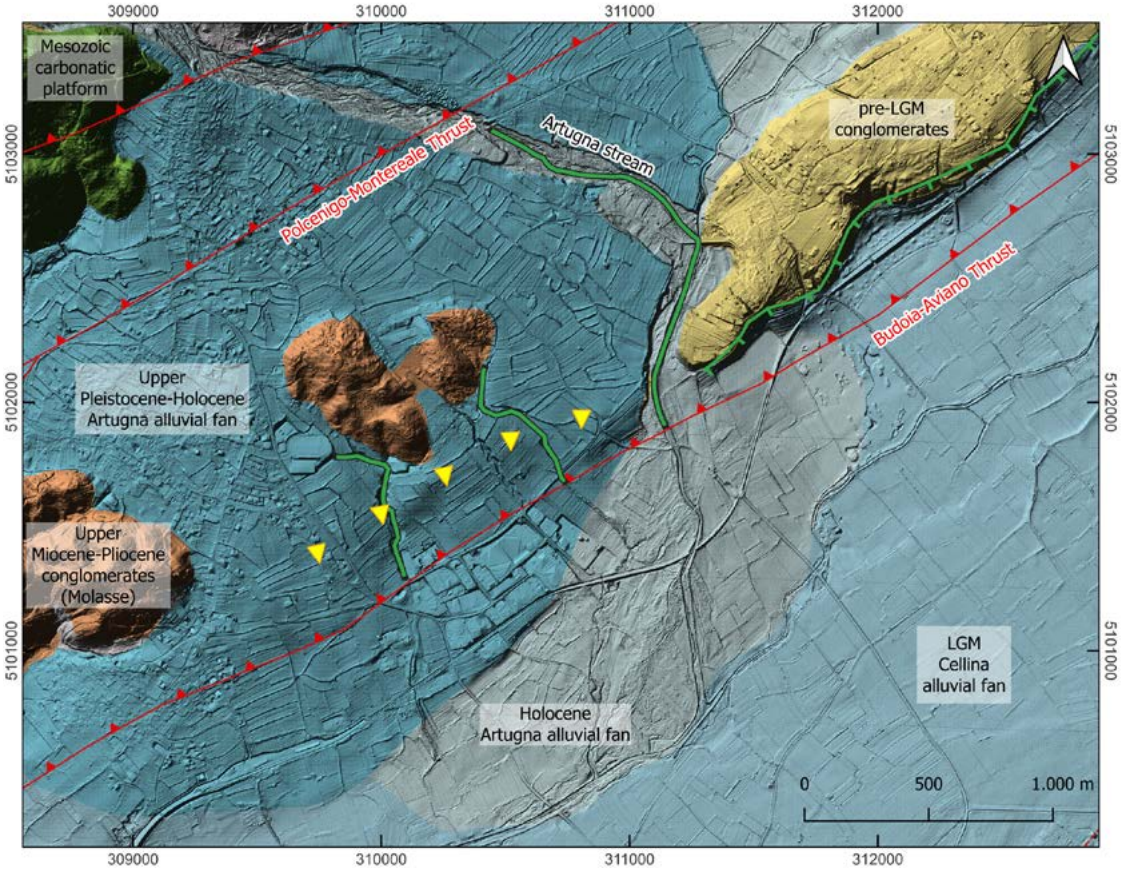

Figure 2 Morphotectonic evidence of fault-related anticline growth on the Upper Pleistocene-Holocene alluvial fan of the Artugna River. Yellow triangles: surficial warping; green line: drainage anomalies; green line with ticks: scarp.

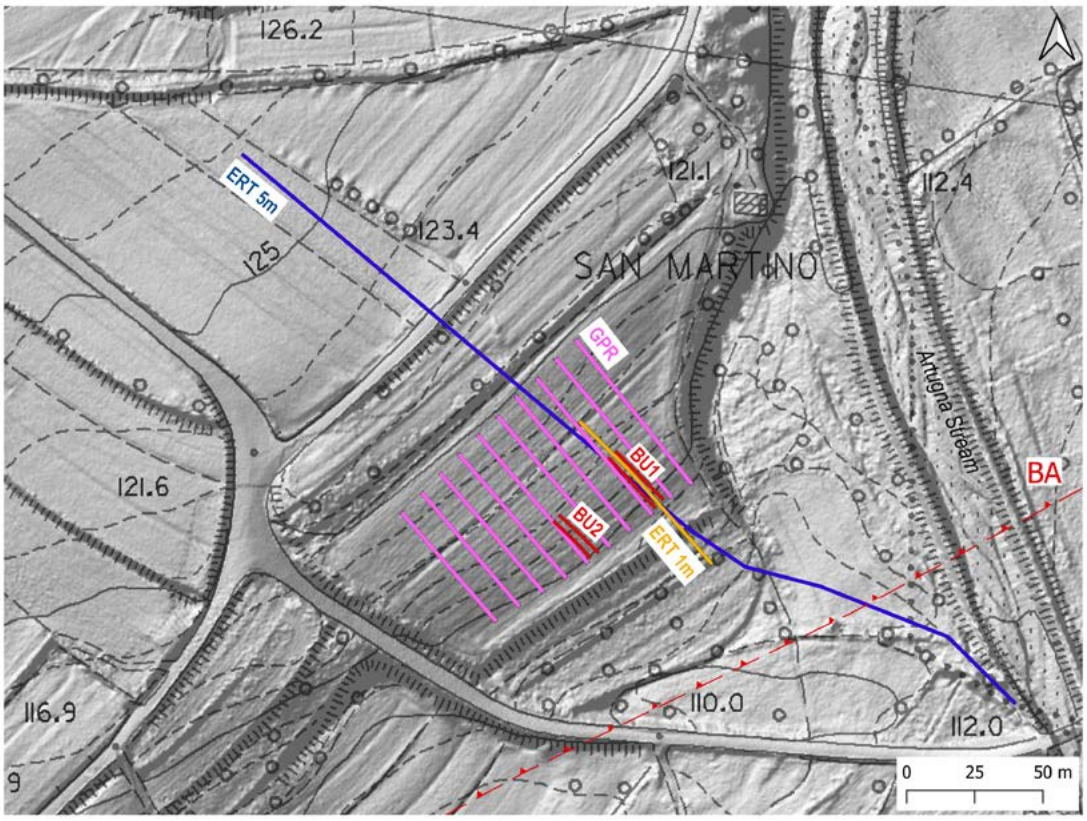

Figure 3 Geophyisical profiles (pink line: GPRs; blue and yellow: deep and shallow ERTs) and palaeoseismological trenches (BU1 and BU2) carried out on the Artugna alluvial fan.

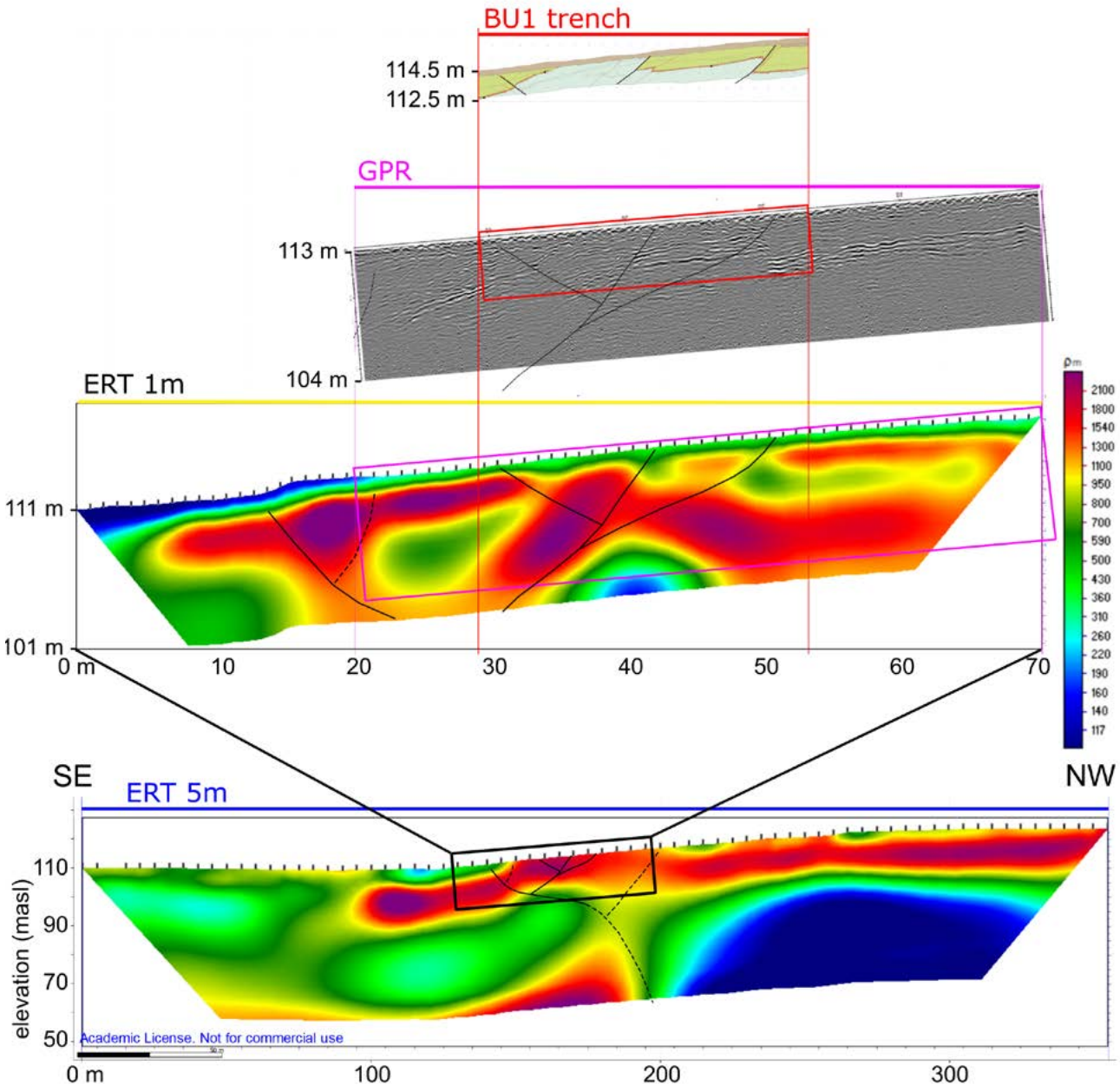

Figure 4 Multiscale investigations workflow. (a): from ERT 5m to ERT1m; (b): from ERT1m to palaeoseismological trench [Rizzo et al., 2024].

Results

The excavated trenches intersected Upper Pleistocene-Holocene sands and gravels of the Artugna River alluvial fan displaced by a set of medium-to-high angle, N-verging reverse faults. At about 2 m-depth from the ground surface, we identified a palaeosoil separating two alluvial fan units. Radiocarbon dating of the palaeosoil sample gave an age of 16,310-16,050 cal. B.C. The palaeoseismological analysis allowed us to estimate a cumulative slip, measured on all the observed fault planes on the order of at least 4.5 m (Figure 5).

The reverse fault planes identified within the two trenches define circa 20 m-wide area of surficial deformation, developed in the hanging-wall block of the main S-verging thrust plane (not intersected by the trenches) and characterized by an ENE-WSW trending.

Figure 5 The western wall of the Budoia 1 trench.

Considering the overall dimensions of this deformation area, both along- and across-strike, this poses a critical issue for such intensely urbanised area, characterised by industrial complexes, urban centres and sensitive infrastructures of Budoia and Aviano localities. Therefore, the palaeoseismological evidence collected so far provide crucial information for more properly estimating the seismic hazard of the area, either relative to ground shaking scenarios and surface faulting-deformation assessments. Both aspects should be indeed carefully considered during regional planning of land use and when developing actions for seismic risk mitigation.

References

Areggi, G., Pezzo, G., Merryman Boncori, J.P., Anderlin, L., Rossi, G., Serpelloni, E., Zuliani,D., and Bonini, L., (2023). *Present-day surface deformation in North-East Italy using In-SAR and GNSS data*. Remote Sensing, 15 (1704). https://doi.org/10.3390/rs15061704

Bernardis, G., Poli, M.E., Renner, G., Snidarcig, A., and Zanferrari, A., (1996). *Le tre sequenze sismiche del 1996 a Claut (Prealpi Carniche).* Atti del 15° Convegno GNGTS, Roma 11-13 novembre 1996, 343-348, Roma.

Devoti, R., Esposito, A., Pietrantonio, G., Pisani, A., and Riguzzi, F., (2011). *Evidence of large scale deformation patterns from GPS data in the Italian subduction boundary*. Earth Planet. Sci. Lett., 311, 230-241. https://doi.org/10.1016/j.epsl.2011.09.034

Galadini, F., Poli, M.E., and, Zanferrari, A., (2005). *Seismogenic sources potentially responsible for earthquakes with M > 6 in eastern Southern Alps (Thiene-Udine sector, NE Italy).* Geophysical

Journal International, 161, 739-762. https://doi.org/10.1111/j.1365-246X.2005.02571.x
Locati, M., Camassi, R., Rovida, A., Ercolani, E., Bernardini, F., Castelli, V., Caracciolo, C.H., Tertulliani, A., Rossi, A., Azzaro, R., D'Amico, S., and Antonucci, A. (2022). *Database Macrosismico Italiano (DBMI15), versione 4.0*. Istituto Nazionale di Geofisica e Vulcanologia (INGV). https://doi.org/10.13127/DBMI/DBMI15.4
Poli, M.E., Monegato, G., Zanferrari, A., Falcucci, E., Marchesini, A., Grimaz, S., Malisan, P., and Del Pin, E. (2015). *Seismotectonic characterization of the western Carnic pre-alpine area between Caneva and Meduno (Ne Italy, Friuli)*. DPC-INGV-S1 Project "Base-knowledge improvement for assessing the seismogenic potential of Italy" (D6/a2.1).
Poli, M.E., Falcucci, E., Gori S., Monegato, G., Zanferrari, A., Affatato, A., Baradello, L., Böem, G., Dal Bo, I., Del Pin, E., Forte, E., Grimaz, S., and Marchesini, A., (2021). *Paleoseismological evidence for historical ruptures along the Meduno Thrust (eastern Southern Alps, NE Italy)*. Tectonophysics, 818. https://doi.org/10.1016/j.tecto.2021.229071
Poli, M.E., Patricelli, G., Monegato, G., and Zanferrari, A., (2024). *Structural inheritances, fault segmentation and seismogenic potential at the front of the eastern Southern Alps (central Carnic Prealps, NE Italy)*. Tectonophysics, 883. https://doi.org/10.1016/j.tecto.2024.230390
Rizzo, E., Colella, A., Lapenna, V., and Piscitelli, S., (2004). *High-resolution images of the fault controlled High Agri Valley basin (Southern Italy) with deep and shallow Electrical Resistivity Tomographies*. Physics and Chemistry of the Earth, 29 (4-9), 321-327. https://doi.org/10.1016/j.pce.2003.12.002
Rizzo E., Giampaolo V., Mucchi F., Boldrin P., De Martino G., Poli M.E., Patricelli G., Marchesini A. and Caputo R. (2024). *Multiscale geophysical investigation on the Budoia-Aviano thrust system (NE Italy): first results*. GNGTS 2024.
Serpelloni, E., Vannucci, G., Anderlini, L., and Bennett, R.A., (2016). *Kinematics, seismotectonics and seismic potential of the eastern sector of the European Alps from GPS and seismic deformation data*. Tectonophysics, 688, 157-181. https://doi.org/10.1016/j.tecto.2016.09.026

Segmentation of the external front of the Eastern Southern Alps: the Arba-Ragogna case study (NE-Italy)

Giulia Patricelli[1,2,3,*], Maria Eliana Poli[1,3], Giovanni Monegato[4], and Adriano Zanferrari[1]

[1]Università di Udine, Dipartimento di Scienze AgroAlimentari, Ambientali e Animali, Udine, Italy
[2]Università di Ferrara, Dipartimento di Fisica e scienze della Terra, Ferrara, Italy
[3]Centro Interuniversitario per la Sismotettonica 3D con Applicazioni Territoriali (CRUST), Chieti, Italy
[4]Consiglio Nazionale delle Ricerche, Istituto di Geoscienze e Georisorse, Padova, Italy

Corresponding author: giulia.patricelli@uniud.it

Structural inheritances play a key role in the geological evolution of the continental lithosphere. In the Eastern Southern Alps (ESA), the Cenozoic to present-day tectonic history is marked by episodes of inversion and reactivation of pre-existing structures, which often controlled the segmentation of the frontal thrust systems [e.g., Doglioni, 1992a; 1992b; Castellarin et al., 1992; Galadini et al., 2005; Zanferrari et al., 2013].
This study investigates the relationships between inherited structures and structural segmentation in a set of active faults along the external front of the Eastern Southern Alps (ESA) in the Carnic Prealps (NE Italy). By integrating geological and morphotectonic data with subsurface interpretations derived from a dense grid of industrial seismic profiles (courtesy of ENI E&P), we explore how the inherited Paleogene Dinaric thrust front (NW-SE trending and west-verging) has influenced the propagation of the Pliocene-Quaternary thrust systems in the region.
Specifically, we reinterpret the geometry and kinematics of the Arba-Ragogna Thrust System, previously treated as a single structure [Galadini et al., 2005; Burrato et al., 2008; Zanferrari et al., 2008a; Poli et al., 2009], and propose its subdivision into two distinct segments: the Arba-Sequals (AS) and the Ragogna (RA) Thrusts [Poli et al., 2024]. This segmentation reflects both surface and subsurface structural variability and highlights the role of inherited Dinaric features in shaping the modern thrusts architecture.

Regional tectonic framework

The study area is located along the external front of the ESA in Friuli, at the transition between the Carnic Prealps and the adjacent Friulian piedmont plain.
This sector has recorded a complex geodynamic evolution, shaped by a Mesozoic extensional regime followed by compressional tectonics during the Cenozoic. Two main tectono-sedimentary phases characterize the Cenozoic evolution of the ESA: the Late Cretaceous-Middle Eocene Dinaric event and the Middle Miocene-Quaternary Neoalpine event [Doglioni and Bosellini, 1987; Doglioni, 1990; Castellarin and Cantelli, 2000].
Regarding the first compressional event, the inherited NW-SE trending Dinaric external thrust front is still recognizable in the Friuli Plain as the Palmanova-Pozzuolo Thrust System (PA-PZ, Figure 1), whose activity generated a structural high trending NW-SE [Placer et al., 2010]. The northwesternmost extent of this inherited Dinaric front is represented by the Monte Ciaurlec Thrust, which is now embedded within the Southalpine orogenic belt [Zanferrari et al., 2008b].
During the latest Oligocene-Early Miocene, the Veneto-Friuli region functioned as distal foreland of the Alpine Chain *s.s.* Starting from the Middle Miocene onward, the ESA underwent significant shortening during the Neoalpine tectonic event, marked by two main compressional

phases: a Serravallian-Tortonian phase ($\sigma_1 \approx$ NNW-SSE) and a Messinian-Pliocene phase ($\sigma_1 \approx$ NW-SE) [Castellarin et al., 1992; Caputo, 1996; Fantoni et al., 2002].

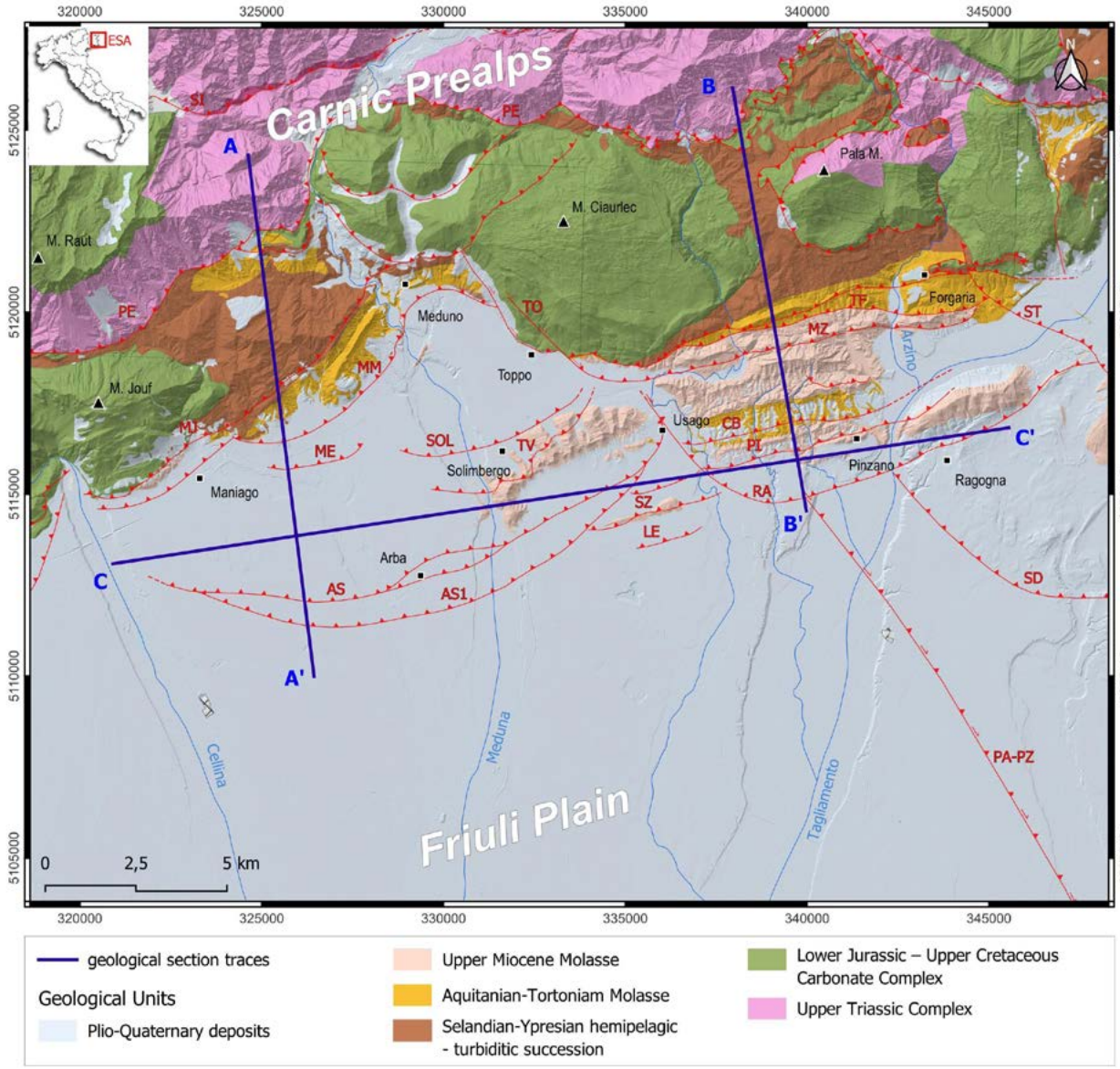

Figure 1 Geological map of the eastern Carnic Prealps (modified from Carulli et al. [2000], Carulli [2006], Zanferrari et al. [2008a; 2013] and Monegato and Poli [2015]). Acronyms: AS: Arba-Sequals Thrust, CB: Costabeorchia Th., LE: Lestans Th., ME: Meduno Th., MJ: Monte Jouf Th., MM: Maniago-Meduno Th., MZ: Manazzons Th., PA-PZ: Palmanova-Pozzuolo Th., PE: Periadriatic Th., PI: Pinzano Th., RA: Ragogna Th., SD: San Daniele Th., SI: Silisia Th., ST: Susans-Tricesimo Th., SOL: Solimbergo Th., SZ: San Zenone Th., TO: Toppo transfer Fault, TF: Toppo-Forgaria Th., TV: Travesio Th.

These Neoalpine deformations overprinted and partially reactivated the pre-existing Dinaric structures (particularly the Palmanova-Pozzuolo front, which experienced transpressive reactivation) and triggered the development of new WSW-ENE trending reverse faults -such as the Terenzano and Medea thrusts - characterized by dip-slip kinematics [Venturini, 1987; Poli, 1996; Patricelli and Poli, 2020]. This led to the persistence of the structural high and influenced sedimentation. A comparable structural evolution affected the Monte Ciaurlec

inherited Thrust, which was reactivated and shifted southwestward relative to the PA-PZ System due to its incorporation into the Southalpine thrust belt.
Concerning the present activity of these structures, the recent instrumental data show low seismic activity. However, historical records report two moderate earthquakes in 1776 (Mw 5.8) and 1794 (Mw 5.96) [Rovida et al., 2022]. The 1776 event has been attributed to the Meduno Thrust [Poli et al., 2021], while the source of the 1794 earthquake remains uncertain.

Methodology

This study was based on a multidisciplinary approach:

- a grid of seismic reflection profiles kindly supplied by ENI E&P has been analysed for reconstructing the structural arrangement at depth;
- the 1-meter resolution DTM has been analysed for conducting a detailed geological survey in selected areas to validate the morphological observations;
- three geological cross sections have been reconstructed by adopting a velocity model extracted from the literature [Zanferrari et al., 2008a; 2008b; Toscani et al., 2016; Patricelli and Poli, 2020; Poli et al., 2024] (Table 1) and integrating subsurface and field data.

SEISMOSTRATIGRAPHIC UNIT	VELOCITY P-WAVES [m/s]
Pliocene - Quaternary Units	2000
Upper Tortonian - lower Messinian Molasse	3500
Lower Serravalian - Tortonian Molasse	3000
Aquitanian - Langhian Cavanella Group	4100
Lower Eocene - hemipelagic and turbiditic units	3600
Lower Jurassic - Upper Cretaceous Carbonate platform units	5800

Table 1 Velocity model adopted for the 2D depth seismic lines conversion.

Results

Within the stratigraphic succession cropping out in the study region we identified five main complexes:

a. the Upper Triassic Complex;
b. the Lower Jurassic - Upper Cretaceous Carbonate Complex;
c. the Selandian-Ypresian hemipelagic - turbiditic succession unconformably covering the Cretaceous carbonates;
d. the mostly terrigenous Miocene sediments;
e. the Pliocene-Quaternary continental succession, which has been controlled by the merging of Tagliamento Cellina, Meduna and Arzino alluvial fans during their Quaternary evolution [Avigliano et al., 2002; Paiero and Monegato, 2003; Monegato et al., 2007; 2010; Fontana et al., 2014; 2019; Monegato and Poli, 2015]. Particularly, the last aggradation phase is related to the Tagliamento glacier outwash deposition during the Last Glacial Maximum in the Alps.

The structural model developed for the Carnic Prealps reveals four main thrust systems with documented Pleistocene to Holocene tectonic activity: the Maniago-Meduno (MM), Toppo-Forgaria (TF), Arba-Sequals (AS), and Ragogna (RA) Thrust Systems (Figure 1).
The Maniago-Meduno (MM) and Toppo-Forgaria (TF) Systems are located at the base of the carbonate anticlines of Mt. Jouf and Mt. Ciaurlec, respectively, and are connected by the dextral Toppo transfer Fault (TO). These thrusts cause the overthrusting of the Aquitanian-Tortonian Molasse units onto the upper Tortonian-lower Messinian Molasse. In front of them, the Arba-Sequals (AS) and Ragogna (RA) Thrust Systems develop. Both systems deform the Miocene Molasse succession, but exhibit markedly different structural styles. In the western sector, the three reverse splays AS, AS1 and AS2 which compose the Arba-Sequals Thrust System cut through the stratigraphic sequence and involve the Pliocene-Quaternary cover, giving rise to the Sequals anticline: a broad folding plunging 15°-20° towards the SW (section AA'; Figure 2). Differently, the eastern portion of the external front is represented by the Ragogna Thrust System composed by the Costabeorchia (CB), Pinzano (PI) and Ragogna (RA) thrusts. The RA Thrust System causes a tight (circa N80°) trending anticline (Ragogna anticline) and propagates up to the topographic surface (section BB'; Figure 2).

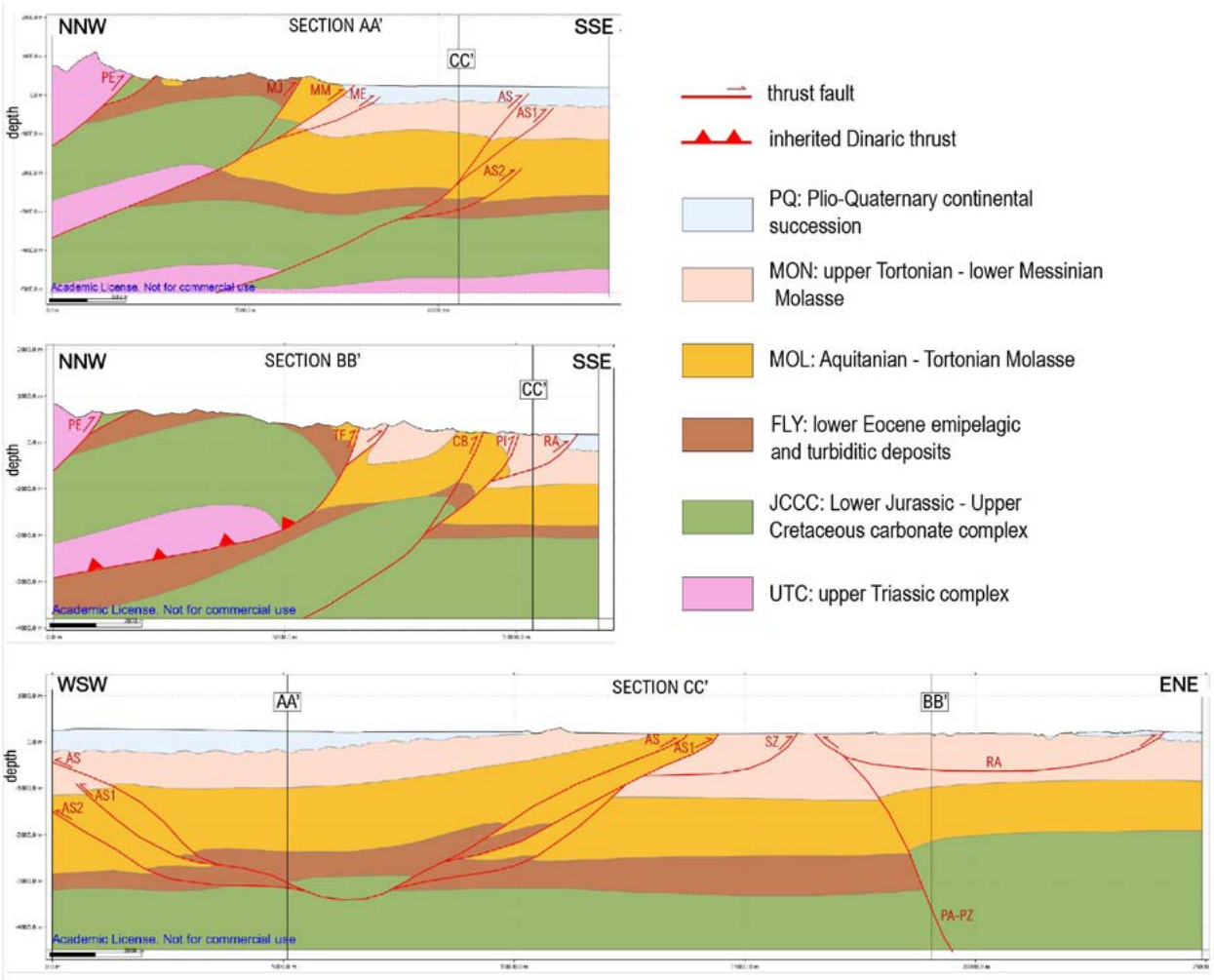

Figure 2 Geological cross sections of the study area. See locations in Figure 1. Acronyms: AS, AS1, AS2: Arba-Sequals Thrust System; CB: Costabeorchia Th.; MM: Maniago-Meduno Th.; ME: Meduno external splay of MM Th; MJ: Mt. Jouf Th.; PA-PZ: Palmanova-Pozzuolo Th.; PE: Periadriatic Th.; PI: Pinzano Th.; RA: Ragogna Th.; SZ: San Zenone Th.; TF: Toppo-Forgaria Th.; TO: Toppo transfer Fault.

Geometric differences between the Sequals and Ragogna anticlines suggest a strong control by inherited structures, particularly the buried Dinaric structural high bounded by the Palmanova-Pozzuolo structure (PA-PZ) (section CC'; Figure 2). While the western sector (Arba-Sequals Thrust System) formed in the footwall of the inherited Dinaric structures, the eastern sector (Ragogna Thrust System) developed above a structural high. The lateral termination between AS and RA aligns with the buried Dinaric front (section CC'; Figure 2), suggesting that the inherited structure strongly controlled the propagation of the external Southalpine front during the Neoalpine phase.

In this regard, if considering the polyphase tectonic history of the study area, by the onset of Neoalpine deformation the region had already been shaped by Dinaric tectonics: the NW-SE elongated carbonate anticline (Palmanova-Pozzuolo-Mt. Ciaurlec) overthrusted the Dinaric foredeep. The Neoalpine compressive phase (started during Miocene) reactivated these structures, giving rise to the SE-verging Southalpine thrust belt. The Toppo transfer zone developed along a pre-existing weak zone and facilitated the southeastward migration of the Toppo-Forgaria (TF) Thrust relative to Maniago-Meduno (MM) Thrust, creating space for the Molasse deposition. The Dinaric inheritances control over the progressive south-eastward propagation of the thrust front continued also during the upper Miocene and Pliocene-Quaternary, when the Arba-Sequals and Ragogna Thrust Systems, representing the external front, developed.

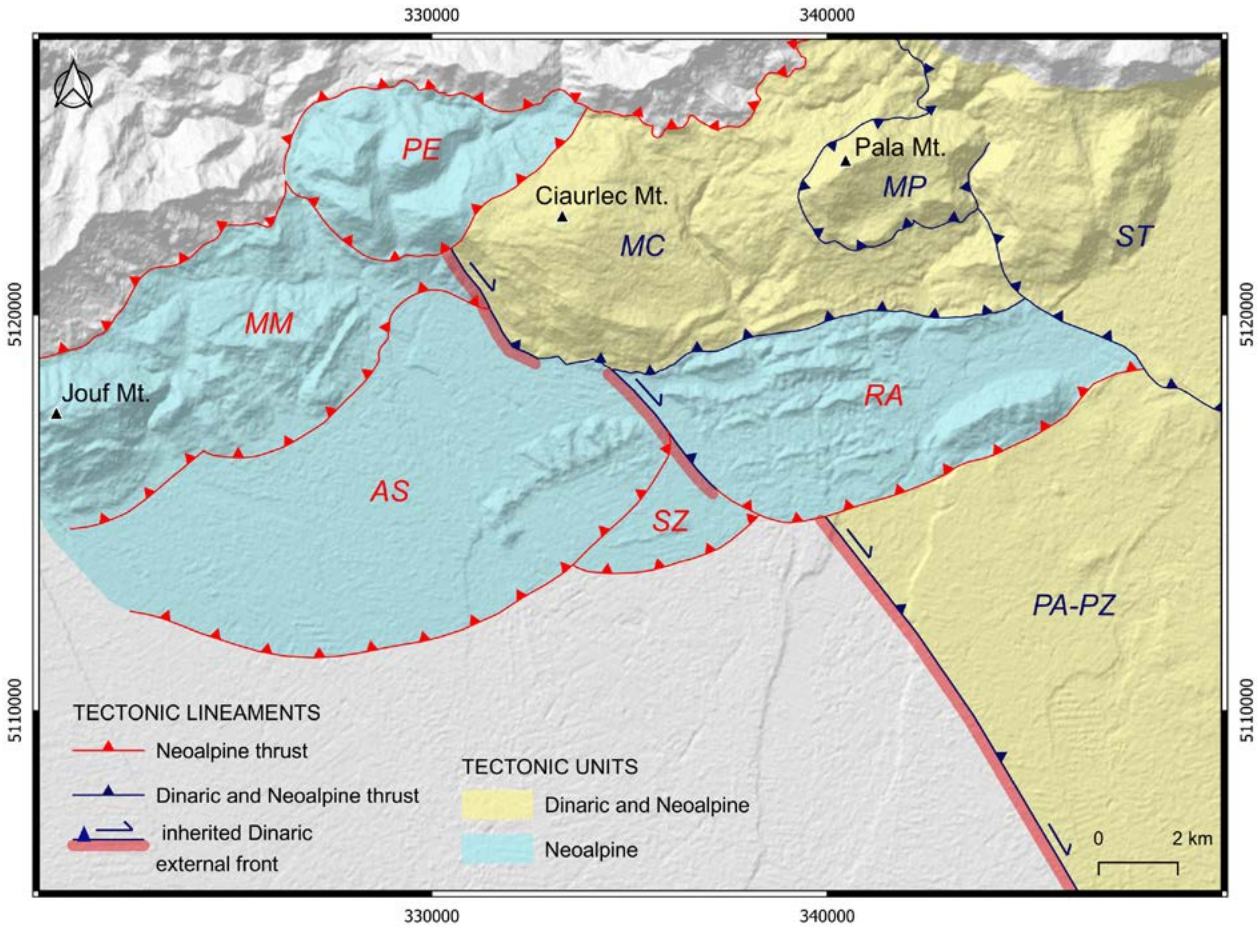

Figure 3 Tectonic lineaments and tectonic units of the study area. Acronyms: AS: Arba-Sequals; MC: Monte Ciaurlec; MM: Maniago-Meduno; MP: Monte Pala; PA-PZ: Palmanova-Pozzuolo; PE: Periadriatic; RA: Ragogna; ST: Susans-Tricesimo; SZ: San Zenone.

Discussion and concluding remarks

Using a multidisciplinary approach, we investigated the active thrust front of the eastern Southern Alps, between the Cellina and Tagliamento rivers. By integrating geophysical surveys, geological and morphotectonic field data with geological cross-sections, we reconstructed the polyphase tectonic evolution of the Carnic Prealpine boundary. Our results highlight the Quaternary activity of four main thrust systems: Maniago-Meduno (MM), Toppo-Forgaria (TF), Arba-Sequals (AS), and Ragogna (RA).

The evolution of this sector has been strongly influenced by the deep structural high of the Friulian Carbonate Platform, which is associated with the Palaeogene Dinaric front and trends NW-SE across the Friuli Plain. This inherited structure controlled the propagation of the Neogene-Quaternary front and led to the development of two distinct structural sectors: a western sector in the footwall (Meduno-Maniago and Arba-Sequals Thrusts) and an eastern sector in the hanging-wall block (Toppo-Forgaria and Ragogna Thrusts).

The Toppo and Ragogna lateral ramps developed along this inherited structure and presently act as structural boundaries, since they document the segmentation of the Southalpine external front. These results align with analog and numerical models that show how inherited discontinuities favor the development of transfer zones, such as lateral ramps and tear faults, which control thrust propagation. Specifically, inherited offsets in the structural backstop influence thrusts geometry and segment the frontal wedge, leading to asymmetric deformation styles on either side of the transfer zone [Calassou et al., 1993; Ruh et al., 2013]. These findings have important seismotectonic implications for the seismic hazard assessment of the area: considering that the outer front is segmented in two portions (AS and RA), the estimated seismogenic potential is lower compared to the potential of a single, continuous source. However, the possibility that the two fault segments may rupture together, or that the activation of one may trigger the other, cannot be ruled out.

References

Avigliano, R., Calderoni, G., Monegato, G., and Mozzi, P., (2002). *The late Pleistocene- Holocene evolution of the Cellina and Meduna alluvial fans (Friuli, NE Italy)*. Mem. Soc. Geol. It. 57, 133-139.

Burrato, P., Poli,M.E., Vannoli, P., Zanferrari, A., Basili, R., and Galadini, F., (2008). *Sources of Mw 5+ earthquakes in northeastern Italy and western Slovenia: an updated view based on geological and seismological evidence.* Tectonophysics, special volume "Earthquake Geology: methods and applications" guest editors: R. Caputo & S.B. Pavlides 453, 157-176. https://doi.org/10.1016/j.tecto.2007.07.009

Calassou, D., Larroque, C., and Malavieille, J., (1993). *Transfer zones of deformation in thrust wedges – an experimental study*. Tectonophysics, 221(3-4), 325-344.

Caputo, R., (1996). *The polyphase tectonics of Eastern Dolomites, Italy*. Mem. Sci. Geol., 48, 93-106.

Carulli, G.B., (2006). *Carta geologica del Friuli Venezia Giulia alla scala 1:150000*. Regione Autonoma Friuli Venezia Giulia - Direzione centrale ambiente ed energia – Servizio Geologico, S.E.L.C.A. Firenze.

Carulli, G.B., Cozzi, A., Longo Salvador, G., Pernacic, E., Podda, F., and Ponton, M., (2000). *Carta geologica delle Prealpi Carniche*. In: Pubbl. n◦ 44, Edizioni Museo Friulano Storia Naturale, Udine.

Castellarin, A., and Cantelli, L., (2000). *Neo-Alpine evolution of the Southern Eastern Alps*. J. Geodyn. 30, 251-274.

Castellarin, A., Cantelli, L., Fesce, A.M., Mercier, J.L., Picotti, V., Pini, G.A., Prosser, G. and, Selli, L., (1992). *Alpine compressional tectonics in Southern Alps. Relationships with the N-Apennines*. Annales Tectonicae 6 (1), 62-94.

Doglioni, C., (1990). *Thrust Tectonics example from the venetian Alps*. Studi Geologici Camerti, Sp. issue 1990, 117-129.

Doglioni, C., (1992a). *The Venetian Alps Thrust Belt*. In: Thrust Tectonics. McKlay, K.R. (Ed.), Chapman and Hall, London, pp. 319-324.

Doglioni, C., (1992b). *Relationships between Mesozoic extensional tectonics, stratigraphy and Alpine inversion in the Southern Alps*. Eclogae Geol. Helv. 85 (1), 105-126.

Doglioni, C., and Bosellini, A., (1987). *Eoalpine and mesoalpine tectonics in the Southern Alps*. Geol. Rundsch. 76, 735-754.

Fantoni, R., Catellani, D., Merlini, S., Rogledi, S., and Venturini, S., (2002). *La registrazione degli eventi deformativi cenozoici nell'avampaese Veneto-Friulano*. Mem. Soc. Geol. It. 57, 301-313.

Fontana, A., Mozzi, P., and Marchetti, M., (2014). *Alluvial fans and megafans along the southern side of the Alps.* Sediment. Geol. 301, 150-171. https://doi.org/10.1016/j. sedgeo.2013.09.003

Fontana, A., Monegato, G., Rossato, S., Poli, M.E., Furlani, S., and Stefani, C., (2019). *Carta delle Unit`a geologiche della pianura del Friuli Venezia Giulia alla scala 1:150.000 e note illustrative*. Regione Autonoma Friuli Venezia Giulia - Servizio Geologico, Trieste, p. 80.

Galadini, F., Poli, M.E., and Zanferrari, A., (2005). *Seismogenic sources potentially responsible for earthquakes with M≥6 in the eastern Southern Alps (Thiene-Udine sector, NE Italy).* Geophys. J. Int. 161, 739-762. https://doi.org/10.1111/j.1365- 246X.2005.02571.x

Monegato, G., and Poli, M.E., (2015). *Tectonic and climatic inferences from the terrace staircase in the Meduna valley, eastern Southern Alps, NE Italy*. Quat. Res. 83, 229–242.

Monegato, G., Ravazzi, C., Donegana, M., Pini, R., Calderoni, G., and Wick, L., (2007). *Evidence of a two-fold glacial advance during the last Glacial Maximum in the Tagliamento end moraine system (eastern Alps).* Quat. Res. 68, 284-302.

Monegato, G., Lowick, S.E., Ravazzi, C., Banino, R., Donegana, M., and Preusser, F., (2010). *Middle to late Pleistocene chronology and palaeoenvironmental evolution of the south-eastern Alpine Foreland: the Valeriano Creek succession (NE Italy).* J. Quat. Sci. 25, 617-632.

Paiero, G., and Monegato, G., (2003). *The Pleistocene evolution of Arzino alluvial fan and western part of Tagliamento morainic amphitheatre (Friuli, NE Italy).* Il Quaternario, 16 (1), 185-193.

Patricelli, G., and Poli, M.E., (2020). *Quaternary tectonic activity in the north-eastern Friuli Plain (NE Italy).* Boll. Geofis. Teor. Appl. 61 (3), 309-332. https://doi.org/10.4430/ bgta0319

Placer, L., Vrabec, M., and Celarc, B., (2010). *The base for understanding of the NW Dinarides and Istria Peninsula tectonics.* Geologija 53, 55-86. https://doi.org/10.5474/ geologija.2010.005

Poli, M.E., (1996). *Analisi strutturale del Monte di Medea (Friuli orientale-Gorizia).* Atti Ticinesi Sci. Terra, ser. spec. 3, 99-114.

Poli, M.E., Zanferrari, A., and Monegato, G., (2009). *Geometria, cinematica e attività pliocenico-quaternaria del sistema di sovrascorrimenti Arba-Ragogna (Alpi Meridionali orientali, Italia NE).* Rend. Online Soc. Geol. Ital. 5, 172-175.

Poli, M.E., Falcucci, E., Gori, S., Monegato, G., Zanferrari, A., Affatato, A., Baradello, L., Böem, G., Dal Bo, I., Del Pin, E., Forte, E., Grimaz, S., and Marchesini, A., (2021). *Paleoseismological evidence for historical ruptures along the Meduno Thrust (eastern Southern Alps, NE Italy).* Tectonophysics, 818, 229071.

Poli, M.E., Patricelli, G., Monegato, G., and Zanferrari, A., (2024). *Structural inheritances, fault segmentation and seismogenic potential at the front of the eastern Southern Alps (central Carnic Prealps, NE Italy).* Tectonophysics 883, 230390. https://doi.org/10.1016/j. tecto.2024.230390

Rovida, A., Locati, M., Camassi, R., Lolli, B., Gasperini, P., and Antonucci, A., (2022). *Catalogo*

Parametrico dei Terremoti Italiani (CPTI15), versione 4.0. Istituto Nazionale di Geofisica e Vulcanologia. https://doi.org/10.13127/CPTI/CPTI15.4

Ruh, J.B., Gerya, T., and Burg, J.P., (2013). *High-resolution 3D numerical modelling of thrust wedges: Influence of d´ecollement strength on transfer zones*. Geochem. Geophys. Geosyst. 14 (4), 1131-1155.

Toscani, G., Marchesini, A., Barbieri, C., Di Giulio, A., Fantoni, R., Mancin, N., and Zanferrari, A., (2016). *The Friulian-venetian Basin I: architecture and sediment flux into a shared foreland basin*. Ital. J. Geosci. 135 (3), 444-459. https://doi.org/ 10.3301/IJG.2015.35

Venturini, S., (1987). *Nuovi dati sul Tortoniano del sottosuolo della Pianura Friulana*. Gortania - Atti del Museo Friulano di Storia Naturale 9, 5-16.

Zanferrari, A., Avigliano, R., Grandesso, P., Monegato, G., Paiero, G., and Poli, M.E., (2008a). *Geological map and explanatory notes of the Geological Map of Italy at the scale 1: 50.000: sheet 065 "Maniago"*. APAT - Servizio Geologico d'Italia - Regione Autonoma Friuli Venezia Giulia 2008, 224. www.isprambiente.gov.it/Media/carg/fr iuli.html

Zanferrari, A., Avigliano, R., Monegato, G., Paiero, G., and Poli, M.E., (2008b). *Geological map and explanatory notes of the Geological Map of Italy at the scale 1: 50.000: sheet 066 "Udine"*. APAT - Servizio Geologico d'Italia - Regio-ne Autonoma Friuli Venezia Giulia, p. 176. www.isprambiente.gov.it/Media/carg/friuli.html

Zanferrari, A., Masetti, D., Monegato, G., and Poli, M.E., (2013). *Geological map and explanatory notes of the Geological Map of Italy at the scale 1:50.000: sheet 049 "Gemona del Friuli"*. ISPRA - Servizio Geologico d'Italia - Regione Autonoma Friuli Venezia Giulia 262. www.isprambiente.gov.it/Media/carg/friuli.html

The influence of pre-existing structures on the foredeep evolution and structural style: the case studio in the Western Emilian Arc, Central Po Plain (Italy)

Ada De Matteo[1,2,*], Giovanni Toscani[1,2], and Silvio Seno[1,2]

[1]Università di Pavia, Dipartimento di Scienze della Terra e dell'Ambiente, Pavia, Italy
[2]Centro Interuniversitario per la Sismotettonica 3D con Applicazioni Territoriali (CRUST), Chieti, Italy

Corresponding author: ada.dematteo@unipv.it

Introduction

Within the framework of the NASA4SHA research project aimed at investigating fault complexities in active thrust systems of Northern Italy, the University of Pavia Research Unit (RU) was responsible for analysing the western portion of the Emilian Arc (Figure 1) by developing analogue models of thrust systems. Due to its geological setting, characterized by the presence of structural highs that may have influenced the advance of the thrust systems under investigation, the central Po Plain represents an excellent case study for assessing the role of pre-existing structures in the evolution of the foredeep basins and in determining the structural style.

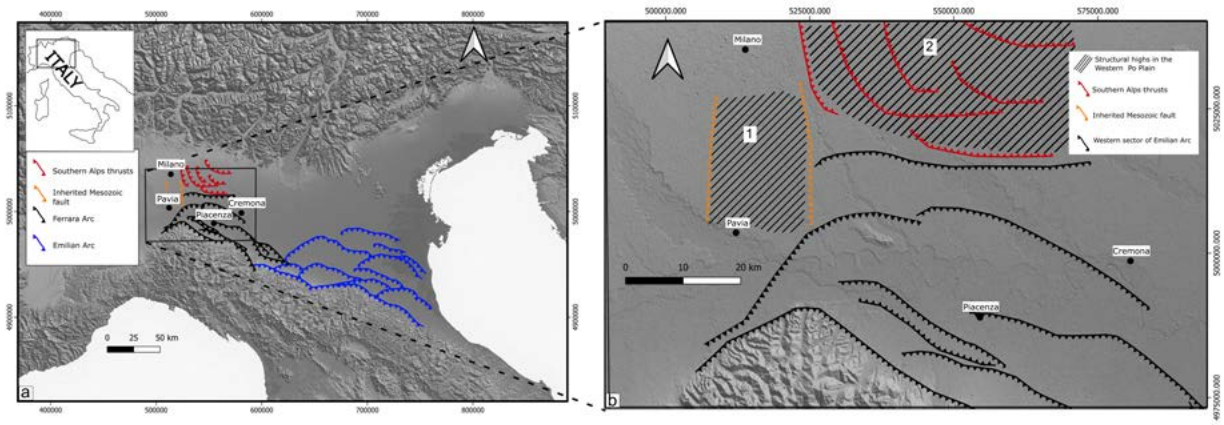

Figure 1 (a) Geological setting. (b) Simplified structural map of buried thrusts in the western sector of the Emilian Arc, distinguished by structural setting (in red the Southern Alps buried fronts, in black the Northern Apennines ones, in yellow the inherited lineaments). The two striped areas (1 and 2) represent the structural highs that existed prior to the formation of the Apennine mountain ranges.

The tectonic framework of the central Po Plain is characterized by the complex interaction between the Southern Alps (SA) and the Northern Apennines (NA). The SA consist of a south-verging fold-and-thrust belt that is partially buried beneath the Pliocene-Pleistocene sedimentary cover, whereas the NA are a north-verging fold-and-thrust belt that displays an outcropping segment separated from the buried part beneath the Neogene-Quaternary sediments by the Pedeapenninic Thrust Front [Castellarin et al., 1992; Fantoni and Franciosi, 2010; Ghielmi et al., 2010; Toscani et al., 2014]. The evolution of the Po Plain is strongly influenced by the interaction between the Alpine and Apennine tectonic systems (e.g. [Carminati and Doglioni,

2012; Livani et al., 2018; Maesano et al., 2015]). The area has experienced south-vergent Alpine compressional events since the Middle Eocene, followed by NNE-vergent Apenninic compression since the Lower Miocene.
Regional Quaternary tectonics at the Po Plain–Apennines hinge has been dominated by northward thrusting and folding. Local transpression has occurred along lateral ramps and the Southern Alps thrusts have been reactivated at a deeper level [Bresciani and Perotti, 2014; Burrato et al., 2003; Maesano et al., 2015; Maestrelli et al., 2018]. Zuffetti and Bersezio [2021] documented secondary extensional faulting in the San Colombano hill.
These belong to a group of Quaternary intra-basin reliefs that rise above the average elevation of the alluvial plain [Desio, 1965] and form over the culmination of the deep ramp folds of the Apennine thrust belts. A detailed structural characterization of the area was provided on the basis of the analysis of a dense dataset of seismic reflection profiles and wells data (courtesy of Eni as part of the PhD project of Daniel Barrera, University of Pavia).
Analogue modelling has long been used to understand, test and constrain geometric and structural styles in different tectonic settings as well as to analyse the influence of various parameters on the kinematics of thrust-and-fold belts. In this study, scaled analogue models were performed to investigate the evolution of the thrust system buried beneath the Pliocene-Quaternary sediments of the Po Plain foreland [Amadori et al., 2019], focusing on the interaction between two opposite verging chains during the Neogene-Quaternary tectonic phases. To investigate the factors controlling the kinematic complexity of the arc-shaped thrusts that characterize the westernmost sector of the Emilian Arc and its interaction with the presence of opposite verging South-Alpine thrusts, we carried out a series of models simulating the effects of the mapped structural highs and related rheological variations of the central Po Plain subsurface (Figure 1). The goal of the models was to evaluate whether, and in what matter, inherited foreland structures and buried thrust fronts influence the geometry, kinematics and slip distribution of the Northern Apennines fronts.
In particular, these models help determine whether deformation occurs homogeneously along strike or it becomes segmented since the early stages of thrust development. Moreover, they provide valuable tools analysing the strain distribution along the outermost arc fronts. Finally, slip-rate calculation and the assessment of slip variation along strike for the main identified thrusts (computed by our RU in another Working Package of the same project) enabled comparison between the kinematic behaviour of the modelled thrusts and those derived from the seismic data.

Methods

The experimental set-up consists of a sandbox with three fixed sides and one movable side, driven by a PC-controlled hydraulic piston (Figure 2). The scale ratio between models and nature is approximately 4×10^{-6}, meaning that 4 mm in the model correspond to ~1 km in nature.
To simulate relatively competent natural rocks, such as sandstones, we used quartz sand with grain size ranging from 100-300 μm and internal friction angle (φ) close to 33°.
We modelled an oversimplified stratigraphic sequence similar to that of the buried thrust front of the Northern Apennines and Southern Alps beneath the central part of the Po Plain foreland. "Brittle" sand layers of different colours were used to highlight tectonic structures, making them easier to be observed on photographs and to measure displacements along faults and distances between different structures.
Since this work aims to simulate the recent kinematic and tectonic evolution of the structures buried beneath the Po Plain, we did not reproduce the earlier tectonic phases that led to the

formation of the two exposed chain. Therefore, the models presented hereinafter start from the assumption that the orogenic wedges of the two chains were already formed.
Three different analogue models have been analysed. The first (M1) is a basic and simple model, consisting only of a horizontal sand layer (Figure 3) used for “reference”. The second model (M2) includes two basal blocks to simulate the presence of two structural highs (Figure 3), namely the Southern Alps buried fronts and the reactivated Lacchiarella high (1 and 2 in Figure 2a, respectively). The third model (M3; Figure 3) combines both the blocks simulating structural highs and different friction values across different sectors of the model.

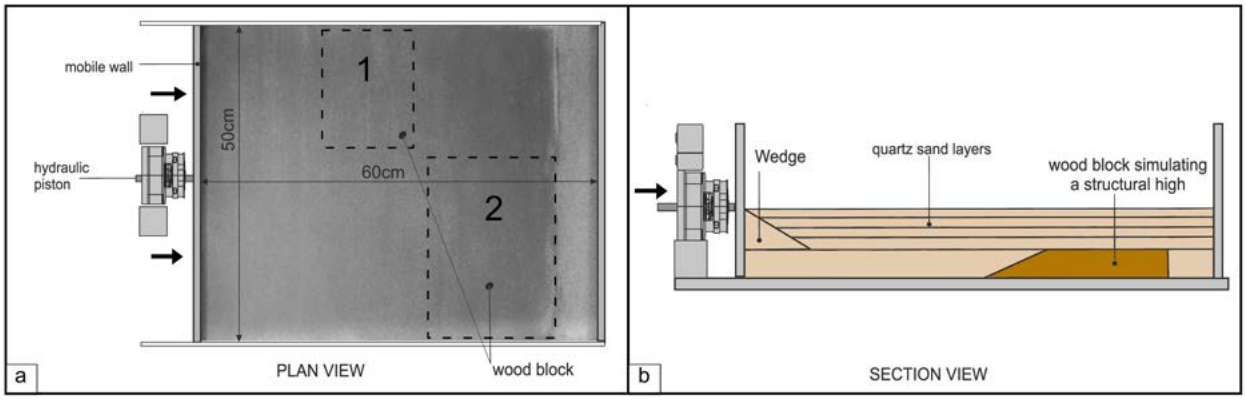

Figure 2 Sandbox configuration. a) plan view of a 60x50 cm sandbox filled with 4 cm of quartz sand. The dashed black rectangles represent the wood blocks (covered by sand) used to simulate the presence of structural highs (1: Lacchiarella high; 2: South Alpine front). b) section view of the same configuration. Black arrows indicate the direction of movement of the mobile wall, driven by the hydraulic piston.

Results

To estimate the vertical and horizontal deformations, we monitored the experiments using four digital cameras. The image sets were processed into sequences of 3-D surface models through structure-from-motion photogrammetry, allowing vertical deformation analyses (Figure 3a). At the end of the deformation, all models were cut and several cross sections examined (Figure 3b) and quantitatively analysed to produce 3D reconstructions of the displacement pattern. Horizontal deformation was assessed by tracking feature displacements within the vertical camera image sequence using PIVlab (a free and open-source Particle Image Velocimetry - PIV - software) [Thielicke and Stamhuis, 2014]. This analysis also allowed determining strain rates along the outermost front of the arc (Figure 3c).
The first clear difference is that in the “reference” model (M1), the thrust front advances in a “homogeneous” manner, in sequence and, as the wall advances, the thrust propagates forward while maintaining a single, continuous front. In contrast, in models that include structural highs (M2) and, even more so, with differences in friction (M3), the thrust front propagates, and advances segmented into several parallel fronts moving at different speeds and accommodating different amounts of shortening. The cross sections show that the presence of a structural high slows down the advance of the thrust front. Indeed, the thrusts struggle to advance beyond the blocks and also exhibit changes both in slope and wavelength (Figure 3). The thrust front develops slightly where there is the Lacchiarella high (1), while the deformation is more pronounced in correspondence with the structural high of the Southern Alps, which is located slightly further ahead than that of Lacchiarella.

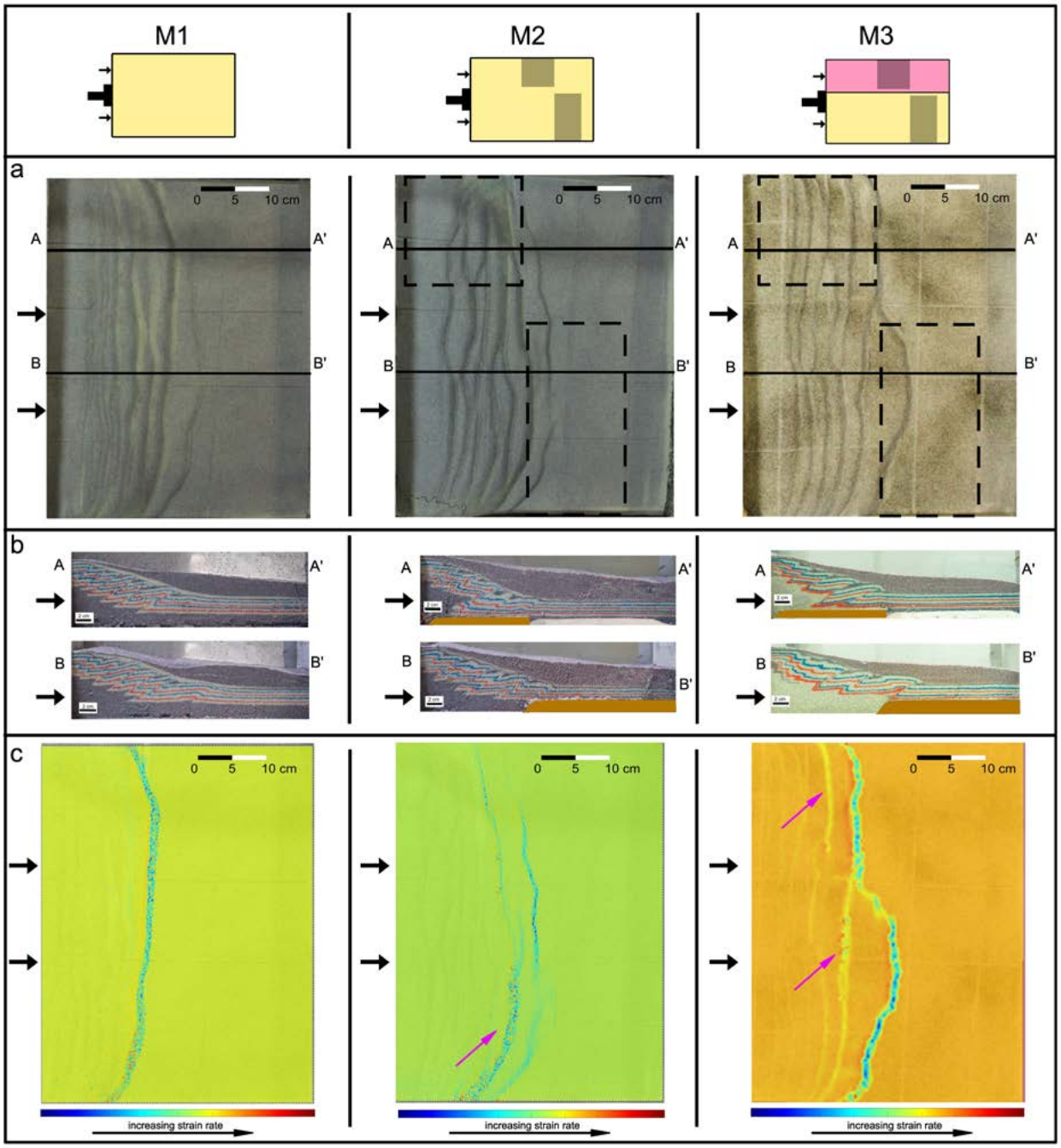

Figure 3 Main analogue models' results. a) top view at the end of the experiment; b) sections of the models at the end of the experiment (section traces visible in a), the dashed black rectangles represent the wood blocks/buried structural highs (covered by sand); c) strain rate analysis of one of the last deformation phases of the experiment. The purple arrows indicate the thrust fronts where tectonic activity is more concentrated. The pink area in M3 represents the sector with higher basal friction.

The difficulty of thrust propagation in the presence of a block that hinders its advancement is further emphasised by the development of backthrusts (Figure 3b, M3 section B-B') and by the strain rate analysis (Figure 3c). When the forward propagation of the thrust is slowed by a structural high, and the deformation cannot involve outermost foreland sectors, inner thrust(s) reactivation occurs. In M2 and even more in M3 models, a highly inhomogeneous deformation distribution is evident both in map (non-rectilinear thrust front traces) and in section (different slip

amount along structures). Furthermore, if structural highs are present, the lateral segmentation and the reactivation of inner thrusts is also evidenced by the strain rate analysis.

Conclusions

Sand box models analysis demonstrates that the presence of inherited structures and/or opposite verging buried fronts significantly affect both kinematics and spatial distribution (along-strike variations) of tectonic deformation. The slip distribution and the along-strike deformation are rather inhomogeneous; also, the thrust kinematics does not follow the usual sequence of deformation from the inner to the outer sectors of the chain but show evidence of out-of-sequence reactivation of inner thrusts and external thrusts with little or no activity during the final deformation phases. In some sectors, the PIV analysis shows that inner thrusts register higher strain values than the outer ones. Finally, it is clear that the model that best replicates the structural setting of the westernmost portion of the Emilian arc is the most complex one (M3), in which both structural highs and rheological inhomogeneities coexist making the Apennine front development and geometry strongly non-cylindrical and diachronous.

References

Amadori, C., Toscani, G., Di Giulio, A., Maesano, F.E., D'Ambrogi, C., Ghielmi, M., and Fantoni, R., (2019). *From cylindrical to non-cylindrical foreland basin: Pliocene-Pleistocene evolution of the Po Plain-Northern Adriatic basin (Italy).* Basin Research, 31(5), 991-1015. https://doi.org/10.1111/bre.12369

Bresciani, I., and Perotti, C.R., (2014). *An active deformation structure in the Po Plain (N Italy): the Romanengo anticline*. Tectonics 33, 2059–2076. https://doi.org/10.1002/ 2013TC003422.

Burrato, P., Ciucci, F., and Valensise, G., (2003). *An inventory of river anomalies in the Po Plain, Northern Italy: evidence for active blind thrust faulting*. Annals of Geophysics 46. https://doi.org/10.4401/ag-3459.

Carminati, E., and Doglioni, C., (2012). *Alps vs. Apennines: The paradigm of a tectonically asymmetric Earth*. Earth-Science Reviews, 112(1–2), 67–96. https://doi.org/10.1016/j.earscirev.2012.02.004

Castellarin, A., Cantelli, L., Fesce, A.M., Mercier, J.L., Picotti, V., Pini, G.A., Prosser, G., and Selli, L., (1992). *Alpine compressional tectonics in the Southern Alps. Relationships with the N-Apennines*. Annales Tectonicae, VI(1), 62-94.

Fantoni, R., and Franciosi, R., (2010). *Tectono-sedimentary setting of the Po Plain and Adriatic foreland*. Rendiconti Lincei, 21(Suppl. 1), 197-209. https://doi.org/10.1007/s12210-010-0102-4

Ghielmi, M., Minervini, M., Nini, C., Rogledi, S., Rossi, M., and Vignolo, A., (2010). *Sedimentary and tectonic evolution in the eastern Po-Plain and northern Adriatic Sea area from Messinian to Middle Pleistocene (Italy)*. Rendiconti Lincei, 21(Suppl. 1), 131-166. https://doi.org/10.1007/s12210-010-0101-5

Maestrelli, D., Benvenuti, M., Bonini, M., Carnicelli, S., Piccardi, L., and Sani, F., (2018). *The structural hinge of a chain-foreland basin: Quaternary activity of the Pede-Apennine Thrust front (Northern Italy).* Tectonophysics 723, 117–135. https://doi.org/ 10.1016/j.tecto.2017.12.006.

Livani, M., Scrocca, D., Arecco, P., and Doglioni, C., (2018). *Structural and Stratigraphic Control*

on Salient and Recess Development Along a Thrust Belt Front: The Northern Apennines (Po Plain, Italy). Journal of Geophysical Research: Solid Earth, 123(5), 4360–4387. https://doi.org/10.1002/2017JB015235

Maesano, F.E., D'Ambrogi, C., Burrato, P., and Toscani, G., (2015). *Slip-rates of blind thrusts in slow deforming areas: Examples from the Po Plain (Italy)*. Tectonophysics, 643, 8–25. https://doi.org/10.1016/j.tecto.2014.12.007

Thielicke, W., and Stamhuis, E., (2014). *Pivlab towards user-friendly, affordable and accurate digital particle image velocimetry in matlab*. Journal of Open Research Software (2). https://doi.org/10.5334/jors.bl

Toscani, G., Bonini, L., Ahmad, M.I., Di Bucci, D., Di Giulio, A., Seno, S., and Galuppo, C. (2014). *Opposite verging chains sharing the same foreland: Kinematics and interactions through analogue models (Central Po Plain, Italy)*. Tectonophysics, 633(1), 268-282. https://doi.org/10.1016/j.tecto.2014.07.019

Zuffetti, C., and Bersezio, R., (2021). Space–time geological model of the Quaternary syntectonic fill of a foreland basin (Po basin, Northern Italy). Sediment. Geol. 421, 105945 https://doi.org/10.1016/j.sedgeo.2021.105945

Results of historical seismology investigations carried out as part of PRIN 2020 NASA4SHA within Working Package 7

Romano Camassi[1], Maria Serafina Barbano[2,3,4], Sofia Baranello[1], Viviana Castelli[1,*], Andrea Faoro[1]

[1]Istituto Nazionale di Geofisica e Vulcanologia - INGV, Sezione di Bologna, Italy
[2]Università di Catania, Dipartimento di Scienze Biologiche, Geologiche e Ambientali, Catania, Italy
[3]Istituto Nazionale di Geofisica e Vulcanologia, Osservatorio Etneo, Catania, Italy
[4]Centro Interuniversitario per la Sismotettonica 3D con Applicazioni Territoriali (CRUST), Chieti, Italy

Corresponding author: viviana.castelli@ingv.it

Italy is a country where high-energy earthquakes (M≥6.0) are scarce and M 7.0 has been rarely exceeded in the last millennium, according to the current CPTI15 v. 4.0 catalogue [Rovida et al., 2022]. Conversely, damaging earthquakes of medium-to-low magnitude (M<6.0) and shallow depth, are frequent and can cause much damage, if in relatively circumscribed areas.
Italy is also a densely populated country, with a building heritage that includes a great number of "old", "ancient" and "very ancient" structures (many of them of great historical and artistic value, and affected by high levels of vulnerability) and it also hosts the largest number of UNESCO sites in the world. In such a situation, even a moderately damaging earthquake can result in huge loss of life and heritage, and economic and social damage.
With these preconditions, being able to make a correct assessment of seismic hazard and seismic risk at a level as detailed as possible is a major strategic objective in Italy.
To reach this end, it is not enough to gain in-depth knowledge of the relatively few high-magnitude historical earthquakes. It is also, if not actually more important, to devote time and care to the improvement of knowledge on as many as possible of the comparatively "minor" damaging earthquakes that have affected the national territory in the near and far-off past. This means not only studying, and periodically updating knowledge on those earthquakes that are already known to the seismic catalogue, but also to devote time to identifying and studying those damaging earthquakes of the near and far-off past that, for a variety of reasons, are still unknown to the seismic catalogue, and –last but not least– to improve the quality of the catalogue by weeding out "fake earthquakes" that could have been included in them by mistake. As previous historical seismology studies show, there is still much space for improvement in all these directions [Molin et al., 2008; Camassi et al., 2011; Castelli et al., 2016].
In line with these requirements, the WP7 "Historical Seismology" of the PRIN 2020 NASA4SHA project identified among its main objectives the improvement of the seismic catalogue CPTI15 v.4.0 [Rovida et al., 2022] and the database of macroseismic observations DBMI15 v.4.0 [Locati et al., 2022] by updating the existing studies and drafting new studies (where missing) on moderate-energy earthquakes located in some of the various areas of interest for the NASA4SHA Project. The choice fell on four areas for which, according to previously acquired knowledge, it was realistic and reasonable to expect that significant results could be achieved within the project time-frame. These areas include: the portion of Emilian plain between Modena and Ferrara; the Treviso Prealps, the Friulian Prealps; and finally the town of Ferrara and its surroundings.

Investigation on Emilian Plain earthquakes

In this case, the aim of the study was improving knowledge on moderately damaging earthquakes located in that portion of the Emilian plain (roughly located between the provincial capitals of Ferrara and Modena) that was most affected by the seismic sequence of 2012.
According to the pre-1900s "seismological tradition"[1], local seismicity in this area was almost nil before the 2012 events. However, a recent census of "unknown" and "neglected" earthquakes [Camassi et al., 2011] led to the discovery of a damaging earthquake occurred in Finale Emilia on 6 April 1639. This earthquake was included in the CPTI15 v. 4.0 catalogue [Rovida et al., 2022] with Mw 5.3 and a single intensity data point (I = VII-VIII MCS in Finale Emilia). The present study improved knowledge on this earthquake by retrieving information on another three damaged localities (Figure 1). The study also led to the discovery of other two previously unknown earthquakes, located in the Carpi area on 15 December 1761 and 11 May 1778.

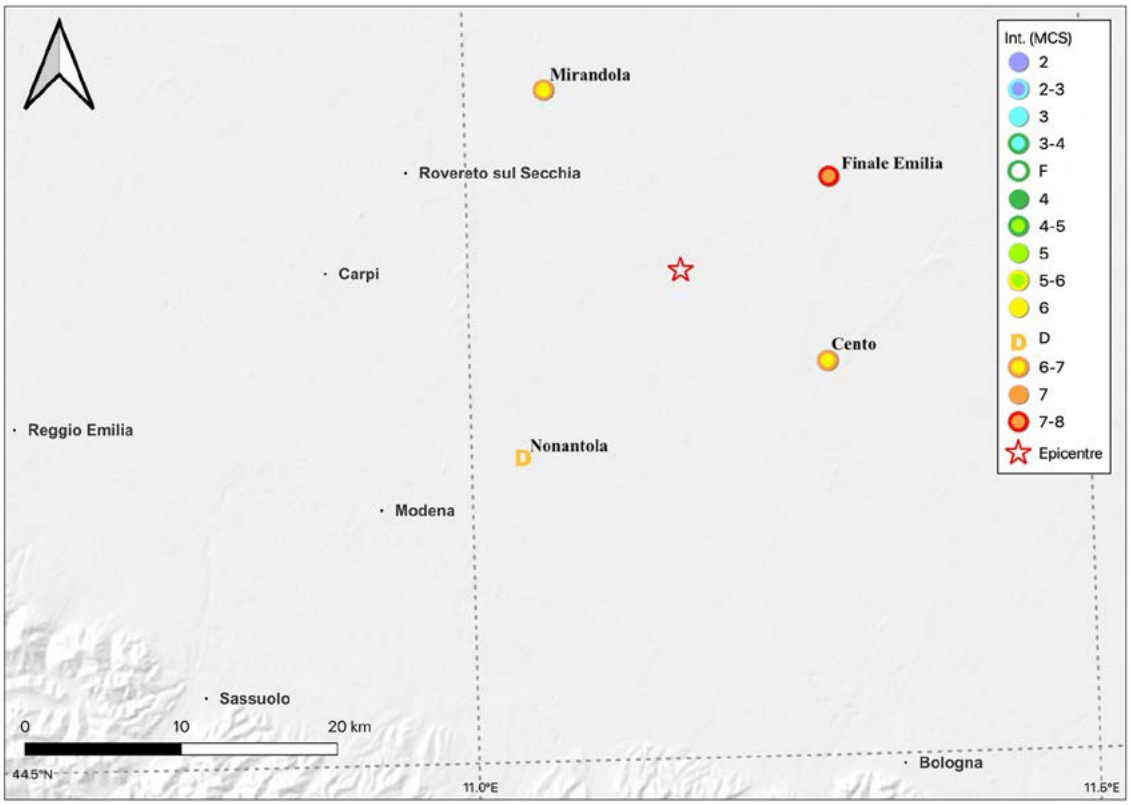

Figure 1 New macroseismic intensity map for the 6 April 1639 Finale Emilia earthquake.

Investigation on Treviso Prealps earthquakes

In this case, the aim of the study was to improve knowledge on eight earthquakes located in the territories of the present-day Provinces of Treviso and Belluno between the years 1709 and 1949. The current version of the CPTI15 catalogue [Rovida et al., 2022] lists seven of these earthquakes with epicentral parameters derived from old or preliminary reference studies.

[1]A centuries-old complex of descriptive studies of Italian local, regional, and national seismicity that was the main source of information on pre-1900s earthquakes for early Italian parametric catalogues.

The last one (1949) is a "neglected" earthquake, that is one that –owing to some compiler's mistake– failed to be included in the first Italian parametric earthquake catalogue [Postpischl, 1985] and thus was forgotten by later catalogues.
The level of knowledge achieved for these earthquakes by the study is very high and, in some cases, conclusive, though some additional research could be useful for: checking a few references to possible damage effects of the 1709 earthquake in the Belluno and Cadore areas; exploring local archives to look for confirmation of damage wrought by the earthquake of 1719 in Friuli; and improving knowledge on damage caused by the 1756 earthquake in Treviso. It would also be very interesting to carry out an integrated study of three earthquakes located in the same area affected by the 1949 earthquake, in the following decade (1956, 1959, and 1960).
This study, together with a previous one dedicated to "minor" damaging earthquakes of the Asolo area [Baranello, 2023], makes a significant contribution to the advancement of knowledge on the historical seismicity of the Veneto and Friuli Prealps (Figure 2).

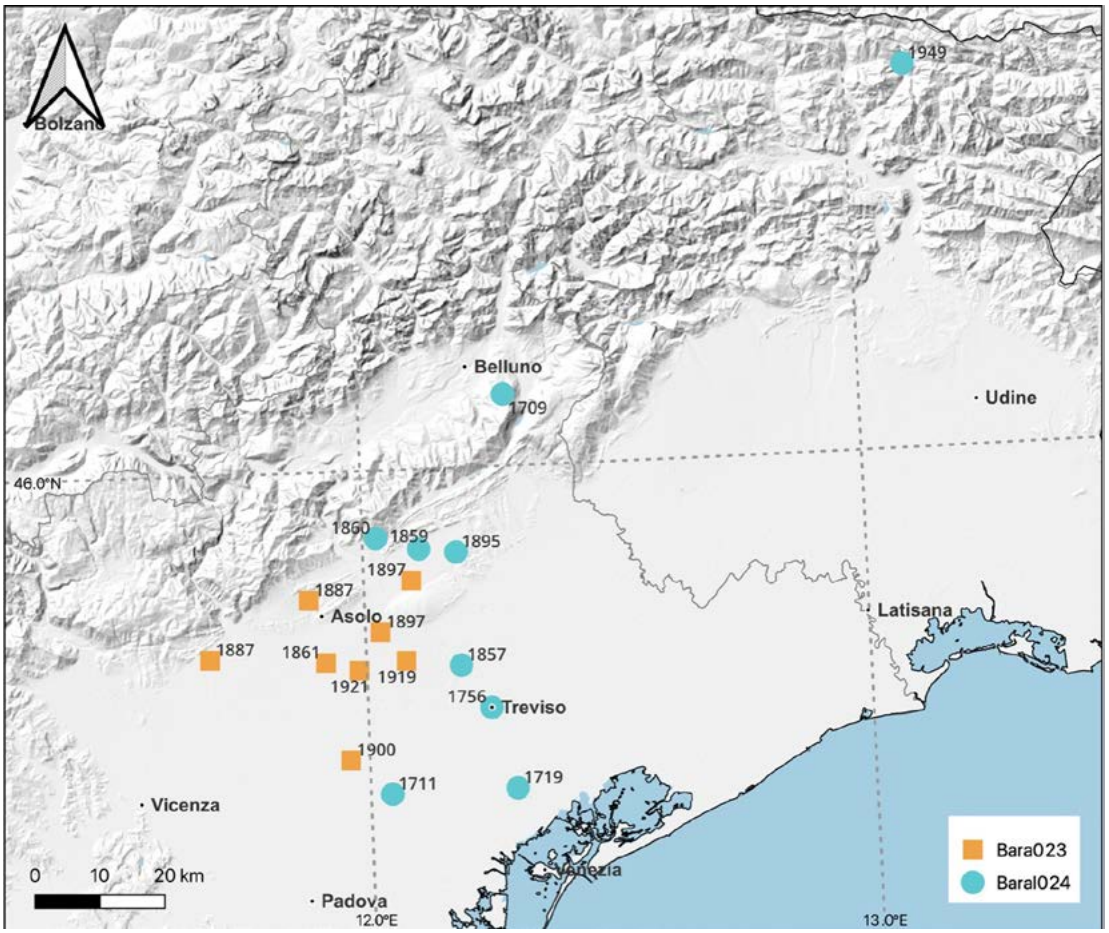

Figure 2 Treviso area earthquakes studied in the frame of the NASA4SHA Project (blue dots) and previously studied Asolano earthquakes (yellow squares).

A few traces of local earthquakes dated between the late 14th century, and the mid-16th century remain to be explored. If confirmed, these events could significantly improve the seismic histories of Treviso and the other main towns of the area. These considerations highlight how much room for improvement there still is in our knowledge of the seismic history of various areas of our country. For further details see Baranello et al. [2025].

In this case, the study concerned five Mw ≥ 5 local earthquakes of the 1700s (1700, 1776, 1788, 1789, 1794). The reference studies from which the current earthquake catalogues derive their epicentral parameters, were carried out in the 1990s and were of better quality than average, having been based not only on an extensive analysis of pre-1900s earthquake compilations, but also on original historical research carried out in local parish archives. All the same, the new study did significantly increase the number of macroseismic observations available for these earthquakes, particularly for those of 1700 and 1776 (Table 1), thus enhancing the stableness and reliability of the epicentral parameters.
The improvement in knowledge is particularly significant for the earthquake of 10 July 1776 (Carnic Prealps), whose effects turned out to have been far more severe than previously believed (Figure 3 and 4). For further details see Baranello et al. [2025b-c].

			Rovida et al. (2022) reference studies			This study		
Year	Mo	Da	Epicentral area	IDP	Imax	Epicentral area	IDP	Imax
1700	7	28	Carnia	28	9	Raveo	38	9-10
1776	7	10	Prealpi Friulane	19	8-9	Prealpi Carniche	29	9-10
1788	10	20	Carnia	9	8-9	Tolmezzo	12	9
1789	08	04	Prealpi Friulane	5	5-6	Tramonti di Sotto	6	7-8
1794	6	7	Prealpi Friulane	19	9	Prealpi Friulane	20	9
1794	6	30	Prealpi Friulane	8	7-8	Prealpi Friulane	10	7-8

Table 1 Data provided by previous studies and by the present study for the Friulan Prealps/Carnia earthquakes. Legend: "IDP": Intensity data points"; "Imax": maximum observed intensity (MCS).

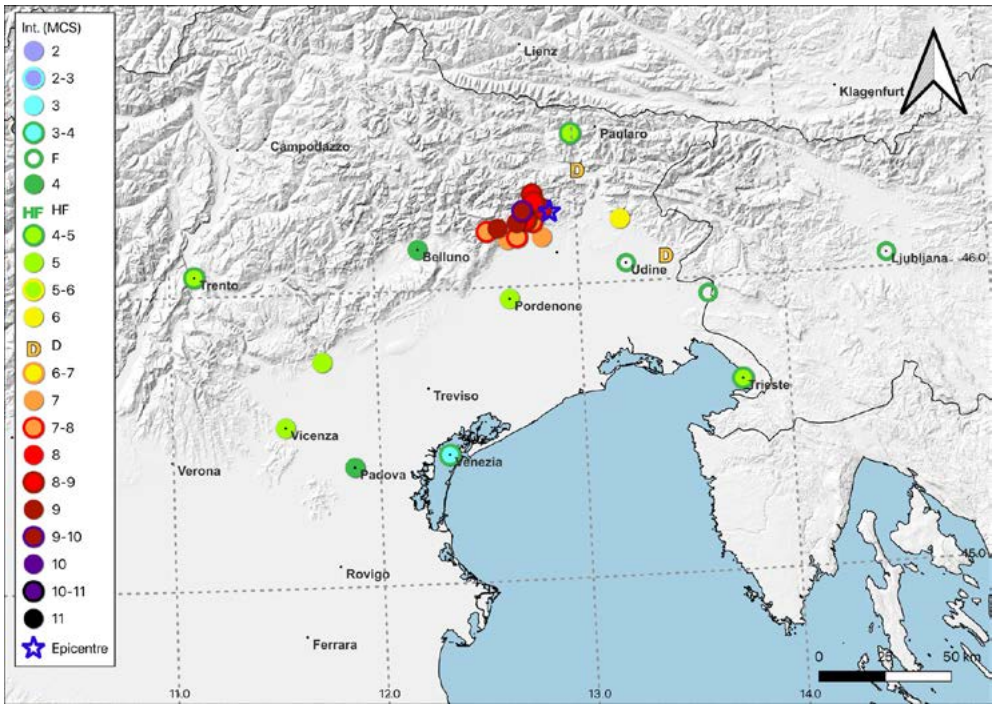

Figure 3 Intensity distribution of the earthquake of 10 July 1776 (Carnic Prealps) after this study (modified from Baranello et al. [2025c]).

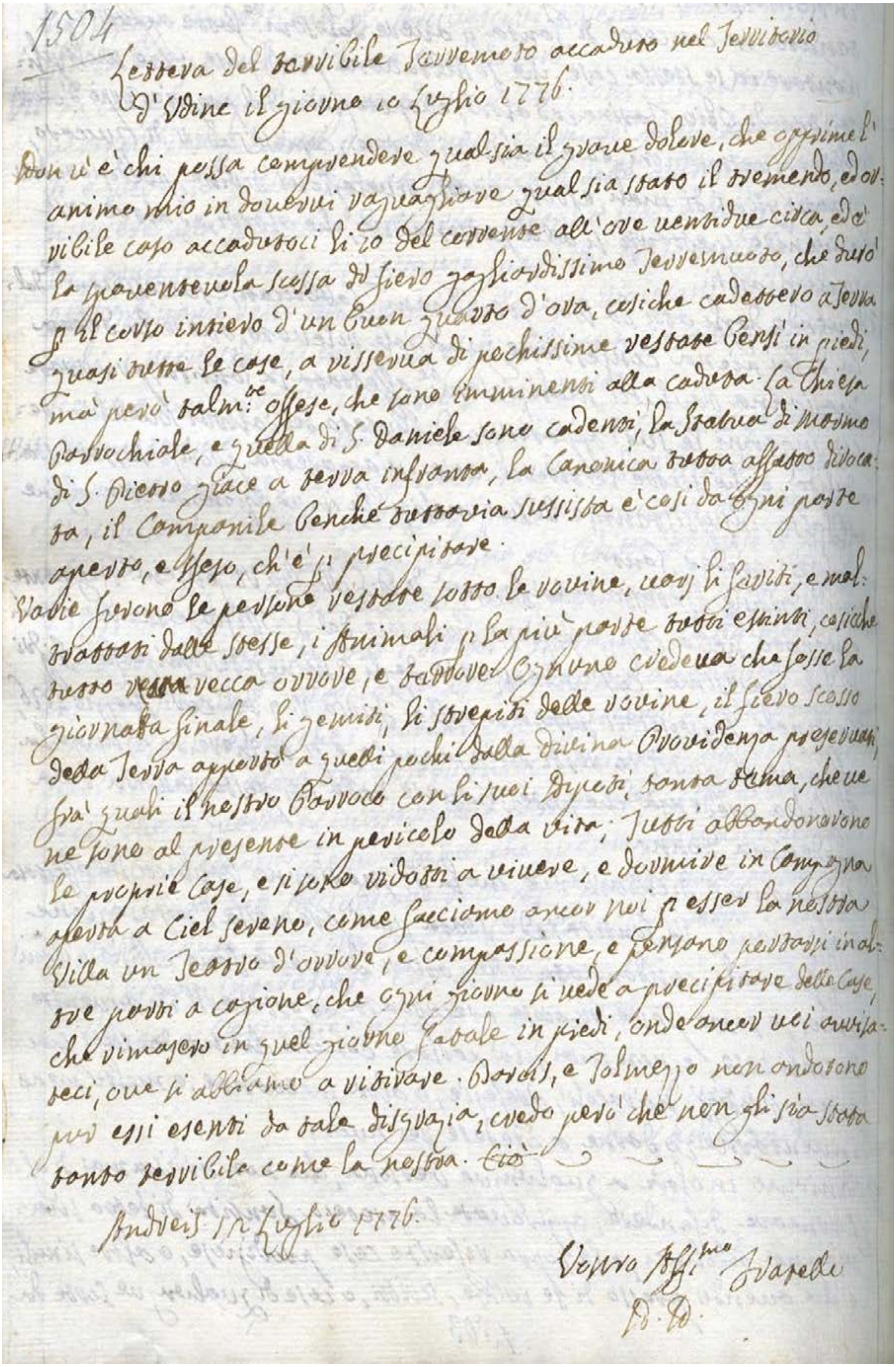

1504
Lettera del terribile Terremoto accaduto nel Territorio d'Udine il giorno 10 Luglio 1776.

Non vi è chi possa comprendere qual sia il grave dolore, che opprime l'animo mio in dovervi ragguagliare qual sia stato il tremendo, ed orribile caso accadutoci li 10 del corrente all'ore ventidue circa, ed è la spaventevole scossa di fiero gagliardissimo Terremuoto, che durò per il corso intiero d'un buon quarto d'ora, cosicchè caddero a terra quasi tutte le case, a riserva di pochissime restate bensì in piedi, ma però talm.te offese, che sono imminenti alla caduta. La Chiesa Parrocchiale, e quella di S. Daniele sono cadenti, la Statua di marmo di S. Pietro giace a terra infranta, la Canonica tutta affatto diroccata, il Campanile benchè tuttavia sussista è così da ogni parte aperto, e leso, ch'è p. precipitare. Varie furono le persone restate sotto le rovine, uccisi li feriti, e maltrattati dalle scosse, i Animali p. la più parte tutti estinti, cosicchè tutto ~~recca~~ recca orrore, e terrore. Ognuno credeva che fosse la giornata finale, li gemiti, li strepiti delle rovine, il fiero scosso della Terra apportò a questi pochi dalla divina Providenza preservati, fra' quali il nostro Parroco con li suoi Diretti, tanta tema, che ne sono al presente in pericolo della vita; Tutti abbandonarono le proprie Case, e si sono ridotti a vivere, e dormire in Campagna aperta a Ciel sereno, come facciamo ancor noi p. esser la nostra Villa un Teatro d'orrore, e compassione, e temono restarvi inal-tre parti a cagione, che ogni giorno si vede a precipitare delle Case, che rimasero in quel giorno fatale in piedi, onde ancor voi avvisa-teci, ove si abbiamo a ritirare. Barcis, e Tolmezzo non andarono per essi esenti da tale disgrazia, credo però che non gli sia stata tanto terribile come la nostra. Ciò

Andreis in Luglio 1776.

Vostro Aff.mo Fratello
P. D.

Figure 4 A previously unknown contemporary description that helped improving knowledge on the 1776 earthquake (BMCVE [1776]).

Investigation on Ferrara area earthquakes

A professional research grant provided by the NASA4SHA Project allowed to carry out an in-depth study of all the earthquakes located by the current catalogue in Ferrara and its immediate surroundings in the time-window 13th-16th centuries, excepted only the major seismic sequence of 1570-1574 (Ferrara) and the 1624 Argenta earthquake, both having been recently and extensively studied. The epicentral parameters with which most of the studied earthquakes are listed in the current catalogue [Rovida et al., 2022] are derived from very old studies [ENEL, 1985]. A few others were never studied at all; the current catalogue having simply adopted the epicentral parameters assessed for them by the Postpischl [1985] catalogue. Our research aimed at revising/updating the old reference studies and to provide new studies for the earthquakes that lacked them. To improve knowledge, an extended survey of the large body of unpublished local chronicles and histories, written in the 14th-19th centuries and preserved in the public libraries of Ferrara and Modena was carried out. In this case too, the work produced significant results, especially in terms of a "cleaning up" of the catalogue, thanks to the identification of several earthquakes that turned out to be non-existent, and others whose intensities were downsized (Table 2). An extended technical report including monographs of all the studied earthquake is about to be submitted for publication in the INGV journal *Quaderni di Geofisica*. For further details see Faoro et al. [2025].

			Rovida et al. [2022] reference studies			This study		
Year	Mo	Da	epicentral area	IDP	Imax	epicentral area	IDP	Imax
1234	03	20	Ferrara	1	7	*Non-existent earthquake*		
1285	12	13	Ferrara	1	7	Ferrara	1	4
1339	11	16	Ferrara	1	6	*Non-existent earthquake*		
1409	08	17	Ferrara	1	6	Ferrara	1	4
1410	05	09	Ferrara	1	6-7	*Non-existent earthquake*		
1411	01	09	Ferrara	1	7	*Non-existent earthquake*		
1425	08	10	Ferrarese	2	7	Ferrara	1	6-7
1483	03	03	Ferrara	1	5-6	Ferrara	1	4-5
1487	01	11	Ferrara	2	5	Ferrarese?	2	5
1508	10	26	Ferrarese	1	5	Ferrarese	1	5
1561	11	24	Ferrarese	3	6-7	Ferrarese	3	6-7
1594	10	03	Ferrara	1	5	*Non-existent earthquake*		

Table 2 Ferrara area earthquakes, with a comparison between data provided by previous studies and by the present study. Legend: "IDP": Intensity data points"; "Imax": maximum observed intensity (MCS).

Conclusions

The historical seismology studies carried out within the frame of the NASA4SHA Project led to a consistent improvement of the information base for each of the studied earthquakes, in

terms of quality of the basic information retrieved and of number of localities for which an intensity degree could be assessed (IDP or intensity data points).
The in-depth research carried out on minor damaging earthquakes and on unknown damaging earthquakes, (i.e. earthquakes not listed by previous studies/parametric catalogues) within the frame of the NASA4SHA Project confirms that, despite the advancement of historical seismological studies carried out in the last decades, there is still significant room for improvement in knowledge concerning the seismic histories of the considered areas.
Last but not least, an important result of these studies is the identification of some non-existent earthquakes, whose cancellation from the Italian seismic catalogue will result in a significant improvement of the catalogue's quality.

References

Baranello, S., (2023). *Materiali per un catalogo dei terremoti italiani. Terremoti "minori" dell'Asolano (1861-1921)*. Quad. Geofis., 186: 1-158, https://doi.org/10.13127/qdg/158

Baranello, S., Camassi, R., and Castelli, V., (2025a). *Materiali per un catalogo dei terremoti italiani. Terremoti del Trevigiano e Bellunese tra '700 e '900*. Quad. Geof., 197: 1-150. https://doi.org/10.13127/qdg/197

Baranello, S., Barbano, M.S., Rossetti, A., Castelli, V., and Camassi, R., (2025b). Digital resources and their role in improving knowledge on 18th century earthquakes in Carnia (Friuli, Italy). Bulletin of Geophysics and Oceanography [in press].

Baranello, S., Barbano, M.S., Rossetti, A., Castelli, V., and Camassi, R., (2025). *Materiali per un catalogo dei terremoti italiani. Forti terremoti delle Prealpi Carniche nel XVIII secolo*. Quad. Geofis., 199: 1-168, https://doi.org/10.13127/qdg/199, [in press].

BMCVE [Venezia, Biblioteca del Museo Correr], (1776). Lettera del terribile terremoto accaduto nel territorio d'Udine il giorno 10 luglio 1776, ms.Correr 1141/1504 (=Misc. Correr XII 1427-1541).

Camassi, R., Castelli, V., Molin, D., Bernardini, F., Caracciolo, C.H., Ercolani, E., and Postpischl, L., (2011). *Materiali per un catalogo dei terremoti italiani: eventi sconosciuti, rivalutati o riscoperti*. Quad. Geof., 96: 1:53 + 391 pp.

Castelli, V., Camassi, R., Cattaneo, M., Cece, F., Menichetti, M., Sannipoli, E.A., and Monachesi, G., (2016). *Materiali per una storia sismica del territorio di Gubbio: terremoti noti e ignoti, riscoperti e rivalutati*. Quad. Geof., 133: 1-196. https://doi.org/10.13127/qdg/133

ENEL, (1985). *Studi e indagini per l'accertamento della idoneità tecnica delle aree suscettibili di insediamento di impianti nucleari per le Regioni Piemonte, Lombardia e Puglia: indagini di sismica storica*. ISMES-SGA Technical Reports, Roma, Italy, (unpublished).

Faoro, A., Camassi, R., and Castelli, V., (2025). *Pre-1500s earthquakes in Ferrara (NE Italy) and an overrated source: first results of a critical revision*. Bulletin of Geophysics and Oceanography, 66(2): 133-146, https://doi.org/10.4430/bgo00476

Locati, M., Camassi, R., Rovida, A., Ercolani, E., Bernardini, F., Castelli, V., Caracciolo, C.H., Tertulliani, A., Rossi, A., Azzaro, R., D'Amico, S., and Antonucci, A., (2022). *Database Macrosismico Italiano DBMI15, versione 4.0. Istituto Nazionale di Geofisica e Vulcanologia (INGV)*. https://doi.org/10.13127/dbmi/dbmi15.4

Molin, D., Bernardini, F., Camassi, R., Caracciolo, C.H., Castelli, V., Ercolani, E., and Postpischl, L., (2008). *Materiali per un catalogo dei terremoti italiani: revisione della sismicità minore del territorio nazionale*. Quad. Geofis., 57: 1-78 + 1444 pp.

Postpischl, D., (1985). *Catalogo dei terremoti italiani dall'anno 1000 al 1980*. Progetto Finalizzato Geodinamica. Quaderni de «La Ricerca Scientifica», n.114, v. 2B, 137 pp.

Rovida, A., Locati, M., Camassi, R., Lolli, B., Gasperini, P., and Antonucci, A., (2022). *Catalogo Parametrico dei Terremoti Italiani (CPTI15), versione 4.0*. Istituto Nazionale di Geofisica e Vulcanologia (INGV). https://doi.org/10.13127/CPTI/CPTI15.4

Improving Seismic Catalogs and Microseismicity Imaging in the Montello area (NE Italy)

Maria Adelaide Romano[1], Rita de Nardis[2,3], Gemma Cipressi[1,2], Monica Sugan[1], and Laura Peruzza[1,*]

[1]Istituto Nazionale di Oceanografia e di Geofisica Sperimentale - OGS, Trieste, Italy
[2]Università "G. d'Annunzio", Chieti-Pescara, Italy
[3]Centro Interuniversitario per la Sismotettonica 3D con Applicazioni Territoriali (CRUST), Chieti, Italy

Corresponding author: lperuzza@ogs.it

Introduction

The northeastern sector of Italy, particularly the Montello-Collalto region within the Eastern Southern Alps, is a structurally complex and seismically active area. Despite historical large-magnitude earthquakes - such as the 1695 Asolo event (Mw 6.5) - the underlying seismogenic sources remain only partially understood. Much of this uncertainty stems from deeply buried tectonic structures (e.g., the Montello thrust system) and the coexistence of natural and potentially induced seismicity, notably due to the presence of the Collalto underground gas storage (UGS) facility.
In this context, in the frame of the activities planned by Work Package 7 of the PRIN Project NASA4SHA, two complementary research streams have emerged: 1) a multi-year effort to consolidate and unify seismic data into a comprehensive Montello-Collalto seismic catalog, enabling better discrimination of tectonic vs. anthropogenic activity [Cipressi et al., 2024; 2025], and 2) a methodological evaluation of earthquake location workflows, confronting machine learning (M_L) pipelines with conventional manual procedures [Sugan et al., 2023; 2024; 2025].

Study Area and framework

The Montello-Collalto area lies along the active mountain front of the eastern Southern Alps, shaped by compressional tectonics since the Miocene. The region is dominated by a buried thrust system, notably the Montello thrust, which seismogenic potential is still highly debated (see e.g., Romano et al. [2019]; Picotti et al. [2022]; Talone et al. [2025] and references therein). Key seismogenic characteristics of this area include evidence of devastating historical earthquakes, moderate to small seismic sequences in the last five decades and debated interpretations of the geologic and geodetic data with hypothesized creeping behavior of the main fault system. In addition, the Montello area hosts strategic infrastructure, such as the Collalto UGS, which requires the most careful seismic hazard assessment, and a detailed microseismic monitoring for safety and compliance [Priolo et al., 2015].

The Montello-Collalto seismic catalog

Cipressi et al. [2024; 2025] outline the goal of building a long-duration, unified seismic catalog for the Montello-Collalto region. The catalog spans 1925 to 2023, integrating data from 9 catalogs, including national, regional, and local networks.

Earthquake locations, originally given by using Hypo71 code [Lee and Lahr, 1975], a 3-layer, 1D regional velocity model with fixed Vp/Vs=1.78 and no topographic/station corrections, have been reprocessed using NonLinLoc code [Lomax, 2001], with 1D/3D velocity models with variable Vp/Vs, topographic and stations corrections determined statistically. The final catalog improved location accuracy and magnitude consistency and provided further insights into the Montello thrust systems (Figure 1). No clear evidence of induced seismicity has been found so far.

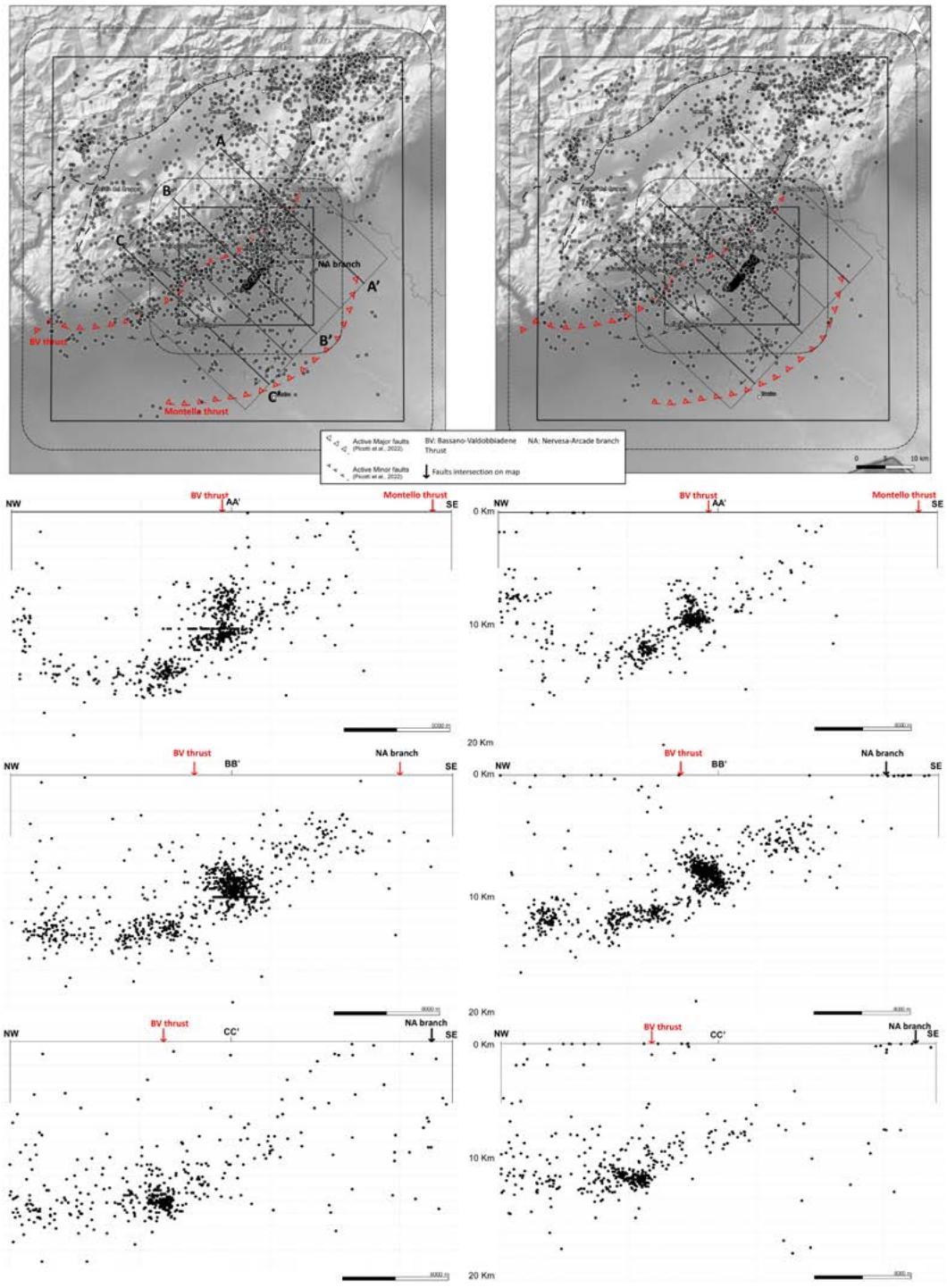

Figure 1 Comparison of the earthquake locations as originally collected (frames in the left column) and after the reprocessing using NLLOC [Lomax, 2001] (right column): the events mapped in the panels on top are plotted along three cross-sections in the frames below. They confirm the listric geometry of the Montello thrust, and the existence of at least an antithetic structure (mainly visible in section BB'). Revised clusters of seismicity are more precisely defined in space than the original ones. Modified from Cipressi et al. [2025].

Evaluating machine learning-enhanced seismic processing

During the initial phases of the NASA4SHA Project, Sugan et al. [2023] tested the LOC-FLOW [Zhang et al., 2022] machine learning (M_L) enhanced workflow using PhaseNet [Zhu and Beroza, 2019] for the automatic P and S pick detections (Figure 2). They used as test case a single, very productive microearthquake sequence, which occurred in August 2021 near Refrontolo (TV), in the Montello area. The workflow has been successively more finely tuned and refined, to become a tool of off-line, automatized processing in case of other sequences in northeastern Italy [Sugan et al., 2024; 2025].

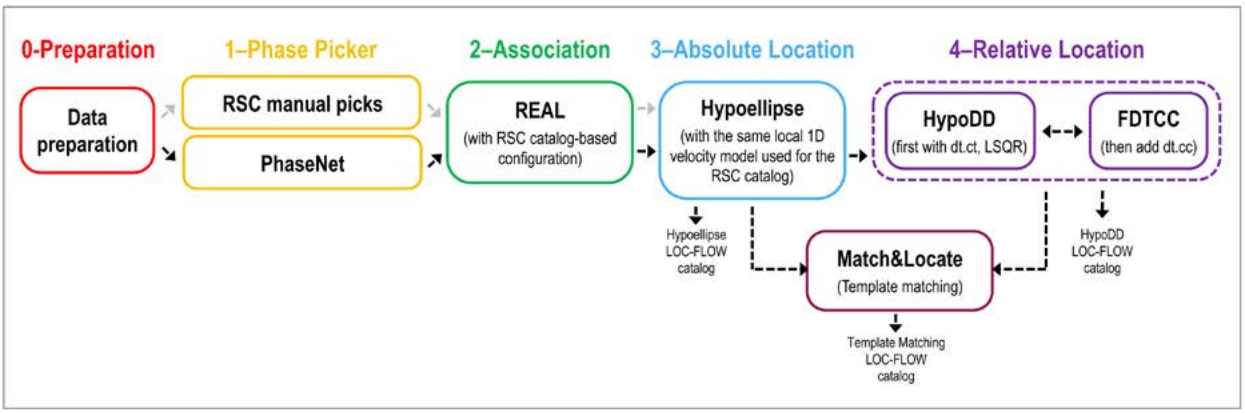

Figure 2 Workflow developed for off-line automatized processing of Refrontolo seismic sequence (taken from Sugan et al. [2023]), based on LOC-FLOW [Zhang et al., 2022]. RSC: Collalto Seismic Network [Priolo et al., 2015]. Some modules have been implemented (e.g. Hypoellipse code for absolute location [Lahr, 1999]), and tailored for the local and regional networks of OGS [Sugan et al., 2024; 2025].

In the case of the 2021 sequence, the M_L approach recovered nearly but not all the events previously manually identified (374 events with maximum magnitude M_L=2.5, see Peruzza et al. [2022], Sugan et al. [2023], and Figure 3), thus suggesting that complementary methods (e.g. template matching) for event identification must be applied in case of very productive sequences of microearthquakes.

Conclusions and Future Directions

These research efforts are complementary, and together, they allow for real-time surveillance and long-term tectonic analysis in complex settings like northeastern Italy. In particular:

- machine learning workflow is focused on automation and performance assessment; it enables fast, scalable detection and improved completeness;
- multi-scale cataloging, instead, focusses on the construction of a long-term, integrated, uniform seismic catalog to provide reliable datasets for interpreting the local and regional seismicity.

Both approaches can provide new clarity on active fault geometries, thus enhancing in real-time a better monitoring of the evolution of seismicity and, in a more long-term perspective, retrospective hazard assessment, and seismotectonic analyses.
This integrated work represents a blueprint for advanced seismic monitoring. Future steps

include clustering analysis, offshore station deployment, and applications of M_L approach to improve risk management at the national scale.

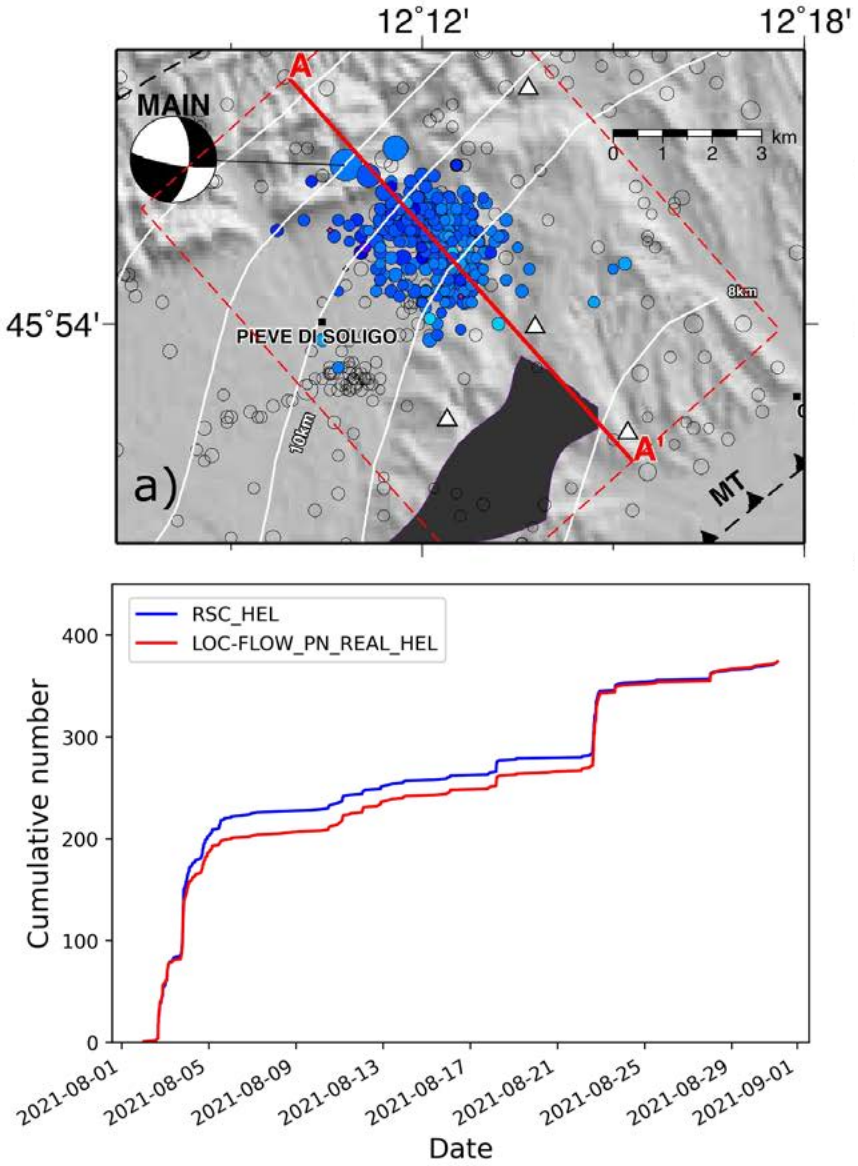

Figure 3 ML workflow applied to the test case of the 2021 Refrontolo sequence (modified from Sugan et al. [2023]). Top panel: map of the events identified and located with manual control [Peruzza et al., 2022]; Bottom panel: cumulative number of events versus time as identified by different procedures (manual and ML workflow in blue and red, respectively, see Sugan et al. [2023] for details).

Acknowledgments

The research activities here described have been carried out in the frame of the Italian PRIN Project (Research Projects of National Interest) "Fault segmentation and seismotectonics of active thrust systems: the Northern Apennines and Southern Alps laboratories for new Seismic Hazard Assessments in northern Italy (NASA4SHA)", PI R. Caputo, UR Responsible L. Peruzza, and they are related to the Work Package 7 "Review of historical and instrumental seismicity".

References

Cipressi, G.M., Romano, M.A., Bernardi, P., Diez, E., Franceschinel, F., Garbin, M., Guidarelli, M., Klin, P., Laurenzano, G., Moratto, L., Peruzza, L., Pettenati, F., Plasencia Linares, M.P., Priolo, E., Rebez, A., Romanelli, M., Sandron, D., Santulin, M., Sarao, A., Tamaro, A., Lavecchia, G., and de Nardis, R., (2025). *A comprehensive seismic catalog of the Montello-Collalto area (Eastern Southern Alps, Italy) for seismotectonic and induced seismicity purpose.* Abstract at GNGTS 2025. https://hdl.handle.net/20.500.14083/42923

Cipressi, G.M., Romano, M.A., Bernardi, P., Eduardo, D., Franceschinel, F., Garbin, M., Guidarelli, M., Klin, P., Laurenzano, G., Moratto, L., Peruzza, L., Pettenati, F., Milton, P., Priolo, E., Rebez, A., Romanelli, M., Sandron, D., Santulin, M., Saraò, A., Tamaro, A., Lavecchia, G., and de Nardis, R., (2024). *Building a comprehensive seismic catalog of the Montello-Collalto area (Eastern Southern Alps, Italy) for seismotectonic and induced seismicity purposes*. Congr. Società Geologica Italiana, 2-5 settembre 2024, Bari. https://hdl.handle.net/20.500.14083/40406

Lahr, JC., (1999). *HYPOELLIPSE: a computer program for determining local earthquake hypocentral parameters, magnitude and first motion pattern (Y2K compliant version*), US Department of the Interior, US Geological Survey: Reston, VA. Open-File Rep. 99–23, version 1.1, 119 pp.

Lee, W.H.K., and Lahr, J.C., (1975). *Hypo 71 (revised): a computer program for determining hypocenter, magnitude and first motion pattern of local earthquakes*. U.S. Geological Survey, Menlo Park, CA, USA, Open File Report 75-311, 113 pp.

Lomax, A.. (2001). *NonLinLoc: A Non-Linear, Probabilistic Earthquake Location Method*. Retrieved from https://alomax.free.fr/nlloc.

Peruzza, L., Romano, M. A., Guidarelli, M., Moratto, L., Garbin, M., and Priolo, E., (2022). *An unusually productive microearthquake sequence brings new insights to the buried active thrust system of Montello (Southeastern Alps, Northern Italy).* Front. Earth Sci., 10, 1044296. https://doi.org/10.3389/feart.2022.1044296

Picotti, V., Romano, M.A., Ponza, A., Guido, F.L., and Peruzza, L., (2022). *The Montello Thrust and the Active Mountain Front of the Eastern Southern Alps (Northeast Italy).* Tectonics, 41, e2022TC007522. https://doi.org/10.1029/2022TC007522

Priolo, E., Romanelli, M., Plasencia Linares, M.P., Garbin, M., Peruzza, L., Romano, M.A., Marotta, P., Bernardi, P., Moratto, L., Zuliani, D., and Fabris, P., (2015). *Seismic Monitoring of an Underground Natural Gas Storage Facility: The Collalto Seismic Network.* Seismological Research Letters, 86 (1), 109–123. https://doi.org/10.1785/0220140087

Romano, M.A., Peruzza, L., Garbin, M., Priolo, E., and Picotti, V., (2019). *Microseismic Portrait of the Montello Thrust (Southeastern Alps, Italy) from a Dense High-Quality Seismic Network*. Seismological Research Letters, 90 (4), 1502-1517, https://doi.org/10.1785/0220180387

Sugan, M., Peruzza, L., Romano, M.A., Guidarelli, M., Moratto, L., Sandron, D., Plasencia Linares, M.P., and Romanelli, M., (2023). *Machine learning versus manual earthquake location workflow: testing LOC-FLOW on an unusually productive microseismic sequence in northeastern Italy*. Geomatics, Natural Hazards and Risk, 14 (1), 2284120. https://doi.org/10.1080/19475705.2023.2284120

Sugan, M., Peruzza, L., Romano, M.A., Guidarelli, M., Moratto, L., Sandron, D., Plasencia Linares, M.P., and Romanelli, M., (2024). *Comparing Machine Learning to Manual Earthquake Location procedures: evaluating the performance of LOC-FLOW on a microseismic sequence occurred in Collalto area (NE Italy)*. 42nd GNGTS, Ferrara, Italy, https://hdl.handle.net/20.500.14083/30065

Sugan, M., Magrin, E., and Magrin, A., (2025). *LOC-FLOW Sviluppo di un flusso di lavoro automatico ML-based per il Monitoraggio Sismico.* https://ricerca.ogs.it/handle/20.500.14083/45043

Talone, D., Romano, M.A., De Siena, L., Guidarelli, M., Santulin, M., Peruzza, L., Lavecchia, G.,

and de Nardis, R., (2025). *Underground Gas Storage as benchmark for seismic attenuation tomography in a tectonically complex region (north-eastern Italy)*. Geophysical Research Letters, 52, e2025GL117956. https://doi.org/10.1029/2025GL117956

Zhang, M., Liu, M., Feng, T., Wang, R., and Zhu, W., (2022). *LOC-FLOW: an end-to-end machine-learning-based high-precision earthquake location workflow*. Seismol Res Lett., 93(5), 2426–2438. https://doi.org/10.1785/0220220019

Zhu, W., and Beroza, G.C., (2019). *PhaseNet: a deep-neural-network based seismic arrival-time picking method*. Geophys. J. Int., 216 (1), 261–273. https://doi.org/10.1093/gji/ggy423

Advancing multi scale seismic hazard assessment in Italy: unified moment magnitude catalog and integrating k_0 corrections in the source parameters estimation

Luca Moratto[1,*], Angela Saraò[1], Gabriele Tarchini[1,2], Enrico Priolo[1]

[1]Istituto Nazionale di Oceanografia e di Geofisica Sperimentale - OGS, Trieste, Italy
[2]Università di Genova, Dipartimento di Scienze della Terra, Ambientali e della Vita, Genoa, Italy

Corresponding author: lmoratto@ogs.it

Introduction

The Work Package 7 of the PRIN Project NASA4SHA dealt with the review of historical and instrumental seismicity in the areas of interest; for this purpose OGS performed and published new studies focused on the compilation of a complete moment magnitude catalog for Northeastern Italy and the surrounding areas [Tarchini et al., 2025], and on the improvement the estimation of source parameters by correcting for k_0 derived from ambient noise [Moratto et al., 2025].

In the first study, Tarchini et al. [2025] computed M_W values using the data acquired from the Istituto Nazionale di Oceanografia e di Geofisica Sperimentale (OX) network; their catalog contains 11,685 low to moderate magnitude earthquakes ($-0.70 \leq M_L \leq 4.35$) suitable for independent M_W calculation and it spans from 2016 to 2023 covering geographical coordinates from 10.0° to 14.5° N longitude and 44.5° to 47.0° E latitude. The accuracy of the moment magnitude estimates was improved by incorporating new, homogeneous local magnitude (M_L) estimates. A newly developed automated routine allowed for near real-time M_W estimation and continuous updating of the seismic catalog. An empirical relationship between M_W and M_L was established specifically for the study region. The catalog is regularly updated as new data becomes available and is accessible online, to promote collaboration and further research in the field of seismic studies.

In the second study, Moratto et al. [2025] estimated the high-frequency attenuation (k_0) from ambient seismic noise and improved the robustness of source parameter estimation for microearthquakes in a complex region such as the High Agri Valley. The k_0 correction leads to reliable corner frequency estimations down to $M_W \approx 1.2$, recognizing particularly small stress drops (~0.1 MPa) in the smallest events.

Thanks to the PRIN 2020 initiative NASA4SHA, these studies contribute significantly to the improvement of seismic hazard assessment and risk mitigation strategies in Italian seismic active areas.

Moment Magnitude Catalog for the Northeastern Italy

The moment magnitude (M_W) is a critical measure for quantifying the energy released during seismic events, as it is considered the most reliable magnitude scale, that avoids saturation at larger magnitudes and is directly related to the size of the rupture area; the M_W values are essential for understanding the physical mechanisms also for the regions characterized by the low-to-moderate magnitude earthquakes. The estimation of M_W for small seismic events is challenging, because the low signal-to-noise ratio makes the analysis less reliable and small

earthquakes are often only recorded by a few nearby stations, making M_W estimates more station-dependent and less stable.

Therefore, it is essential to create a robust M_W catalog for small to moderate earthquakes occurred in Northeastern Italy, a region characterized by frequent seismic activity due to tectonic interactions. Indeed, the seismic activity in Northeastern Italy, particularly due to the Adriatic microplate interacting with the Eurasian plate, necessitates a reliable estimation of M_W, which is essential also for seismic hazard assessment.

The study utilized the response spectra to estimate the moment magnitude, adopting the methodology proposed by Atkinson et al. [2014], which was calibrated specifically for Northeastern Italy by Moratto et al. [2017]. Response spectra were calculated from vertical waveforms to limit potential site effects and used as input in the empirical relationships to obtain accurate M_W estimates. A new automated routine is implemented to process seismic data in near real-time, which enables prompt updates to the catalog and enhances the overall efficiency of data handling. The procedure selected only waveforms recorded at a maximum epicentral distance of 80 km to avoid unmodelled complexity in the propagation effects.

As results, a comprehensive dataset that includes 11,685 earthquakes (Figure 1) including the M_W estimations and the related processed waveforms are freely available on Zenodo [Moratto et al., 2024]. In the final catalog the earthquakes are characterized also by their magnitudes and locations, and the catalog provides essential information such as depth, seismic moment, and associated local magnitudes. M_L was computed utilizing both the relationships proposed by Hutton and Boore [1987] (M_L(H&B)) and by Bragato and Tento [2005] (M_L(B&T)).

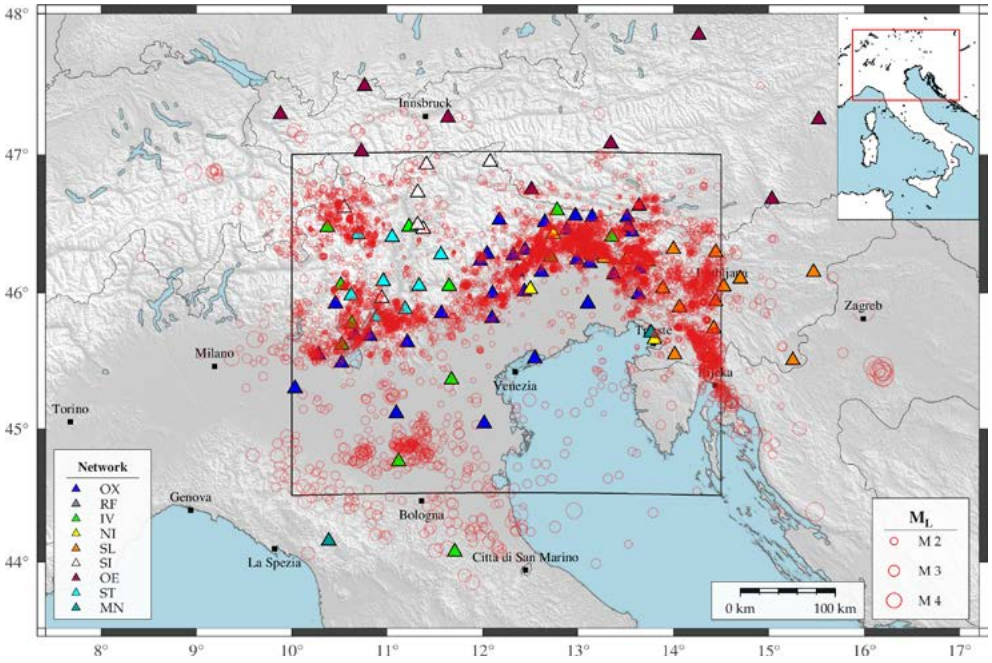

Figure 1 Map of the seismicity analyzed by Tarchini et al. [2025], represented by circles, with dimensions proportional to the M_L values. The stations used are from the OX network and other surrounding networks; the black rectangle marks the study area monitored by the OGS. Figure taken from Tarchini et al. [2025].

A new empirical relationship between M_W and M_L was derived for the region, which demonstrates improved accuracy and better reflects the seismic behavior observed in Northeastern Italy (Figure 2). The slope of the relationship (0.70 ≈ 2/3) matches the scaling parameter proposed by Hanks and Kanamori [1979]. For values in the range $2.0 < M_L < 3.0$, M_L and M_W exhibit

closer agreement, with a consistent 1:1 magnitude scaling. Below 2.0, the scaling shifts to 2:3, likely due to anelastic attenuation affecting signal propagation paths [Moratto et al., 2017].

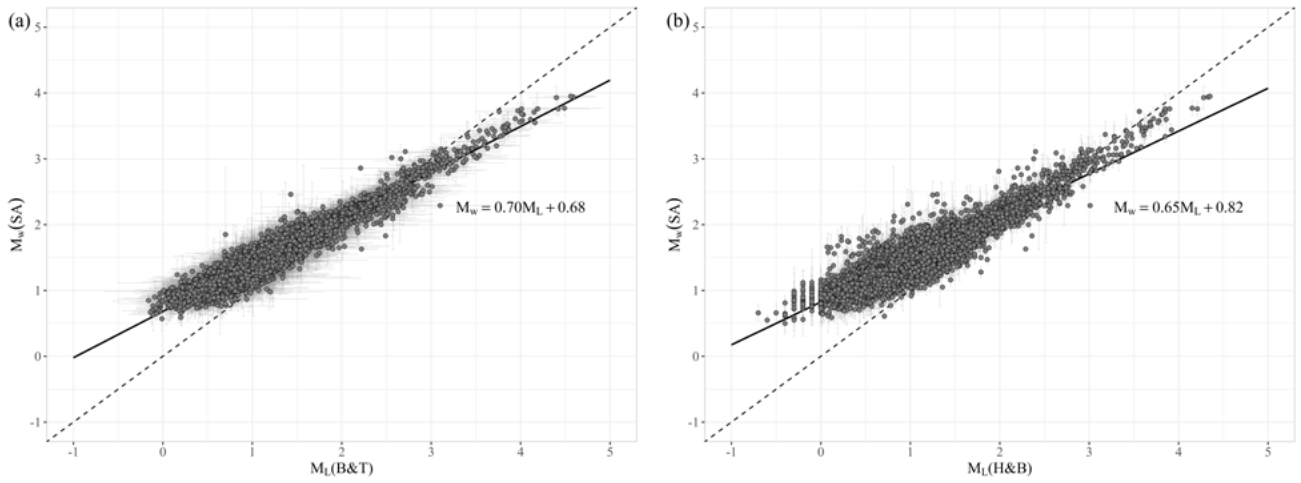

Figure 2 (a) Comparison between M_L(B&T) and M_W(SA). The dashed line represents the 1:1 correlation, whereas the gray solid line indicates the best-fit linear regression. (b) Similar to (a) but comparing M_L(H&B) and M_W(SA). Figure taken from Tarchini et al. [2025].

The results also included a comparative analysis of the M_W values derived from the response spectra with those extracted from the moment tensor solutions for specific events with $M_W \geq 3.5$ (Figure 3). The mean absolute difference between the new M_W estimates and those calculated by time-domain moment tensor analysis was found to be 0.066, with a standard deviation of 0.157. This indicates a strong agreement between the two methodologies, which emphasizes the validity of the newly developed estimation approach.

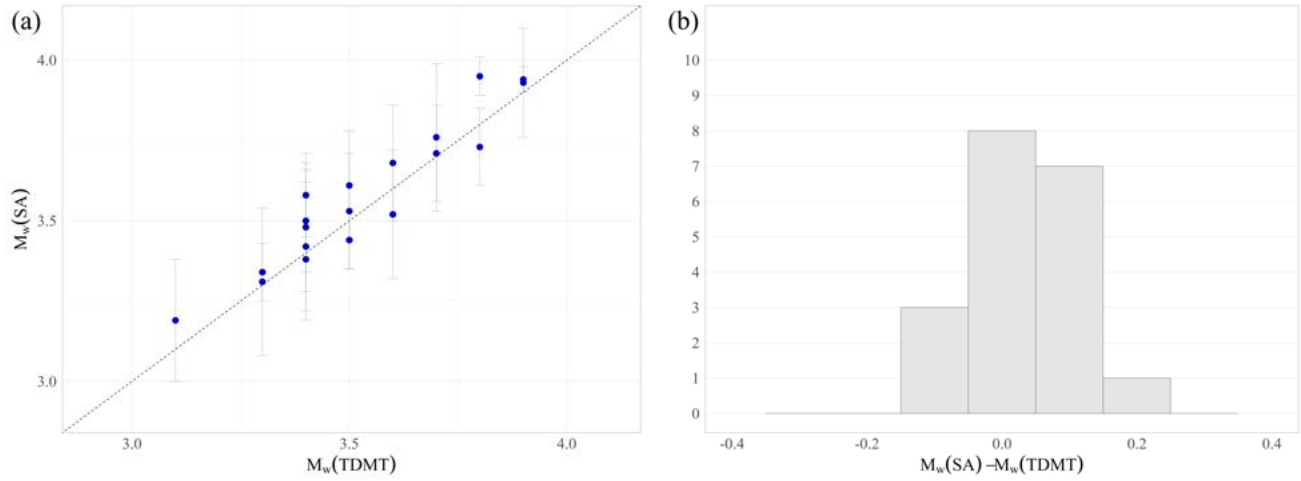

Figure 3 (a) Comparison between M_W(SA) values derived in this study with those computed by Saraò et al. [2021] using time-domain moment tensor (TDMT) analysis; the dotted line represents the 1:1 correlation. (b) Histogram of residuals between our Mw values and those computed by Saraò et al. [2021]. The mean absolute difference between the new Mw estimates and those calculated by time-domain moment tensor analysis was found to be 0.066, with a standard deviation of 0.157. Figure taken from Tarchini et al. [2025].

The study shows that the M_W estimations for smaller earthquakes can be influenced by noise, leading to possible overestimations in certain cases. The results suggest that adjustments to the approach, such as the use of response spectra calculated at 0.3 seconds instead of 1.0 second for very small events, lead to more reliable estimates. This refinement is crucial for producing accurate magnitude data, especially in a region with a high percentage of low-magnitude earthquakes.

Integrating the k_0 corrections in the source parameters estimation

The determination of the source parameters (e.g., corner frequency and stress drop) for low-magnitude earthquakes (microearthquakes) poses a major challenge. The attenuation of high frequencies distorts seismic spectra, acting as a low-pass filter and often leading to underestimated corner frequency estimates. This effect makes it difficult to accurately assess the properties of seismic sources, which are crucial for understanding both natural and induced seismicity.
Moratto et al. [2025] therefore adopted the approach proposed by Butcher et al. [2020], who estimated the high-frequency attenuation parameter (k_0) using ambient seismic noise rather than relying on the earthquakes themselves. They analyzed noise displacement spectra in the 15-40 Hz band at eight broadband stations of the High Agri Valley Geophysical Observatory. The estimations of k_0 values at the selected stations ranged from 0.02 to 0.04 s and were well constrained within the analyzed frequency range.
These k_0 estimates were then integrated into the SourceSpec code [Satriano, 2024], and the displacement amplitude spectra were corrected in high-frequency content for near-site attenuation during the inversion of source parameters. The method was tested on 72 microearthquakes (M_W spanning between 0.4 and 2.7) from the Castelsaraceno sequence of August 2020 in the Southwestern High Agri Valley (Figure 4).

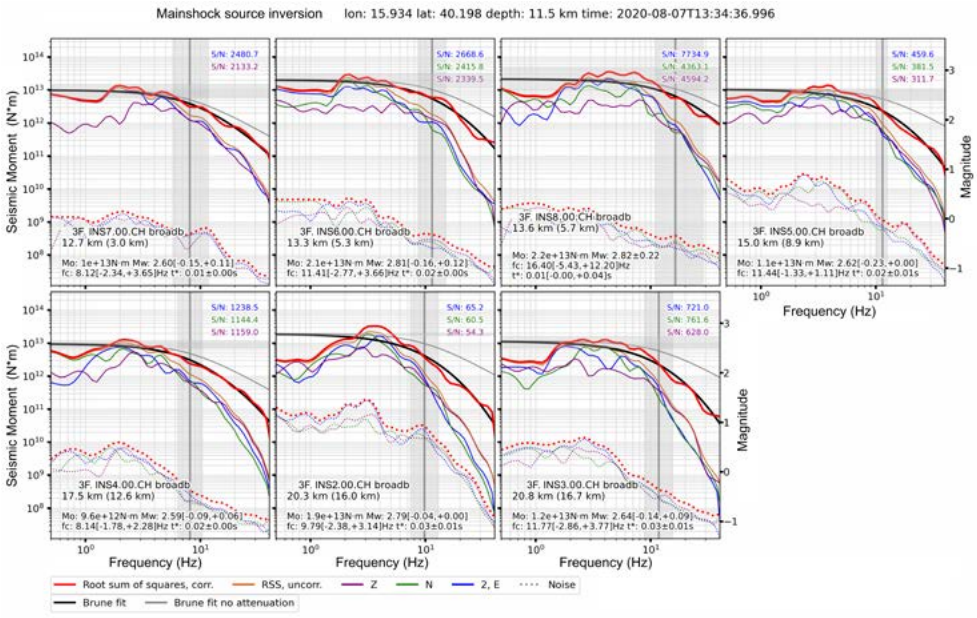

Figure 4 Displacement amplitude spectra computed with the SourceSpec code for the inversion of the mainshock source parameters. Signal (solid lines) and noise (dashed lines) spectra are shown for each station. The corrected signal root-sum-of-squares spectrum used for the inversion is shown in red, together with the fitted Brune source spectrum (black). The expected Brune source spectrum without attenuation is also shown for comparison (grey). Figure taken from Moratto et al. [2025].

The results show that a spectral cut-off near 10 Hz occurs for earthquakes with M_W < 2.0, if the k_0 correction is not taken into account. By applying the k_0 correction, this cut-off was removed, lowering the magnitude threshold for a reliable corner frequency estimation to M_W ≈ 1.2, which is almost an order of magnitude improvement. Additionally, for events with M_W < 1.5, post-correction stress drops aligned with roughly 0.1 MPa, which is about ten times lower than for larger earthquakes (M_W > 2.0). In this case, the scaling between corner frequency–seismic moment ($fc–M_0$) also approached self-similarity. These results suggest that smaller earthquakes may follow a different physical rupture mechanism.

Conclusions and Future Outlook

Together, these studies can take to significant advancements made in seismic hazard assessment in Italy through the integration of a unified moment magnitude catalog and the application of k_0 corrections in source parameter estimations. The results demonstrate the importance of utilizing robust methodologies, such as the automated near-real-time M_W estimation, to enhance the accuracy and reliability of moment magnitude estimates for small to moderate earthquakes, and the k_0 corrections derived from ambient seismic noise to obtain more reliable estimation of the source parameters.

The compilation of the moment magnitude catalog, which includes 11,685 earthquakes, provides a comprehensive dataset essential for understanding seismic activity in Northeastern Italy.

Furthermore, the k_0 corrections have improved the estimations of corner frequencies and stress drops for microearthquakes.

Future research should focus on continuing the refinement of these methodologies and expanding the catalog as new seismic data becomes available. Additionally, the developments achieved within this project regarding the k_0 corrections, and the availability of M_W catalog will be a significant help to obtain reliable source parameters estimation for small earthquakes occurred in Northeastern Italy.

Acknowledgments

The research activities here described have been carried out in the frame of the Italian PRIN Project (Research Projects of National Interest) “Fault segmentation and seismotectonics of active thrust systems: the Northern Apennines and Southern Alps laboratories for new Seismic Hazard Assessments in northern Italy (NASA4SHA)”, PI R. Caputo, UR Responsible L. Peruzza, and they are related to the Work Package 7 “Review of historical and instrumental seismicity”.

References

Atkinson, G., Wesley Greig, D., and Yenier, E., (2014). *Estimation of moment magnitude (M) for small events (M < 4) on local networks*. Seismological Research Letters, 85, 1116-1124. https://doi.org/10.1785/0220130180

Bragato, P.L., and Tento, A., (2005). *Local magnitude in Northeastern Italy*. Bulletin of the Seismological Society of America, 95, 579–591. https://doi.org/10.1785/0120040100

Butcher, A., Luckett, R., Kendall, J.M., and Baptie, B., (2020). *Seismic magnitudes, corner frequencies, and microseismicity: using ambient noise to correct for high-frequency attenuation*. Bulletin of the Seismological Society of America, 110, 1260-1275. https://

doi.org/10.1785/0120190032
Hanks, T.C., and Kanamori, H., (1979). *A moment magnitude scale*. Journal of Geophysical Research, 84, 2348–2350. https://doi.org/10.1029/JB084iB05p02348
Hutton, L.K., and Boore, D.M., (1987). *The M_L scale in southern California*. Bulletin of the Seismological Society of America, 77, 2074-2094, https://doi.org/10.1785/BSSA0770062074
Moratto, L., Saraò, A., and Priolo, E., (2017). *Moment magnitude (Mw) estimation of weak seismicity in Northeastern Italy*. Seismological Research Letters, 88, 1455-1464. https://doi.org/10.1785/0220170063
Moratto, L., Tarchini, G., and Saraò, A., (2024). *Catalog of NE Italy earthquakes Mw with related velocimetric time series* [Data set], Zenodo. https://doi.org/10.5281/zenodo.12794785.
Moratto, L., Panebianco, S., Satriano, C., Stabile, T.A., and Priolo, E., (2025) *Using ambient noise k_0 estimation to improve microearthquake source parameters assessment in the High Agri Valley*. Geophysical Journal International 242 (2), ggaf191. https://doi.org/10.1093/gji/ggaf191
Saraò, A., Sugan, M., Bressan, G., Renner, G., and Restivo, A., (2021). *A focal mechanism catalogue of earthquakes that occurred in the southeastern Alps and surrounding areas from 1928-2019*. Earth System Science Data, 13, 2245-2258. https://doi.org/10.5194/essd-13-2245-2021
Satriano, C., (2024). *SourceSpec - Earthquake source parameters from P- or S-wave displacement spectra* (1.7), Zenodo. https://zenodo.org/records/4779492.
Tarchini, G., Moratto, L.,and Saraò, A. (2025). *A comprehensive moment magnitude catalog for the Northeastern Italy region*. Seismological Research Letters, 96, 2714-2723. https://doi.org/10.1785/0220240303

Towards a unified probabilistic fault displacement hazard assessment: combining physics-based simulations and OpenQuake engine implementation

Yen-Shin Chen[1,2], Luca Moratto[1], Marco Pagani[2], Hugo Fernandez[1,3], and Laura Peruzza[1,*]

[1]Istituto Nazionale di Oceanografia e di Geofisica Sperimentale - OGS, Trieste, Italy
[2]GEM Foundation, Pavia, Italy
[3]Università "G. D'Annunzio", Dipartimento di Ingegneria e Geologia, Chieti-Pescara, Italy

Corresponding author: lperuzza@ogs.it

Introduction

The accurate estimation of surface fault displacement hazards remains a critical component of seismic hazard and risk assessment, particularly for linear infrastructures and high-consequence facilities. While empirical data and statistical fault displacement models have long been the foundation of Probabilistic Fault Displacement Hazard Assessment (PFDHA), recent advances emphasize the integration of physics-based modeling and computational frameworks. The recent contributions by Moratto and Peruzza [2024] and by Chen et al. [2025], obtained within the frame of activities of the PRIN Project NASA4SHA, offer complementary steps in this direction. The former addresses the mechanistic understanding and modeling of dip-slip permanent ground displacement, while the latter provides a computational infrastructure for probabilistic hazard integration within the OpenQuake Engine. Together, they set the stage for a new generation of transparent, reproducible, and physically grounded PFDHA workflows.
Thanks to these activities, a new light is shed for understanding active compressive systems in Northern Italy, and for improving seismic hazard assessments of critical infrastructures. Testing and prototypal applications for a few selected structures are ongoing.

Physics-Based Modeling of Dip-Slip Displacement

Moratto and Peruzza [2024] explore permanent surface displacements caused by dip-slip faulting, particularly for moderate-magnitude events (M5.5-7.0), which are underrepresented in empirical datasets. They employ pseudo-dynamic rupture simulations [Moratto et al., 2015] to model both the along-strike and across-strike variability of surface deformation. These simulations incorporate realistic kinematic parameters such as slip distribution, rupture velocity, and fault geometry. A forward modelling pipeline simulates static, permanent, ground surface displacement (PD) for normal (dip slip) earthquakes typical of Apennine extensional tectonics. Input distributions span strike, dip, rake, rupture length/width, down dip extent, slip heterogeneity, and crustal elastic properties (Figure 1). From these simulations, they derive fault static offset (permanent displacement, PD), and off trace vertical/horizontal PD attenuation curves. Model ensembles are translated into displacement exceedance probabilities conditioned on magnitude and distance, providing inputs directly usable in PFDHA for infrastructure that intersects mapped faults.
The key results and insights of this analysis are:

- the modeled displacement fields are consistent with field data from Central Italy (see also materials from Fault2SHA Laboratories CA and FDH [1]), demonstrating the credibility of

physics-based approaches to reproduce observed displacement patterns;

- this study provides valuable insights into near-fault variability, which is essential for capturing the tail behavior of displacement exceedance curves - an area where empirical models often lack resolution;
- the approach quantifies both aleatory (random) and epistemic (knowledge-based) uncertainties in displacement estimates, providing critical input for hazard analyses.

This study provides a physically constrained foundation that can be incorporated into probabilistic models. By generating realistic displacement fields beyond the range of empirical observations, it directly addresses data gaps and improves hazard estimates for scenarios that cannot be fully captured by statistical regressions alone.

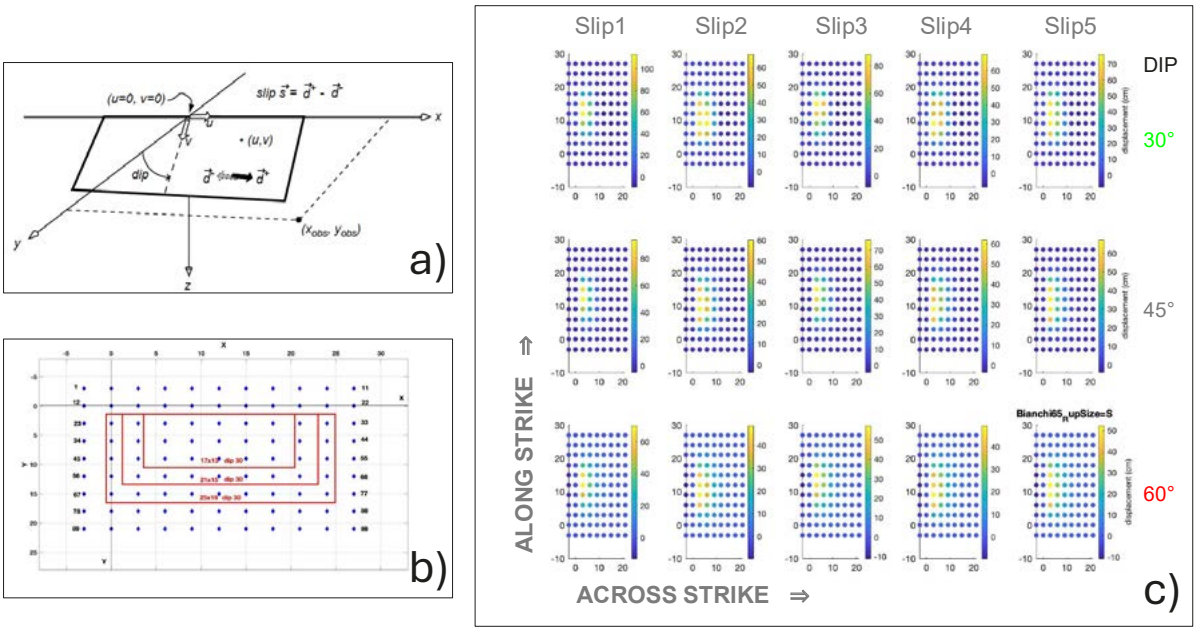

Figure 1 Example of PD's for a normal fault for a M=6.5 event: a) geometry sketch of the fault; b) receivers' location, and different rupture sizes; c) modelled PD obtained with one velocity model and one rupture size: rows represent three dip angles assigned the fault, columns five slip distribution models taken from literature.

Probabilistic Fault Displacement Hazard Assessment in the OpenQuake Engine

Chen et al. [2025] focus on developing a prototype PFDHA module within the open-source OpenQuake Engine [Pagani et al., 2014]. While the OpenQuake Engine framework is widely used for Probabilistic Seismic Hazard Assessment (PSHA), this work extends its capabilities to surface rupture hazards, creating a standardized computational pipeline (Figure 2).
Key innovations are:

- a modular architecture: Adapts OpenQuake's PSHA components to handle surface rupture probability (CPSR) and displacement exceedance, enabling seamless integration with seismic source models;
- Flexible Displacement Models: the framework supports multiple empirical and statistical Fault Displacement Models (FDMs), while remaining open for the integration of physics-based

approaches such as those previously mentioned [Moratto and Peruzza, 2024];

- distributed vs. principal fault rupture: the implementation addresses both types of rupture hazards, generating probabilistic exceedance curves relevant to different engineering contexts;
- transparency and reproducibility: all workflows are coded in Python, leveraging the open-source ethos of OpenQuake, which facilitates peer review, model updates, and widespread adoption.

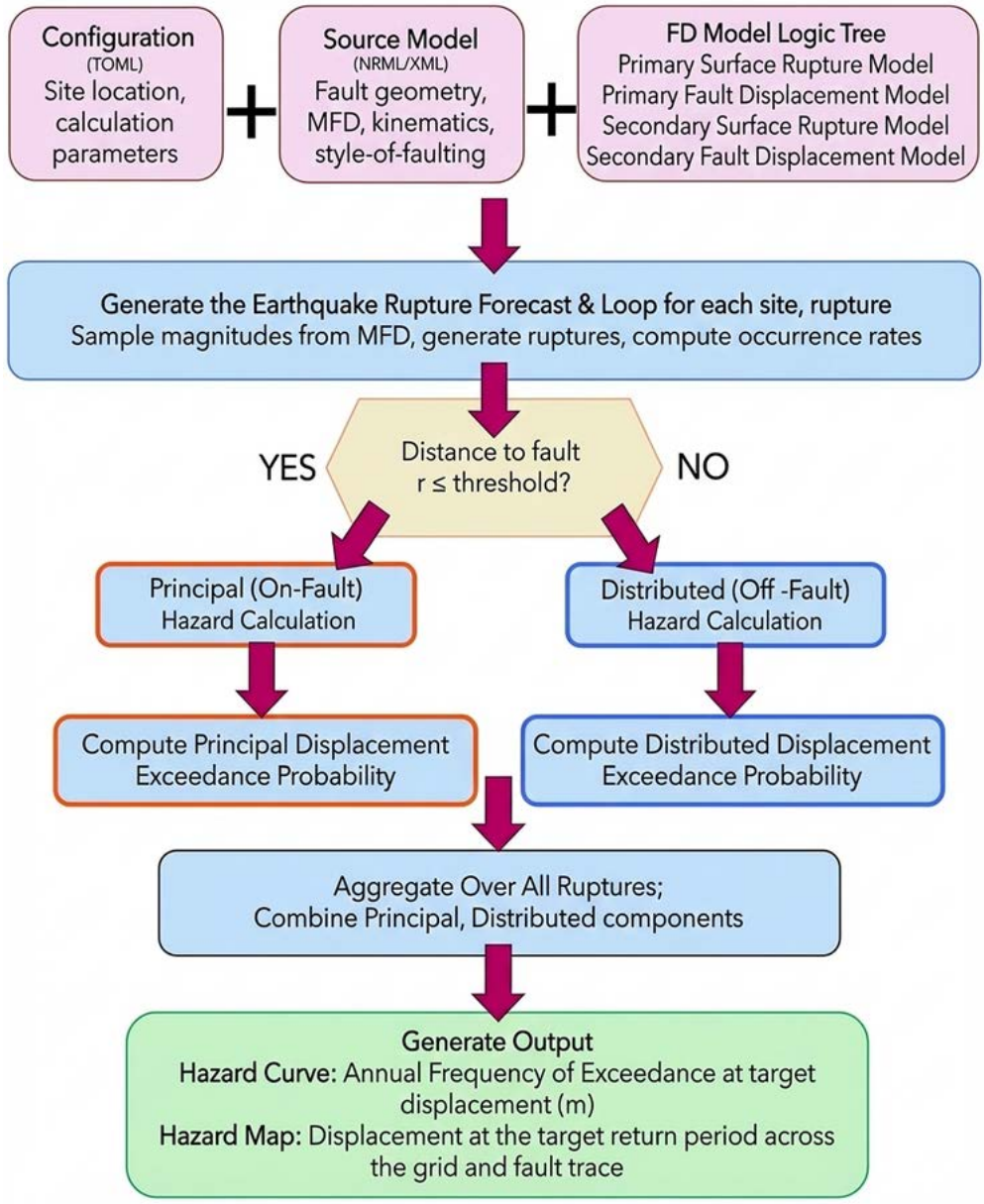

Figure 2 Workflow of the implementations done for PFDHA on the OQ Engine.

Figure 2 summarizes the end-to-end workflow used to compute fault-displacement hazard with OpenQuake Engine primitives. The software is modularized, separating geometry handlers, rupture occurrence and fault displacement calculators, model registries, and result composers; it affords (i) plug-and-play extension to new empirical or physics-based models, (ii) transparent, reproducible workflows, and (iii) efficient computation via vectorized gridding and parallel execution. It also supports both hazard curves and hazard map calculations.

Sites can be specified as single points or as rectangular footprints, which is practical for near-fault infrastructure such as dams and tunnels.
The accompanying applications to synthetic scenarios (Figures 3 and 4) document the set of surface rupture and fault-displacement models currently implemented in the software and

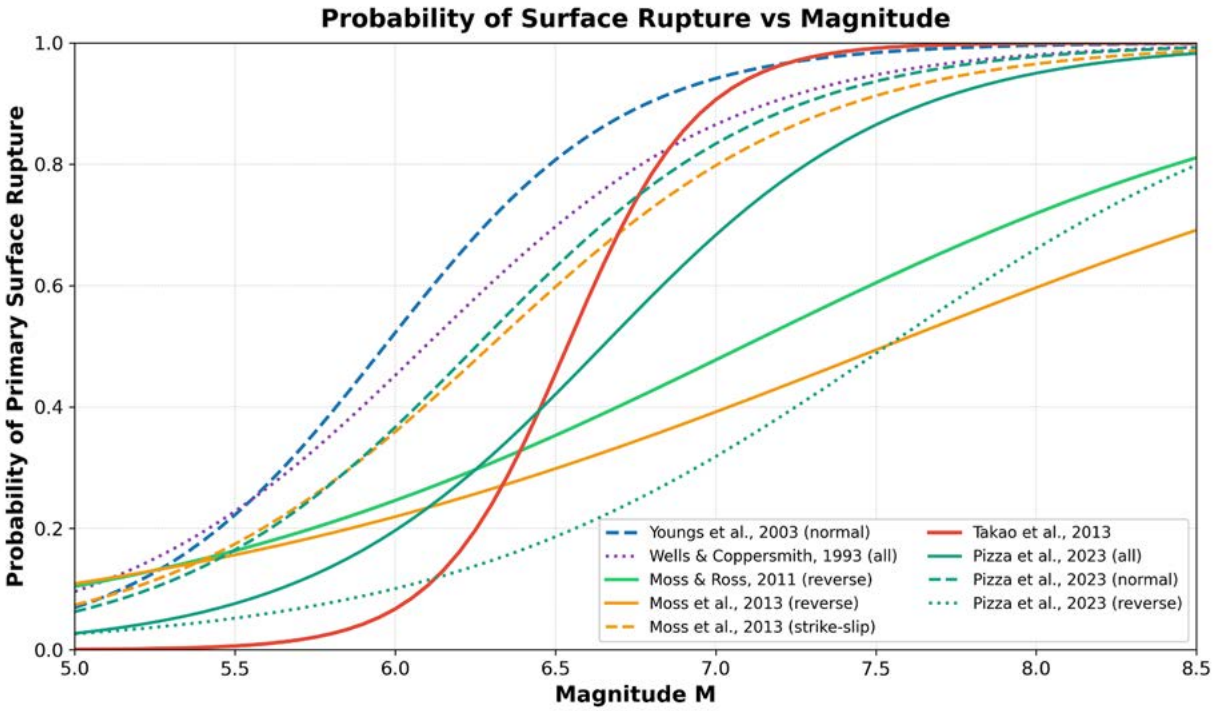

Figure 3 Primary surface-rupture probability as a function of magnitude M for the models implemented in the prototype. Curves shown include: YEA03 [Youngs et al., 2003]: all and normal variants; WC93 [Wells and Coppersmith, 1993]; MR11 [Moss and Ross, 2011]; M13 [Moss, 2013]: strike-slip and reverse; PZ23 [Pizza et al., 2023]: all/normal/reverse; TK13 [Takao et al., 2013]. Style-agnostic models are labelled "all," whereas style-specific variants are plotted as indicated. Full reference of various models are given in Valentini et al. [2025].

illustrate their relative behavior model assumptions, mechanisms (strike-slip, reverse, normal) and magnitudes. The sensitivity panels intentionally emphasize inter-model differences rather than validation of any single model, while also demonstrating the framework's ability to swap alternative models and to encode epistemic uncertainty via logic trees. In addition, Figure 5 demonstrates the output hazard curves at the Mount Vettore Fault site (42.76° N, 13.27° E), located on the principal fault trace near a rupture end (x/L = 0.05), and overlays the reference Youngs et al. [2003] curve for the Norcia exercise (characteristic Mw = 6.7 with mean annual rate α = 4.03×10−4). KEA24, MEA24 (DAD, DMD), and YEA03 (DAD, DMD) -produce consistent curve shapes with systematic divergence at larger target displacement, reflecting model-specific tail behavior. Although most one-to-one overlays with the source publications are not shown for brevity, the resulting hazard curves and occurrence probabilities are in good agreement with ranges reported by the respective authors. After final verification, the new code will be integrated in the latest version of OQ and released on GEM public repository [2].
The computational functionalities developed so far answer to the needs of having a flexible and tested framework for fault displacement hazard evaluations, applicable to the segments of active thrust systems identified in the Northern Apennines and Southern Alps by the PRIN NASA4SHA Project.

Complementarity and integration potential in the frame of NASA4SHA Project

The two works here summarized represent the major contribution obtained by some participants of the OGS research unit, in Work Package 9 of the PRIN 2020 Project NASA4SHA.
They represent distinct yet synergistic advancements. Moratto and Peruzza [2024] provide the physics-based inputs needed to enhance empirical FDMs, offering detailed spatial patterns and variability of surface rupture for dip-slip faults. Chen et al. [2025], in turn, supply the computational backbone that can integrate these physics-based results into a fully probabilistic hazard framework.

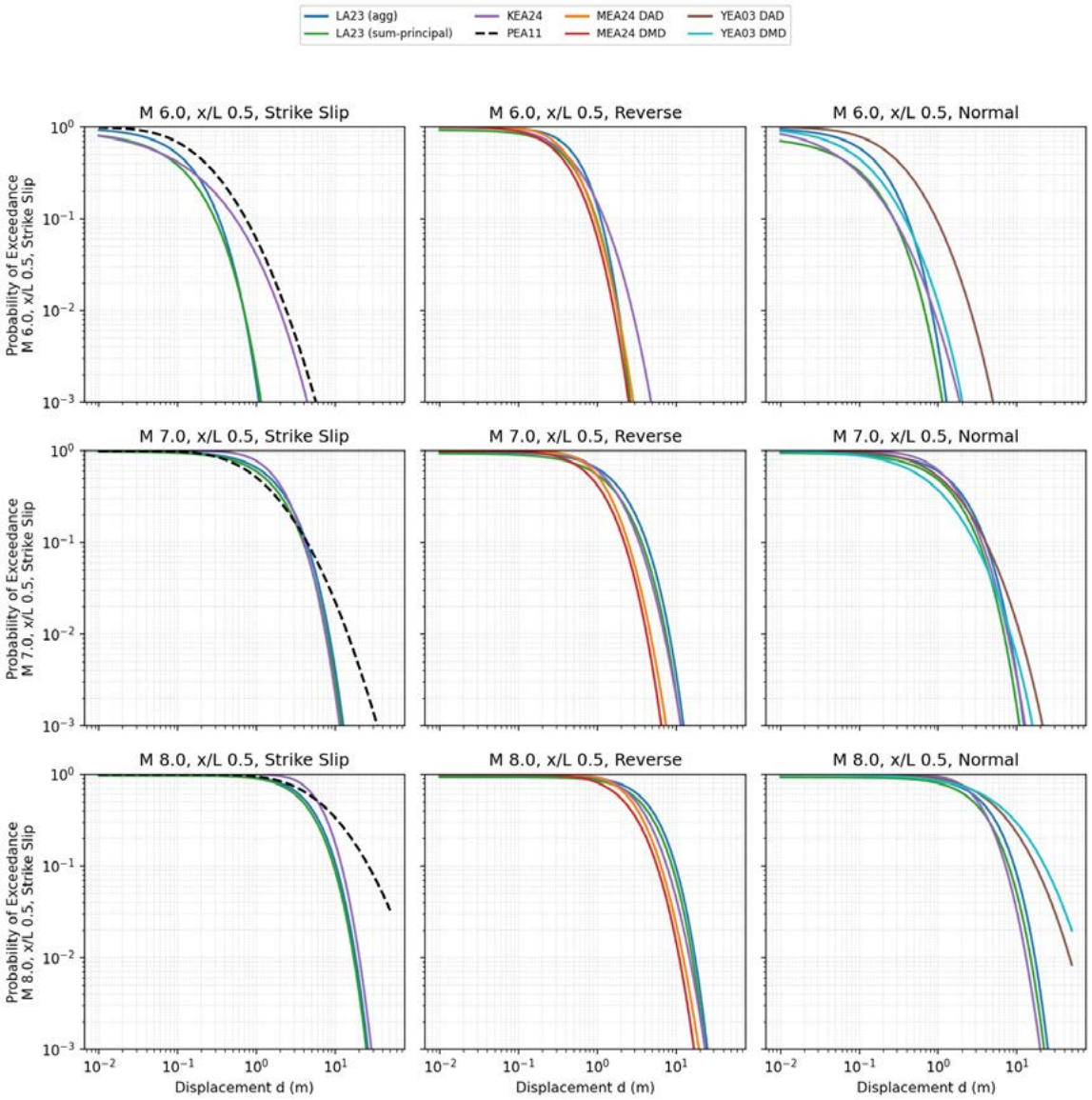

Figure 4 Probability of exceedance of surface displacement at the rupture midpoint (x/L = 0.5) for various magnitudes using the available primary fault displacement models in our software. The strike-slip panels plot four models with consistent styling across magnitudes: PEA11 [Petersen et al., 2011], black dashed; LA23-agg [Lavrentiadis et al., 2023], aggregate/net, blue solid; LA23-SoP [Lavrentiadis et al., 2023], sum-of-principal/net, blue dashed); KUEHN24 [Kuehn et al., 2024], Box-Cox, folded, green solid). The reverse and normal panels (when available and applicable) may additionally include KEA24 [Kuehn et al., 2024], MEA24-D/AD and MEA24-D/MD [Moss et al., 2024], and YEA03-D/AD and YEA03-D/MD [Youngs et al., 2003].

The last mile will be combining the detailed physics-based displacement modeling with the probabilistic, modular computational framework; it will enable the construction of a next-generation PFDHA framework that is:

- physically grounded by incorporating realistic rupture dynamics and displacement heterogeneity beyond purely empirical relations;
- probabilistically robust by capturing uncertainty through logic trees and stochastic rupture realizations, allowing hazard assessments with quantified confidence levels;
- modular and open-source by facilitating flexible incorporation of new models, datasets, and rupture styles while encouraging transparency and community collaboration;
- applicable across fault types and scales by extending hazard estimation to dip-slip and other complex fault systems often neglected in traditional models;
- adaptable to engineering needs by producing displacement exceedance curves, and rupture probabilities relevant to infrastructure risk assessments and regulatory compliance.

This integrated framework has the potential to provide critical support for seismic risk mitigation in densely populated and industrialized areas.

Conclusions and Future Outlook

The synergic efforts conducted in the frame of WP9 of the NASA4SHA Project have led to the development of brand-new probabilistic computational tools and physics-based simulations that, combined, can significantly advance fault displacement hazard science. Future developments should focus on:

- direct integration of simulated displacement fields into OpenQuake's logic-tree framework;
- expanding coverage to complex rupture geometries and oblique-slip scenarios;
- validating against high-resolution geodetic data (InSAR, LiDAR) from recent earthquakes;
- building a community-driven, open database of physics-based and empirical FDMs for global use.

The complementary nature of these studies bridges the gap between process-based understanding and probabilistic risk assessment, paving the way toward a more unified, transparent, and reliable PFDHA methodology.

Acknowledgments

The research activities here described have been carried out in the frame of the Italian PRIN Project (Research Projects of National Interest) "Fault segmentation and seismotectonics of active thrust systems: the Northern Apennines and Southern Alps laboratories for new Seismic Hazard Assessments in northern Italy (NASA4SHA)", PI R. Caputo, UR Responsible L. Peruzza, and they are related to the Work Package 9 "Fault-based ERF models and PFDHA at selected areas".

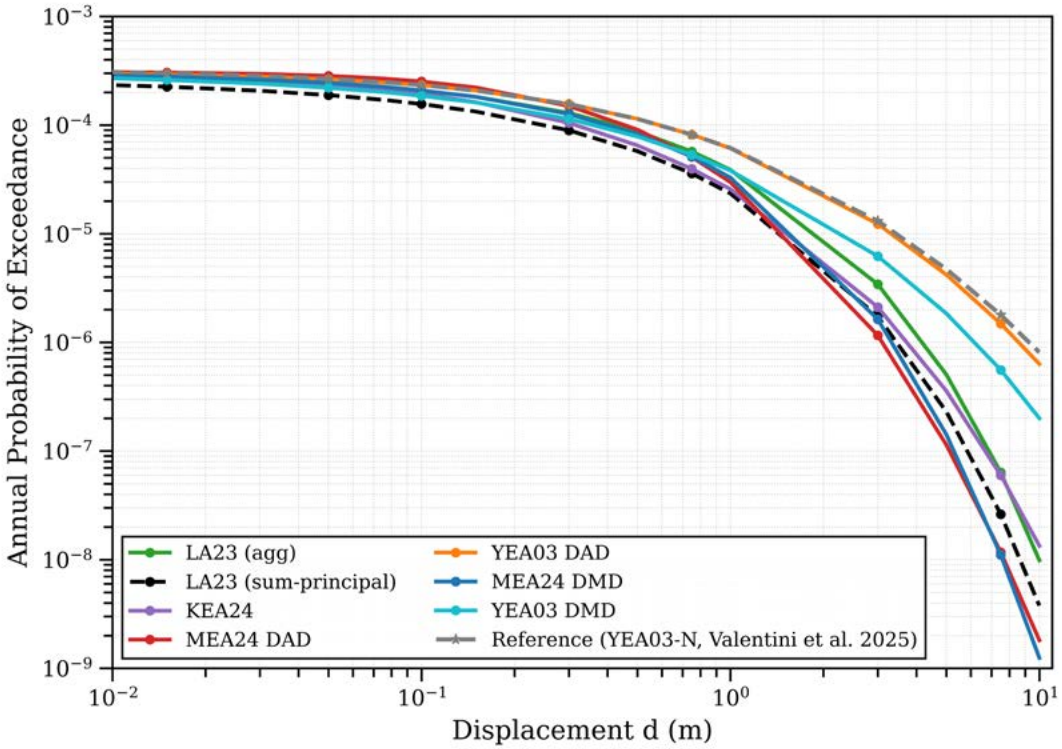

Figure 5 Fault displacement hazard curve for the Norcia test case. Annual probability of exceedance vs. displacement for the Mount Vettore Fault at the site (42.767° N, 13.278° E), located on the principal fault trace near a rupture end (x/L=0.05). Colored curves show the implemented models-LA23 (agg), LA23 (sum-principal), KEA24, MEA24 (DAD, DMD), and YEA03 (DAD, DMD). The gray dashed curve is the reference from Youngs et al. [2003] as reported for the Norcia case in Valentini et al. [2025], assuming a characteristic event of Mw = 6.7 with mean annual rate $\alpha = 4.03\times10^{-4}$. The figure emphasizes inter-model differences under identical common inputs.

References

Chen, Y.S., Pagani, M., Fernandez, H., and Peruzza, L., (2025). *Prototypal Implementation of Probabilistic Fault Displacement Hazard Assessment Using the OpenQuake Engine Components*. 43 Convegno GNGTS, Atti, Bologna. https://hdl.handle.net/20.500.14083/43865

Kuehn, N.M., Kottke, A.R., Sarmiento, A.C., Madugo, C.M., and Bozorgnia, Y., (2024). *A fault displacement model based on the FDHI database*. Earthquake Spectra. https://doi.org/10.1177/87552930241291077

Lavrentiadis, G., and Abrahamson, N., (2023). *Fault-displacement models for aggregate and principal displacements*. Earthquake Spectra. https://doi.org/10.1177/87552930231201531

Moratto, L., Vuan, A., and Saraò, A., (2015). *A hybrid approach for broadband simulations of strong ground motion: the case of the 2008 Iwate–Miyagi Nairiku earthquake*. Bull. Seism. Soc. Am., 105, 2823-2829. https://doi.org/10.1785/0120150054

Moratto, L., and Peruzza, L., (2024). *Permanent ground displacement for dip slip faulting: a modelling approach*. 39 ESC General Assembly, Corfu. https://hdl.handle.net/20.500.14083/31304

Moss, R.E.S., and Ross, Z.E., (2011). *Probabilistic fault displacement hazard analysis for reverse faults*. Bulletin of the Seismological Society of America, 101(4), 1542–1553. https://doi.org/10.1785/0120100248

Moss, R.E.S., Stanton, K.V., and Buelna, M.I., (2013). *The impact of material stiffness on the*

likelihood of fault rupture propagating to the ground surface. Seismological Research Letters, 84(3), 485–488. https://doi.org/10.1785/0220110109

Moss, R.E.S., Thompson, S.C., Kuo, C.-H., Younesi, K., and Baumont, D., (2024). *Probabilistic fault displacement hazard analysis for reverse faulting*. Earthquake Spectra. https://doi.org/10.1177/8755293024128856

Pagani, M., Monelli, D., Weatherill, G., Danciu, L., Crowley, H., Silva, V., Henshaw, P., Butler, L., Nastasi, M., Panzeri, L., Simionato, M., and Vigano, D., (2014). *OpenQuake Engine: An open hazard (and risk) software for the Global Earthquake Model*. Seismological Research Letters, 85 (3), 692-702. https://doi.org/10.1785/0220130087

Petersen, M.D., Dawson, T.E., Chen, R., Cao, T., Wills, C.J., Schwartz, D.P., and Frankel, A.D., (2011). *Fault displacement hazard for strike-slip faults*. Bulletin of the Seismological Society of America, 101(2), 805–825. https://doi.org/10.1785/0120100035

Pizza, M., Ferrario, M.F., Thomas, F., Tringali, G., and Livio, F. (2023). *Likelihood of primary surface faulting: Updating of empirical regressions*. Bulletin of the Seismological Society of America, 113(5), 2106–2118. https://doi.org/10.1785/0120230019

Takao, M., Tsuchiyama, J., Annaka, T., and Kurita, T. (2013). *Application of probabilistic fault displacement hazard analysis in Japan*. Journal of Japan Association for Earthquake Engineering, 13(1), 17–36. https://doi.org/10.5610/jaee.13.17

Valentini, A., Visini, F., Boncio, P., Scotti, O., and Baize, S., (2025). *Twenty-five years of probabilistic fault displacement hazard assessment*. Reviews of Geophysics, 63, e2024RG000875. https://doi.org/10.1029/2024RG000875

Youngs, R.R., Arabasz, W.J., Anderson, R.E., Ramelli, A.R., Ake, J.P., Slemmons, D.B., McCalpin, J.P., Doser, D.I., Fridrich, C.J., Swan, F.H., Rogers, A.M., Yount, J.C., Anderson, L.W., Smith, K.D., Bruhn, R.L., Knuepfer, P.L.K., Smith, R.B., dePolo, C.M., O'Leary, D.W., Coppersmith, K.J., Pezzopane, S.K., Schwartz, D.P., Whitney, J.W., Olig, S.S., Toro, G.R., (2003). *A Methodology for Probabilistic Fault Displacement Hazard Analysis (PFDHA)*. Earthq. Spectra 19, 191–219. https://doi.org/10.1193/1.1542891

Wells, D., and Coppersmith, K., (1993). *Likelihood of surface rupture as a function of magnitude*. Seismological Research Letters, 64(1).

Sitography

[1] https://fault2sha.net/labs/

[2] https://github.com/gem/oq-engine/

APPENDIX

Additional papers from the NASA4SHA Project

Baranello S., Camassi R., and Castelli V., (2023a). *In the wake of a big quake*. IASPEI, Berlino, luglio 2023.

Baranello S., Camassi R., and Castelli V., (2023b). *Forgotten Earthquakes and Where to Find Them (and Also Why…)*. 8th International Colloquium on Historical Earthquakes, Palaeo-Macroseismology and Seismotectonics, 17-20 September 2023 - Lixouri, Greece, Bulletin of the Geological Society of Greece, Sp. Publ. 11, Ext. Abs. 00035, pp. 129-132.

Baranello S., Camassi R., and Castelli V., (2024). *Behind the Italian catalogues: overlooked but far from negligible earthquakes*. Ann. Geophys., 67, 2, SE220, 2024. https://doi.org/10.4401/ag-9096

Baranello S., Camassi R., and Castelli V., (2024). *Materiali per un catalogo dei terremoti italiani. Terremoti del Trevigiano e Bellunese tra '700 e '900*. Quad. Geofis., 197: 1150. https://doi.org/10.13127/qdg/197

Barbano M.S., Baranello S., Rossetti A., Castelli V., and Camassi R., (2025). *Updating knowledge on 18th century Carnia earthquakes*. 43° convegno nazionale GNGTS, Bologna, 11-14 febbraio 2025.

Baranello S., Barbano M.S., Rossetti A., Castelli V., Camassi R., (2025). Materiali per un catalogo dei terremoti italiani. Forti terremoti delle Prealpi Carniche nel XVIII secolo. Quad. Geofis., 199: 1-168, https://doi.org/10.13127/qdg/199

De Matteo A., Barrera D., Seno S., Di Giulio A., Toscani G., (2025). *The influence of pre-existing structures on the foredeep evolution and structural style: integrated analysis of Plio-Pleistocene fault kinematics in the Central Po Plain (Italy)*. GeoMod 2025, Lisbon 7-12 September, Abstract Volume.

Faoro A., Camassi R., and Castelli V., (2024). *Early results of a systema c revision of Ferrarese seismicity of the 13th-15th centuries*. 42° GNGTS National Conference 13 - 16 febbraio 2024 Ferrara.

Faoro A., Camassi R. and Castelli V., (2025). *Pre-1500s earthquakes in Ferrara (N Italy) and their sources: early results of a critical revision*. Bull. Geophys. Ocean., 66(2), 133-146. https://doi.org/10.4430/bgo00476

Galvani A., Albano M., Braitenberg C., Brighen F., Caputo C., Carnemolla F., Cheloni D., De Guidi G., Devo R., Magrin A., Pellegrinelli A., Pietrantonio G., Rossi G., Stramondo S., Tunini L., and Zuliani D., (2024). *PRIN 2020 NASA4SHA Project: A Combined Regional Velocity Field of Northern Italy*. 42° GNGTS National Conference 13 - 16 febbraio 2024 Ferrara.

Giuffrida S., Anderlini L., Graham S., Carnemolla F., Brighenti F., de Guidi G., Cannavò F., and Caputo R., (2025). *Investigating the interseismic coupling degree of the northern Apennines external Arc in Emilia Romagna region, (northern Italy)*. Bull. Geol. Soc. Greece, Sp. Publ. Sp. Publ. 15, 099, 488-490.

Moratto L., Panebianco S., Satriano C., Stabile T.A., and Priolo E., (2025). *Using ambient noise k_0 estimation to improve microearthquake source parameters assessment in the High Agri Valley*. Geophysical Journal International 242 (2), ggaf191. https://doi.org/10.1093/gji/ggaf191

Poli M.E., Patricelli G., Falcucci E., Gori S., Paiero G., Rizzo E., Marchesini A., and Caputo R., (2024). *New palaeoseismological evidence of coseismic surface rupture across the Carnic Prealpine front (NE-Italy): the Budoia-Aviano thrust system*. 42° GNGTS National Conference 13 - 16 febbraio 2024 Ferrara.

Poli M.E., Patricelli G., Monegato G., and Zanferrari A., (2024). *Structural inheritances, fault segmentation and seismogenic potential at the front of the eastern Southern Alps (central Carnic Prealps, NE Italy)*. Tectonophys., 883, 230390. https://doi.org/10.1016/j.tecto.2024.230390

Talone D., Romano M.A., De Siena L., Guidarelli M., Santulin M., Peruzza L., Lavecchia G., and de Nardis R., (2025). *Underground Gas Storage as benchmark for seismic attenuation tomography*

in a tectonically complex region (north-eastern Italy). Geophysical Research Letters, 52, e2025GL117956. https://doi.org/10.1029/2025GL117956

Tarchini G., Moratto L., and Saraò A., (2025). *A comprehensive moment magnitude catalog for the Northeastern Italy region*. Seismological Research Letters, 96, 2714-2723. https://doi.org/10.1785/0220240303

Tibaldi A., de Nardis R., Torrese P., Bressan S., Pedicini M., Talone D., Bonali F.L., Corti N., Russo E., and Lavecchia G., (2023). *A multi-scale approach to the recent activity of the Stradella thrust in the seismotectonic context of the Emilia Arc (northwestern Italy)*. Tectonophys., 857, 229853. https://doi.org/10.1016/j.tecto.2023.229853

Tibaldi A., Barrera D., Bonali F.L., Corti N., and Toscani G., (2025). *Out-of-sequence recent thrusting revealed by surface and subsurface data under the Po Plain, Italy*. Journal of Structural Geology, 201, 105556. https://doi.org/10.1016/j.jsg.2025.105556

Zampieri D., Roghi G., Preto N., and Dalconi M.C., (2023). *The Debated Discovery of Dolomite and the Proposal of a New Geosite at Borcola Pass (Eastern Italian Pre-Alps) in Honor of Giovanni Arduino*. Geoheritage, 15:53. https://doi.org/10.1007/s12371-023-00816-x

QUADERNI di GEOFISICA

ISSN 1590-2595 https://istituto.ingv.it/it/le-collane-editoriali-ingv/quaderni-di-geofisica.html/

I QUADERNI DI GEOFISICA (QUAD. GEOFIS.) accolgono lavori, sia in italiano che in inglese, che diano particolare risalto alla pubblicazione di dati, misure, osservazioni e loro elaborazioni anche preliminari che necessitano di rapida diffusione nella comunità scientifica nazionale ed internazionale. Per questo scopo la pubblicazione on-line è particolarmente utile e fornisce accesso immediato a tutti i possibili utenti. Un Editorial Board multidisciplinare ed un accurato processo di peer-review garantiscono i requisiti di qualità per la pubblicazione dei contributi. I QUADERNI DI GEOFISICA sono presenti in "Emerging Sources Citation Index" di Clarivate Analytics, e in "Open Access Journals" di Scopus.

QUADERNI DI GEOFISICA (QUAD. GEOFIS.) welcome contributions, in Italian and/or in English, with special emphasis on preliminary elaborations of data, measures, and observations that need rapid and widespread diffusion in the scientific community. The on-line publication is particularly useful for this purpose, and a multidisciplinary Editorial Board with an accurate peer-review process provides the quality standard for the publication of the manuscripts. QUADERNI DI GEOFISICA are present in "Emerging Sources Citation Index" of Clarivate Analytics, and in "Open Access Journals" of Scopus.

RAPPORTI TECNICI INGV

ISSN 2039-7941 https://istituto.ingv.it/it/le-collane-editoriali-ingv/rapporti-tecnici-ingv.html/

I RAPPORTI TECNICI INGV (RAPP. TEC. INGV) pubblicano contributi, sia in italiano che in inglese, di tipo tecnologico come manuali, software, applicazioni ed innovazioni di strumentazioni, tecniche di raccolta dati di rilevante interesse tecnico-scientifico. I RAPPORTI TECNICI INGV sono pubblicati esclusivamente on-line per garantire agli autori rapidità di diffusione e agli utenti accesso immediato ai dati pubblicati. Un Editorial Board multidisciplinare ed un accurato processo di peer-review garantiscono i requisiti di qualità per la pubblicazione dei contributi. RAPPORTI TECNICI INGV (RAPP. TEC. INGV) publish technological contributions (in Italian and/or in English) such as manuals, software, applications and implementations of instruments, and techniques of data collection. RAPPORTI TECNICI INGV are published online to guarantee celerity of diffusion and a prompt access to published data. A multidisciplinary Editorial Board and an accurate peer-review process provide the quality standard for the publication of the contributions.

MISCELLANEA INGV

ISSN 2039-6651 https://istituto.ingv.it/it/le-collane-editoriali-ingv/miscellanea-ingv.html

MISCELLANEA INGV (MISC. INGV) favorisce la pubblicazione di contributi scientifici riguardanti le attività svolte dall'INGV. In particolare, MISCELLANEA INGV raccoglie reports di progetti scientifici, proceedings di convegni, manuali, monografie di rilevante interesse, raccolte di articoli, ecc. La pubblicazione è esclusivamente on-line, completamente gratuita e garantisce tempi rapidi e grande diffusione sul web. L'Editorial Board INGV, grazie al suo carattere multidisciplinare, assicura i requisiti di qualità per la pubblicazione dei contributi sottomessi. MISCELLANEA INGV (MISC. INGV) favours the publication of scientific contributions regarding the main activities carried out at INGV. In particular, MISCELLANEA INGV gathers reports of scientific projects, proceedings of meetings, manuals, relevant monographs, collections of articles etc. The journal is published online to guarantee celerity of diffusion on the internet. A multidisciplinary Editorial Board and an accurate peer-review process provide the quality standard for the publication of the contributions.

Progetto grafico
Barbara ANGIONI
Istituto Nazionale di Geofisica e Vulcanologia

Ufficio Editoriale
Francesca DI STEFANO | Coordinatore

Segreteria di redazione
segreteria.collane-editoriali@ingv.it

Editing | Produzione | Grafica redazionale
Barbara ANGIONI
Massimiliano CASCONE
Francesca DI STEFANO
Patrizia PANTANI

ISTITUTO NAZIONALE DI GEOFISICA E VULCANOLOGIA